THESE DE DOCTORAT DE SORBONNE UNIVERSITE

Spécialité Ecologie Microbienne
« Sciences de la Nature et de l'Homme : évolution et écologie » (ED227)

Présentée par

Mathilde FERRIEUX

En vue de l'obtention du grade de
DOCTEUR de SORBONNE UNIVERSITE

Adaptation à la température et à la limitation en fer chez un représentant majeur du phytoplancton marin, la picocyanobactérie *Synechococcus*

Soutenue le 9 septembre 2022, devant le jury composé de :

Pr. GARCIA-FERNANDEZ José Manuel ..... Rapporteur
Université de Cordoue

Dr. VAN-WAMBEKE France ..... Rapportrice
MIO - Mediterranean Institute of Oceanography

Dr. LEPERE Cécile ..... Examinatrice
Université de Clermont-Ferrand

Pr. CORMIER Patrick ..... Examinateur
CNRS, Roscoff

Dr. PARTENSKY Frédéric ..... Co-encadrant de thèse
CNRS, Roscoff

Dr. GARCZAREK Laurence ..... Directrice de thèse
CNRS, Roscoff

Station Biologique de Roscoff
UMR 7144 Adaptation et Diversité en Milieu Marin
Equipe ECOMAP (Ecology of Marine Plankton)

Résumé

Les océans sont fortement impactés par le changement global, qui provoque une augmentation de la température de surface mais aussi une expansion des zones pauvres en Fer (Fe) alors que ce micronutriment limite déjà la croissance du phytoplancton dans près de 30 % de l'océan mondial. Dans ce contexte, on peut se demander si et comment le phytoplancton marin est capable de s'adapter à cette limitation et quelles seront les conséquences de l'appauvrissement en Fe sur la capacité des océans à séquestrer le CO_2 via la pompe à carbone biologique. De par son abondance, son ubiquité, la disponibilité de nombreuses souches et génomes, *Synechococcus* constitue l'un des modèles biologiques les plus pertinents disponibles à ce jour pour étudier les processus moléculaires impliqués dans l'adaptation du phytoplancton aux changements environnementaux en cours dans l'océan. Alors que les populations naturelles de *Synechococcus* ont longtemps été considérées comme dominées par quatre clades (I-IV), l'importance écologique d'un cinquième clade (appelé CRD1) a récemment été mise en évidence dans les zones limitées en Fe de l'océan mondial. En outre, il a été démontré que le clade CRD1 englobe 3 unités taxonomiques distinctes écologiquement significatives (ESTUs CRD1A à C), occupant des niches thermiques distinctes. Afin de mieux comprendre les rôles respectifs de la carence en Fe et de la température sur la distribution et la diversification génétique de *Synechococcus*, la comparaison de souches représentatives de chacun des trois ESTUs de CRD1 avec des membres des clades I-IV, utilisés comme références de thermotypes froids (I, IV) ou chauds (II, III) et colonisant des environnements riches en Fe, a permis de valider l'existence de trois thermotypes distinctes au sein au clade CRD1. De plus, l'acquisition de paramètres physiologiques supplémentaires à partir de cultures acclimatées à différentes températures et différents degrés de limitation en Fe a également révélé des spécificités des souches CRD1 par rapport aux autres clades. Des analyses comparatives des génomes de *Synechococcus* disponibles ont également suggéré que la dominance de ce clade dans les zones pauvres en Fe pourrait reposer sur une réduction du nombre de gènes codant pour des protéines riches en Fe et sur une augmentation du nombre de gènes codant pour des protéines utilisant des métaux alternatifs comme co-facteurs et surtout des protéines impliquées dans le transport, l'assimilation et le stockage du Fe. Enfin, l'analyse des métagénomes de *Tara* Oceans a révélé des gènes spécifiquement présents ou absents dans les niches pauvres en Fe qui ont permis de confirmer les résultats de génomique comparative et d'identifier de nouveaux gènes candidats potentiellement impliqués dans les mécanismes d'adaptation à la carence en Fe et à la température.

Abstract

The oceans are strongly impacted by global change, which is predicted to cause an increase of sea surface temperature but also an expansion of iron-poor areas (Fe). This micronutrient limits phytoplankton growth in nearly 30% of the global ocean. In this context, one may wonder if/how marine phytoplankton is able to adapt to such limitation and what will be the consequences of Fe depletion on the ocean ability to sequester CO2 via the biological carbon pump. Due to its abundance, ubiquity, the availability of numerous strains and genomes, Synechococcus constitutes one of the most relevant biological models available nowadays to study the molecular processes involved in the adaptation of phytoplankton to the environmental changes occuring the ocean. While natural populations of Synechococcus were long thought to be dominated by four clades (I-IV), the ecological importance of a fifth clade (called CRD1) has recently been demonstrated in Fe-limited areas of the world ocean. Furthermore, the CRD1 clade has been shown to encompass 3 distinct Ecologically Significant Taxonomic Units (ESTUs, CRD1A to C), occupying distinct thermal niches. In order to better understand the respective roles of Fe deficiency and temperature on the distribution and genetic diversification of Synechococcus, we compared the physiology of representative strains of each of the three CRD1 ESTUs with members of clades I-IV, used as controls for cold (I, IV) or warm (II, III) thermotypes and Fe-replete environments to validate the existence of three distinct thermotypes within the CRD1 clade. Moreover, the acquisition of additional physiological parameters from cultures acclimated to different temperatures and different degrees of Fe limitation also revealed specificities of CRD1 strains compared to other clades. Comparative analyses of Synechococcus genomes have also suggested that the dominance of this clade in Fe-depleted areas may rely on a reduction in the number of genes coding for Fe-rich proteins and an increase of genes coding for proteins using alternative metals as co-factors and especially involved in Fe transport, assimilation and storage. It made it possible to confirm the results of comparative genomics and to identify new candidate genes potentially involved in the mechanisms of adaptation to Fe and temperature. Finally, the analysis of Tara oceans metagenomes revealed genes specifically present of absent in the Fe-poor niches which made it possible to confirm the results of comparative genomics and to identify novel genes potentially involved in adaptation mechanisms to Fe-depletion and temperature.

Remerciements

TRUGAREZ VRAS D'AN HOLL !

Tout d'abord, je souhaiterais remercier les membres du jury d'avoir accepté de lire et évaluer ce travail. Merci aux deux rapporteurs de cette thèse, France Van-Wambeke et José-Manuel Garcia Fernandez et aux deux examinateurs, Cécile Lepère et Patrick Cormier. Je remercie également Anne-Claire Baudoux, Eva Bucciarelli et Catherine Leblanc qui ont accepté de suivre ce travail durant les comités de thèse. Merci d'avoir porté un regard bienveillant sur mon travail et de m'avoir fait relativiser sur la condition de doctorant.

Un grand merci à Laurence pour avoir accepté de travailler ensemble une première fois en stage puis d'avoir voulu continuer l'aventure en doctorat. Je pense également à Fred, merci d'avoir co-encadré ce travail. Vous formez une équipe si chouette ! Grâce à vous, je me suis découverte une patience sans limite (ou presque) pour faire pousser ces petites bêtes et surtout les CRD1, pas des plus dociles ! On y est arrivés !!!!

Depuis janvier 2018 j'en ai fait des rencontres ! Surtout dans un environnement comme la Station Biologique !

Momo, j'ai été ravie de travailler avec toi sur des fichiers excel relevant du casse-tête chinois, des miliers de bloblots ou encore des récoltes d'ARN semblables à des sprints de jeux olympiques. On aura surtout beaucoup ri et chanté. Bientôt les tresses pour se rappeler nos racines sur les chemins de Babylone (Babylone). Floflo, merci d'avoir été mon binôme de fous rires au Gulf Stream. Un jour on arrivera à faire interdire le panais et les cocos de Paimpol. Merci aussi pour toutes tes petites attentions pendant ces quatre ans, il est évident que tu as contribué à mon bien-être au sein de la Station et pour ça un milliard de fois merci ! Grande pensée à Fabienne, pour toutes les discussions en pause café ou à la porte de ton bureau. Merci également de m'avoir fait me sentir si styyyyylée certains matins et pour ta bonne humeur ! Merci à Pris d'avoir supporté ma paillasse, visuellement pas des plus agréables quand on aime l'ordre. Domi, Domi, Domi… je te remercie pour les discussions (sur les phares, l'actualité, la politique…), les croque-monsieurs/les gaufres, la cytométrie et les nombreux débugg de Guava. On avait dit qu'on partait en même temps, j'ai pris un petit rab'. Plein de pensées pour Sarah, membre honorable du GS et Estelle, je n'aurai pas imaginé meilleure partenaire de campagne

TONGA ! Merci à Céline d'avoir contribué à faciliter mon arrivée à la Station en dénouant les nœuds de l'administration, mais aussi pour avoir été une partenaire exemplaire aux fêtes d'été/noël. Je remercie chaleureusement chacun des membres de PhytopK, ce fut un plaisir de partager avec vous les pauses café du matin, les sessions repiquages sous la hotte, les repas au Gulf, toujours dans une ambiance joviale. D'ailleurs, merci à l'équipe du Gulf Stream ! Franck, Barbara, Maryline, Pascale, Jean-Jacques et tous les autres, toujours un plaisir de venir manger chez vous ! D'une manière générale, je remercie toutes les personnes croisées au détour d'un couloir, propice à un sourire, un bonjour, un café ou une discussion. Mais aussi à tous les autres… Je mentionnerai Fredo et Stéphane ! Merci pour tous les moments partagés autour d'un repas ou d'un verre, au Ty Pierre par exemple... Fredo pour ton regard bienveillant et Stéphane pour tes traits d'esprit. Je suis si ravie d'avoir croisé votre chemin que j'espère recroiser un jour avec grand plaisir ! Gwenn, merci de m'avoir fait découvrir le pilâtes avec Francky et bien rire à Panos.

On arrive à la partie des amis, pas la plus facile à écrire (en plus il fait chaud, on vit une canicule à Roscoff, c'est un fait rare pour être mentionné dans cette partie !) Je commencerai par le premier ami rencontré ici... Martin ! Heureusement qu'il a fallu brancher un incubateur dès mes premiers jours à la Station… Ker Gac'henot, sache qu'il existe des Amitiés où l'on sait qu'on ne se quittera jamais, il est évident que celle-ci en fait partie 🦫. Naturellement, Damien, tu as ta place dans cette catégorie 🧢 ! Ton rire ne cessera jamais de raisonner dans mon esprit (et me hanter parfois ahah) ! Merci d'avoir formé avec moi une sacrée team… Dont Erwan a souvent été la victime… Merci Erwan d'avoir ri à presque toutes mes blagues et de m'en avoir fait des milliers 🌊. Alicia et Laura, mes brocantes adorées, merci d'avoir été présentes même à 400km d'ici, si vous saviez l'affection que je vous porte 🌺. Pensée pour Jade, ma partenaire de balade, toujours partante pour un petit kir breton ou un kir de chez Coco 🐧. Léna, mes sessions de repiquages ont été des plus agréables à tes côtés, ne parlons pas du paddle ! De vraies professionnelles, toujours dans la maîtrise malgré les attaques de sternes 😼. Je pense également à Bertille, clairement mon compagnon de Domac 🍟 et bien plus ! Louison, d'abord stagiaire, puis binôme, puis amie et enfin coloc', il me semble qu'on ne se quitte plus ! Merci d'avoir été là même quand on se disait « mais quel enfer ! » après avoir effectué des milliers de suivis de Fv/Fm, de récoltes d'HPLC, etc… jusque pas d'heures en

mangeant de délicieuses Lombardi tout en profitant de ciels étoilés comme je n'en avais jamais vu ❤️. Parmi les copains de galère : Ulysse ! Tu es toujours d'un grand soutien même quand tu es loin (merci Slack !). Sache que tu es une vraiment « une bonne personne » 🎸 ! Capitaine Dan, merci pour ta gentillesse sans limite, ta disponibilité et ton écoute. Merci aussi de m'avoir fait découvrir la magnifique Île de Batz, la pêche au casier et les remontées de filets 🚤 ! Karine, merci de m'écouter, d'accepter d'aller se promener à pas d'heures et de suivre le petit démon que je peux être 🧩.
Merci aux copains pour les bons moments passés au cours de session jeu de rôle, apéro, tournoi de palets, plages, camping, etc… : Florian, Lancelot, Charlotte, Stéphane, Laura P., Steph', les Kerloc'h, Polo, Maël, Hugo, Eystein, Pym, Lisa, Jérémy, Mariana, Yasmine, Camille P., Ben, Sam, PG, Guillaume, Kévin, Yacine, Jana, Valéria, Marie-Morgane, Myriam, Camille T.B., Victor, Emilie, Justine, Théophile, Alexis, Antonin, Aurélien etc… Dans un autre registre, c'était si chouette de rencontrer les copains du Centre Nautique : Adrienne, Lilou, Léo, Yann et Malo ! Les copains de Plougoulm : Maïna, Angèle, Boris, Ewen, Léna et Antho. Et forcément, mon séjour roskovite n'aurait pas été le même sans le Ty Pierre ❤️.
Merci à toute l'équipe de m'avoir fait me sentir quasiment à la maison et d'avoir toujours porté une attention toute particulière à mon passage. Merci Sam, Yvan, Goul', Do', Polo, Zoé, Jo, Manue, Marine et tous les autres…

Merci à mes parents, Rémy & Catherine, et ma soeur Anne. Merci pour votre soutien sans faille. Je m'excuse pour la distance que je nous ai imposé ces dernières années et pour les appels laissés sans réponse. Je vous remercie d'avoir fait de moi la personne que je suis aujourd'hui, je vous dois énormément.

Et pour finir, **MERCI ROSCOFF** de m'avoir fait me sentir chez moi dès les premières minutes en Finistère Nord, même les jours de pluie, de vent, de tempêtes… Tu m'auras marqué par la beauté de ton paysage, de tes couchers de soleil tous plus spectaculaires les uns que les autres, tes marées si impressionnantes, ton eau souvent froide (voire très froide), ton charme, tes parties de palets interminables, les éclats de rire qui y ont retenti, le bruit des vagues, les cris des goëlands et j'en passe…

Je repasserai te voir pour sûr.

Et comme on dit en breton : « *Kenavo*, *ar wech all* »

Table des matières

Liste des figures

Table des abréviations

ADN	Acide désoxyribonucléique
AMZ	Zones marines anoxiques
APC	Allophycocyanine
ARN	Acide ribonucléique
ARTO	« Alternative Respiratory Terminal Oxidase »
β-car	β-carotène
CAG	Cluster de gènes adjacents
Chl *a*	Chlorophylle *a*
CLOG	Cluster de gènes orthologues
DFOB	Deferoxamine mésilate
DMS	Diméthylsulfure
DMSO	Diméthylsulfoxyde
DMSP	Diméthylsulfoniopropionate
DOM	Matière organique dissoute
ESTU	Ecologically Significant Taxonomic Unit
Fe / Fe' / FeL / dFe / Fe^{2+} / Fe^{3+}	Fer / Fer inorganique / Fer lié / Fer dissous / Fer ferreux / Fer Ferrique
FNR	Ferrédoxine-$NADP^+$ réductase
FSC	Forward Scattering
F_V/F_M	Rendement quantique moyen du photosystème II
GOS	Global Ocean Survey
HL	« High-light »
HNLC	« High-nutrient, low chlorophyll »
LL	« Low-light »
MAG	« Metagenomes Assembled Genomes »
NPQ	« Non-photochemical quenching »
OCP	Caroténo-protéine orange
OTU	Unité taxonomique opérationnelles
PBP	Phycobiliprotéine
PBS	Phycobilisome
PCB	Phycocyanobiline
PEB	Phycoérythrobiline
POM	Matière organique particulaire
PSI	Photosystème I
PSII	Photosystème II
PUB	Phycourobiline

ROS	Espèces réactives de l'oxygène
SAG	« Single Amplified Genomes »
SC	Sous-cluster
T_{min} / T_{max} / T_{opt}	Température minimale / maximale / optimale
WGS	« Whole Genome Sequencing »
Zea	Zeaxanthine

Introduction

1. Les picocyanobactéries marines, des organismes modèles pour étudier la réponse aux variations des conditions environnementales

1.1. Le phytoplancton

1.1.1. Généralités

Les océans recouvrent presque 71% de la surface de la Terre et leur profondeur moyenne est d'environ 3,8 km. Ce vaste environnement est habité par une très grande diversité d'organismes, allant des virus aux baleines bleues. Les organismes les plus abondants dans l'environnement marin appartiennent au plancton (du grec : πλαγκτός ou planktos, à la dérive), qui regroupe l'ensemble des organismes dérivant au gré des courants. Le plancton constitue 95% de la biomasse marine et présente une très grande diversité taxonomique, écologique et morphologique, et notamment de taille (6 ordres de grandeurs : du pico au méga-plancton ; Fig. 1). On trouve en effet aussi bien des formes libres que symbiotiques ou parasitiques. Les organismes du plancton présentent également une forte diversité de régimes trophiques, comprenant les phototrophes, les hétérotrophes et les mixotrophes. La fraction végétale du plancton, appelée également phytoplancton, désigne l'ensemble des organismes microscopiques capables de réaliser la photosynthèse oxygénique et vivant dans la zone euphotique, c'est-à-dire la zone éclairée de la colonne d'eau pouvant atteindre jusqu'à 250m de profondeur dans les eaux les plus claires comme les parties centrales de l'Océan Pacifique.

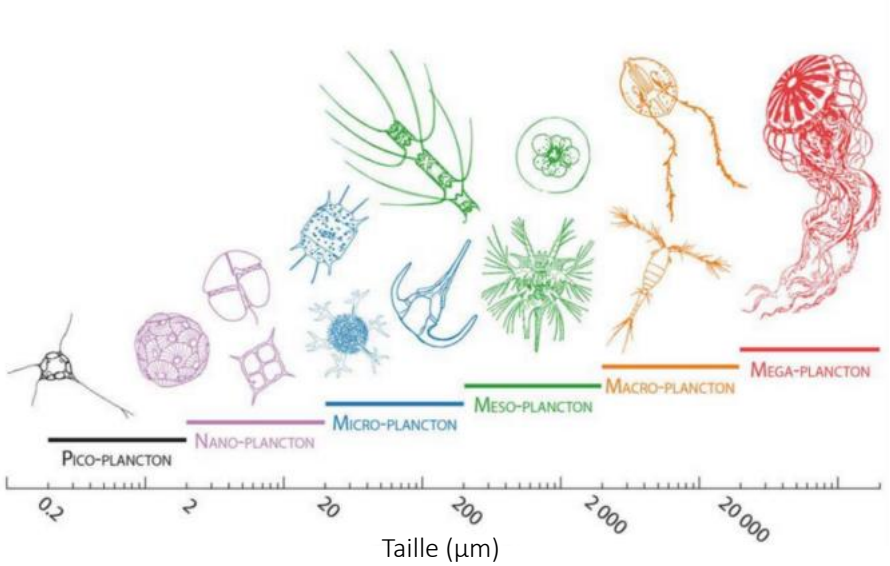

Figure 1 | Classification du plancton en différentes classes de taille. Issue de Biard 2015

1.1.2. Rôle dans la pompe biologique

Même s'il représente seulement 1% de la biomasse des organismes photosynthétiques, le phytoplancton est tout de même responsable de presque 46% de la production primaire nette globale, soit $48{,}5.10^{12}$ kg de CO_2 par an (Field et al., 1998). Il joue un rôle essentiel au sein de l'écosystème marin, notamment dans les grands cycles biogéochimiques tels que le cycle du carbone. De par leur activité photosynthétique, ces organismes fixent le CO_2 atmosphérique, qui est ensuite converti en matière organique. Cette matière organique a différents destins possibles : environ la moitié constitue la base d'un réseau trophique complexe (Field et al., 1998)Fig. 2). En effet, elle est consommée par les niveaux trophiques supérieurs via le broutage par des organismes hétérotrophes ou mixotrophes qui sont à leur tour consommés par les métazoaires. L'autre moitié est quant à elle excrétée sous forme de matière organique dissoute (DOM) ou particulaire (POM) au cours de la croissance et à la mort des organismes phytoplanctoniques. Cette DOM/POM est recyclée en matière inorganique grâce aux bactéries hétérotrophes et mixotrophes, c'est ce que l'on appelle la « boucle microbienne » (Azam et al., 1983 ; Sherr & Sherr, 2002 ; Fig. 2). Une partie des nutriments organiques, tels que les acides aminés, est reminéralisée par les bactéries mais seule une fraction de ces nutriments est à nouveau disponible sous forme inorganique et est utilisée par les organismes phytoplanctoniques. La fraction restante, représentant environ 2% du carbone fixé initialement par le phytoplancton n'étant pas recyclée *via* la boucle microbienne, va être exporté vers les couches profondes et être séquestrée dans les sédiments durant des millénaires. Ce phénomène est appelé : la pompe biologique à carbone (Guidi et al., 2016). Enfin, les virus participent également à la libération de DOM/POM à travers la lyse virale d'organismes phytoplanctoniques et de bactéries *via* le « shunt viral » qui représente environ 25% du carbone fixé grâce à la photosynthèse (Wilhelm & Suttle, 1999 ; Guidi et al., 2016). Ainsi, en plus d'être à la base du réseau trophique marin, le phytoplancton limite la quantité de CO_2 présent dans l'atmosphère et participe à la régulation du climat.

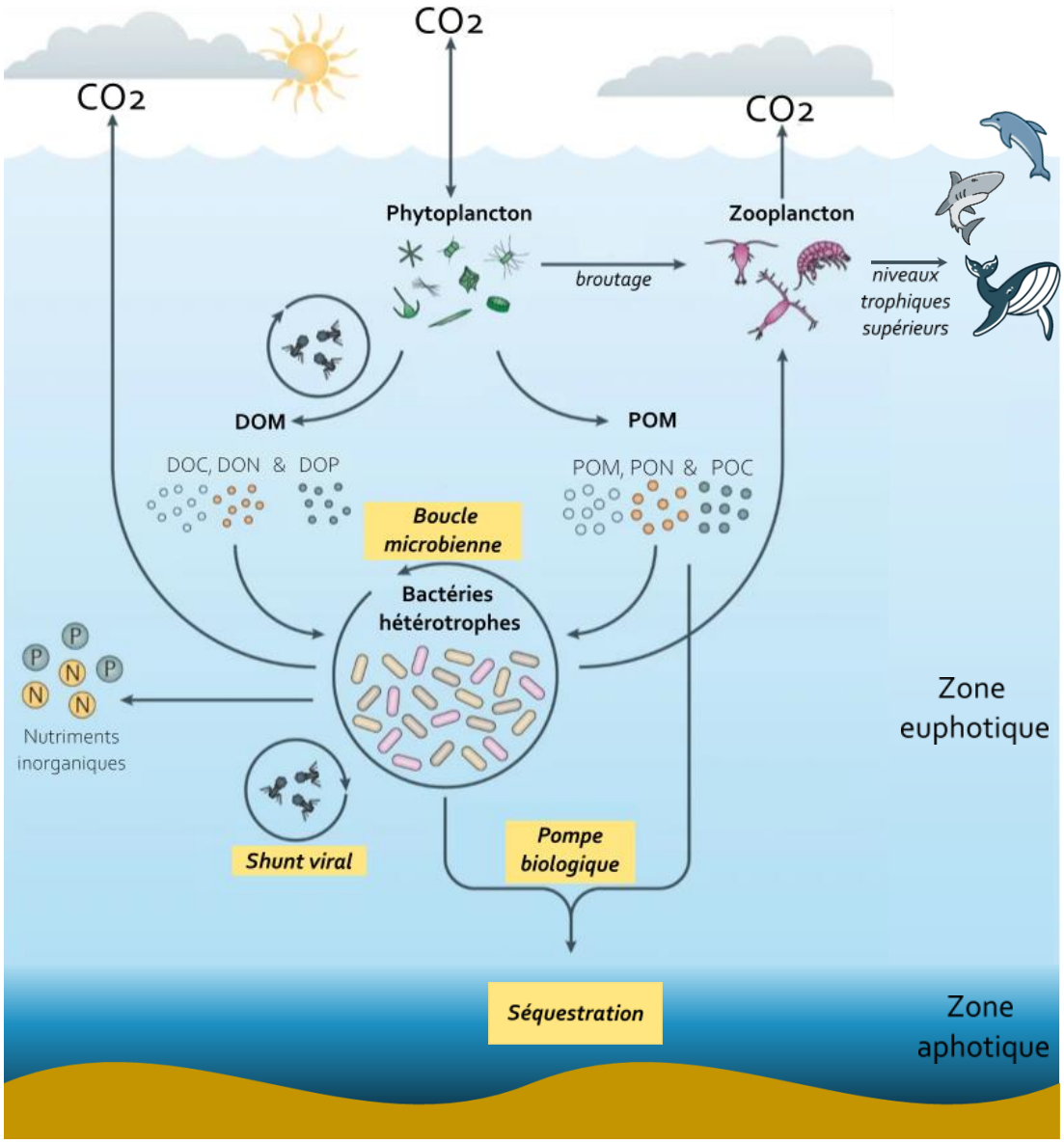

Figure 2 | Cycle du carbon océanique. DOM : matière organique dissoute (incluant DOC, DON et DOP pour carbone, azote et phosphate organiques dissouts, respectivement) et POM : matière organique particulaire (incluant POC, PON et POP, pour carbone, azote et phosphate organiques particulaires, respectivement ; d'après Buchan et al., 2014).

1.2. Découverte et morphologie des picocyanobactéries marines

De par leurs très petites tailles, les organismes du picophytoplancton, c'est-à-dire le phytoplancton de taille comprise entre 0.2 et 2-3 µm (Sieburth et al., 1978 ; Johnson & Sieburth, 1979 ; Vaulot et al., 2008), et notamment la composante procaryotique dominée par les picocyanobactéries, n'ont été découverts que depuis les années 1970, grâce à l'apparition de nouvelles techniques d'échantillonnage et d'analyse, telles que la microscopie à épifluorescence et la cytométrie en flux. En effet c'est en 1979, grâce à la microscopie à épifluorescence, que John Waterbury découvrit des cyanobactéries planctoniques sphériques fluoresçant en orange, une propriété typique de la phycoérythrine (Waterbury et al., 1979). Ces organismes de petite taille (entre 0,8 et 2 µm de diamètre), très ubiquistes et abondants, sont retrouvés jusqu'à 400m de profondeur et à des concentrations pouvant excéder 10^6 cellules/ml (Saito et al., 2005). Waterbury et ses collaborateurs leur assigna le nom de genre *Synechococcus* en se basant sur leur morphologie et leur physiologie (Waterbury et al., 1979 ; Waterbury, 1986). En 1988, c'est grâce à la cytométrie en flux que Sallie Chisholm et ses collaborateurs découvrent un nouveau genre de cyanobactéries de plus petite taille (de 0,5 à 0,8 µm de diamètre) et qui se différencient des *Synechococcus* par l'absence de fluorescence orange, et par la seule présence de fluorescence rouge due à la chlorophylle (Chisholm et al., 1988). La caractérisation physiologique et phylogénétique de cette lignée très proche des *Synechococcus*, a conduit à la baptiser *Prochlorococcus* (Chisholm et al., 1992).

Les cyanobactéries sont des bactéries à Gram-. Elles possèdent en effet deux membranes, externe et plasmique, séparées par une épaisse couche de peptidoglycanes, proche de celle que l'on retrouve chez les bactéries de type Gram+. La surface externe et la structure de la paroi sont variables selon les souches. Les thylakoïdes, lieu où se produisent les réactions de la phase claire de la photosynthèse, forment des réseaux de membranes intracellulaires. En plus de la différence de taille, la disposition des membranes thylakoïdales au sein du cytoplasme représente une des grandes différences entre les deux genres de picocyanobactéries. Chez *Synechococcus*, les membranes sont disposées en cercles concentriques très espacés tandis que chez *Prochlorococcus*, elles sont plus compactes. Cette différence est due à la structure et la composition respective de leurs complexes collecteurs de lumière. En effet, chez *Synechococcus*, on retrouve de gros complexes antennaires, localisés à la surface des membranes thylakoïdales : les

phycobilisomes (PBS ; Sidler, 1994). En revanche chez *Prochlorococcus*, l'énergie lumineuse est capturée grâce des complexes pigments-protéines intramembranaires (appelé Pcb pour Prochlorophyte-chlorophyll binding proteins), et qui nécessitent donc beaucoup moins d'espace intermembranaire (La Roche et al., 1996)

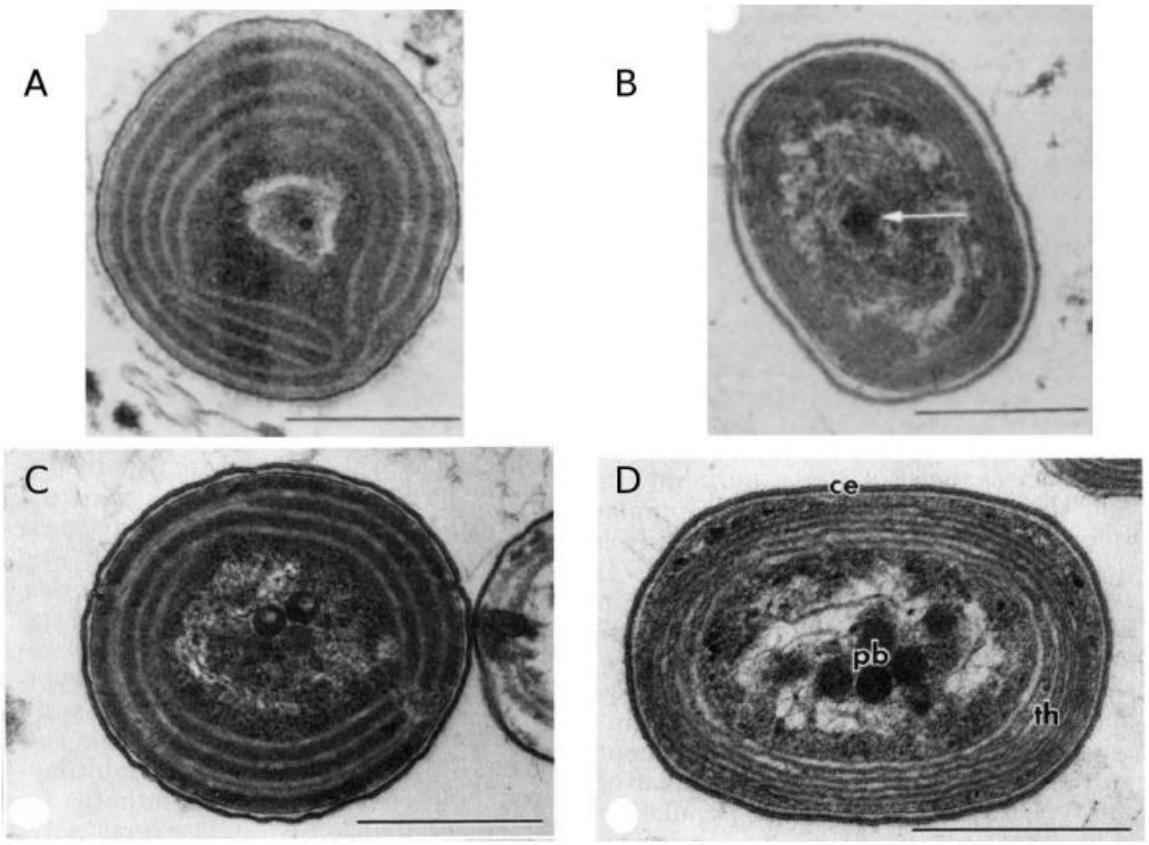

Figure 3 | Photographies en microscopie électronique de cellules de Synechococcus et *Prochlorococcus*. (**A**) *Synechococcus* (Echelle : 0,5µm, source : Chisholm et al., 1988). (**B**) *Prochlorococcus* (Echelle : 0,5µm, source : Chisholm et al., 1988). (**C**) *Synechococcus* (Echelle : 0,5µm, source : Johnson et Sieburth, 1979). (**D**) *Prochlorococcus* (Echelle : 0,2µm, source : Johnson et Sieburth, 1979). Th : thylakoïdes, pb : carboxysomes (polyhedral bodies), ce : enveloppe cellulaire.

1.3. Distribution globale et importance écologique des picocyanobactéries

Les picocyanobactéries marines sont très abondantes dans l'océan global. En effet, ce groupe est ubiquiste et domine numériquement la communauté phytoplanctonique dans les eaux oligotrophes (Partensky et al., 1999; Scanlan et al., 2009), avec une abondance globale estimée de $2{,}9 \times 10^{27}$ et 7×10^{26} cellules pour les deux genres majeurs, *Prochlorococcus* et *Synechococcus* respectivement (Flombaum et al., 2013; Whitman et al., 1998).

Synechococcus présente une aire de répartition très vaste, puisqu'on le retrouve dans la couche éclairée de tous les environnements marins de l'équateur jusqu'aux régions sub-polaires (Paulsen et al., 2016 ; Fig. 4). C'est dans les régions riches en nutriments, comme les upwellings ou les régions côtières, que l'on observe la plus forte abondance de ce genre, avec des concentrations pouvant atteindre $3,7x10^6$ cellules/ml, notamment dans le Dôme du Costa Rica (Saito et al., 2005). Dans les régions plus oligotrophes, *Synechococcus* est également présent mais à des concentrations plus faibles, de l'ordre de 10^3 cellules/ml dans l'Atlantique ou le Pacifique et 10^4 cellules/ml en Méditerranée (Partensky et al., 1999; Scanlan et al., 2009). *Prochlorococcus* présente quant à lui une aire de répartition plus réduite. En effet, il est quasiment absent à hautes latitudes (au-delà de 50°N ou 40°S) et plus généralement dans les eaux froides (< 10°C ; Flombaum et al., 2013; Johnson et al., 2006) Cependant, il domine très largement dans les régions oligotrophes où son abondance dépasse fréquemment 10^5 cellules/ml. Dans les régions où ses deux genres coexistent, *Prochlorococcus* est en général plus abondant que *Synechococcus,* en particulier dans les zones oligotrophes. On observe également des différences de répartition en fonction de la profondeur. *Synechococcus* est plus abondant en surface, et ce jusque 150 m, tandis que *Prochlorococcus* est retrouvé jusqu'à 200-250m de profondeur, c'est-à-dire sur l'ensemble de la zone éclairée (Partensky et al., 1999). Cette abondance et cette ubiquité en font des organismes de choix pour étudier les mécanismes d'adaptation et d'acclimatation aux variations des conditions environnementales.

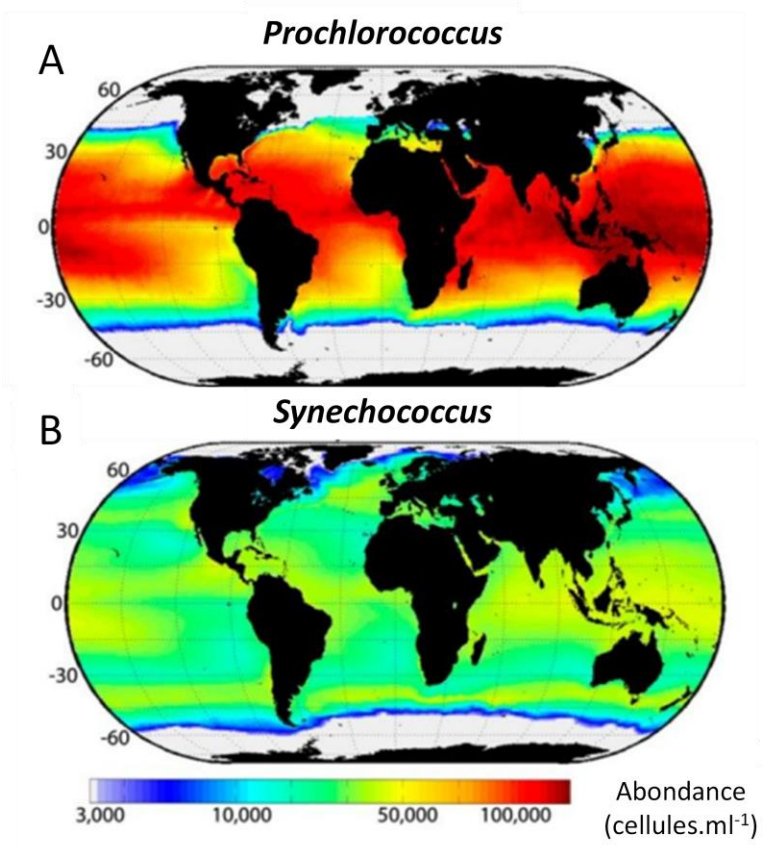

Figure 4 |Distribution latitudinal de (A) *Prochlorococcus* et (B) *Synechococcus*. D'après Flombaum et al., 2013.

1.4. Diversité et évolution des picocyanobactéries marines

Les cyanobactéries planctoniques marines seraient apparues au cours du Néoprotérozoïque (entre 1 milliard et 542 millions d'années) à partir de cyanobactéries ancestrales benthiques côtières ou d'eau douce (Sánchez-Baracaldo et al., 2022). Chez les cyanobactéries marines, le genre *Synechococcus* constitue un groupe polyphylétique au sein duquel on trouve des souches marines, dulcicoles et halotolérantes (Scanlan et al., 2009). Les *Synechococcus* marins sont rassemblés dans une branche phylogénétique profonde bien séparée des autres cyanobactéries, appelée « cluster 5 » (Herdman et al., 2001), lui-même séparé en 3 groupes phylogénétiques tels qu'initialement définis sur la base de l'ARNr 16S (Dufresne et al., 2008). Le sous-cluster (SC) 5.2 rassemble des représentants d'eau douce et halotolérants. Dans le milieu marin, les membres de ce groupe ne se trouvent en abondance significative uniquement dans les eaux côtières influencées par les rivières, telles que la baie de Chesapeake (Cai et al., 2010; F. Chen et al., 2004, 2006), l'estuaire de la Pearl river (Xia et al., 2015; Xia, Partensky, et al., 2017) et

dans les zones à faible salinité telles que la mer Baltique (Haverkamp et al., 2008). Bien que moins bien connu, le SC 5.3 comporte aussi bien des souches marines, qui peuvent représenter une part importante de la communauté de *Synechococcus* dans les zones pauvres en phosphore (Farrant et al., 2016a; Huang, Wilhelm, et al., 2012; Sohm et al., 2015; Zwirglmaier et al., 2008), que lacustres, ces dernières n'ayant été mises en évidence que très récemment (Cabello-Yeves, Picazo, et al., 2018). Enfin, le SC 5.1 rassemble essentiellement des souches marines et constitue le SC le plus abondant et diversifié en milieu océanique, avec 10 à 15 clades définis au sein cette lignée selon le marqueur génétique utilisé. Si le gène de l'ARNr 16S est assez peu résolutif, il est possible de subdiviser le SC 5.1 de manière plus fine en utilisant des marqueurs à haute résolution, tels que *rpoC1* qui code pour la sous-unité β de l'ARN polymérase (Toledo & Palenik, 1997), la région intergénique située entre les ARNr 16S et 23S appelée ITS (pour « internal transcribed spacer » ; Ahlgren & Rocap, 2006; Choi et al., 2013; Rocap et al., 2002), le gène *ntcA* codant pour une protéine nécessaire à l'expression de tous les gènes impliqués dans le métabolisme de l'azote (Penno et al., 2006) ou encore le gène petB codant pour le cytochrome b6. Par exemple, ce dernier marqueur a permis de subdiviser le SC 5.1 en 15 clades phylogénétiques et une trentaine de sous-clades (Mazard et al., 2012).

Au sein de la radiation des *Synechococcus*, les *Prochlorococcus* constitue une lignée monophylétique, elle-même subdivisée en une branche monophylétique correspondant aux phototypes HL (High-Light) et un groupe polyphylétique correspondant aux phototypes LL (Low-Light; Moore et al., 1998; cf. paragraphe suivant).

1.5. Diversité génétique et biogéographie

1.5.1. Prochlorococcus

La lumière joue un rôle prépondérant dans la distribution écologique de *Prochlorococcus.* En effet, on distingue les phototypes HL et LL qui sont retrouvés à des profondeurs différentes du gradient vertical de lumière et présentent des preferenda lumineux de croissance très différents (Moore et al., 1998; Moore & Chisholm, 1999). Chacun des phototypes de *Prochlorococcus* a été subdivisé en différents clades occupant des niches écologiques distinctes. Le clade HLI domine à haute latitude dans les eaux tempérées qui subissent un mélange hivernal, tandis que le clade HLII domine à basses latitudes dans les eaux chaudes et stratifiées (Bouman et al., 2006; Chandler et al., 2016; Z. I. Johnson et al., 2006; Zwirglmaier et al., 2008). Les clades HLIII, HLIV et HLV sont

spécifiquement retrouvés dans des environnements riches en azote et phosphore mais pauvres en fer (Farrant et al., 2016; S. Huang et al., 2012; Rusch et al., 2010; West et al., 2011) appelées zones HNLC (« High-Nutrient, Low Chlorophyll », (Behrenfeld & Kolber, 1999). Les membres des clades HLIII et HLIV se seraient notamment adaptés aux zones pauvres en fer en diminuant leur besoin en fer et en acquérant la possibilité d'utiliser des sidérophores produits par d'autres organismes (Malmstrom et al., 2013; Rusch et al., 2010). Enfin, le clade HLVI est plus rare et beaucoup moins étudié, mais il semble que les membres de ce clade soient adaptés à des lumières plus faibles que les HLI et HLII puisqu'elles se situent plus en profondeur, dans la partie inférieure de la zone euphotique (Huang et al., 2012).

Alors que les principaux facteurs permettant d'expliquer la distribution des *Prochlorococcus* du phototype HL sont donc assez bien identifiés (lumière, température et disponibilité en fer; Biller et al., 2015; Martiny et al., 2015), la distribution géographique et les facteurs environnementaux impliqués sont par contre moins bien connus pour les clades au sein du phototype LL. Dans les environnements stratifiés et tropicaux, le clade LLI est capable de coloniser les eaux de profondeur intermédiaire par rapport aux clades HL et LL stricts, mais on le retrouve jusqu'en surface dans les eaux mélangées à hautes latitudes (Johnson et al., 2006; Malmstrom et al., 2010). A noter que Farrant et collaborateurs (2016) ont mis en évidence une microdiversité au sein du clade LLI, dont un sous-groupe phylogénétique (LLIB) dominerait le clade LLI spécifiquement dans les eaux de surface des zones HNLC de l'Océan Indien et de l'Océan Pacifique. Il semble donc que l'adaptation à la carence en fer ne soit pas restreinte aux seuls clades HLIII et HLIV de *Prochlorococcus*. A l'inverse des LLI, les clades LLII/III et LLIV sont systématiquement localisés à la base de la zone euphotique, là où l'intensité lumineuse est faible (Malmstrom et al., 2010; Zinser et al., 2006). Enfin, les clades LLV et LLVI (aussi appelés AMZ-I et II, respectivement) sont présents dans les zones marines anoxiques (AMZs pour 'anoxic marine zones') en mer d'Arabie et dans la partie Est de l'Océan Pacifique Nord et Sud (Lavin et al., 2010; Ulloa et al., 2021).

1.5.2. Synechococcus

Pour *Synechococcus*, du fait de la forte diversité génétique au sein de ce genre, la biogéographie des différents clades est moins bien connue que pour *Prochlorococcus.* Cependant, différentes études environnementales ont pu mettre en évidence les

principaux facteurs environnementaux influençant la distribution des clades dominant la communauté *in situ* (Farrant et al., 2016; Gutiérrez-Rodríguez et al., 2014; S. Huang et al., 2012; Sohm et al., 2015; Xia et al., 2019; Zwirglmaier et al., 2008). Ainsi, les clades I et IV du SC 5.1 co-existent à hautes latitudes (au-delà de 30°N/S) dans les eaux tempérées ou froides (7 – 18°C), riches en nutriments (Tai & Palenik, 2009; Zwirglmaier et al., 2007, 2008) avec une répartition qui s'étend jusqu'à 82.5 °N (Paulsen et al., 2016) et une augmentation progressive du rapport clade I/IV avec la latitude (Doré et al., 2022). Le clade II domine quant à lui dans les eaux plus chaudes de l'océan ouvert (22 – 28°C) limitées en azote et constitue globalement le clade le plus abondant de *Synechococcus* dans l'océan (Farrant et al., 2016; S. Huang et al., 2012; Sohm et al., 2015). Le clade III, qui co-existe avec le clade WPC1 et le SC 5.3 (précédemment appelé clade X), est abondant dans les régions oligotrophes carencées en phosphate, telles que la Méditerranée ou le Golfe du Mexique (Farrant et al., 2016; Mella-Flores et al., 2011). Enfin, les membres du clade CRD1 dominent la population de *Synechococcus* dans les zones pauvres en fer, et notamment dans le Pacifique (35°N à 33°S) ainsi que dans plusieurs zones de l'Atlantique et de l'Océan Indien (Ahlgren et al., 2020; Farrant et al., 2016; Sohm et al., 2015). Mis à part ces lignées dominantes dans les zones océaniques, peu de choses sont connues quant à la distribution des autres clades de *Synechococcus*, à l'exception du clade VIII que l'on retrouve essentiellement dans les estuaires et les eaux euryhalines (Hunter-Cevera et al., 2016; Xia, Guo, et al., 2017). De même, une étude récente a montré que les clades V et VI semblent limités aux régions côtières de salinité intermédiaire (Doré et al., 2022). Dans l'ensemble, il semble donc que les niches environnementales occupées par les *Synechococcus* soient principalement définies par quatre facteurs environnementaux : la température, la disponibilité en fer et en phosphate et la salinité (Ahlgren & Rocap, 2012; Doré et al., 2022; Farrant et al., 2016; Hunter-Cevera et al., 2016; Sohm et al., 2015; Xia, Guo, et al., 2017; Zwirglmaier et al., 2008).

La plupart de ces études de diversité ont considéré les membres du même clade, comme appartenant à un même écotype, c'est-à-dire un groupe d'organismes apparentés partageant la même niche écologique (Coleman & Chisholm, 2007; Koeppel et al., 2013). Cependant, l'utilisation de marqueurs à haute résolution taxonomique (*petB, rpoC1,* ITS) a révélé la présence au sein des clades majeurs de *Synechococcus* de plusieurs populations génétiquement homogènes occupant des niches distinctes, suggérant que le niveau du

clade ne serait peut-être pas le niveau taxonomique le plus pertinent sur le plan écologique (Farrant et al., 2016; Mazard et al., 2012; Xia et al., 2019; Xia, Partensky, et al., 2017), comme c'est également le cas pour *Prochlorococcus* (Larkin et al., 2016; Martiny et al., 2009a). Dans ce contexte, la délimitation d'ESTUs (pour 'Ecologically Significant Taxonomic Units'), c'est-à-dire d'ensembles d'unités taxonomiques opérationnelles (OTUs *petB* à 94% d'identité nucléotidique) appartenant au même clade et dont les aires de distributions sont similaires *in situ,* a permis de définir des écotypes plus robustes au sein de chaque clade et de préciser leur distribution *in situ* (Farrant et al., 2016); Fig. 5). Par exemple, deux ESTUs ont été définis au sein du clade II de *Synechococcus*, l'ESTU dominant (IIA) étant retrouvé comme celui-ci dans les eaux chaudes limitées en azote, alors que l'ESTU IIB colonise spécifiquement les eaux froides et mélangées, une niche qu'il partage avec les ESTUs dominant des clades I et IV (IA et IVA). Dans le cas du clade CRD1, trois ESTUs (CRD1 A – C) ont été définis, tous présents dans les zones carencées en fer mais colonisant des niches thermiques distinctes. En effet, l'ESTU CRD1B colonise les eaux froides en co-occurrence avec les ESTUs IA et IVA (Atlantique Nord et Sud à moyennes latitudes, upwelling du Chili), l'ESTU CRD1C domine dans les zones tempérées chaudes

(régions HNLC du Pacifique et de l'Océan Indien), tandis que l'ESTU CRD1A a une aire de répartition qui englobe celles des deux autres (Farrant et al., 2016).

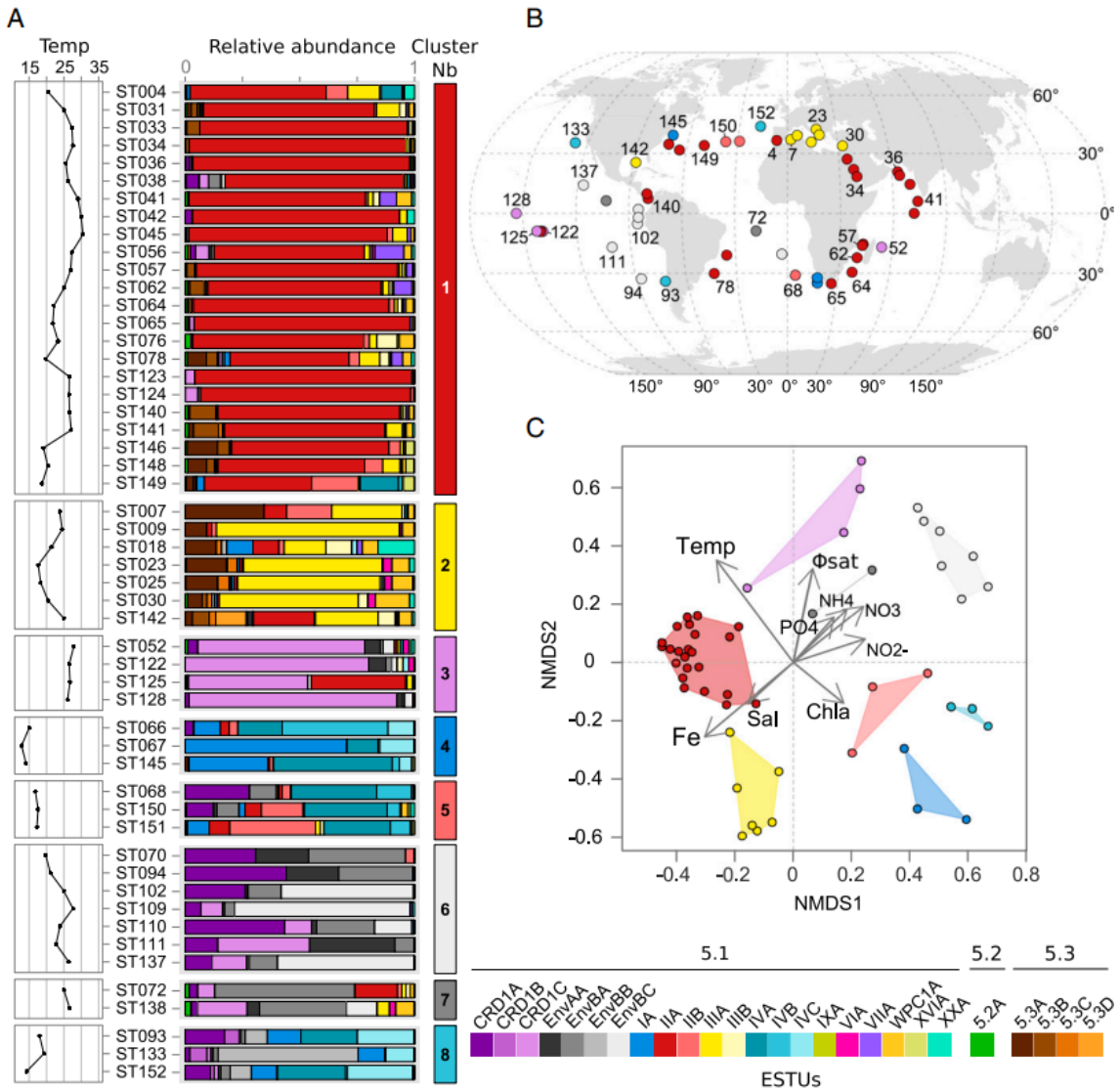

Figure 5 | Biogéographie des ESTUs de *Synechococcus* à partir des métagénomes de Tara Oceans en fonction des paramètres physico-chimiques. (**A**) Abondances relatives des ESTUs de Synechococcus à chaque station, regroupées par assemblages (clusters), comme déterminées grâce à l'indice de dissimilarité de Bray-Curtis. Les encarts de gauche représentent la température de l'eau à chaque station (T°C). (**B**) Distribution des assemblages d'ESTUs le long du transect de Tara Oceans. (**C**) Analyse NMDS des paramètres physico-chimiques et des assemblages. Issu de Farrant et al., 2016.

1.6. Diversité génomique et adaptation

1.6.1. Les apports de la génomique comparative

Dans le contexte d'un changement climatique rapide, les picocyanobactéries marines présentent un intérêt majeur dans l'étude des processus d'adaptation aux variations des conditions environnementales, de par leur temps de génération rapide et

leur abondance dans le milieu naturel. Les premières analyses de génomique comparative, ont notamment permis de mettre en évidence que les génomes de picocyanobactéries marines étaient plus petits que ceux des cyanobactéries d'eau douce (Larsson et al., 2011; Shih et al., 2013). Cette diminution de taille est maximale chez *Prochlorococcus* à l'exception des clades à la base de la radiation (LLIV et sans doute LLV et VI) et s'accompagne d'une forte diminution du contenu en GC% (Dufresne et al., 2005, 2008; Kettler et al., 2007; Partensky & Garczarek, 2011; Scanlan et al., 2009). La multiplication de génomes séquencés soit à partir de souches (WGS pour 'Whole Genome Sequencing' ; Cabello-Yeves et al., 2018; Doré et al., 2020; Lee et al., 2019; Yan et al., 2021), soit de cellules uniques (SAGs pour 'Single Amplified Genomes' ; Berube et al., 2019; Kashtan et al., 2014; Malmstrom et al., 2013; Pachiadaki et al., 2019; Ulloa et al., 2021), soit de metagenomes (MAGs 'Metagenomes Assembled Genomes' ; (Cabello-Yeves et al., 2018b; Haro-Moreno et al., 2018; Kashtan et al., 2014) a permis de mieux comprendre l'histoire évolutive qui a conduit à la diversification génomique au sein de cette radiation et à l'adaptation des différentes lignées à diverses niches environnementales. La comparaison des génomes le plus complets a notamment permis d'identifier les gènes communs, accessoires et uniques (Doré et al., 2020; Dufresne et al., 2008; Kettler et al., 2007; Scanlan et al., 2009; Fig. 6). Les gènes communs, c'est-à-dire partagés par tous les membres d'un taxon, représentent entre 39 à 69% du génome total et permettent d'assurer les fonctions indispensables au métabolisme général des cellules et notamment à leur mode de vie autotrophe (Doré et al., 2020). A l'inverse, les gènes uniques sont spécifiques d'un génome et beaucoup d'entre eux sont de petite taille et de fonction inconnue. Enfin, les gènes accessoires sont retrouvés dans un sous-set de génomes (2 à n-1) et sont parfois spécifiques d'un taxon donné (SC, clade ou sous-clade), ce qui suggère qu'ils pourraient jouer un rôle dans l'adaptation de ces organismes à une niche écologique particulière. Dans ce contexte, la comparaison de 81 génomes non redondants de picocyanobactéries, incluant 28 génomes de *Prochlorococcus* et 53 *Synechococcus* ou *Cyanobium* a par exemple permis de montrer que bien qu'ils soient très éloignés d'un point de vue phylogénétique, les membres du clade VIII et du SC 5.2, qui colonisent tous deux les eaux saumâtres, se retrouvent côte à côte dans un arbre basé sur le contenu en gènes, du fait qu'ils ont en commun un certain nombre de gènes potentiellement impliqués dans l'adaptation aux variations de salinité (Doré et al., 2020).

De même, cette étude a confirmé et complété des études précédentes (par exemple : (Berube et al., 2015, 2019; Martiny et al., 2006, 2009; Scanlan et al., 2009) montrant qu'un certain nombre de gènes accessoires seraient potentiellement lié à l'adaptation à la limitation en nutriments (azote, phosphate, fer), tandis qu'assez peu de gènes se sont avérés spécifiques des thermotypes froids de *Synechococcus* (clades I et IV). En revanche, bien qu'éloignés d'un point de vue phylogénétique, ces deux thermotypes froids présentent de nombreuses substitutions spécifiques, notamment dans des gènes potentiellement impliqués dans la réponse au stress lumineux et oxydatif, dans la voie de synthèse du β-carotène, un caroténoïde potentiellement impliqué dans la réduction du stress oxydatif induit par le froid (Pittera et al., 2014) ou encore des sous-unités α et β de la phycocyanine, potentiellement impliqués dans la thermostabilité des PBS (Pittera et al., 2017). Globalement, ces résultats tendent à soutenir le modèle d'évolution du génome bactérien "Maestro Microbe" (Larkin & Martiny, 2017) qui postule que certains traits phénotypiques, tels que les preferenda thermiques, auraient évolué par l'optimisation progressive des séquences protéiques plutôt que par le gain et la perte de gènes (Doré et al., 2020). Il est également important de noter que les gènes accessoires et uniques sont le plus souvent situés dans des îlots génomiques, qui correspondent à des régions hypervariables du génome (Coleman et al., 2006; Dufresne et al., 2008; Martiny et al., 2006, 2009; Scanlan et al., 2009). Ces îlots génomiques sont notamment enrichis en gènes issus de transferts horizontaux, via des phages (Dufresne et al., 2008; Lindell et al., 2004) ou encore des vésicules extracellulaires (Biller et al., 2014, 2022). Plus récemment, il a été mis en évidence chez *Prochlorococcus* (Hackl et al., 2020) et *Synechococcus* (Grébert et al., 2022) qu'un certain nombre d'ilots génomiques comprennent de nouveaux éléments génétiques mobiles, appelés 'tycheposons'. Ces éléments seraient impliqués dans l'intégration et la transposition de gènes et notamment de gènes importants pour l'adaptation à la niche tels que des gènes de transport et/ou d'assimilation de macro- et micro-nutriments (azote et phosphore, fer, zinc, cuivre), de réponse à différents stress (thermique et oxydatif) ou encore impliqués dans l'adaptation à la qualité de la lumière ambiante.

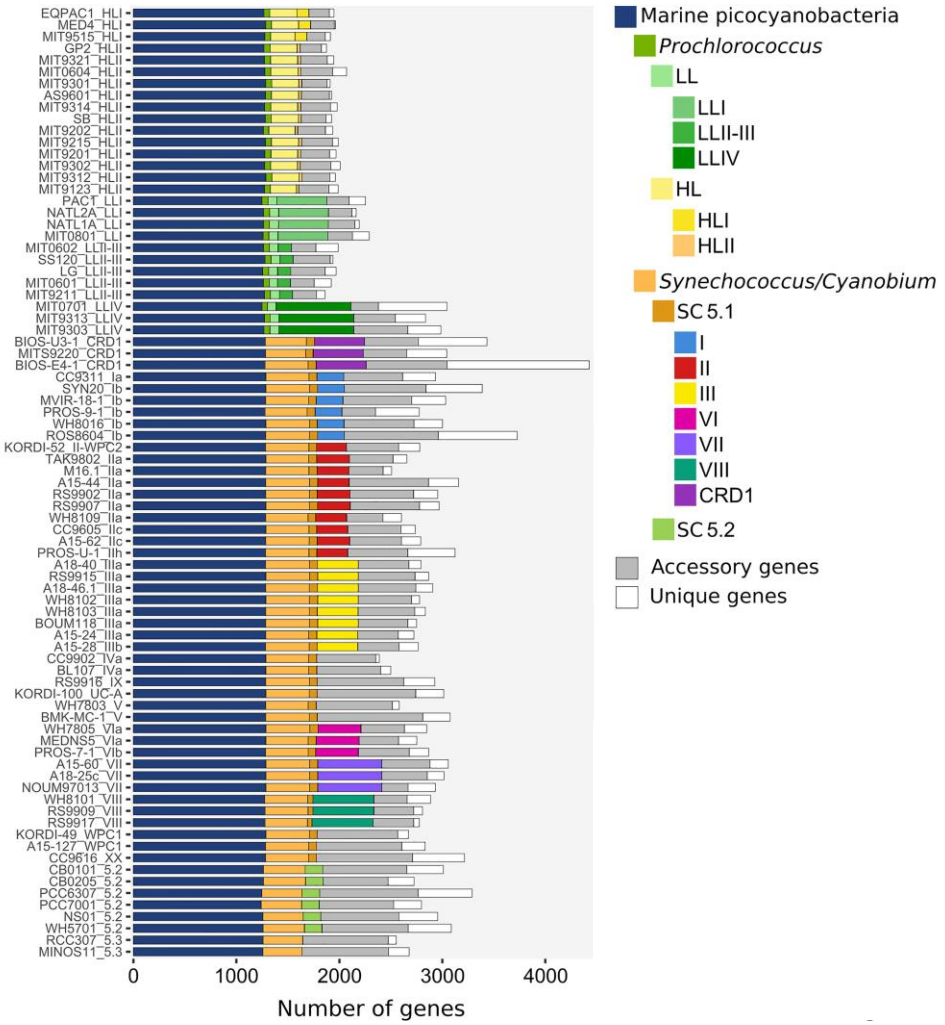

Figure 6 | Gènes core, accessoires et uniques de picocyanobactéries marines. Distribution des clusters de gènes orthologues (CLOGs) dans les génomes picocyanobactérien. D'après Doré et al., 2020.

1.6.2. Identification de gènes de niches à partir de données environnementales

Afin de mieux comprendre le lien entre l'évolution des génomes et l'adaptation aux différentes niches environnementales, quelques études ont utilisé une approche complémentaire à la génomique comparative consistant à utiliser des génomes de référence pour recruter des lectures issues de métagénomes marins, dont le nombre a considérablement augmenté ces dernières années avec la popularisation des techniques de NGS (Ahlgren et al., 2020; Delmont & Eren, 2018; Garcia et al., 2020; Kent et al., 2016; Ustick et al., 2021). En effet, la très grande diversité génomique des *Prochlorococcus* et *Synechococcus* marins n'est pas distribuée au hasard dans l'océan puisque les communautés colonisant des niches particulières ne sont pas seulement distinctes d'un

point de vue génétique mais se caractérisent également par un contenu spécifique en gènes accessoires (Garcia et al., 2020; Kent et al., 2016). Ainsi, l'identification de gènes spécifiquement présents ou absents dans les différentes niches écologiques a permis de préciser les mécanismes potentiellement impliqués dans l'adaptation aux différents facteurs environnementaux. Les premières études à ce niveau ont concerné *Prochlorococcus* avec la mise en évidence, à partir des données de l'expédition Global Ocean Survey (GOS), de la présence d'ilots génomiques impliqués dans le transport et l'assimilation du phosphore (Martinez et al., 2010; A. C. Martiny et al., 2006) ou des nitrites/nitrates (Martiny et al., 2009) dans les zones limitées en ces nutriments. Plus récemment, plusieurs études ont étendu cette approche à la recherche plus systématique de gènes spécifiques de niches écologiques particulières (Kent et al., 2016) et plus spécifiquement des zones carencées en fer aussi bien pour *Prochlorococcus* que pour *Synechococcus* (Ahlgren et al., 2020; Hogle et al., 2022). Ces études ont notamment permis de mettre en évidence différentes stratégies d'adaptation à cette limitation, incluant l'élimination de gènes codant pour des protéines utilisant le fer comme cofacteur, le remplacement du fer par d'autres cofacteurs métalliques ou encore l'acquisition de gènes impliqués dans le stockage de fer et dans le transport et l'assimilation de sidérophores (Ahlgren et al., 2020; Hogle et al., 2022; Rusch et al., 2010).

Réciproquement, les variations spatiales dans les populations naturelles de *Prochlorococcus* de l'abondance relative de ces différents gènes constituant des biomarqueurs de la limitation en nutriments, ont également été utilisées pour réaliser une carte globale des zones limitées en azote, phosphore et fer (Hogle et al., 2022; Ustick et al., 2021) ; Fig. 7), qui confirme et précise celles réalisées sur la base des mesures chimiques de ces éléments (Moore et al., 2013). Ces études ont notamment permis de mettre en évidence l'importance des zones co-limitées en azote/phosphore, azote/fer ou encore phosphore/fer (Ustick et al., 2021) et également de révéler de nouvelles zones géographiques potentiellement limitées en fer telles que le gyre de l'Atlantique sud en surface et le maximum profond de chlorophylle des zones oligotrophes des océans Pacifique et Atlantique Sud (Hogle et al., 2022).

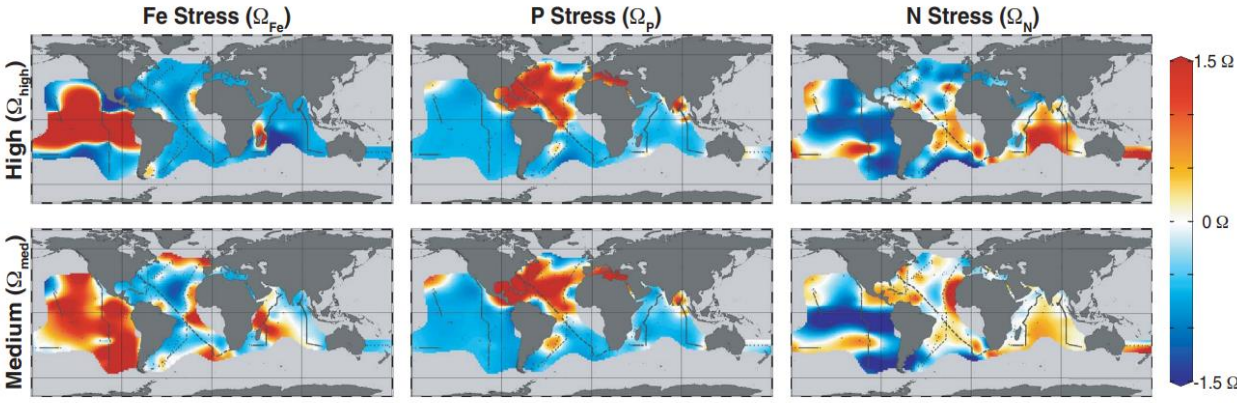

Figure 7 | Distribution globale de *Prochlorococcus* en fonction du stress en nutriments et de sa sévérité. Sur la base de leur rôle biochimique, les gènes ont été regroupés par type de stress (Fe, P et N) et leur sévérité (high ou medium). D'après Ustick et al., 2021.

1.7. Appareil photosynthétique et diversité pigmentaire

1.7.1. Photosynthèse oxygénique

La photosynthèse consiste en la fixation de gaz carbonique par les organismes photoautotrophes en utilisant l'énergie lumineuse afin de synthétiser la matière organique, une réaction qui libère de l'oxygène comme produit de dégradation de l'eau via une série de réactions dont l'équation globale peut s'écrire de la façon suivante :

$$6\ CO_2 + 6\ H_2O + photons \rightarrow C_6H_{12}O_6 + 6\ O_2$$

De ce fait, l'apparition des cyanobactéries, les premiers microorganismes oxyphototrophes, serait responsable de l'oxygénation de l'atmosphère primitive de la Terre (Soo et al., 2017).

Les premières étapes de la photosynthèse dite « phase claire » sont réalisée au sein des membranes thylakoïdales par quatre complexes multiprotéiques : le photosystème I (PSI), le photosystème II (PSII), le cytochrome b_6f et l'ATP synthase (Fig. 8). Cette phase consiste en l'absorption de l'énergie lumineuse via une antenne photo-collectrice. Cette énergie est ensuite transférée à une paire spéciale de molécules de chlorophylle *a* (Chl *a* ; P680) située au niveau du centre réactionnel du PSII, qui est composé d'un dimère de protéines (D1 et D2). Les molécules de Chl *a* sous leurs formes excitées (P680*) dissipent l'énergie d'excitation en émettant un électron à une molécule de phéophytine ($Pheo_{D1}$). Les électrons sont ensuite transférés aux deux plastoquinones (Q_A et Q_B), les molécules de Chl *a* excitées (P680*) passant ainsi sous forme oxydée ($P680^+$). Ces molécules via la dissociation de l'eau vont capturer un électron du complexe

d'évolution de l'oxygène (Oxygen Evolving Complex - OEC). Deux molécules d'eau sont alors oxydées tandis qu'une molécule de dioxygène est formée et quatre protons sont libérés dans le lumen du thylakoïde. Via plusieurs réactions redox, les électrons sont ensuite transférés vers le cytochrome b_6f puis le PSI. Le cytochrome b_6f joue un rôle majeur dans la chaîne de transfert d'électron entre le PSII et le PSI, en allouant une partie de l'énergie produite pour faire traverser les protons à travers la membrane thylakoïdale, permettant ainsi la formation d'un gradient électrochimique. La mise en place de ce gradient permettra ensuite de fournir l'énergie nécessaire à l'ATP synthase pour phosphoryler l'ADP en ATP. La fonction du PSI est de catalyser le transfert d'un électron induit par la lumière entre le cytochrome c_6 (donneur d'électrons), se trouvant dans le lumen des thylakoïdes, et la ferrédoxine (molécule acceptrice) située dans le cytoplasme. Comme pour le PSII, l'énergie lumineuse est collectée au sein du PSI grâce à des pigments photosynthétiques (Chl *a* et β-carotène). L'énergie produite est ensuite transférée vers une paire de molécules de Chl *a* (P700), qui sous leurs formes excitées (P700*) émettent des électrons qui sont transférés jusqu'à un accepteur terminal, $NADP^+$, via une chaîne de transport d'éléctrons constituée notamment de la ferrédoxine-$NADP^+$ réductase (FNR), une flavoprotéine permettant la formation de NADPH.

Les dernières étapes de la photosynthèse sont regroupées sous le terme de « phase sombre », qui correspondent au cycle de Calvin-Benson (Fig. 8) et sont

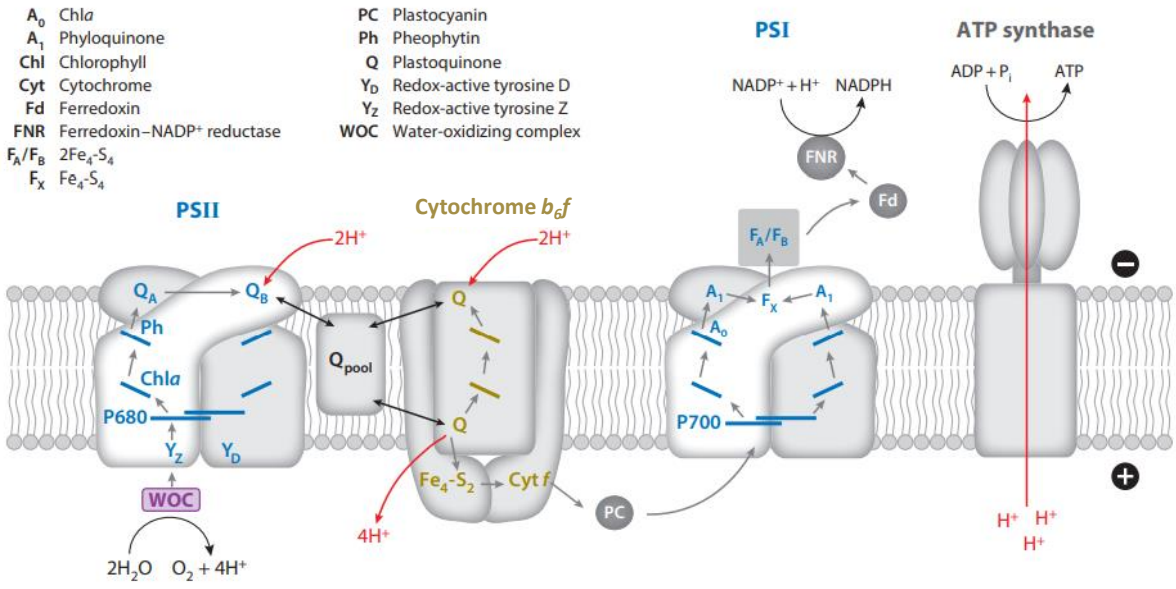

Figure 8 | Complexes impliqués dans la phase claire de la photosynthèse. Fischer et al., 2016.

complètement indépendantes de la lumière. L'ATP et le NADPH nouvellement produits sont utilisés pour fixer le CO_2 grâce à la RuBisCO (Ribulose-1,5-), bisphophate carboxylase/oxygenase la protéine la plus abondante sur Terre (Ellis, 1979). Les molécules à trois carbones issues du cycle de Calvin-Benson entrent dans la composition de toutes les biomolécules (ADN, ARN, protéines, lipides, etc.).

1.7.2. Les antennes photocollectrices

Chez les *Synechococcus* marins, comme chez la majorité des cyanobactéries à l'exception de certains *Prochlorococcus* (Ulloa et al., 2021) et quelques autres genres de cyanobactéries (*Prochloron*, *Prochlorothrix* et *Acaryochloris*) regroupés sous le terme 'oxyphotobactéries vertes' (Partensky & Garczarek, 2010), la capture de la lumière est réalisée par une antenne couplée aux photosystèmes et constituée d'un macrocomplexe extra-membranaire nommé phycobilisome (PBS). Les PBS des *Synechococcus* marins sont composés d'un cœur de 2 à 5 cylindres protéiques ainsi que de 6 à 8 bras périphériques (Adir, 2005). Ils sont formés de diverses protéines pigmentées, les phycobiliprotéines (PBPs ; Glazer, 1985), l'ensemble étant maintenu par des protéines de liaison (Fig. 9). Les PBPs se répartissent en trois classes : l'allophycocyanine (APC) qui compose le cœur, la phycocyanine (PC) pour la partie proximale des bras, et la phycoérythrine (PE) pour la partie distale. Elles ont des couleurs variées, attribuables aux chromophores (ou phycobilines) qui leur sont liés de façon covalente. Les trois chromophores présents chez les *Synechococcus* marins sont la phycocyanobiline (PCB, A_{max} = 620 nm, pigment bleu), la phycoérythrobiline (PEB, A_{max} = 550 nm, rose) et la phycourobiline (PUB, A_{max} = 495 nm, orange). Bien que proches structurellement puisqu'il s'agit d'isomères, ces phycobilines ont des propriétés spectroscopiques très différentes (Glazer, 1985). Trois types pigmentaires peuvent être définis en se basant sur la composition en PBPs des bras des PBS (Six et al., 2007c) : i) le type 1, exclusivement constitué de PC qui lie de la PCB ; ii) le type 2 composé de PC et de PEI qui lient PCB et PEB ; iii) le type 3 composé de PC, PEI et PEII qui lient PCB, PEB et PUB. Ce dernier type pigmentaire peut être subdivisé en trois sous-types différenciables par leur contenu relatif en PUB et PEB (Humily et al., 2013; Six et al., 2007). En effet, leur rapport PUB:PEB peut être faible (sous-type 3a), intermédiaire (sous-type 3b), élevé (sous-type 3c) ou variable (sous-type 3d). Les organismes du sous-type 3d sont nommés 'acclimateurs chromatiques' de type 4 (CA4) puisqu'ils sont capables de faire varier leurs contenus en PUB et PEB en fonction de la qualité spectrale

de la lumière (Everroad et al., 2006; Humily et al., 2013; Palenik, 2001). L'analyse de la distribution des différents types pigmentaires à l'échelle globale a permis de montrer que cette diversité pigmentaire, qui ne semble pas être corrélée à la phylogénie des souches (Six et al., 2007c), pourrait permettre aux cellules de s'adapter à différentes conditions lumineuses en collectant les longueurs d'onde les plus abondantes dans une niche lumineuse donnée (Grébert et al., 2018). La plupart des gènes codant pour les bras des PBS sont regroupés dans une région génomique spécialisée, appelée région PBS, dont la composition varie selon le type pigmentaire et dont la complexification progressive au cours de l'évolution a récemment été étudiée par génomique comparative (Grébert et al., 2022). Par ailleurs, la capacité d'acclimatation chromatique serait conférée par la présence d'un ilot génomique supplémentaire, qui existe sous deux configurations en termes de contenu en gène et localisation dans le génome : CA4-A et CA4-B (Grébert et al., 2021; Humily et al., 2013; Sanfilippo et al., 2019).

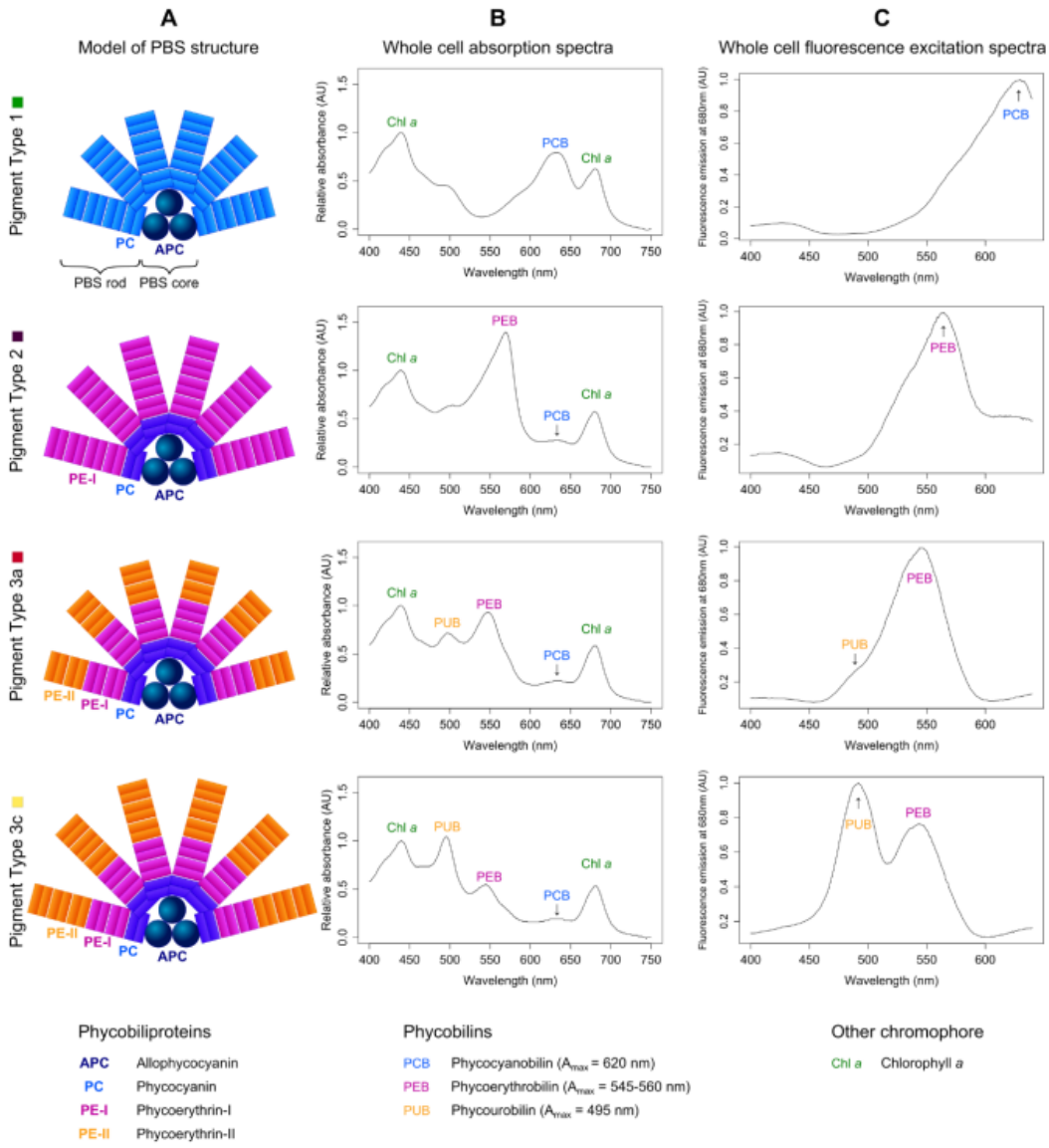

Figure 9 | Composition du phycobilisome et propriétés d'aborption des différents types pigmentaires. A. Structure des phycobilisomes. B. Spectres d'absorption. C. Spectres d'excitation. Grébert et al., 2018.

2. Influence de la température et du fer sur les picocyanobactéries marines

2.1. La variabilité des paramètres environnementaux dans l'océan

L'environnement marin étant un milieu très dynamique, les paramètres physico-chimiques, et notamment la température, la concentration en nutriments ou encore la quantité et qualité de la lumière, sont sujets à d'importantes fluctuations aussi bien spatiales que temporelles (journalière, saisonnières, multi-annuelles). La variabilité de ces paramètres influence fortement la diversité génétique des organismes qui y vivent mais également leur aire de répartition. C'est la zone euphotique, caractérisée par des gradients inverses en température, lumière et nutriments, qui présente la plus forte variabilité (Fig. 10). En effet, la quantité de lumière décroît de manière exponentielle en

fonction de la profondeur et les différentes longueurs d'ondes de la lumière blanche sont progressivement filtrées, induisant une modification de la qualité spectrale de la lumière (Partensky & Garczarek, 2017). Le rouge est filtré dès les premiers mètres de la colonne d'eau, le bleu étant capable de pénétrer le plus profondément. A noter que la composition de l'eau de mer en particules organiques et minérales, absorbant essentiellement dans le bleu, et la composition en phytoplancton, qui absorbe principalement dans le bleu et le rouge de par leur contenu en chlorophylle, impactent également la pénétration de la lumière dans la colonne d'eau (Holtrop et al., 2021).

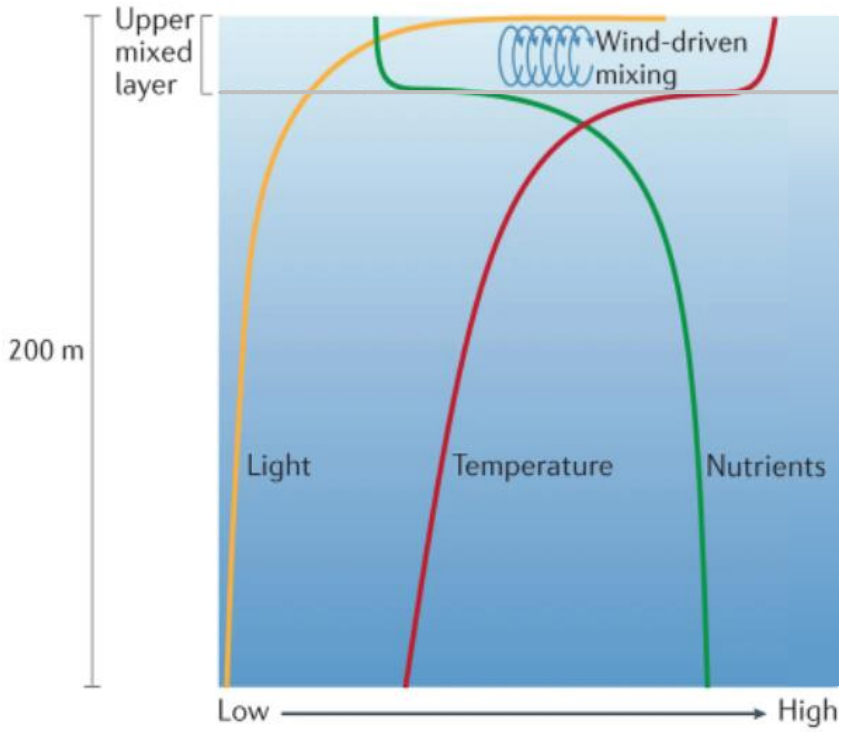

Figure 10 | Variabilité des paramètres abiotiques (lumière, température et concentration en nutriments) en fonction de la profondeur. D'après Biller et al., 2015.

La combinaison des paramètres environnementaux ayant un impact sur la croissance des microorganismes délimite dans le milieu marin un certain nombre de niches écologiques, définies par Hutchinson, (1957) comme une combinaison de caractéristiques environnementales (ou hypervolume) où chaque dimension de l'espace représente une ressource (azote, phosphore, fer, etc.) ou une condition (température, irradiance, pH, etc.) de l'environnement dans laquelle les populations sont capables de maintenir une croissance nette positive. Hutchinson distingue ainsi deux types de niches :

- La niche fondamentale qui réunit toutes les ressources et conditions environnementales nécessaires à l'existence d'un organisme et qui est physiologiquement et génétiquement déterminée.
- La niche environnementale réalisée, qui est le plus souvent comprise dans la niche fondamentale, mais est réduite notamment du fait des interactions biotiques (compétition, prédation, allélopathie, etc.).

Afin de s'adapter à ces différentes niches écologiques et répondre aux variations des conditions environnementales dans l'océan global, les picocyanobactéries marines ont mis au point des stratégies sophistiquées, comme le suggère leur distribution très ubiquiste (Scanlan, 2012).

2.2. Effets de la température

2.2.1. Les gradients de température sur le globe

De par sa forme et sa position vis-à-vis du soleil, l'ensoleillement et la température de la Terre ne sont pas homogènes. 25% du rayonnement incident du soleil est directement réfléchis vers l'espace grâce aux aérosols et aux nuages tandis que 6% sont réfléchis par la surface de la terre et des océans. Ainsi, 69% de l'énergie solaire réussit à traverser l'atmosphère et être absorbée par les continents et les océans. Aux basses latitudes, les rayons atteignant la surface de la Terre traversent une couche atmosphérique fine. A l'inverse à hautes latitudes l'angle d'incidence étant plus faible, la couche atmosphérique traversée est alors plus épaisse (Fig. 11). Ainsi, l'énergie incidente diminue de l'équateur jusqu'aux pôles, entraînant un gradient latitudinal de température. D'après Greenwood & Wing, 1995, en partant de l'équateur, la température moyenne des océans varierait d'environ 0,4°C par degré de latitude. A l'équateur on trouve généralement des eaux dont la température est supérieure à 30°C et pouvant même atteindre jusque 36°C comme dans le Golfe Persique. Tandis qu'aux pôles, on enregistre des températures comprises entre 2°C et -1,8°C.

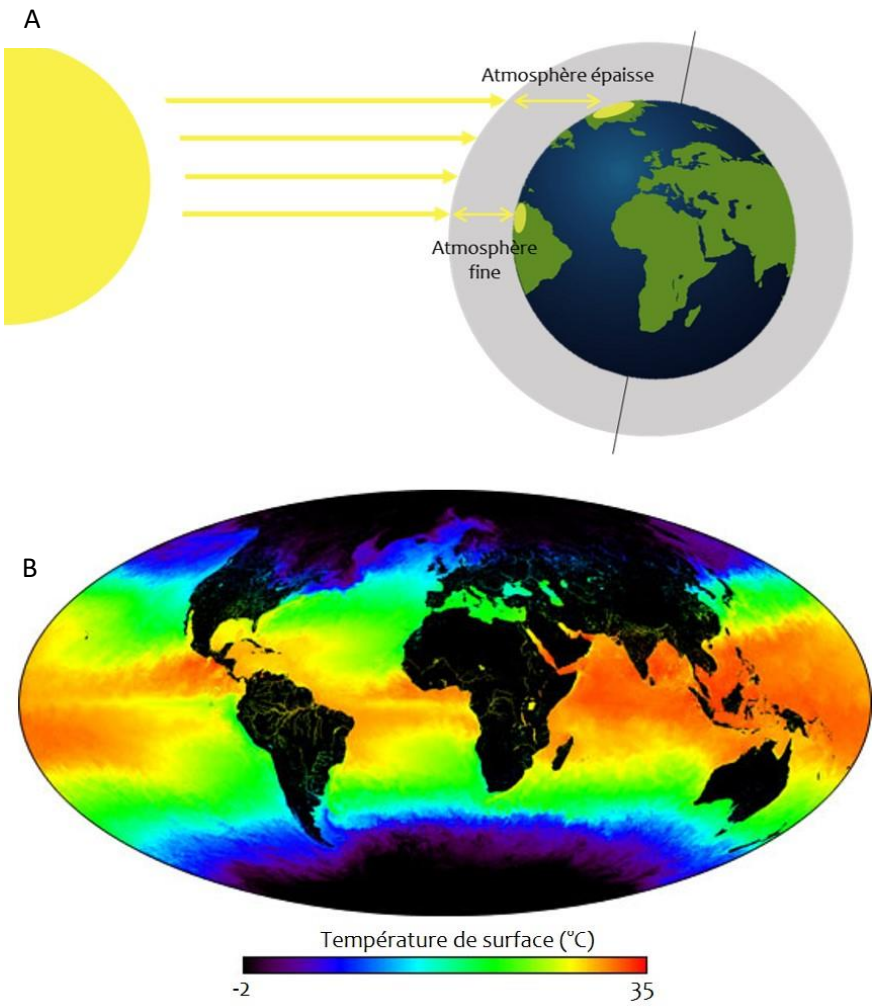

Figure 11 | Variations de la quantité d'énergie solaire atteignant la surface de la Terre en fonction de la latitude et gradient de température. (**A**) Schéma expliquant l'influence de l'angle d'incidence de l'énergie solaire et de l'épaisseur de l'atmosphère sur la quantité de lumière arrivant à la surface de la Terre en fonction de la latitude, entraînant un gradient de température des eaux de surface (**B** ; source : NASA).

Ce gradient présente certaines anomalies, telles qu'au niveau des 'upwellings' qui provoquent de brusques changements de température très localisés, comme par exemple au large des côtes du Pérou/Chili, de la Californie, de la Mauritanie et de la Namibie. Ces phénomènes consistent en une remontée d'eau froide profonde due à l'action du vent qui, en déplaçant les masses d'eau chaude superficielles, vont permettre la remontée d'eau froide profonde. En plus d'entraîner une modification de la température de l'eau de surface, les upwellings provoquent également une remontée de nutriments (Kämpf & Chapman, 2016). C'est pourquoi on observe très souvent des maximums de chlorophylle *a* dans les zones d'upwelling.

Les gyres constituent également un type d'anomalie au gradient latitudinal de températures. Ce type de formation est issu du frottement entre différentes masses d'eau. Une partie d'une masse d'eau A va se dissocier au contact d'une masse d'eau B en formant une sorte de méandre puis une boucle indépendante à la masse d'eau A. Suivant le type de courant dont le gyre est issu, il peut être plutôt chaud (par exemple : courant du Gulf Stream ou du Kurashio) ou froid (p.ex. courant du Benguela ou de Californie ou encore anneaux d'Agulhas, Villar et al., 2015). Ce gyre nouvellement formé peut mesurer jusqu'à 500 km de diamètre et perdurer durant des mois. Il forme alors un nouvel environnement à part entière et différent des eaux qu'il traverse. Globalement, la température constitue donc un facteur extrêmement variable dans l'environnement marin, tant en fonction de la latitude que de la profondeur, et constitue un paramètre déterminant pour la diversité et la répartition des organismes phytoplanctoniques (Sunagawa et al., 2015).

2.2.2. Effets de la température sur la croissance des cellules

Typiquement la forme des courbes de croissance des microalgues en fonction de la température est une cloche asymétrique (Fig 11), les taux de croissance mesurés à chaque température correspondant à un équilibre entre les activités anaboliques et cataboliques des cellules (Ras et al., 2013). Les activités anaboliques correspondent ici à la phase claire de la photosynthèse, phase durant laquelle les molécules d'ATP et de NADPH sont produites grâce à l'énergie lumineuse, tandis que les activités cataboliques correspondent à la consommation de ces molécules via le cycle de Calvin-Benson résultant en la production de carbone organique permettant la synthèse de biomasse et la division cellulaire. L'ensemble de ces réactions étant majoritairement enzymatiques, elles sont très sensibles à la température (J.-H. Chen et al., 2022). La définition du preferendum thermique d'un organisme est basé sur 3 températures remarquables : la température optimale de croissance (T_{opt} ; Fig 11), associée au taux de croissance maximum atteint, la température minimale (T_{min}) et la température maximale (T_{max}), correspondant aux limites de tolérance thermique de cet organisme. En s'éloignant du T_{opt}, l'énergie produite par la cellule n'est plus uniquement allouée à la croissance via la division cellulaire mais elle est également utilisée pour le maintien et la réparation cellulaire. Ainsi, on observe une diminution du taux de croissance de part et d'autre de la T_{opt}, traduisant un déséquilibre entre la croissance et la réparation, et donc une diminution de la fitness des cellules. En

dessous de $T_{opt,}$ le taux de croissance diminue progressivement, du fait du ralentissement de l'activité enzymatique, qui peut être en partie compensée par une augmentation de concentrations en carboxylases et en ribosomes qui permet de réorienter le métabolisme vers la croissance plutôt que la réparation. De plus, pour survivre à basses températures, certaines cellules se sont adaptées et produisent des protéines dites « anti-gel ». Au-dessus de $T_{opt,}$ on observe en revanche une chute drastique du taux de croissance, pouvant s'expliquer par une augmentation de l'activité enzymatique associée à une dénaturation des protéines (Dill et al., 2011).

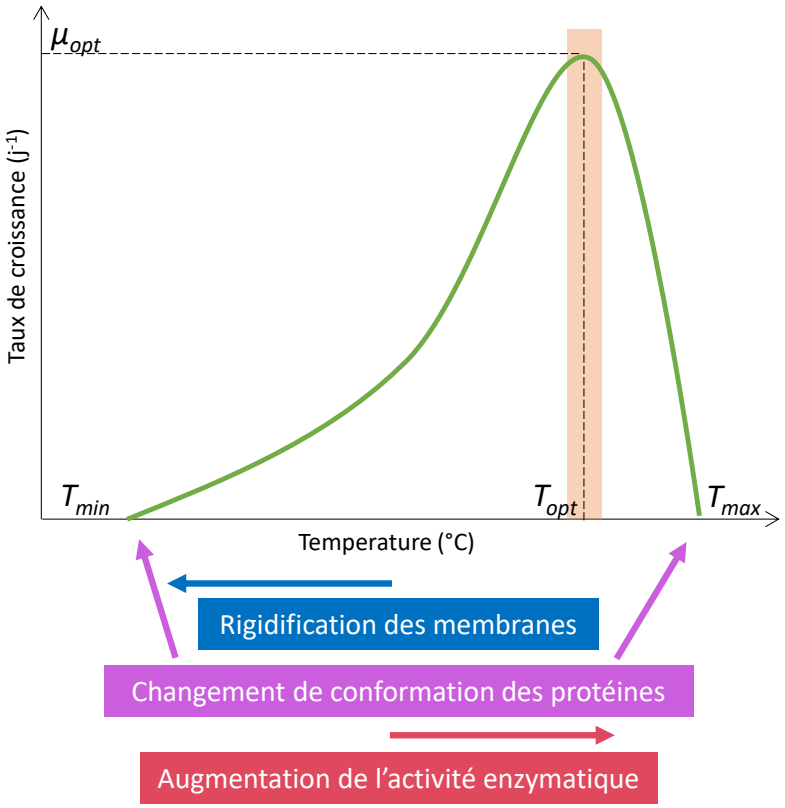

Figure 12 | Exemple d'une courbe de croissance de phytoplancton en fonction de la température.

2.2.3. Effets de la température sur la composition lipidique des membranes

La température est connue pour être l'un des facteurs majeurs portant atteinte à l'intégrité des membranes, un des composants cellulaires les plus thermosensibles, en affectant ses propriétés physiques (Cossins et al., 1977; Pehowich et al., 1988). Elle a notamment un effet sur la fluidité des membranes et de ce fait sur l'activité des protéines membranaires dans leur ensemble (Breton et al., 2019; Mikami & Murata, 2003). Des températures basses vont entraîner une diminution de la fluidité membranaire, pouvant

aller jusqu'au gel des membranes, tandis que de fortes températures vont entraîner leur fluidification, pouvant dans les cas extrêmes induire la désintégration de la matrice lipidique. Afin de s'adapter aux variations de température de leur environnement, les organismes photosynthétiques ont donc besoin de réguler la fluidité de leurs membranes (Mackey et al., 2013; Pittera et al., 2017; Varkey et al., 2016).

Chez les picocyanobactéries marines, des études récentes ont montré qu'en réponse à des variations de température, la fluidité membranaire variait essentiellement en fonction du degré d'insaturation et de la longueur des acides gras fixés au glycérol de la tête polaire alors que la proportion relative des 4 types de lipides membranaires (monogalactosyldiacylglycérol ou MGDG, digalactosyldiacylglycérol ou DGDG, sulfoquinovosyldiacylglycérol ou SQDG et phosphatidylglycérol ou PG) ne variait pas significativement, le MGDG constituant toujours le lipide dominant (Biller et al., 2014; Breton et al., 2019; Pittera et al., 2017). Alors que chez les cyanobactéries d'eau douce, les deux chaines d'acides gras sont constituées de 14 à 18 carbones (Los & Mironov, 2015), les lipides membranaires des picocyanobactéries marines incluent très majoritairement du C14 et C16, le rapport C14:C16 augmentant en réponse à l'acclimatation au froid ou à un stress thermique froid (Pittera et al., 2017). Ces conditions induisent également l'insertion d'insaturations, c-à-d de doubles liaisons, à des positions spécifiques dans les chaînes d'acides gras des 3 lipides majoritaires (MGDG, DGDG, et SQDG) résultant de l'action d'enzymes spécialisées, les désaturases. Alors que tous les *Synechococcus* marins possèdent le gène *desC3*, qui code pour une enzyme désaturant en position Δ9, une seconde Δ9-désaturase, *desC4*, est principalement présente dans les thermotypes froids (clades I, IV) et dans les eaux inférieures à 20°C. Parmi les deux gènes codant pour les Δ12-désaturases, *desA2* est spécifique des clades II et III et retrouvé dans les eaux chaudes, alors que *desA3* est présent dans les génomes des clades I, III et IV et est retrouvé dans les eaux inférieures à 20 °C, colonisées par les clades I et IV, ou entre 17 et 25°C dans les eaux dominées par le clade III. Il est donc possible que la présence des gènes *desA2* et *desA3* dans le clade III puisse conférer un avantage adaptatif aux membres de ce clade, qui sont soumis à des variations thermiques saisonnières beaucoup plus fortes que leurs homologues (sub)tropicaux du clade II (Breton et al., 2019). Dans l'ensemble, il semble donc que la capacité des *Synechococcus* à moduler le degré d'insaturation de leurs lipides

membranaires joue un rôle essentiel dans leur capacité d'adaptation à différentes niches thermiques.

2.3. Effets de la carence en fer

2.3.1. La limitation en fer dans les océans

Les éléments traces étaient largement disponibles dans l'océan primitif (4,6 – 4,0 milliards d'années), ce qui explique que le fer, le nickel ou encore le cobalt soient retrouvés en tant que co-facteurs dans de nombreuses réactions métaboliques (Falkowski, 2006; Saito et al., 2003). En ce qui concerne le Fe, alors que la forme réduite (Fe^{2+}), soluble dans l'eau de mer, constituait la forme dominante de ce métal (Canfield, 1998), sa disponibilité a diminué après l'apparition et la prolifération des photoautotrophes et notamment des cyanobactéries. En effet, l'évènement de Grande Oxygénation de l'atmosphère terrestre (GOE pour 'Great Oxygenation Event'), survenu entre 2,5 et 2,2 milliards d'années, a provoqué une oxygénation de l'océan, entrainant alors une oxydation de la plupart du Fe présent dans l'eau de mer (Sánchez-Baracaldo et al., 2022). Le fer ferreux (Fe^{2+}) s'est oxydé en fer ferrique (Fe^{3+}) et en hydroxydes de fer, créant alors les conditions de carence telles que nous les connaissons actuellement dans une grande partie de l'océan. En effet, même si le Fe est un des éléments les plus abondants sur Terre, sa biodisponibilité dans certains environnements aquatiques est extrêmement faible et ceci à cause de sa faible solubilité dans les environnements neutres à basiques (Boyd et al., 2007; Sutak et al., 2020; Tagliabue et al., 2017). C'est notamment le cas des régions dites HNLC pour 'High Nutrient, Low Chlorophyll', dans lesquelles l'azote et le phosphore inorganiques sont disponibles en concentrations non limitantes et pourtant la biomasse phytoplanctonique y est faible car le fer n'y est présent qu'à des concentrations de l'ordre du nano- au picomolaire (Behrenfeld & Kolber, 1999; Martin et al., 1994). Ce zones HNLC couvrent de vastes régions océaniques (Martin & Fitzwater, 1988) et incluent le Pacifique équatorial, le Pacifique subarctique et l'Océan austral (Coale et al., 2004; Martin et al., 1994; Tsuda et al., 2003). Ce métal est également limitant dans d'autres régions telles que l'Atlantique nord et plusieurs zones d'upwelling côtiers (Blain et al., 2004; Hutchins & Bruland, 1998). Dans l'ensemble, ces zones limitées ou co-limitées en fer représenteraient entre 35 et 50 % de l'océan mondial selon les groupes phytoplanctoniques (Moore et al., 2002).

2.3.2. Les sources de fer dans les océans

De nos jours, une grande partie du fer disponible dans la couche de surface des océans est issue de dépôts atmosphériques qui peuvent être d'origine anthropique ou naturelle et notamment issus des poussières désertiques (Bonnet & Guieu, 2004; Bressac et al., 2021; Duce & Tindale, 1991; Jickells et al., 2005). Les sédiments de la marge continentale générés par l'érosion constituent également une source de Fe importante, en particulier dans le Pacifique Nord (Lam & Bishop, 2008). De façon plus localisée, un enrichissement en Fe peut également avoir comme origine les sources hydrothermales et le volcanisme sous-marin (Horner-Devine et al., 2015), un phénomène récemment étudié lors de la campagne océanographique TONGA (Chefs de mission : S. Bonnet et C. Guieu, nov-dec 2019, http://tonga-project.org/web/). Dans les régions polaires et tempérées, les phénomènes de fonte de glacier et de ruissellement des rivières constituent également une source en fer pour l'environnement marin et même la principale en milieu côtier (Guieu & Martin, 2002; Raiswell, 2013). Enfin, certains processus physiques tels que la resuspension de sédiments par les courants ou encore les upwellings, entraînant une remontée de nutriments présents dans les masses d'eau profondes, jouent également un rôle dans la disponibilité du fer pour les communautés planctoniques (Boyd et al., 2005; Fig. 13).

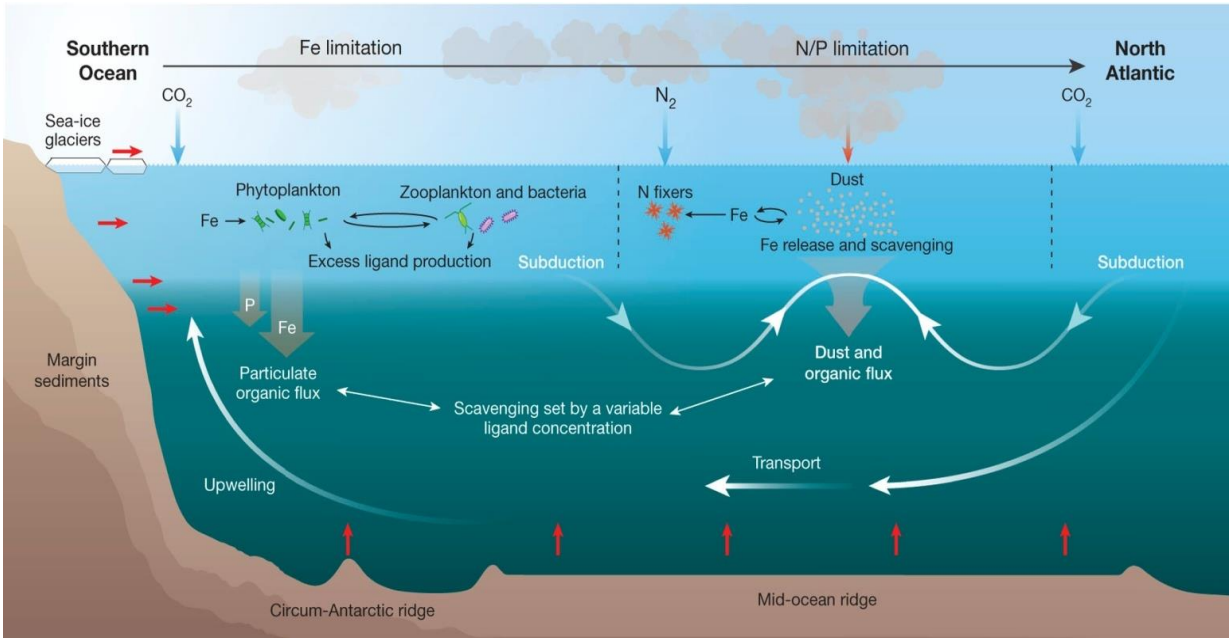

Figure 13 | Représentation des processus majeurs du cycle du Fe, modèle centré sur l'Océan Atlantique. (D'après Tagliabue et al., 2017)

2.3.3. Spéciation et estimation de la limitation en Fe dans l'océan

Le fait que le Fe biodisponible soit seulement présent à l'état de traces dans l'eau de mer alors qu'il constitue le 4^{ième} élément le plus abondant de la croûte terrestre (5.6% ; Mengel & Kirkby, 1987) est directement lié à la spéciation du fer, c-à-d l'importance relative des différentes formes physico-chimiques du Fe présentes dans l'eau de mer. D'un point de vue physique, le Fe peut être séparé en trois fractions : le Fe particulaire (>0.2 µm), le Fe colloïdal (0.02-0.2 µm) et le Fe dissous (ou soluble ; dFe ; <0.02 µm; Ussher et al., 2010). D'un point de vue chimique, en plus de la spéciation redox déjà évoquée plus haut — qui sépare le Fe^{3+}, plus stable mais très peu soluble, du Fe^{2+}, beaucoup plus soluble mais très rapidement oxydé dans les environnements oxiques — on distingue les stocks inorganiques (Fe') et organiques (FeL pour 'Fe-binding ligand').

Le dFe correspond au principal compartiment à partir duquel les micro-organismes peuvent acquérir le Fe. Dans les océans, 95-99% du dFe est chélaté par des ligands organiques naturels, ce qui impacte grandement la fraction de Fe accessible par les micro-organismes (Gledhill & van den Berg, 1994). Il existe une variété de molécules capables de complexer le fer, parmi lesquels les sidérophores constituent des ligands organiques synthétisés et secrétés par les bactéries (Wandersman & Delepelaire, 2004). Ils permettent la chélation du Fe dans l'eau de mer et ainsi de le rendre disponible pour les bactéries qui disposent de récepteurs appropriés permettant la récupération des complexes sidérophore-Fe (cf. § 2.3.5).

Outre la spéciation physico-chimique, la disponibilité du pool de dFe dépend également des voies d'acquisition du Fe et des différents besoins des organismes (Maldonado et al., 2005). En effet, il est important de noter que du fait du découplage entre la concentration en dFe dans l'océan et de la variabilité des besoins en Fe en fonction des espèces et de leur état physiologique, les concentrations en Fe biodisponible ne peuvent pas être mesurées directement à l'aide d'analyses chimiques (Pankowski & McMinn, 2009). Pour cette raison, la biodisponibilité du Fe est le plus souvent mesurée par des approches indirectes basées sur
i) la mesure de la fluorescence variable de la Chl (Behrenfeld et al., 1996; Kolber & Falkowski, 1993), ii) des expériences de bioaccumulation qui consistent à mesurer les concentrations intracellulaires de Fe après incubation des microorganismes d'intérêt dans un milieu enrichi en ^{55}Fe (Hudson & Morel, 1990), iii) des biorapporteurs tel que le

remplacement de la ferredoxine par la flavodoxine (Erdner & Anderson, 1999; La Roche et al., 1996) ou encore iv) sur la présence/absence d'un ensemble de marqueurs moléculaires de *Prochlorococcus* extraits à partir de données de métagénomique (Ustick et al., 2021). Cette dernière approche a récemment permis de réaliser une cartographie globale de l'état de carence en Fe des communautés phytoplanctoniques (Fig 7).

2.3.4. Rôle du Fer dans les cycles biogéochimiques

De par son rôle de contrôle de la production primaire, et donc de la pompe biologique (cf. §. 1.1.2), la disponibilité en Fe a un impact direct sur les grands cycles biogéochimiques et en particulier le cycle du carbone (Mahowald et al., 2005; Raven & Falkowski, 1999). Le fer joue également un rôle majeur dans le cycle de l'azote, puisque la fixation de l'azote atmosphérique (N_2) par les diazotrophes, capables de réduire ce composé gazeux en ammonium (NH_4^+) est rendue possible grâce à la nitrogénase, une enzyme riche en Fe. De ce fait, le Fe et l'azote sont souvent co-limitants dans l'environnement (Falkowski, 1997; Ustick et al., 2021). A l'inverse, une augmentation des apports en Fe pourrait induire une augmentation de la fixation d'azote, elle-même résultant en une augmentation de la disponibilité en azote inorganique soutenant une production primaire élevée, comme cela se serait produit pendant les périodes glaciaires (Broecker & Henderson, 1998). Enfin, le Fe jouerait également un rôle dans le cycle du diméthylsulfure (DMS, $(CH_3)_2S$), l'apport de Fer pouvant favoriser le développement d'haptophytes (p.ex. *Phaeocystis* ou *Emiliania huxleyi*), de prasinophytes et/ou de dinoflagellés. Ces organismes sont en effet de forts producteurs de dimethylsulfoniopropionate (DMSP, $(CH_3)_2SCH_2CH_2COOH$; Stefels et al., 2007) et donc considérés comme les principaux émetteurs de DMS, qui après oxydation dans l'atmosphère se transforme en sulfure et génère des noyaux de condensation participant à la formation des nuages, qui auraient un effet sur l'albédo et donc le réchauffement climatique (Boyd et al., 2007). De plus, alors que les diatomées et les cyanobactéries sont considérés comme étant de faibles producteurs de DMSP, (Bucciarelli et al., 2013) ont montré une forte augmentation de la production de DMSP dans les cultures de ces organismes carencées en Fe, pouvant atteindre des valeurs comparables à celles des forts producteurs de DMSP. Étant donné les surfaces océaniques affectées par la limitation en fer, cela suggère que le rôle des diatomées et des cyanobactéries dans le cycle du DMS/P pourrait avoir été largement sous-estimé.

2.3.5. La carence en fer chez les cyanobactéries

Le Fe est essentiel au métabolisme et à la croissance des organismes vivants et notamment du phytoplancton dont l'appareil photosynthétique peut contenir jusqu'à 50% du Fe intracellulaire (Behrenfeld & Milligan, 2013 ; Fig.14). Néanmoins, il peut être toxique à forte dose via la réaction de Fenton, qui génère des espèces réactives de l'oxygène lorsque le Fe^{2+} est oxydé en Fe^{3+} par le peroxyde d'hydrogène (Halliwell & Gutteridge, 1992). De ce fait, les organismes photosynthétiques ont développé des mécanismes afin de contrôler étroitement l'homéostasie du Fe et de coordonner les réponses à la carence ou à l'excès de Fe.

Chez les cyanobactéries, la plupart des études décryptant les mécanismes relatifs au métabolisme du Fe portent sur des souches d'eau douce ou halotolérantes. Par exemple, il a été démontré que le transport du Fe était optimisé chez *Synechocystis* sp. PCC 6803. En effet, malgré la faible solubilité du Fe^{3+} à pH neutre, son uptake est facilité grâce au transporteur FutABC, FutA existant sous forme de 2 sous-unités distinctes. Alors que FutA2 est la protéine soluble fixatrice de Fe^{3+} non-chélaté la plus abondante dans l'espace périplasmique, il a été suggéré que FutA1 aurait un rôle dans la protection du PSII en

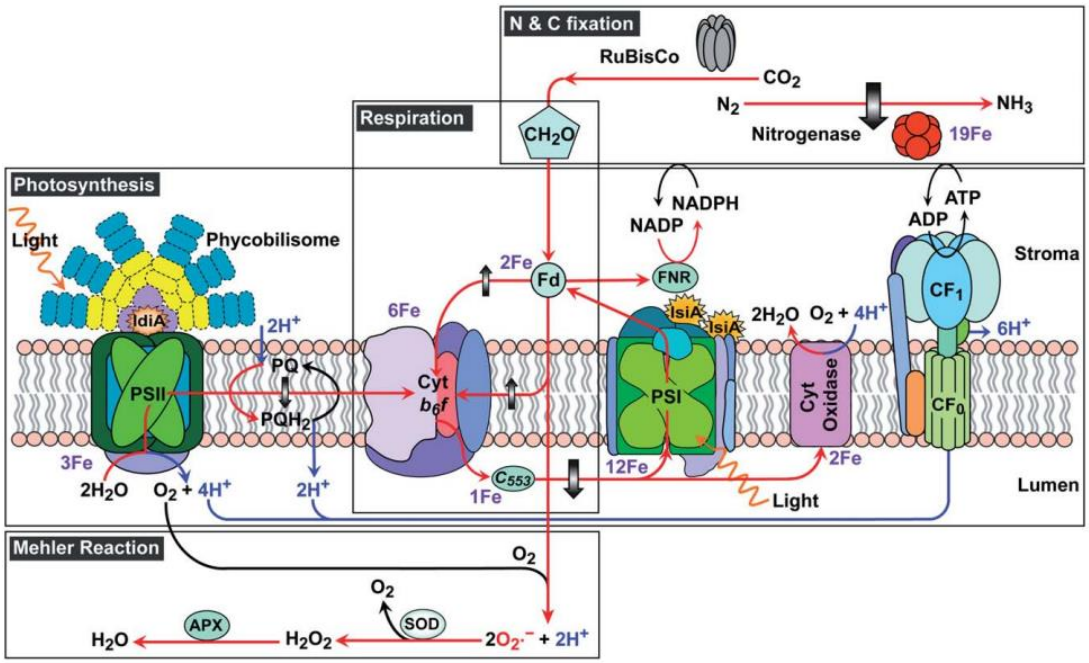

Figure 14 | Schéma des effets de la limitation en Fe sur les taux de transport d'électrons parmi les composants primaires de la photosynthèse, la fixation d'azote, la respiration et des voies de réactions de Mehler chez *Trichodesmium erythraeum* IMS101 (D'après Shi et al., 2007)

conditions de carence en fer, bien que le mécanisme moléculaire impliqué reste à élucider (Badarau et al., 2008; Katoh, Hagino, & Ogawa, 2001). Le Fe^{3+} est ensuite transféré dans le cytoplasme via le transporteur FutB/C (Katoh, Hagino, Grossman, et al., 2001; Katoh, Hagino, & Ogawa, 2001; Kranzler et al., 2014). Il existe également chez la plupart des cyanobactéries d'eau douce un système d'absorption du Fe^{2+}, FeoA/FeoB, qui est activé quand les concentrations en Fe intracellulaire sont faibles (Katoh, Hagino, Grossman, et al., 2001). Shcolnick et collaborateurs ont montré que les gènes *futABC* et *feoB* étaient induits à des niveaux semblables en condition limitée en Fe chez *Synechocystis* sp. PCC 6803 (Shcolnick et al., 2009).

D'autres mécanismes ont été mis en évidence chez les cyanobactéries en réponse à la carence en fer. Parmi ceux-ci, on peut noter le stockage du Fe par des bacterioferritines et des complexes homologues (Dps), qui chez *Synechocystis* sp. PCC 6803 peuvent contenir jusque 50% du quota de Fe cellulaire (Keren et al., 2004; Shcolnick & Keren, 2006). Ces stratégies comprennent également la diminution du rapport PSI/PSII (le PSI contenant 12 atomes de Fe contre 3 pour le PSII) et du nombre de phycobilisomes, dont la synthèse repose sur des molécules contenant du Fe (Behrenfeld & Milligan, 2013; Strzepek et al., 2019). Ainsi, ces altérations de l'appareil photosynthétique, partiellement compensées par la synthèse d'IsiA (pour 'Iron-starvation induced protein A'), un complexe Chl-protéine qui augmente la capacité de capture de la lumière par le PSI (Havaux et al., 2005a), permettrait de réduire les besoins en fer des cyanobactéries. En suivant la même logique, plusieurs autres mécanismes impliquent le remplacement de molécules complexes contenant du Fe par d'autres qui en sont dépourvues ou utilisent un métal alternatif comme cofacteur. C'est notamment le cas des ferredoxines, des protéines contenant un centre Fe-S, qui en conditions limitées en Fe sont remplacées par des flavodoxines non métalliques dans la chaîne de transport des électrons (Bradley et al., 2019; Le Brun et al., 2010; Shcolnick et al., 2009). C'est également le cas des hèmes où l'atome de Fe est remplacé par d'autres cofacteurs comme le Zn, Mn, Co, etc. (Morrissey & Bowler, 2012), du cytochrome *c6* remplacé par la plastocyanine contenant du Cu (Sandström et al., 2002) ou encore des superoxydes dismutases (SOD) qui présentent des formes alternatives qui fixent différents métaux (Chadd et al., 1996; Jiang et al., 2020).

Un autre type de stratégie repose sur l'optimisation du transport et de l'acquisition du Fe soit sous sa forme liée (FeL) à des ligands organiques tels que des sidérophores soit

sous sa forme libre inorganique (Fe' ; Shaked & Lis, 2012). Dans tous les cas, le Fe^{3+} n'étant pas directement assimilable par les cellules, il doit tout d'abord être réduit en Fe^{2+} par des reductases, soit dans le milieu environnant, soit au niveau des membranes (voie de transport réductif du Fe' ou FeL). Alors que peu de cyanobactéries sont capables de synthésiser des sidérophores, nombre d'entre elles possèdent des transporteurs de sidérophores, suggérant qu'ils utilisent ceux produits par les bactéries environnantes comme cela a été notamment montré chez *Trichodesmium* (Basu et al., 2019). Ce système de transport comprend des récepteurs dépendants de TonB (TBDR pour 'TonB-dependent receptors') qui assurent le transport spécifique des sidérophores à travers la membrane externe, en utilisant l'énergie dérivée de la force proton-motrice transmise par le complexe TonB-ExbB-ExbD et les transporteurs FecBCDE, situés au niveau de la membrane plasmique. En ce qui concerne les reductases, dont la présence l'existence a été suggérée chez de nombreux organismes phytoplanctoniques eucaryotes et procaryotes, cette réaction implique i) soit des enzymes situées au niveau de la surface de la membrane externe tel que le système ARTO (pour 'alternate respiratory terminal oxidase'), ii) soit des molécules libérées dans le milieu environnant, telles que les substances humiques ou des ions superoxides ('electron shuttle ' ; Rose et al., 2005).

Enfin, tout comme la plupart des bactéries, les cyanobactéries sont capables de détecter les concentrations de fer cytosolique (Fe^{2+}) grace au facteur de transcription Fur (pour 'ferric uptake regulator') et de réguler en fonction les gènes impliqués dans le métabolisme du fer (Chappell & Webb, 2010; Fillat, 2014; Morrissey & Bowler, 2012; Riediger et al., 2021). Chez *Synechococystis* sp PCC 6803, le régulon Fur comprend 33 gènes, codant pour des transporteurs et des enzymes impliqués dans l'assimilation et le stockage du fer, ainsi qu'un ARN non codant, IsaR1, qui régule un certain de nombre de gènes impliqués dans la réponse à la carence en fer mais ne possèdant pas de Fur-Box dans leur région promotrice (Riediger et al., 2021). Plus généralement, il semble que la régulation du transport, du stockage et de l'utilisation du fer résulte de l'interaction entre le régulon Fur, plusieurs autres facteurs de transcription, la protéase FtsH3 et l'ARNs IsaR1.

Pour l'heure, bien que les picocyanobactéries marines dominent très largement les communautés phytoplanctoniques, peu d'études ont porté sur l'adaptation de ces

organismes à la concentration en Fe (Flombaum et al., 2013; Partensky et al., 1999). L'utilisation de données de métagénomiques a tout d'abord permis de mettre en évidence que les *Prochlorococcus* des clades HLIII/IV colonisant les zones HNLC possédaient un certain nombre de spécificités par rapport aux autres écotypes HL. Ces adaptations incluent la réduction de protéines contenant du fer, telles que la plastoquinol terminal oxidase (PTOX), deux ferredoxines et le cytochrome C_m mais également la capacité de transporter des sidérophores synthétisés par d'autres micro-organismes (Hogle et al., 2022; Malmstrom et al., 2013; Rusch et al., 2010).

En ce qui concerne *Synechococcus*, Mackey et al. (2015) ont montré en comparant la croissance, la photophysiologie et les protéomes de deux souches de *Synechococcus* isolées de différentes niches environnementales que, contrairement au paradigme selon lequel le phytoplancton côtier est moins capable de s'adapter à la limitation de Fe que les espèces de haute mer, la souche côtière (CC9311, clade I) était capable de s'acclimater aux changements de concentration de Fe en modulant l'absorption de Fe, le stockage de Fe et la quantité de protéines photosynthétiques alors que la souche océanique (WH8102, clade III) était dépourvue de cette réponse adaptative. Cependant, aucune de ces deux souches n'a été isolée d'une zone chroniquement pauvre en Fe. Plus récemment, des études de métagénomiques ont également permis de mettre en évidence quelques spécificités des ecotypes Fe de *Synechococcus* par rapport aux autres écotypes, dont la présence spécifique de gènes impliqués dans le transport, le stockage et la régulation du Fe (Ahlgren et al., 2020; Garcia et al., 2020).

2.4. Réponse de l'appareil photosynthétique aux variations des conditions environnementales

L'appareil photosynthétique joue un rôle central dans la réponse des organismes phytoplanctoniques aux variations des conditions environnementales, d'une part parce que son activité régule l'ensemble du métabolisme de la cellule et d'autre part parce que la plupart des stress affecte l'état d'oxydo-réduction cellulaire, conduisant à la génération d'espèces réactives de l'oxygène (ROS pour 'reactive oxygen species') qui peuvent à leur tour endommager les composants cellulaires tels que les lipides, les protéines ou encore l'ADN (Asada, 1994; S. Hirayama et al., 1995; Latifi et al., 2005, 2009; Schwarz & Forchhammer, s. d.; Takahashi & Murata, 2008). Une augmentation importante de la

production de ROS intracellulaires est en effet observée chez les organismes photosynthétiques notamment lorsque le taux de transport des électrons générés lors de la photosynthèse excède leur taux de consommation durant la fixation du CO_2 (Knox & Dodge, 1985; Latifi et al., 2009; Rastogi et al., 2010). Ce déséquilibre se produit non seulement lorsque les cellules sont exposées à un excès de lumière ou de rayonnement UV mais également en réponse à tout stress environnemental, qu'il soit nutritionnel, salin ou thermique, qui induit un ralentissement du métabolisme des cellules (Murata et al., 2007; Pittera et al., 2014, 2017). Par exemple, il a été montré chez la cyanobactérie d'eau douce *Anabaena* sp. PCC 7120 qu'une limitation en fer provoquait une augmentation de 100 fois de la quantité de ROS par rapport aux cellules non carencées (Latifi et al., 2005). La capacité des cyanobactéries à s'adapter à différentes conditions environnementales repose donc en grande partie sur leur capacité à optimiser le fonctionnement de leur appareil photosynthétique dans toutes ces conditions. Pour cela, les cyanobactéries ont développé une série de mécanismes de photoprotection permettant de contrôler l'énergie atteignant les RC et ainsi de limiter et/ou réparer les dommages à l'appareil photosynthétique.

2.4.1. Effet sur les phycobilisomes et les centres réactionnels

En ce qui concerne les antennes, l'étude de la réponse de différentes souches modèles de *Synechococcus* marins à des stress lumineux (Six et al., 2004), UV (Six et al., 2007) ou thermique (Pittera et al., 2017) a permis de montrer que ces conditions induisent un raccourcissement des bras des PBS, voire une déconnection des PBS de la membrane thylacoïdale. De façon intéressante, la thermostabilité de ces PBS varie selon les thermotypes de *Synechococcus,* ce qui suggère que ce phénomène pourrait jouer un rôle important dans la colonisation des différentes niches thermiques (Pittera et al., 2017). La phycocyanine s'est avérée être la moins stable de toutes les phycobiliprotéines en réponse au stress thermique, une sensibilité qui semble liée à deux substitutions dont la distribution varie selon les thermotypes (Pittera et al., 2017).

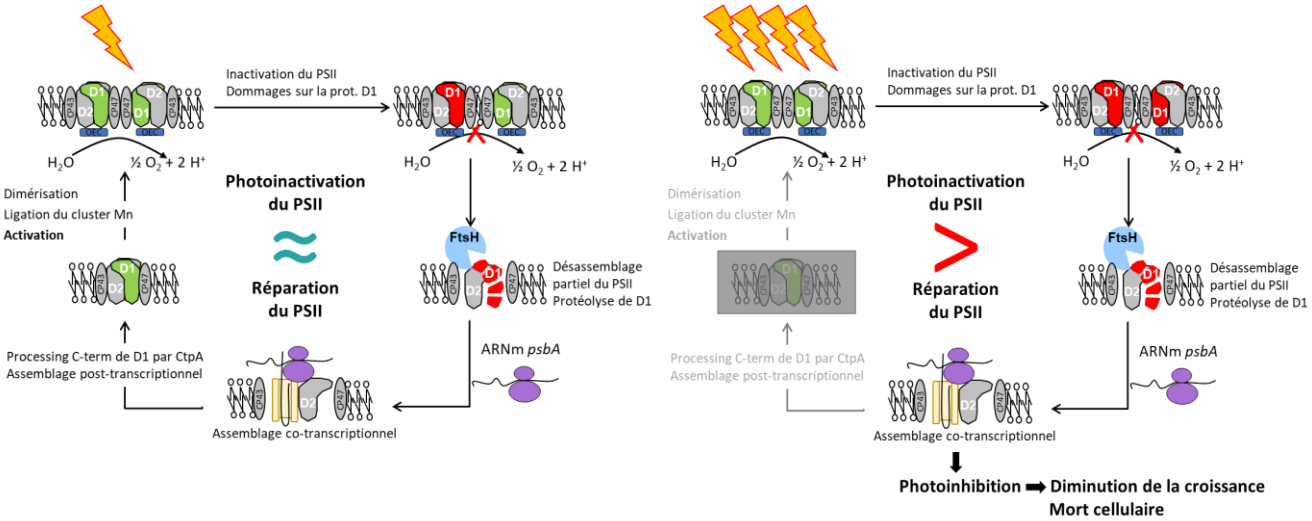

Figure 15 | Cycle de réparation de la protéine D1 du photosystème II (PSII). D'après Garczarek, 2018 et Mulo et al., 2009.

Le centre réactionnel du PSII, composé des deux protéines majeures (D1 et D2, codées par les gènes *psbA* et *psbD*) et qui constitue l'une des cibles privilégiées des ROS et notamment ceux issus de la Chl (P680) à l'état de triplet excité, est également étroitement régulé en réponse aux variations de paramètres abiotiques (Blot et al., 2011; Takahashi & Murata, 2008; Triantaphylidès et al., 2008). Dans des conditions normales et stables de croissance, la protéine D1 agit comme un 'fusible' (Vass, 2012). Elle est très rapidement dégradée puis re-synthétisée, permettant ainsi de protéger le reste de l'appareil photosynthétique d'un excès d'énergie lumineuse. Ce cycle de réparation de D1, qui intervient de façon continue et plus ou moins rapide selon l'intensité lumineuse de croissance, permet de maintenir une activité photosynthétique et un taux de croissance constants (Fig. 15). En revanche, en conditions d'excès de lumière ou en réponse à tout autre stress environnemental entraînant une diminution du métabolisme, la protéine D1 est dégradée plus rapidement qu'elle n'est synthétisée. L'appareil photosynthétique est alors photo-inhibé, entraînant une diminution de la croissance pouvant mener à la mort cellulaire (Murata et al., 2007; Nishiyama et al., 2006; Tyystjärvi, 2008 ; Fig. 15). D'un point de vue moléculaire, la protéine D1 est codée par 3 à 6 copies du gène *psbA* chez les *Synechococcus* marins (Garczarek et al., 2008). Il y a en général une copie qui code pour l'isoforme D1:1, qui présente des performances photosynthétiques optimales et dont les transcrits sont abondants à faible lumière, et 2 à 5 copies qui codent pour l'isoforme D1:2, moins performante d'un point de vue photosynthétique mais

également moins sensible à la photo-inhibition (Garczarek et al., 2008; Sander et al., 2010; Sugiura et al., 2015). Les gènes codant pour cette dernière isoforme sont fortement surexprimés en conditions de stress, notamment ceux dus aux fortes intensités lumineuses, aux radiations UV et aux basses températures (Guyet et al., 2020).

2.4.2. Autres mécanismes de photoprotection

En plus de la régulation de la taille des antennes photosynthétiques et de la réparation du PSII, d'autres mécanismes de photoprotection permettent aux picocyanobactéries de s'acclimater aux variations des conditions environnementales en dissipant l'excès d'énergie lumineuse et/ou en gérant le surplus d'électrons générés par un excès de lumière ou un ralentissement du métabolisme cellulaire.

Un premier mécanisme impliquerait les transitions d'état qui, chez les cyanobactéries, repose sur la mobilité du PBS à la surface des membranes entre le PSII (état 1) et le PSI (état 2 ; Ashby & Mullineaux, 1999). En modifiant la distribution de l'énergie entre les deux PS en fonction de la quantité ou la qualité de la lumière ambiante (Fujita et al., 1994), les transitions d'état contrôleraient l'équilibre entre le transport linéaire d'électrons (impliquant les deux PS et générant à la fois la force proton-motrice qui est génératrice d'ATP et un pouvoir réducteur) et le transport cyclique d'électrons autour du PSI (impliquant uniquement le PSI et générant la force proton-motrice sans production de pouvoir réducteur ; (Mullineaux, 2014). Cependant, le rôle de ce mécanisme dans l'acclimatation à d'autres conditions environnementales que les changements lumineux reste à démontrer.

Grâce à leur activité d'oxydoréductases, les flavoprotéines permettent également aux cyanobactéries de gérer les variations rapides de l'intensité lumineuse en jouant un rôle de puits pour les électrons en surplus, permettant d'éviter la production de ROS (Bersanini et al., 2014; Zhang et al., 2009). Au cours de ce processus, appelé la réaction de Mehler, les électrons récupérés du côté accepteur du PSI sont délivrés à une molécule d'O_2 qui est réduite en H_2O sans danger pour la cellule (Allahverdiyeva et al., 2011, 2013). Alors qu'il existe 4 gènes codant pour des flavoprotéines (flv1-4) chez la cyanobactérie d'eau douce modèle *Synechocystis* sp. PCC 6803 qui sont fortement surexprimés lors de l'exposition à de fortes lumières ou en cas de limitation en carbone (Zhang et al., 2009), seul les gènes *flv1* et *3* sont présents chez toutes les picocyanobactéries marines.

Tout comme les flavoprotéines, la protéine PTOX (pour 'plastoquinol terminal oxidase'), présente chez certaines souches de *Synechococcus* et dans la plupart des souches de *Prochlorococcus* HL et LLI, pourrait également permettre d'éviter l'accumulation de plastoquinones réduites et donc la production de ROS (Bailey et al., 2008; Scanlan et al., 2009). Chez *Prochlorococcus,* le gène correspondant est surexprimé en condition de fortes lumières (Steglich et al., 2006) et pendant la phase lumineuse chez des cultures acclimatées en cycle jour/nuit (Mella-Flores et al., 2012), ce qui tend à confirmer son rôle dans la régulation de l'état redox des cellules lorsque la lumière est en excès.

Un autre mécanisme de photoprotection consiste en la dissipation de l'énergie lumineuse excédentaire sous forme de chaleur, un phénomène le plus souvent relié au quenching non photochimique de la fluorescence (ou NPQ pour 'non photochemical quenching'). Alors que chez les plantes supérieures, ce mécanisme de photoprotection est en grande partie assuré par le cycle des xanthophylles (Roach & Krieger-Liszkay, 2012), la plupart des cyanobactéries utilisent pour cela une voie impliquant une caroténo-protéine orange (OCP ; Wilson et al., 2006, 2007). Le changement de conformation de cette protéine, qui fixe une molécule de caroténoïde (échinénone), permettrait la fixation de la forme active de l'OCP sur les PBS, responsable de la dissipation de 80 % de l'énergie collectée par le PBS (Boulay et al., 2010; Kirilovsky & Kerfeld, 2012). De façon intéressante, les trois gènes nécessaires à ce mécanisme et codant pour l'OCP, la FRP (Fluorescence Recovery Protein) qui joue un rôle dans le détachement de l'OCP du PBS, et la β-carotène kétolase (CrtW), impliquée dans la synthèse de l'échinénone, sont regroupés dans un même opéron qui constitue les gènes les plus fortement sur-exprimés en réponse à des nombreux stress environnementaux (Guyet et al., 2020; Six et al., 2021) ont récemment montré que chez les *Synechococcus* marins, cet opéron était systématiquement présent dans les thermotypes froids (clades I et IV) et chez les membres du clade III, colonisant des zones soumises à de fortes variations saisonnières de température, mais également dans les communautés naturelles de *Synechococcus* colonisant les eaux inférieures à 20°C. De plus, ce mécanisme serait particulièrement actif chez les souches de *Synechococcus* acclimatées à basse température, suggérant qu'il aurait joué un rôle important dans la colonisation des niches thermiques froides. Par ailleurs, d'autres protéines pourraient également jouer un rôle dans la dissipation de l'excès d'énergie lumineuse. C'est

notamment le cas des HLIPs (pour High-Light Inducible Protein), une famille de protéines particulièrement amplifiée chez les *Prochlorococcus* HL et dont les gènes sont souvent surexprimés en réponse à des nombreux stress environnementaux chez les cyanobactéries en général (Guyet et al., 2020; Havaux et al., 2005b; He et al., 2001; Steglich et al., 2006). Bien que le rôle exact de ces protéines ne soit pas parfaitement compris, il semble qu'elles permettraient d'éviter les dommages aux complexes pigment-protéines en inactivant les singulets de Chl excité ou les singulets d'oxygène (O. Hirayama et al., 1994; L. Huang et al., 2002). De même le gène *isiA*, présent dans certains génomes de *Synechococcus,* est surexprimé en conditions de carence en fer ou d'exposition aux fortes lumières. Les protéines générées forment une couronne de 18 protéines autour des trimères de PSI et permettrait ainsi de limiter les dommages au PSII tout en augmentant la capacités de capture de la lumière par le PSI (Havaux et al., 2005b; Yeremenko et al., 2004).

Ces multiples stratégies utilisées par les picocyanobactéries marines pour préserver l'intégrité et le fonctionnement de la machinerie photosynthétique leur permettent de survivre et de croître dans des conditions environnementales très variées en réagissant rapidement aux variations spatio-temporelles des paramètres physico-chimiques qu'elles rencontrent dans le milieu naturel.

Objectifs

La communauté scientifique a longtemps pensé que seuls quatre clades (I-IV) du SC 5.1 dominaient les communautés naturelles de *Synechococcus* marins. Cependant, un cinquième clade, CRD1, initialement découvert dans le dôme du Costa Rica (Saito et al., 2005), s'est avéré être le clade dominant, en co-occurence avec les membres d'un clade non-encore cultivé (EnvB) dans les vastes zones océaniques limitées en Fe et en particulier dans les zones HNLC du Pacifique (Farrant et al., 2016; Sohm et al., 2015). Néanmoins, au début de ma thèse, aucune étude n'avait porté sur la caractérisation physiologique et génomique des membres de ce clade et seule une étude, essentiellement métagénomique est parue en 2020 (Ahlgren et al., 2020). Ainsi, l'objectif principal de ma thèse a été de mieux comprendre l'influence des paramètres environnementaux, et en particulier de la température et du Fe, sur la physiologie, la diversification génétique, la diversité fonctionnelle, et la distribution de ces organismes *in situ*.

Le premier chapitre de cette thèse s'est focalisé sur le paramètre température. En effet, en analysant la distribution des membres du clade CRD1 à partir des données de métagénomique de l'expédition *Tara* Océans, Farrant et al. (2016) ont pu subdiviser ce clade en trois ESTUs (CRD1A-C), correspondant à trois thermotypes potentiels. Ainsi, l'objectif de ce premier chapitre été de vérifier cette hypothèse par une étude de thermophysiologie comparative à partir de souches en culture, représentatives des différents écotypes, et de mieux définir les niches thermales réalisées des différents thermotypes grâce aux données de métabarcoding et métagénomique issues de diverses campagnes océanographiques.

Le second axe de ma thèse a porté sur la carence en Fe. Au début de ma thèse, la plupart des connaissances disponibles à ce sujet concernait des cyanobactéries d'eau douce modèles assez éloignées du point de vue de leur phylogénie, contenu génomique et habitat de leurs homologues marins. Cet axe de recherche a donc visé par une approche physiologique, génomique et transcriptomique comparative à identifier des mécanismes d'adaptation et d'acclimatation mis en place par les membres du clade CRD1, en comparaison avec des souches représentatives d'autres niches du milieu océanique, leur permettant de survivre dans un environnement pauvre en fer.

Chapitre I :

Acclimatation à la température des écotypes -Fe

Contexte de l'étude

Le but de ce premier chapitre a été de valider au sein du clade CRD1 l'existence d'écotypes distincts vis-à-vis de la température. Récemment, Farrant et collaborateurs ont subdivisé les clades de *Synechococcus* en ESTUs, ce qui a permis de délimiter des écotypes au sein de chaque clade, mais également de définir leurs aires de répartition et d'identifier les facteurs influençant leur distribution géographique *in situ* (Farrant et al., 2016). Ainsi, au sein du clade CRD1, trois ESTUs (CRD1A-C) ont été mis en évidence, présentant des aires de répartition différentes *in situ* et correspondant à de potentiels thermotypes. En revanche, les clades I à IV présentent chacun un ESTU largement majoritaire (IA, IIA, IIIA et IVA) et un ou deux ESTUs minoritaires. Ces ESTUs majoritaires sont donc bien représentatifs de la distribution des clades I à IV dans leur ensemble, à savoir les eaux froides et riches en nutriments, à hautes latitudes pour les clades I et IV et les eaux tropicales, subtropicales et tempérées, pauvres en azote ou en phosphore pour les clades II et III, respectivement (Huang et al., 2012 ; Sohm et al., 2016 ; Kent et al., 2019). D'un point de vue physiologique, alors que plusieurs souches représentatives des clades I à IV ont été caractérisées, ce qui a notamment permis de valider l'existence de thermotypes froids (clades I et IV) et tempérés chauds (clades II et III ; (Breton et al., 2019; Doré et al., 2022; Pittera et al., 2014; Six et al., 2021), les membres du clade CRD1 ont pour le moment très peu été étudiés (Ahlgren et al., 2020). Au cours de ce chapitre, la disponibilité de souches en culture représentatives des trois ESTUs distincts vis-à-vis de la température au sein du clade CRD1 m'a permis de mener la première étude de thermophysiologie sur ce groupe écologiquement important de *Synechococcus.* Dans un premier temps, j'ai déterminé les *preferenda* et limites de croissance des trois souches sélectionnées en comparaison avec des souches représentatives des ESTUs IA à IVA afin de déterminer de manière précise la niche fondamentale de chaque souche. J'ai également acquis plusieurs paramètres (photo)physiologiques, tels que le contenu pigmentaire, l'activité photosynthétique, ou encore la réparation du photosystème II afin de mieux comprendre les mécanismes d'acclimatation mis en place par les cellules en réponse aux variations de la température. Enfin, cette étude a également permis de redéfinir les niches environnementales réalisées à partir d'un large set de données regroupant plus de 413 sites d'échantillonnage issus de diverses campagnes

océanographiques, telles que *Tara* Oceans, *Tara* Polar Circle et l'Ocean Sampling Day 2014 (OSD2014), ou encore du site de suivi à long terme SOMLIT-ASTAN au large de Roscoff.

Contribution

Les cultures utilisées lors de cette étude ont été fournies par la Collection de Cultures de Roscoff (RCC) et sélectionnées sur la base de leur représentativité dans l'environnement. J'ai d'abord complété les quelques points de croissance acquis auparavant par des membres de mon équipe en poursuivant l'acclimatation à la température de l'ensemble des cultures (8 souches) afin de compléter leurs gammes de tolérance thermique. Pour comprendre comment la température affecte la physiologie des cellules et en particulier l'appareil photosynthétique, j'ai acquis un panel de paramètres renseignant sur l'état physiologique des cellules dans différentes conditions de culture. J'ai notamment mis en place des expériences de stress en fonction de la température et organisé la récolte des échantillons avec l'aide des membres de mon équipe. J'ai ensuite activement participé au traitement des échantillons, à l'analyse des données physiologiques et à l'interprétation des résultats obtenus.

Comparative thermophysiology of marine *Synechococcus* CRD1 strains isolated from different thermal niches in iron-depleted areas

Résumé de l'article en français

Les cyanobactéries marines du genre *Synechococcus* sont omniprésentes dans l'océan, une caractéristique probablement liée à leur grande diversité génétique. Parmi les principales lignées, les clades I et IV sont retrouvés préférentiellement dans les eaux tempérées et froides riches en nutriments, tandis que les clades II et III préfèrent les eaux chaudes, pauvres en azote ou en phosphore. L'existence de tels thermotypes froids (I/IV) et chauds (II/III) est corroborée par la caractérisation physiologique de souches représentatives de ces environnements. Il a récemment été démontré qu'un cinquième clade, CRD1, domine la communauté de *Synechococcus* marins dans les zones pauvres en fer de l'océan mondial et comprend trois 'unités taxonomiques écologiquement significatives' distinctes (ESTUs CRD1A-C) occupant différentes niches thermiques, ce qui suggère qu'il existerait différents thermotypes au sein de ce clade.

Au cours de cette étude, en utilisant la thermophysiologie comparative de souches représentatives de ces trois ESTUs CRD1, nous montrons que la souche CRD1A, MITS9220, est un thermotype chaud, la souche CRD1B, BIOS-U3-1, un thermotype tempéré-froid et la souche CRD1C, BIOS-E4-1, un thermotype tempéré-chaud sténotherme. Etonnamment, le thermotype CRD1B s'est avéré présenter peu de traits et/ou de caractéristiques génomiques typiques des thermotypes froids. En revanche, des traits physiologiques spécifiques des souches CRD1 par rapport à leurs homologues des clades I, II, III et IV ont peu être mis en évidence, notamment un taux de croissance et un rendement quantique maximal du photosystème II plus faibles à la plupart des températures et un taux de réparation plus élevé de la protéine D1. L'ensemble de ces données suggère que chez les membres du clade CRD1, l'adaptation à la carence en fer est prioritaire par rapport à l'adaptation à la température, même si la présence de plusieurs thermotypes CRD1 pourrait expliquer pourquoi le clade CRD1 dans son ensemble occupe la majeure partie des eaux limitées en fer.

Article published in Frontiers in Microbiology

frontiers | Frontiers in Microbiology

ORIGINAL RESEARCH
published: 09 May 2022
doi: 10.3389/fmicb.2022.893413

Comparative Thermophysiology of Marine *Synechococcus* CRD1 Strains Isolated From Different Thermal Niches in Iron-Depleted Areas

*Mathilde Ferrieux[1], Louison Dufour[1], Hugo Doré[1†], Morgane Ratin[1], Audrey Guéneuguès[2], Léo Chasselin[2], Dominique Marie[1], Fabienne Rigaut-Jalabert[3], Florence Le Gall[1], Théo Sciandra[1], Garance Monier[1], Mark Hoebeke[4], Erwan Corre[4], Xiaomin Xia[5], Hongbin Liu[6], David J. Scanlan[7], Frédéric Partensky[1] and Laurence Garczarek[1,8]**

[1] Sorbonne Université, CNRS, UMR 7144 Adaptation and Diversity in the Marine Environment (AD2M), Station Biologique de Roscoff (SBR), Roscoff, France, [2] Sorbonne Université, CNRS, UMR 7621 Laboratoire d'Océanographie Microbienne (LOMIC), Observatoire Océanologique de Banyuls/mer, Banyuls, France, [3] Sorbonne Université, CNRS, Fédération de Recherche FR2424, Station Biologique de Roscoff, Roscoff, France, [4] CNRS, FR 2424, ABiMS Platform, Station Biologique de Roscoff (SBR), Roscoff, France, [5] Key Laboratory of Tropical Marine Bio-Resources and Ecology, South China Sea Institute of Oceanology, Chinese Academy of Sciences, Guangzhou, China, [6] Department of Ocean Science, The Hong Kong University of Science and Technology, Kowloon, Hong Kong SAR, China, [7] University of Warwick, School of Life Sciences, Coventry, United Kingdom, [8] CNRS Research Federation (FR2022) Tara Océans GO-SEE, Paris, France

Marine *Synechococcus* cyanobacteria are ubiquitous in the ocean, a feature likely related to their extensive genetic diversity. Amongst the major lineages, clades I and IV preferentially thrive in temperate and cold, nutrient-rich waters, whilst clades II and III prefer warm, nitrogen or phosphorus-depleted waters. The existence of such cold (I/IV) and warm (II/III) thermotypes is corroborated by physiological characterization of representative strains. A fifth clade, CRD1, was recently shown to dominate the *Synechococcus* community in iron-depleted areas of the world ocean and to encompass three distinct ecologically significant taxonomic units (ESTUs CRD1A-C) occupying different thermal niches, suggesting that distinct thermotypes could also occur within this clade. Here, using comparative thermophysiology of strains representative of these three CRD1 ESTUs we show that the CRD1A strain MITS9220 is a warm thermotype, the CRD1B strain BIOS-U3-1 a cold temperate thermotype, and the CRD1C strain BIOS-E4-1 a warm temperate stenotherm. Curiously, the CRD1B thermotype lacks traits and/or genomic features typical of cold thermotypes. In contrast, we found specific physiological traits of the CRD1 strains compared to their clade I, II, III, and IV counterparts, including a lower growth rate and photosystem II maximal quantum yield at most temperatures and a higher turnover rate of the D1 protein. Together, our data suggests that the CRD1 clade prioritizes adaptation to low-iron conditions over temperature adaptation, even though the occurrence of several CRD1 thermotypes likely explains why the CRD1 clade as a whole occupies most iron-limited waters.

Keywords: marine picocyanobacteria, *Synechococcus*, CRD1, thermotype, temperature adaptation

OPEN ACCESS

Edited by:
Susana Agusti,
King Abdullah University of Science and Technology, Saudi Arabia

Reviewed by:
Alexandra Coello-Camba,
IMEDEA (CSIC-UIB), Spain
Cristiana Callieri,
National Research Council (CNR), Italy

***Correspondence:**
Laurence Garczarek
laurence.garczarek@sb-roscoff.fr

†Present address:
Hugo Doré,
Department of Ecology, Evolution and Marine Biology, University of California, Santa Barbara, Santa Barbara, CA, United States

Specialty section:
This article was submitted to Aquatic Microbiology, a section of the journal Frontiers in Microbiology

Received: *10 March 2022*
Accepted: *31 March 2022*
Published: *09 May 2022*

Citation:
Ferrieux M, Dufour L, Doré H, Ratin M, Guéneuguès A, Chasselin L, Marie D, Rigaut-Jalabert F, Le Gall F, Sciandra T, Monier G, Hoebeke M, Corre E, Xia X, Liu H, Scanlan DJ, Partensky F and Garczarek L (2022) Comparative Thermophysiology of Marine Synechococcus CRD1 Strains Isolated From Different Thermal Niches in Iron-Depleted Areas. Front. Microbiol. 13:893413. doi: 10.3389/fmicb.2022.893413

INTRODUCTION

Marine picocyanobacteria contribute to the biogeochemical cycling of various elements, most notably carbon, contributing ∼25% of ocean net primary productivity, of which the *Synechococcus* genus alone is responsible for about 16% (Flombaum et al., 2013). The large geographic distribution of these organisms, extending from the equator to subpolar waters, is largely attributable to their extensive genetic and functional diversity (Zwirglmaier et al., 2008; Farrant et al., 2016; Doré et al., 2020). Amongst the nearly 20 clades within subcluster (SC) 5.1, the most abundant and diversified *Synechococcus* lineage in oceanic ecosystems (Dufresne et al., 2008; Scanlan et al., 2009; Ahlgren and Rocap, 2012), only four (clades I, II, III, and IV) were thought to largely dominate *in situ*. Clades I and IV mainly thrive in temperate and cold, nutrient-rich waters, while clades II and III reside in warm, oligotrophic or mesotrophic areas (Zwirglmaier et al., 2008; Mella-Flores et al., 2011), suggesting the existence of cold (I/IV) and warm (II/III) *Synechococcus* "thermotypes." This hypothesis was subsequently confirmed by work demonstrating that strains representative of these different clades exhibit distinct thermal *preferenda* (Mackey et al., 2013; Pittera et al., 2014; Breton et al., 2020; Six et al., 2021), a feature notably linked to differences in the thermostability of light-harvesting complexes (Pittera et al., 2017), lipid desaturase gene content (Pittera et al., 2018) and the ability of some strains to induce photoprotective light dissipation at colder temperatures using the orange carotenoid protein (OCP; Six et al., 2021). Field studies using global ocean datasets have allowed to refine the respective ecological niches of the different thermotypes, with clade I extending further north than clade IV (Paulsen et al., 2016; Doré et al., 2022) and clades II and III predominating in N- and P-depleted waters, respectively, but also to highlight the importance of a fifth clade within SC 5.1, the CRD1 clade (Farrant et al., 2016; Sohm et al., 2016; Kent et al., 2019). Initially thought to be limited to the Costa Rica dome area (Saito et al., 2005; Gutiérrez-Rodríguez et al., 2014), the latter clade was recently found to be a major component of *Synechococcus* communities in iron (Fe)-depleted areas (Farrant et al., 2016; Sohm et al., 2016; Ahlgren et al., 2020). Furthermore, analysis of the global distribution of these organisms using high-resolution marker genes has highlighted large within-clade microdiversity associated with niche differentiation in marine *Synechococcus* (Farrant et al., 2016; Larkin and Martiny, 2017; Xia et al., 2019), as also observed in *Prochlorococcus* (Kashtan et al., 2014; Larkin et al., 2016). Using the *petB* gene encoding cytochrome b_6, Farrant et al. (2016) showed that most major clades encompassed several Ecologically Significant Taxonomic Units (ESTUs), i.e., genetically related subgroups within clades occupying distinct oceanic niches. This is notably the case for ESTU IIB that occupies a cold thermal niche in sharp contrast with IIA, the dominant ESTU within clade II that occupies warm, mesotrophic, and oligotrophic Fe-replete waters. Similarly, three distinct ESTUs with distinct thermal niches were identified within the CRD1 clade and the co-occurring clade EnvB (a.k.a. CRD2; Ahlgren et al., 2020): (i) CRD1B/EnvBB are found in cold mixed waters in co-occurrence with ESTUs IA, IVA and IVC, (ii) CRD1C/EnvBC dominate in warm, high-nutrient low-chlorophyll (HNLC) regions such as the central Pacific Ocean, and (iii) CRD1A/EnvBA are present in both environments and thus span a much wider range of temperatures than CRD1B and C (Farrant et al., 2016). This suggests that these three CRD1 ESTUs could correspond to different thermotypes.

In order to test this hypothesis, we used strains representative of each of the three CRD1 ESTUs to determine the fundamental thermal niches of these organisms as compared to typical cold (clades I and IV) and warm (clades II and III) thermotypes. Furthermore, given the strong influence of temperature on optimal functioning of the photosynthetic apparatus in marine *Synechococcus* (Pittera et al., 2014, 2017; Guyet et al., 2020), we also examined the effect of temperature acclimation on the photophysiology of CRD1 ESTUs compared to their clade I and IV counterparts and show that CRD1 thermotypes actually differ more strongly in this respect to members of clades I–IV than from each other.

MATERIALS AND METHODS

Strains and Growth Conditions

The eight *Synechococcus* spp. strains used in this study were retrieved from the Roscoff Culture Collection (RCC[1]), including representative strains of the three known CRD1 ESTUs (CRD1A—C) and one or two of each of the four dominant clades in the field (clades I—IV) used as controls (**Table 1** and **Supplementary Figure 1**). Cells were grown in 50 mL flasks (Sarstedt, Germany) in PCR-S11 culture medium (Rippka et al., 2000) supplemented with 1 mM sodium nitrate. Cultures were acclimated for at least 2 weeks in temperature-controlled chambers across a range of temperatures dependent on the thermal tolerance of each strain and under a continuous light of 75 μmol photons m^{-2} s^{-1} (hereafter μE m^{-2} s^{-1}) provided by a white-blue-green LED system (Alpheus, France). For each experiment, cultures were grown in triplicate, inoculated at an initial cell density of ∼3 × 10^6 cells mL^{-1}, and samples were harvested daily to measure growth rate and fluorescence parameters as described below.

In order to compare the capacity of strains to repair the D1 subunit of photosystem II (PSII; see "Measurement of PSII Repair Rate" section), cultures grown in 250 ml flasks at 75 μE m^{-2} s^{-1} were acclimated at 18, 22, and 25°C, temperatures at which all strains were able to grow, were subjected to high light stress (375 μE m^{-2} s^{-1}). Exponentially growing cultures were sampled at T0 and after 15, 30, 60, and 90 min of stress, before shifting cultures back to the initial light conditions and then sampling again after 15, 30, 60 min, and 24 h of recovery (R). While D1 repair measurements were performed at all-time points, cell concentrations were measured by flow cytometry only at T0, T30 min, T90 min, R30 min, and R24 h and liposoluble pigment content was determined only at T0.

[1]https://roscoff-culture-collection.org/

TABLE 1 | Characteristics of the *Synechococcus* strains used in this study.

Strains name	MVIR-18-1	A15-62	M16.1	WH8102	BL107	BIOS-E4-1	BIOS-U3-1	MITS9220
RCC #[a]	2,385	2,374	791	539	515	2,534	2,533	2,571
Subcluster[b]	5.1	5.1	5.1	5.1	5.1	5.1	5.1	5.1
Clade[b]	I	II	II	III	IV	CRD1	CRD1	CRD1
ESTU[b]	IA	IIA	IIA	IIIA	IVA	CRD1C	CRD1B	CRD1A
Pigment type[c]	3aA	3dB	3a	3c	3dA	3cA	3dA	3dA
Ocean	Atlantic	Atlantic	Atlantic	Atlantic	Med. Sea	Pacific	Pacific	Pacific
Region	North Sea	Offshore Mauritania	Gulf of Mexico	Caribbean Sea	Balearic Sea	South East Pacific	Chile upwelling	Equatorial Pacific
Isolation latitude	61°00' N	17°37' N	27°70' N	22°48' N	41°72' N	31°52' S	34°00' S	0°00' N
Isolation longitude	1°59' E	20°57' W	91°30' W	65°36' W	3°33' E	91°25' W	73°22' W	140°00' W

[a]*Roscoff Culture Collection*, [b]*Farrant et al. (2016)*, [c]*Humily et al. (2013)*.

Flow Cytometry

Culture aliquots (200 μl) sampled for flow cytometry were fixed using 0.25% (v/v) glutaraldehyde (grade II, Sigma Aldrich, United States) and stored at −80°C until analysis (Marie et al., 1999). Cell concentrations were estimated using a Guava easyCyte flow cytometer (Luminex Corporation, United States) and maximum growth rates (μ_{max}) were calculated as the slope of the linear regression of ln (cell density) vs. time during the exponential growth phase. *Synechococcus* cells were identified based on their red (695 nm) and orange (583 nm) fluorescence, proxies for their chlorophyll *a* and phycoerythrin content, respectively. Fluorescence, forward scatter and side scatter values were normalized to that of standard 0.95 μm beads using Guavasoft software (Luminex Corporation, United States).

Fluorescence Measurements

The maximum PSII quantum yield (F_V/F_M) was estimated using a Pulse Amplitude Modulation fluorimeter (Phyto-PAM II, Walz, Germany) during the exponential growth phase after 10 min dark acclimation followed by addition of 100 μM of the PSII blocker 3-(3,4-dichlorophenyl)-1,1-dimethylurea (DCMU, Sigma-Aldrich, United States; Campbell et al., 1998).

The PSII quantum yield was calculated as:

$$F_V/F_M = (F_M - F_0)/F_M$$

where F_0 is basal fluorescence, F_M maximal fluorescence level and F_V variable fluorescence (Campbell et al., 1998; Six et al., 2007).

Fluorescence excitation (with emission set at 580 nm) and emission (with excitation set at 530 nm) spectra were generated using a LS-50B spectrofluorometer (Perkin-Elmer, United States) as described in Six et al. (2004). The fluorescence excitation ratio ($Exc_{495:550\ nm}$) was used as a proxy for the PUB:PEB ratio. Phycobilisome (PBS) rod length and the degree of coupling of the PBS to PSII reaction center chlorophylls was then assessed using fluorescence emission spectra by calculating the phycoerythrin (PE, F_{max} = 565–575 nm) to phycocyanin (PC, F_{max} = 645–655 nm) ratio as well as the PC to PBS terminal acceptor (TA; F_{max} = 680 nm) ratio, respectively (Pittera et al., 2017).

Pigment Analyses

Triplicate cultures were harvested during the exponential phase when F_V/F_M was maximum for each temperature condition. Cultures (50 mL) were subjected to centrifugation in the presence of 0.01% (v/v) pluronic acid (Sigma-Aldrich, Germany) at 4°C, 14,000 × g for 7 min, using an Eppendorf 5804R (Eppendorf, France). Pellets were resuspended and transferred to 1.5 ml Eppendorf tubes and centrifuged at 4°C, 17,000 × g for 2 min using an Eppendorf 5417R centrifuge (Eppendorf, France). Once the supernatant was removed samples were stored at −80°C until further analysis. Pigment content was subsequently assessed using calibrated high-performance liquid chromatography (HPLC 1100 Series System, Hewlett Packard, St Palo Alto, CA), as previously described (Six et al., 2005).

Measurement of the Photosystem II Repair Rate

Each culture acclimated to 75 μE m^{-2} s^{-1} and 18, 22 or 25°C was split into two new 50 mL flasks (Sarstedt Germany) with one used as a control and the other flask supplemented with lincomycin (0.5 mg mL^{-1} final concentration, Sigma-Aldrich, United States) in order to inhibit protein synthesis and thus D1 repair (Guyet et al., 2020). Both sub-cultures were then subjected to light stress by exposing cultures to 375 μE m^{-2} s^{-1} continuous light (at the same temperature), and F_V/F_M measured at different time points as described above. The PSII repair rate for each strain at each temperature was determined from the coefficient differences between the exponential curves fitted over the 90 min time course of F_V/F_M measurements for control and +lincomycin samples. This light stress experiment was replicated on four independent cultures.

Determination of the Realized Environmental Niches of Major *Synechococcus* Ecologically Significant Taxonomic Units

The realized niches of CRD1 and clades I-IV ESTUs were determined using *petB* reads extracted from metagenomic data from the *Tara* Oceans and *Tara* Polar circle expeditions, the Ocean Sampling Day (OSD; June 21st 2014) campaign, and *petB* metabarcodes from (i) various oceanographic cruises (CEFAS,

BOUM, Micropolar, RRS Discovery cruise 368 and several in the northwestern Pacific Ocean as detailed in Xia et al., 2017), (ii) two individual sampling sites in the Mediterranean Sea (Boussole, Point B) as well as (iii) a bi-monthly sampling at the long-term observatory site SOMLIT ("Service d'Observation en Milieu Littoral")-Astan located 2.8 miles off Roscoff between July 2009 and December 2011 (**Supplementary Table 1**).

petB metagenomic recruitment using the *Tara* and OSD datasets was performed as described previously (Farrant et al., 2016). *Synechococcus petB* sequences from both metagenomes and metabarcodes were used to define operational taxonomic units (OTUs) at 97% identity using Mothur v1.34.4 (Schloss et al., 2009) that were then taxonomically assigned using a *petB* reference database (Farrant et al., 2016). OTUs encompassing more than 3% of the total *Synechococcus* reads for a given sample were grouped into ESTUs and used to determine the whole temperature range occupied by each of the five major *Synechococcus* ESTUs.

Comparative Genomics

The Cyanorak *v2.1* information system (Garczarek et al., 2021)[2] was used to compare the phyletic pattern i.e., the presence/absence pattern of each cluster of likely orthologous genes (CLOG) in each strain, for CRD1 strains and their clades I-IV counterparts for a number of selected genes potentially involved in adaptation to low temperature based on previous literature (see section "Results").

RESULTS

The Fundamental Thermal Niches of CRD1 vs. Clades I–IV Strains

In order to determine the temperature optima and boundary limits of the different CRD1 strains and to compare them to those of typical cold and warm *Synechococcus* thermotypes, representative strains of each of the three CRD1 ESTUs and strains of clades I, II, III, and IV were grown over a range of temperatures from 6 to 36°C. The growth responses of all strains to temperature followed a typical asymmetric bell-shaped curve over the selected temperature range (**Figure 1**), with a progressive rise in growth rate (μ) until T_{opt} (the temperature associated with maximum μ: μ_{max}) was reached, and a sharp decline above T_{opt}. BIOS-U3-1 (CRD1-B) was able to grow between 12 and 29°C with a T_{opt} at 25°C ($\mu_{max} = 0.78 \pm 0.02\ d^{-1}$), a growth pattern most similar to that of the clade IV strain BL107, while the clade I strain MVIR-18-1 was able to grow at much lower temperatures, down to 8°C but could not grow above 25°C (**Figure 1A**). MITS9220 (CRD1-A) and BIOS-E4-1 (CRD1-C) displayed thermal growth characteristics more similar to the clade II (A15-62 and M16.1) and III (WH8102) strains, representatives of warm thermotypes (**Figure 1B**). While most strains in this category displayed a minimal growth temperature of 16°C, large variations between strains were observed at the highest thermal boundary limit (T_{max}). Maximum growth temperature was obtained for M16.1 (II; T_{max}: 34°C), then A15-62 (II) and WH8102 (III; both with T_{max} at 32°C), MITS9220 (CRD1-A; T_{max}: 31°C) and finally for BIOS-E4-1 (CRD1-C; T_{max}: 30°C). The latter strain also displayed the highest minimal growth temperature (T_{min}: 18°C) and thus possesses the narrowest temperature range for growth of all the strains studied (12°C vs. 15–18°C). It is also worth noting that CRD1 strains display a lower maximum growth rate and more generally lower growth rates at most temperatures than their clade I, II, III, and IV counterparts.

[2]http://www.sb-roscoff.fr/cyanorak/

The Environmental Realized Niches of CRD1 vs. Clades I–IV Strains

We then compared the fundamental thermal niches of all studied strains, i.e., the whole temperature range over which they can grow in a laboratory setting in the absence of biotic interactions (e.g., competition or predation), with environmental realized niches (*sensu* Pearman et al., 2008) of the corresponding ESTUs. For this, we determined the distribution limits of each of these ESTUs along the *Tara* Oceans and *Tara* Polar circle transects, 203 samples from OSD2014 and additional oceanographic cruises and individual sampling sites, altogether encompassing 413 samples worldwide covering a wide range of temperature conditions (**Figure 1**, **Supplementary Figure 2**, and **Supplementary Table 1**). This made it possible to have much finer estimates of the limits of the thermal niches of the different ESTUs than in the study performed by Farrant et al. (2016), in particular for the cold adapted ESTUs, which were poorly represented in the initial *Tara* Oceans dataset (**Supplementary Figure 2**).

This analysis showed that the CRD1B ESTU displayed a reduced thermal tolerance range in the environment (14–24.5°C) compared to the BIOS-U3-1 strain in culture (12–29°C), while the typical cold thermotypes colonized larger thermal niches *in situ* than their representative strains (**Figure 1A**). Environmental realized niches indeed ranged from 2.5 to 24°C for ESTU IA (compared to 8–25°C for MVIR-18-1) and from 8.5 to 25°C for ESTU IVA (compared to 12–29°C for BL107). Interestingly, the median temperature of the CRD1B ESTU is 3°C higher than that observed for ESTUs IA and IVA.

As concerns warm thermotypes, CRD1C displayed a fairly narrow thermal tolerance range *in situ* (22–29.5°C), which, similar to the cold thermotype CRD1B, was even narrower than for its representative strain BIOS-E4-1 (18–30°C; **Figure 1B**). Comparatively, the CRD1A ESTU was detected across a wider temperature range (14–30.5°C) than the other two CRD1 ESTUs and also slightly larger than the corresponding strain in culture (MITS9220, 16–31°C). Still, the most extended temperature range was observed for ESTU IIA and IIIA (12–32°C) that reached significantly lower temperature limits than the corresponding clade II (16 to 32–34°C) and III (16–32°C) strains. Of note, although both IIA and IIIA ESTUs displayed a similar temperature range, the median temperature of ESTU IIA (25°C) was about 3°C higher than that of ESTU IIIA (22°C) and the maximum median temperature was surprisingly observed for the CRD1C ESTU (26.5°C). In this context, it

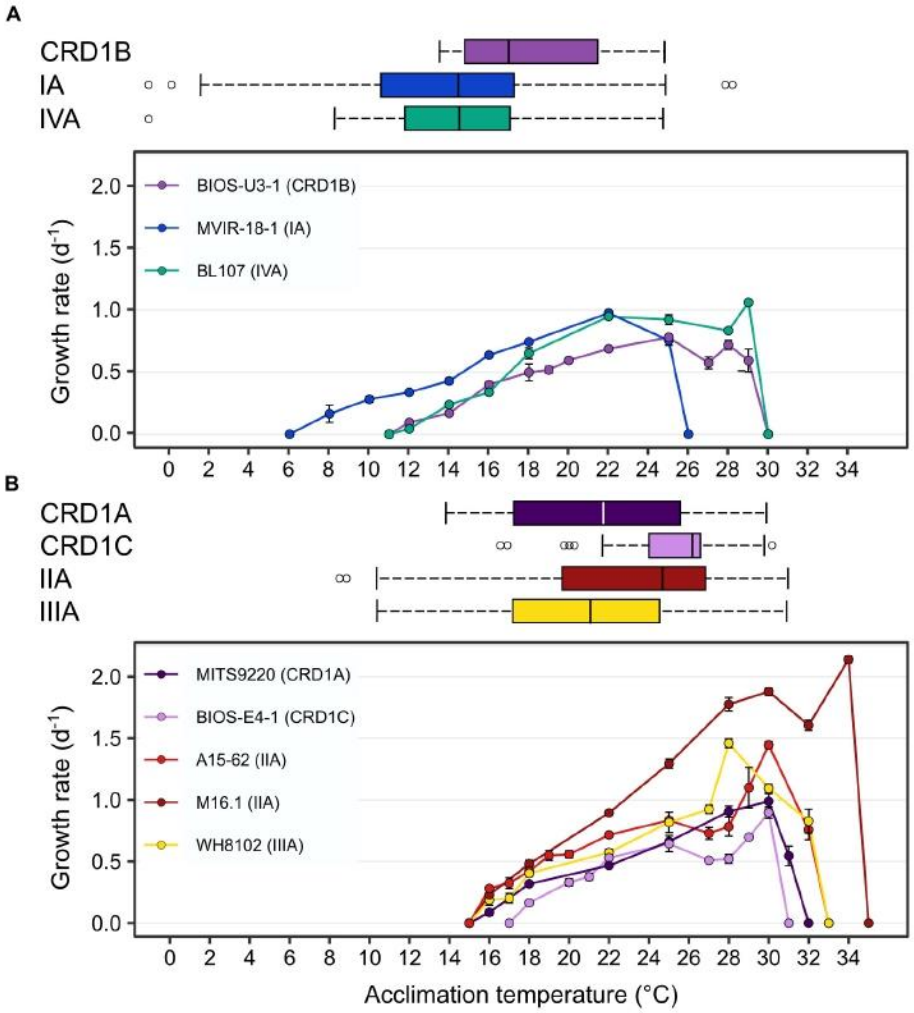

FIGURE 1 | Fundamental thermal niches of CRD1 vs. clade I, II, III, and IV strains and environmental realized niches of the corresponding ESTUs. **(A)** CRD1-B strain BIOS-U3-1 vs. cold thermotypes. **(B)** CRD1-A strain MITS9220 and the CRD1-C strain BIOS-E4-1 vs. warm thermotypes. The insert indicates the strain names and their corresponding ESTU (*sensu* Farrant et al., 2016) between brackets. Each data point is the average of at least 3 biological replicates. Environmental realized niches are indicated as horizontal boxplots for each ESTU above each graph with the whiskers corresponding to 1.5-fold the interquartile range and outliers being plotted as individual points.

is also worth mentioning that although clade II strains are clearly both warm thermotypes, M16.1 displays a significantly higher temperature limit for growth than A15-62 and more generally than all other strains. This suggests that ESTU IIA may encompass two distinct ESTUs, but such a high temperature niche (>32°C) where they could be discriminated is exceptional and not available in our dataset (**Supplementary Table 1**).

Comparative Genomics

In order to assess whether the cold, temperate thermotype BIOS-U3-1 (CRD1B) exhibits similar adaptation mechanisms to those previously described for the cold-adapted clades I and/or IV, we examined a number of clusters of likely orthologous genes (CLOGs) from all *Synechococcus* genomes belonging to clades I-IV and CRD1 present in the Cyanorak *v2.1* information system (Garczarek et al., 2021). First, we looked for the occurrence of two amino-acid substitutions in phycocyanin α- (RpcA) and β-subunits (RpcB), which were shown to differ between cold- (Gly in clades I and IV for RpcA43; Ser in RpcB42) and warm-thermotypes (Ala in clades II and III for RpcA43; Asp in RpcB42), these substitutions being potentially responsible for the differential thermotolerance of this phycobiliprotein between thermotypes (Pittera et al., 2017). In all three CRD1 strains, both sites displayed the warm-type residue (**Supplementary Figures 3A,B**), suggesting that in contrast to typical cold and warm thermotypes, the molecular flexibility of this phycobiliprotein does not differ between CRD1 thermotypes. We then looked at fatty acid desaturases that are essential for regulating membrane fluidity and thus the activity of integral membrane proteins, including photosynthetic complexes (Mikami and Murata, 2003; Pittera et al., 2018; Breton et al., 2020). All three CRD1 strains surprisingly possess in addition

to the core Δ9-desaturase gene *desC3*, a second Δ9-desaturase, *desC4* (**Supplementary Table 2**), previously thought to be specific to cold-adapted strains as well as the Δ12-desaturase *desA3* found in both cold-adapted clades I and IV as well as in clade III, a warm thermotype subjected to much stronger seasonal variability than its (sub) tropical clade II counterparts (Pittera et al., 2018). Furthermore, BIOS-U3-1 also possesses *desA2*, thought to be specific to warm environments, while this gene is in contrast absent from the other two CRD1 warm-adapted strains. Thus, CRD1 strains exhibit a different desaturase gene set and potentially display a larger capacity to regulate membrane fluidity than typical cold- or warm-adapted thermotypes. Finally, while all clades I, III and IV genomes possess the *ocp* operon, involved in the protection of PSII against photoinactivation through the dissipation of excess light energy (Kirilovsky, 2007) and which was recently shown in marine *Synechococcus* to play a key role at low temperature (Six et al., 2021), none of the three CRD1 genomes possess this operon.

Photosynthetic Activity and Pigment Content

PSII quantum yield (F_V/F_M), used as a proxy of photosynthetic activity, was measured for each strain over their whole temperature growth range. Most strains displayed a decrease in this parameter at both low and high boundary limits of their growth temperature range and this effect was particularly striking for BIOS-U3-1, reaching values down to 0.11 at 14°C and 0.32 at 28°C (**Figure 2A**). Besides MVIR-18-1 that exhibited a quite constant F_V/F_M over its whole temperature range, the decrease in F_V/F_M at high temperature was stronger for cold than warm thermotypes that are able to maintain a quite high F_V/F_M in the warmest growth conditions (**Figure 2B**). Finally, as for growth rate, CRD1 strains exhibited lower F_V/F_M at all temperatures than clade I to IV strains.

The $Exc_{495:550nm}$ fluorescence excitation ratio, used as a proxy for PUB:PEB ratio, was consistent with the pigment type of each strain (Humily et al., 2013; **Table 1** and **Supplementary Figure 4A**). This ratio remained pretty constant over the whole temperature range for all strains except for the chromatic acclimator BL107 (pigment type 3dA), for which a sharp increase was observed at its maximal growth temperature (28°C) to reach a value (1.35) intermediate between that typically observed in green light (or white light; 0.6–0.7) and blue light (1.6–1.7). This suggests that the chromatic acclimation process could be affected by growth temperature, at least in this strain. The phycobilisome (PBS) rod lengths and the degree of coupling of PBS to PSII reaction center chlorophylls, as estimated from PE:PC and PE:TA ratios, respectively, showed fairly limited variations over the temperature range, indicating that the phycobiliprotein composition of PBS is quite stable over the growth temperature range of each strain (**Supplementary Figures 4B,C**). One notable exception was a rise in both ratios for strain A15-62 at its minimal growth temperature, likely attributable to the partial decoupling of individual phycobiliproteins and of the whole PBS from PSII, a phenomenon typically observed under stressful conditions (Six et al., 2007; Guyet et al., 2020). It is also worth noting that MITS9220 and to some extent BIOS-E4-1, exhibited a significantly higher PE:PC ratio than the five other strains, potentially indicating a different phycobiliprotein composition and/or length of PBS rods.

In terms of liposoluble pigments, the β-carotene/chlorophyll *a* (β-car/Chl *a*) ratio tended to increase with temperature in BIOS-E4-1 and MITS9220, as observed for the other warm thermotypes, whilst this ratio was more stable in the cold thermotypes BIOS-U3-1 and BL107, and seemed to slightly increase in the lower part of the thermal range for the clade I strain MVIR-18-1 (**Figure 3**). For all strains, these ratios result from a concomitant increase with temperature of Chl *a* and β-car content per cell (**Supplementary Figure 5**), indicating an enhancement of the surface of thylakoids per cell at higher temperatures that was particularly marked for BIOS-E4-1 and A15-62, whilst this variation was fairly limited in the other two CRD1 strains. As these two pigments are present in different proportions in PSI and II (Umena et al., 2011; Xu and Wang, 2017), the higher β-car/Chl *a* ratio measured in clades I and IV strains also suggests that they may have a higher PSII:PSI ratio than all other strains, including BIOS-U3-1, and that this ratio might be more strongly affected by temperature in warm than cold thermotypes.

As concerns the zeaxanthin/chlorophyll *a* (Zea/Chl *a*) ratio, although an increase in this ratio was measured at low temperature for all strains, the amplitude was globally larger for cold than for warm thermotypes, with BIOS-U3-1 behaving very similarly to the clade IV strain BL107 that exhibits the largest variation in this ratio (**Figure 3**). Changes in this ratio likely originate partially from the decrease in Chl *a* content in response to cold, a strategy typically used by cells to regulate light utilization under slow growth conditions (Inoue et al., 2001). However, several strains also displayed an increase in their Zea content per cell at low temperature, a response particularly striking in BIOS-U3-1 and A15-62, but that also seems to occur in M16.1 and in the two other CRD1 strains BIOS-E4-1 and MITS9220 (**Supplementary Figure 5**). Thus, although Zea has been hypothesized to be involved in the photoprotection of cold-adapted strains by dissipating excess light energy under low temperature conditions (Kana et al., 1988; Breton et al., 2020), this process seems to be present in both cold and warm-adapted CRD1 strains and in most warm thermotypes as well. In this context, it is also worth noting that the two clade II strains, A15-62 and M16.1, displayed fairly distinct temperature-induced variations in their Zea:Chl *a* ratios and individual pigment contents, possibly linked to their different isolation temperatures (see section "Discussion" below).

Photosystem II Repair Capacity

The ability of the different strains to repair PSII in response to light stress (375 $\mu E\ m^{-2}\ s^{-1}$) was determined in cultures acclimated to 18, 22, and 25°C by measuring changes in $F_V:F_M$ over time after adding the protein synthesis inhibitor lincomycin, or not (**Supplementary Figure 6**). While a decrease in $F_V:F_M$ ratio during the 90 min light stress period was observed in both cultures supplemented with lincomycin and controls, this ratio

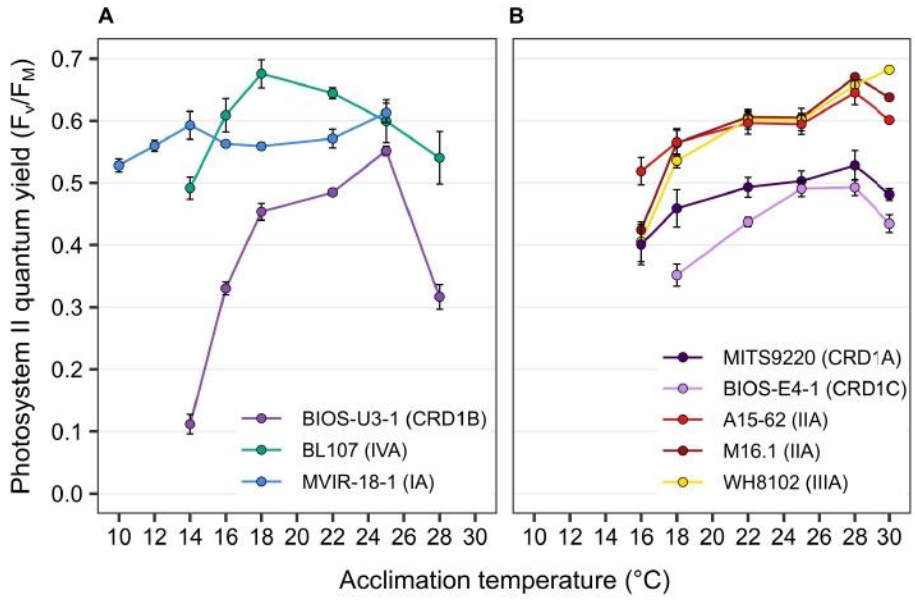

FIGURE 2 | Variation with growth temperature of photosystem II quantum yield (F_V/F_M) for CRD1 vs. clade I, II, III, and IV strains. **(A)** CRD1-B strain BIOS-U3-1 vs. cold thermotypes. **(B)** CRD1-A strain MITS9220 and the CRD1-C strain BIOS-E4-1 vs. warm thermotypes. The insert indicates the strain names and their corresponding ESTU (*sensu* Farrant et al., 2016) between brackets.

only re-increased back up to initial F_V:F_M values, after shifting cultures back to standard light conditions (75 μE m^{-2} s^{-1}), in the control group in most strains and temperature conditions. Thus, all studied strains were able to recover from this light stress, as long as the D1 repair cycle was not inactivated by inhibition of protein synthesis. Yet, a fast decrease in F_V:F_M was observed for all three CRD1 cultures supplemented with lincomycin, while the +/− lincomycin curves overlapped during the first 15–30 min of light stress in most other strains and conditions. This suggests that the initial decrease in F_V:F_M in clades I–IV strains was not due to D1 damage but rather to dissipation of light energy as heat through non-photochemical quenching (Campbell et al., 1998), whilst the damage and hence repair of D1 proteins only occurred later on.

The PSII repair rate (R_{PSII}), as calculated from the time course of F_V:F_M with and without lincomycin, increased with temperature in most strains, except for BIOS-U3-1 that displayed its highest rate at 22°C (**Figure 4**). Strikingly, all three CRD1 strains displayed significantly higher R_{PSII} than clade I-IV strains at all three tested temperatures, a difference ranging from 3- to nearly 40-fold at the lowest common temperature (18°C). Furthermore, CRD1 strains displayed fairly limited variation in R_{PSII} with temperature (ranging from 1.33 to 1.87-fold) compared to the other strains, the strongest increase in R_{PSII} being observed for the clade I strain MVIR-18-1 (21.5-fold) and the clade III strain WH8102 (5.5-fold). This indicates that CRD1 strains exhibit a constitutively high level of PSII repair compared to the other strains whatever the growth temperature and only trigger a moderate increase in R_{PSII} in response to temperature variations.

DISCUSSION

Temperature constitutes one the strongest driving factors that have shaped genetic diversification and niche partitioning in marine cyanobacteria (Scanlan et al., 2009; Flombaum et al., 2013; Biller et al., 2015) and phytoplankton at large (Sunagawa et al., 2015; Delmont et al., 2020). While temperature has caused one major diversification event in *Prochlorococcus*, resulting in the divergence of the cold-adapted HLI from the warm-adapted HLII clades (Johnson et al., 2006; Kettler et al., 2007), several independent temperature-related diversification events also occurred in the *Synechococcus* SC 5.1 radiation, leading to the emergence of clades I and IV (Dufresne et al., 2008; Zwirglmaier et al., 2008). Here, determination of the temperature optimum and boundary limits (i.e., the fundamental niche) of strains representative of the three CRD1 ESTUs identified in the field (Farrant et al., 2016) showed that different thermotypes can also be delineated within the CRD1 clade, which dominates the *Synechococcus* populations in low-Fe areas of the world Ocean. Comparison with representative strains of the cold-adapted *Synechococcus* ecotypes (clades I and IV) on the one hand, and warm-adapted ecotypes (clades II and III) on the other, made it possible to classify (i) the CRD1A strain MITS9220, isolated from the equatorial Pacific Ocean, as a warm thermotype, (ii) the CRD1B strain BIOS-U3-1, isolated from the Chilean upwelling, as a cold temperate thermotype, and finally (iii) the CRD1C strain BIOS-E4-1, isolated from the edge of the South Pacific gyre, a stable, warm, Fe-depleted oceanic region (Claustre et al., 2008), as a warm temperate stenotherm.

As expected from theory (Pearman et al., 2008), the realized environmental thermal niches of CRD1 ESTUs were narrower

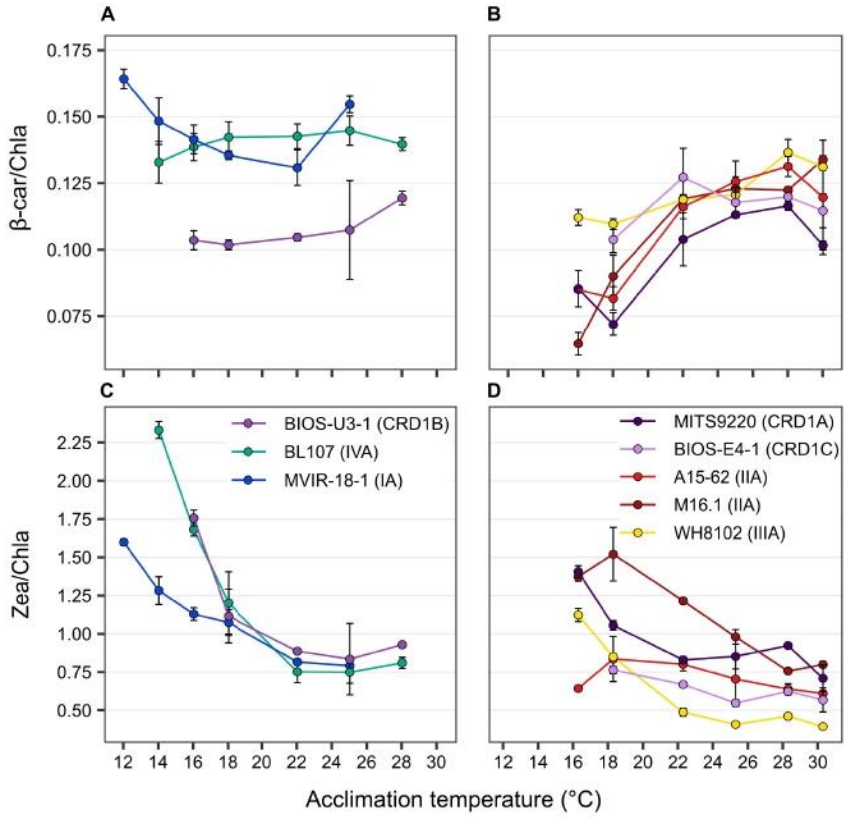

FIGURE 3 | Variation with growth temperature of cellular mass pigment ratios of CRD1 vs. clade I, II, III, and IV strains. **(A,B)** β-carotene (β-car) to chlorophyll *a* (Chla) ratio. **(C,D)** Zeaxanthin (Zea) to Chl*a* ratio with **(A,C)** CRD1-B strain BIOS-U3-1 vs. cold thermotypes and **(B,D)** CRD1-A strain MITS9220 and the CRD1-C strain BIOS-E4-1 vs. warm thermotypes. Inserts indicate strain names and their corresponding ESTUs (*sensu* Farrant et al., 2016) between brackets.

than their fundamental niches (or similar for MITS9220). In contrast, for ESTUs IA to IVA, the realized environmental niche was significantly more extended toward the low thermal limit than the fundamental niches of their representative strains, this expansion being particularly marked for ESTU IA (**Figure 1**). This could be due to passive transport of *Synechococcus* populations by currents into water masses colder than their temperature limits for growth. Alternatively, these ESTUs may exhibit a greater microdiversity than previously assessed (Farrant et al., 2016) and could be subdivided into distinct ESTUs occupying slightly different thermal niches from the current ones, although representative strains to test this hypothesis remain to be isolated. In agreement with the latter hypothesis, Paulsen et al. (2016) measured a positive growth rate of *Synechococcus* natural populations dominated by clade I in waters as cold as 2°C in the vicinity of the Svalbard island. Thus, CRD1 ESTUs appear to be strongly outcompeted by their ESTU IA to IVA counterparts at their lower temperature limits. Consistent with this, comparison of their gene content showed that CRD1 ESTUs, including the cold thermotype CRD1B, lack the main adaptation mechanisms reported so far for typical cold thermotypes. Indeed, all CRD1 strains examined in this study (i) exhibit warm-type substitutions in their α and β-phycocyanin subunits, influencing the thermotolerance of this phycobiliprotein (Pittera et al., 2017; **Supplementary Figures 3A,B**); (ii) possess a different set of desaturase genes, involved in regulation of membrane fluidity (Pittera et al., 2018), than typical warm and cold thermotypes (**Supplementary Table 2**) and (iii) lack the OCP system, involved in the protection of PSII against photoinactivation, which seemingly plays a key role at low temperature (Kirilovsky, 2007; Six et al., 2021). Still, we cannot exclude that CRD1 strains could use alternative strategies to cope with temperature variations and notably to deal with the generation of reactive oxygen species, known to be generated by a variety of factors including low and high temperature (Nishiyama et al., 2006; Latifi et al., 2009). For instance, all CRD1 strains possess the *srxA* gene encoding sulfiredoxin catalyzing the reduction of 2-Cys peroxiredoxin involved in H_2O_2 detoxification (Findlay et al., 2005; Guyet et al., 2020) as well as *isiA* that, besides its role in increasing the light-harvesting efficiency of PSI under conditions of Fe-limitation, was also shown to provide photoprotection to PSII by dissipating excess light energy under oxidative stress conditions (Yeremenko et al., 2004; Ihalainen et al., 2005; **Supplementary Table 2**).

The ability of cyanobacteria to grow over a large temperature range largely relies on their capacity to optimize the functioning of their photosynthetic apparatus, notably at low temperature that induces a general slowing down of cell metabolism (Murata et al., 2007; Pittera et al., 2014, 2017). For this reason, we

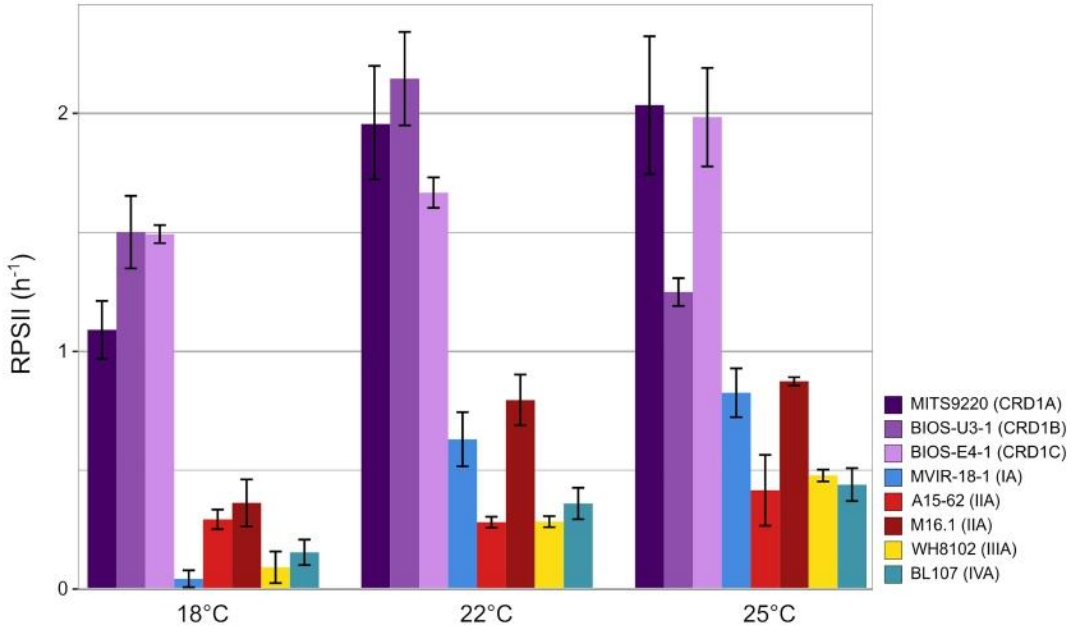

FIGURE 4 | Variation with growth temperature of cumulative photosystem II repair rate (RPSII) of CRD1 vs. clade I, II, III, and IV strains. The insert indicates the strain names and their corresponding ESTU (*sensu* Farrant et al., 2016) between brackets.

also compared the photophysiology of CRD1 and clades I-IV strains at three growth temperatures common to all strains. These analyses showed that all three CRD1 strains exhibit a lower growth rate at most temperatures than clade I to IV strains (**Figure 1**), possibly explaining why they are easily outcompeted by other taxa when Fe is no longer limiting, as observed for instance around the Marquesas Islands (Caputi et al., 2019). Moreover, CRD1 strains also display a lower PSII maximum quantum yield (**Figure 2**), suggesting that PSII is partially photoinactivated, that is their D1 repair cycle does not fully compensate damage to this protein, even under optimal growth temperatures. Consistent with this, the very high turnover rate of the D1 protein measured in all CRD1 strains indicates that their PSII is much more sensitive to light stress than other strains and can only trigger a moderate increase in R_{PSII} in response to both light and temperature variations, possibly indicating that they are adapted to live deeper in the water column than clades I to IV. This sensitivity could be partially linked to the abovementioned absence of the OCP, potentially reducing their ability to dissipate excess light energy, although it must be noted that the clade II strain A15-62 also lacks the OCP system. Interestingly in this context, all cold thermotypes including the CRD1B strain BIOS-U3-1, possess more copies of the D1:2 isoform (3–6 copies, average: 3.9 ± 1.1) than warm thermotypes (2–3 copies, average: 2.2 ± 0.4), this isoform providing a lower quantum yield but higher PSII resistance to photoinhibition than D1:1 (**Supplementary Table 2**; Clarke et al., 1993a,b; Campbell et al., 1995; Garczarek et al., 2008). Moreover, A15-62 is one of the only *Synechococcus* strains to possess two complete copies of the D1:1 isoform, a duplication which could partly explain why, despite the absence of OCP, this atypical clade II strain is able to maintain a high PSII quantum yield over its whole growth temperature range with fairly low D1 repair rates. Interestingly, CRD1 strains also possess a paralog of *psbN*, which was found to be required for the assembly of the PSII reaction center in *Nicotiana tabacum* and would play an important role in the D1 repair cycle (Torabi et al., 2014).

Taken together, both comparative genomics and photophysiological analyses highlighted a number of specificities of CRD1 strains compared to their clade I-IV counterparts, rather than them possessing traits distinctive of cold or warm thermotypes. In this context, it is worth noting that although strains representative of ESTUs IVA and CRD1B exhibit a similar fundamental thermal niche in culture, the higher median temperature of CRD1B in the field indicates that it preferentially thrives in temperate waters (about 18°C, **Figure 1**), where energetically costly temperature adaptation mechanisms might not be essential. This suggests that for members of the CRD1 clade, adaptation to low-Fe conditions likely prevails over adaptation to temperature variations, and/or that adaptation mechanisms to temperature variations might be more complex and diversified than previously thought. Still, in terms of a realized environmental thermal niche, the occurrence of several CRD1 thermotypes likely explains why the CRD1 clade as a whole occupies most Fe-limited areas, a vast ecosystem constituting about 30% of the world Ocean (Moore et al., 2013; Bristow et al., 2017). A notable exception is the Southern Ocean, for which from the little available data shows that *Synechococcus* is scarce south of the polar front (Wilkins et al., 2013; Farrant et al., 2016), consistent with the fairly high low-temperature limit (14°C) of the CRD1B environmental realized niche (**Figure 1**), while low-Fe availability likely limits the growth

of clades I and IV in this area. In contrast, CRD1 growth does not currently appear to be limited by warm temperatures since most oceanic waters display a temperature below 30°C (**Supplementary Figure 2B** and **Supplementary Table 1**). However, one cannot exclude that with global change, some areas of the world Ocean could become warmer than the highest limits determined here for representative strains of CRD1A and C, i.e., 31 and 30°C, respectively. In this context, it is worth mentioning that in the dataset used for this study, several coastal stations, sampled during the OSD campaign reached 31.5°C (**Supplementary Table 1**). Thus, although biogeochemistry global models predict that *Synechococcus* could be one of the winners of the phytoplankton community in a future world Ocean (Flombaum et al., 2013; Schmidt et al., 2020; Visintini et al., 2021), it might well not be able to survive in the warmest low-Fe areas, an ecological niche that is currently expanding (Polovina et al., 2008). Although a few studies have started to analyze the genomic bases of adaptation of *Synechococcus* cells to Fe-limitation in the field (Ahlgren et al., 2020; Garcia et al., 2020), further comparative genomic and physiological studies are still needed to decipher the specific capacity of CRD1 clade members to deal with Fe-limitation which should help predict the future distribution and dynamics of *Synechococcus* taxa in the world Ocean.

DATA AVAILABILITY STATEMENT

The datasets presented in the National Center for Biotechnology Information (NCBI) repository (https://www.ncbi.nlm.nih.gov; PRJNA811120).

AUTHOR CONTRIBUTIONS

MF, HD, and LG designed the experiments. MF, LD, HD, MR, AG, FR-J, TS, LC, and GM collected the samples and performed the physiological measurements. MF and DM ran the flow cytometry analyses. FL isolated several CRD1 strains used in this study. HD, XX, DS, HL, and LG performed sequencing and bioinformatics analyses of metabarcodes. MH, EC, FP, and LG developed and refined the Cyanorak *v2.1* database. MF, HD, FP, and LG made the figures. MF, LD, HD, FP, and LG interpreted results. All authors contributed to the preparation of the manuscript, read, and approved the final manuscript.

FUNDING

This work was supported by the French "Agence Nationale de la Recherche" Programs CINNAMON (ANR-17-CE02-0014-01) and EFFICACY (ANR-19-CE02-0019) as well as the European program Assemble Plus (H2020-INFRAIA-1-2016-2017; grant no. 730984).

ACKNOWLEDGMENTS

We would like to thank Thierry Cariou for providing physico-chemical parameters from the SOMLIT-Astan station and Gwenn Tanguy (Biogenouest genomics core facility) and Monica Moniz for their sequencing of *petB* metabarcodes. We are also most grateful to Nathalie Simon for coordinating the phytoplankton time-series at the SOMLIT-Astan station, Christophe Six for technical hints on PAM fluorimetry and HPLC analyses as well as Priscillia Gourvil and Martin Gachenot from the Roscoff Culture Collection (http://roscoff-culture-collection.org/) and Florian Humily for isolating and/or maintaining the *Synechococcus* strains used in this study. We also thank the support and commitment of the *Tara* Oceans coordinators and consortium, Agnès b. and E. Bourgois, the Veolia Environment Foundation, Région Bretagne, Lorient Agglomeration, World Courier, Illumina, the EDF Foundation, FRB, the Prince Albert II de Monaco Foundation, the *Tara* schooner and its captains and crew.

SUPPLEMENTARY MATERIAL

The Supplementary Material for this article can be found online at: https://www.frontiersin.org/articles/10.3389/fmicb.2022.893413/full#supplementary-material

REFERENCES

Ahlgren, N. A., and Rocap, G. (2012). Diversity and distribution of marine *Synechococcus*: multiple gene phylogenies for consensus classification and development of qPCR assays for sensitive measurement of clades in the ocean. *Front. Microbiol.* 3:213. doi: 10.3389/fmicb.2012.00213

Ahlgren, N. A., Belisle, B. S., and Lee, M. D. (2020). Genomic mosaicism underlies the adaptation of marine *Synechococcus ecotypes* to distinct oceanic iron niches. *Environ. Microbiol.* 22, 1801–1815. doi: 10.1111/1462-2920.14893

Biller, S. J., Berube, P. M., Lindell, D., and Chisholm, S. W. (2015). *Prochlorococcus*: the structure and function of collective diversity. *Nat. Rev. Microbiol.* 13, 13–27. doi: 10.1038/nrmicro3378

Breton, S., Jouhet, J., Guyet, U., Gros, V., Pittera, J., Demory, D., et al. (2020). Unveiling membrane thermoregulation strategies in marine picocyanobacteria. *New Phytol.* 225, 2396–2410. doi: 10.1111/nph.16239

Bristow, L. A., Mohr, W., Ahmerkamp, S., and Kuypers, M. M. M. (2017). Nutrients that limit growth in the ocean. *Curr. Biol.* 27, R431–R510. doi: 10.1016/j.cub.2017.03.030

Campbell, D., Hurry, V., Clarke, A. K., Gustafsson, P., and Öquist, G. (1998). Chlorophyll fluorescence analysis of cyanobacterial photosynthesis and acclimation. *Microbiol. Mol. Biol. Rev.* 62, 667–683. doi: 10.1128/mmbr.62.3.667-683.1998

Campbell, D., Zhou, G., Gustafsson, P., Oquist, G., and Clarke, A. K. (1995). Electron transport regulates exchange of two forms of photosystem II D1 protein in the cyanobacterium *Synechococcus*. *EMBO J.* 14, 5457–5466. doi: 10.1128/MMBR.62.3.667-683.1998

Caputi, L., Carradec, Q., Eveillard, D., Kirilovsky, A., Pelletier, E., Pierella Karlusich, J. J., et al. (2019). Community-level responses to iron availability in open ocean plankton ecosystems. *Glob. Biogeochem. Cycles* 33, 391–419. doi: 10.1029/2018GB006022

Clarke, A. K., Hurry, V. M., Gustafsson, P., and Oquist, G. (1993a). Two functionally distinct forms of the photosystem II reaction-center protein D1 in

the cyanobacterium *Synechococcus* sp. PCC 7942. *Proc. Natl. Acad. Sci. U.S.A.* 90, 11985–11989. doi: 10.1073/pnas.90.24.11985

Clarke, A. K., Soitamo, A., Gustafsson, P., and Oquist, G. (1993b). Rapid interchange between two distinct forms of cyanobacterial photosystem II reaction-center protein D1 in response to photoinhibition. *Proc. Natl. Acad. Sci. U.S.A.* 90, 9973–9977. doi: 10.1073/pnas.90.21.9973

Claustre, H., Sciandra, A., and Vaulot, D. (2008). Introduction to the special section bio-optical and biogeochemical conditions in the South East Pacific in late 2004: the BIOSOPE program. *Biogeosciences* 5, 679–691. doi: 10.5194/bg-5-679-2008

Delmont, T. O., Gaia, M., Hinsinger, D. D., Fremont, P., Guerra, A. F., Eren, A. M., et al. (2020). Functional repertoire convergence of distantly related eukaryotic plankton lineages revealed by genome-resolved metagenomics. *BioRxiv* [Preprint] BioRxiv: 2020.10.15.341214-2020.10.15.341214, doi: 10.1101/2020.10.15.341214

Doré, H., Farrant, G. K., Guyet, U., Haguait, J., Humily, F., Ratin, M., et al. (2020). Evolutionary mechanisms of long-term genome diversification associated with niche partitioning in marine picocyanobacteria. *Front. Microbiol.* 11:567431. doi: 10.3389/fmicb.2020.567431

Doré, H., Leconte, J., Breton, S., Demory, D., Hoebeke, M., Corre, E., et al. (2022). Global phylogeography of marine *Synechococcus* in coastal areas unveils strikingly different communities than in open ocean. *BioRxiv* [Preprint] doi: 10.1101/2022.03.07.483242

Dufresne, A., Ostrowski, M., Scanlan, D. J., Garczarek, L., Mazard, S., Palenik, B. P., et al. (2008). Unraveling the genomic mosaic of a ubiquitous genus of marine cyanobacteria. *Genome Biol.* 9:R90. doi: 10.1186/gb-2008-9-5-r90

Farrant, G. K., Doré, H., Cornejo-Castillo, F. M., Partensky, F., Ratin, M., Ostrowski, M., et al. (2016). Delineating ecologically significant taxonomic units from global patterns of marine picocyanobacteria. *Proc. Natl. Acad. Sci. U.S.A.* 113, E3365–E3374. doi: 10.1073/pnas.1524865113

Findlay, V. J., Tapiero, H., and Townsend, D. M. (2005). Sulfiredoxin: a potential therapeutic agent? *Biomed. Pharmacother.* 59, 374–379. doi: 10.1016/j.biopha.2005.07.003

Flombaum, P., Gallegos, J. L., Gordillo, R. A., Rincón, J., Zabala, L. L., Jiao, N., et al. (2013). Present and future global distributions of the marine Cyanobacteria *Prochlorococcus* and *Synechococcus*. *Proc. Natl. Acad. Sci. U. S. A.* 110, 9824–9829. doi: 10.1073/pnas.1307701110

Garcia, C. A., Hagstrom, G. I., Larkin, A. A., Ustick, L. J., Levin, S. A., Lomas, M. W., et al. (2020). Linking regional shifts in microbial genome adaptation with surface ocean biogeochemistry. *Philos. Trans. R. Soc. B Biol. Sci.* 375:20190254. doi: 10.1098/rstb.2019.0254

Garczarek, L., Dufresne, A., Blot, N., Cockshutt, A. M., Peyrat, A., Campbell, D. A., et al. (2008). Function and evolution of the *psbA* gene family in marine *Synechococcus*: *Synechococcus* sp. WH7803 as a case study. *ISME J.* 2, 937–953. doi: 10.1038/ismej.2008.46

Garczarek, L., Guyet, U., Doré, H., Farrant, G. K., Hoebeke, M., Brillet-Guéguen, L., et al. (2021). Cyanorak v2.1: a scalable information system dedicated to the visualization and expert curation of marine and brackish picocyanobacteria genomes. *Nucleic Acids Res.* 49, D667–D676. doi: 10.1093/nar/gkaa958

Gutiérrez-Rodríguez, A., Slack, G., Daniels, E. F., Selph, K. E., Palenik, B., and Landry, M. R. (2014). Fine spatial structure of genetically distinct picocyanobacterial populations across environmental gradients in the Costa Rica Dome. *Limnol. Oceanogr.* 59, 705–723. doi: 10.4319/lo.2014.59.3.0705

Guyet, U., Nguyen, N. A., Doré, H., Haguait, J., Pittera, J., Conan, M., et al. (2020). Synergic effects of temperature and irradiance on the physiology of the marine *Synechococcus* strain WH7803. *Front. Microbiol.* 11:1707. doi: 10.3389/fmicb.2020.01707

Humily, F., Partensky, F., Six, C., Farrant, G. K., Ratin, M., Marie, D., et al. (2013). A gene island with two possible configurations is involved in chromatic acclimation in marine *Synechococcus*. *PLoS One* 8:e84459. doi: 10.1371/journal.pone.0084459

Ihalainen, J. A., D'Haene, S., Yeremenko, N., van Roon, H., Arteni, A. A., Boekema, E. J., et al. (2005). Aggregates of the chlorophyll-binding protein IsiA (CP43') dissipate energy in cyanobacteria. *Biochemistry* 44, 10846–10853. doi: 10.1021/bi0510680

Inoue, N., Taira, Y., Emi, T., Yamane, Y., Kashino, Y., Koike, H., et al. (2001). Acclimation to the growth temperature and the high-temperature effects on photosystem II and plasma membranes in a mesophilic cyanobacterium *Synechocystis* sp. PCC6803. *Plant Cell Physiol.* 42, 1140–1148. doi: 10.1093/pcp/pce147

Johnson, Z. I., Zinser, E. R., Coe, A., McNulty, N. P., Woodward, E. M. S., and Chisholm, S. W. (2006). Niche partitioning among *Prochlorococcus* ecotypes along ocean-scale environmental gradients. *Science* 311, 1737–1740. doi: 10.1126/science.1118052

Kana, T. M., Glibert, P. M., Goericke, R., and Welschmeyer, N. A. (1988). Zeaxanthin and ß-carotene in *Synechococcus* WH7803 respond differently to irradiance. *Limnol. Oceanogr.* 33, 1623–1626. doi: 10.4319/lo.1988.33.6part2.1623

Kashtan, N., Roggensack, S. E., Rodrigue, S., Thompson, J. W., Biller, S. J., Coe, A., et al. (2014). Single-cell genomics reveals hundreds of coexisting subpopulations in wild *Prochlorococcus*. *Science* 344, 416–420. doi: 10.1126/science.1248575

Kent, A. G., Baer, S. E., Mouginot, C., Huang, J. S., Larkin, A. A., Lomas, M. W., et al. (2019). Parallel phylogeography of *Prochlorococcus* and *Synechococcus*. *ISME J.* 13, 430–441. doi: 10.1038/s41396-018-0287-6

Kettler, G. C., Martiny, A. C., Huang, K., Zucker, J., Coleman, M. L., Rodrigue, S., et al. (2007). Patterns and implications of gene gain and loss in the evolution of *Prochlorococcus*. *PLoS Genet.* 3:e231. doi: 10.1371/journal.pgen.0030231

Kirilovsky, D. (2007). Photoprotection in cyanobacteria: the orange carotenoid protein (OCP)-related non-photochemical-quenching mechanism. *Photosynth. Res.* 93:7. doi: 10.1007/s11120-007-9168-y

Larkin, A. A., and Martiny, A. C. (2017). Microdiversity shapes the traits, niche space, and biogeography of microbial taxa: the ecological function of microdiversity. *Environ. Microbiol. Rep.* 9, 55–70. doi: 10.1111/1758-2229.12523

Larkin, A. A., Blinebry, S. K., Howes, C., Lin, Y., Loftus, S. E., Schmaus, C. A., et al. (2016). Niche partitioning and biogeography of high light adapted *Prochlorococcus* across taxonomic ranks in the North Pacific. *ISME J.* 10, 1555–1567. doi: 10.1038/ismej.2015.244

Latifi, A., Ruiz, M., and Zhang, C. C. (2009). Oxidative stress in cyanobacteria. *FEMS Microbiol. Rev.* 33, 258–278. doi: 10.1111/j.1574-6976.2008.00134.x

Mackey, K. R. M., Paytan, A., Caldeira, K., Grossman, A. R., Moran, D., McIlvin, M., et al. (2013). Effect of temperature on photosynthesis and growth in marine *Synechococcus* spp. *Plant Physiol.* 163, 815–829. doi: 10.1104/pp.113.221937

Marie, D., Partensky, F., Vaulot, D., and Brussaard, C. (1999). Enumeration of phytoplankton, bacteria, and viruses in marine samples. *Curr. Protoc. Cytom* 10, 11.11.1–11.11.15. doi: 10.1002/0471142956.cy1111s10

Mella-Flores, D., Mazard, S., Humily, F., Partensky, F., Mahé, F., Bariat, L., et al. (2011). Is the distribution of *Prochlorococcus* and *Synechococcus* ecotypes in the Mediterranean Sea affected by global warming? *Biogeosciences* 8, 2785–2804. doi: 10.5194/bg-8-2785-2011

Mikami, K., and Murata, N. (2003). Membrane fluidity and the perception of environmental signals in cyanobacteria and plants. *Prog. Lipid Res.* 42, 527–543. doi: 10.1016/S0163-7827(03)00036-5

Moore, C. M., Mills, M. M., Arrigo, K. R., Berman-Frank, I., Bopp, L., Boyd, P. W., et al. (2013). Processes and patterns of oceanic nutrient limitation. *Nat. Geosci.* 6, 701–710. doi: 10.1038/ngeo1765

Murata, N., Takahashi, S., Nishiyama, Y., and Allakhverdiev, S. I. (2007). Photoinhibition of photosystem II under environmental stress. *Biochim. Biophys. Acta Bioenerg.* 1767, 414–421. doi: 10.1016/j.bbabio.2006.11.019

Nishiyama, Y., Allakhverdiev, S. I., and Murata, N. (2006). A new paradigm for the action of reactive oxygen species in the photoinhibition of photosystem II. *Biochim. Biophys. Acta BBA Bioenerg.* 1757, 742–749. doi: 10.1016/j.bbabio.2006.05.013

Paulsen, M. L., Doré, H., Garczarek, L., Seuthe, L., Müller, O., Sandaa, R.-A., et al. (2016). *Synechococcus* in the atlantic gateway to the arctic ocean. *Front. Mar. Sci.* 3:191. doi: 10.3389/fmars.2016.00191

Pearman, P. B., Guisan, A., Broennimann, O., and Randin, C. F. (2008). Niche dynamics in space and time. *Trends Ecol. Evol.* 23, 149–158. doi: 10.1016/j.tree.2007.11.005

Pittera, J., Humily, F., Thorel, M., Grulois, D., Garczarek, L., and Six, C. (2014). Connecting thermal physiology and latitudinal niche partitioning in marine *Synechococcus*. *ISME J.* 8, 1221–1236. doi: 10.1038/ismej.2013.228

Pittera, J., Jouhet, J., Breton, S., Garczarek, L., Partensky, F., Maréchal, É, et al. (2018). Thermoacclimation and genome adaptation of the membrane lipidome

in marine *Synechococcus*. *Environ. Microbiol.* 20, 612–631. doi: 10.1111/1462-2920.13985

Pittera, J., Partensky, F., and Six, C. (2017). Adaptive thermostability of light-harvesting complexes in marine picocyanobacteria. *ISME J.* 11, 112–124. doi: 10.1038/ismej.2016.102

Polovina, J. J., Howell, E. A., and Abecassis, M. (2008). Ocean's least productive waters are expanding. *Geophys. Res. Lett.* 35:L03618. doi: 10.1029/2007GL031745

Rippka, R., Coursin, T., Hess, W., Lichtle, C., Scanlan, D. J., Palinska, K. A., et al. (2000). *Prochlorococcus marinus Chisholm* et al. 1992 subsp. *pastoris* subsp. nov. strain PCC 9511, the first axenic chlorophyll *a2/b2*-containing cyanobacterium (*Oxyphotobacteria*). *Int. J. Syst. Evol. Microbiol.* 50, 1833–1847. doi: 10.1099/00207713-50-5-1833

Saito, M. A., Rocap, G., and Moffett, J. W. (2005). Production of cobalt binding ligands in a *Synechococcus* feature at the Costa Rica upwelling dome. *Limnol. Oceanogr.* 50, 279–290. doi: 10.4319/lo.2005.50.1.0279

Scanlan, D. J., Ostrowski, M., Mazard, S., Dufresne, A., Garczarek, L., Hess, W. R., et al. (2009). Ecological genomics of marine picocyanobacteria. *Microbiol. Mol. Biol. Rev.* 73, 249–299. doi: 10.1128/MMBR.00035-08

Schloss, P. D., Westcott, S. L., Ryabin, T., Hall, J. R., Hartmann, M., Hollister, E. B., et al. (2009). Introducing Mothur: Open-source, platform-independent, community-supported software for describing and comparing microbial communities. *Appl. Environ. Microbiol.* 75, 7537–7541. doi: 10.1128/AEM.01541-09

Schmidt, K., Birchill, A. J., Atkinson, A., Brewin, R. J. W., Clark, J. R., Hickman, A. E., et al. (2020). Increasing picocyanobacteria success in shelf waters contributes to long-term food web degradation. *Glob. Change Biol.* 26, 5574–5587. doi: 10.1111/gcb.15161

Six, C., Joubin, L., Partensky, F., Holtzendorff, J., and Garczarek, L. (2007). UV-induced phycobilisome dismantling in the marine picocyanobacterium *Synechococcus* sp. WH8102. *Photosynth. Res.* 92, 75–86. doi: 10.1007/s11120-007-9170-4

Six, C., Ratin, M., Marie, D., and Corre, E. (2021). Marine *Synechococcus* picocyanobacteria: light utilization across latitudes. *Proc. Natl. Acad. Sci. U.S.A.* 118:e2111300118. doi: 10.1073/pnas.2111300118

Six, C., Thomas, J., Brahamsha, B., Lemoine, Y., and Partensky, F. (2004). Photophysiology of the marine cyanobacterium *Synechococcus* sp. WH8102, a new model organism. *Aquat. Microb. Ecol.* 35, 17–29. doi: 10.3354/ame035017

Six, C., Thomas, J.-C., Thion, L., Lemoine, Y., Zal, F., and Partensky, F. (2005). Two novel phycoerythrin-associated linker proteins in the marine cyanobacterium *Synechococcus* sp. strain WH8102. *J. Bacteriol.* 187, 1685–1694. doi: 10.1128/JB.187.5.1685-1694.2005

Sohm, J. A., Ahlgren, N. A., Thomson, Z. J., Williams, C., Moffett, J. W., Saito, M. A., et al. (2016). Co-occurring *Synechococcus* ecotypes occupy four major oceanic regimes defined by temperature, macronutrients and iron. *ISME J.* 10, 333–345. doi: 10.1038/ismej.2015.115

Sunagawa, S., Coelho, L. P., Chaffron, S., Kultima, J. R., Labadie, K., Salazar, G., et al. (2015). Structure and function of the global ocean microbiome. *Science* 348, 1261359–1261359. doi: 10.1126/science.1261359

Torabi, S., Umate, P., Manavski, N., Plöchinger, M., Kleinknecht, L., Bogireddi, H., et al. (2014). PsbN is required for assembly of the photosystem II reaction center in *Nicotiana tabacum*. *Plant Cell* 26, 1183–1199. doi: 10.1105/tpc.113.120444

Umena, Y., Kawakami, K., Shen, J.-R., and Kamiya, N. (2011). Crystal structure of oxygen-evolving photosystem II at a resolution of 1.9 Å. *Nature* 473, 55–60. doi: 10.1038/nature09913

Visintini, N., Martiny, A. C., and Flombaum, P. (2021). *Prochlorococcus*, *Synechococcus*, and picoeukaryotic phytoplankton abundances in the global ocean. *Limnol. Oceanogr. Lett.* 6, 207–215. doi: 10.1002/lol2.10188

Wilkins, D., Lauro, F. M., Williams, T. J., Demaere, M. Z., Brown, M. V., Hoffman, J. M., et al. (2013). Biogeographic partitioning of Southern Ocean microorganisms revealed by metagenomics. *Environ. Microbiol.* 15, 1318–1333. doi: 10.1111/1462-2920.12035

Xia, X., Cheung, S., Endo, H., Suzuki, K., and Liu, H. (2019). Latitudinal and vertical variation of *Synechococcus* assemblage composition along 170°W transect from the South Pacific to the Arctic Ocean. *Microb. Ecol.* 77, 333–342. doi: 10.1007/s00248-018-1308-8

Xia, X., Partensky, F., Garczarek, L., Suzuki, K., Guo, C., Cheung, S. Y., et al. (2017). Phylogeography and pigment type diversity of *Synechococcus* cyanobacteria in surface waters of the northwestern Pacific Ocean. *Environ. Microbiol.* 19, 142–58. doi: 10.1111/1462-2920.13541

Xu, W., and Wang, Y. (2017). "Function and structure of cyanobacterial photosystem I," in *Photosynthesis: Structures, Mechanisms, and Applications*, eds H. J. M. Hou, M. M. Najafpour, G. F. Moore, and S. I. Allakhverdiev (Cham: Springer International Publishing), 111–168. doi: 10.1007/978-3-319-48873-8_7

Yeremenko, N., Kouřil, R., Ihalainen, J. A., D'Haene, S., van Oosterwijk, N., Andrizhiyevskaya, E. G., et al. (2004). Supramolecular organization and dual function of the IsiA chlorophyll-binding protein in cyanobacteria. *Biochemistry* 43, 10308–10313. doi: 10.1021/bi048772l

Zwirglmaier, K., Jardillier, L., Ostrowski, M., Mazard, S., Garczarek, L., Vaulot, D., et al. (2008). Global phylogeography of marine *Synechococcus* and *Prochlorococcus* reveals a distinct partitioning of lineages among oceanic biomes. *Environ. Microbiol.* 10, 147–161. doi: 10.1111/j.1462-2920.2007.01440.x

Conflict of Interest: The authors declare that the research was conducted in the absence of any commercial or financial relationships that could be construed as a potential conflict of interest.

Publisher's Note: All claims expressed in this article are solely those of the authors and do not necessarily represent those of their affiliated organizations, or those of the publisher, the editors and the reviewers. Any product that may be evaluated in this article, or claim that may be made by its manufacturer, is not guaranteed or endorsed by the publisher.

Ferrieux et al.
Supplementary Figures

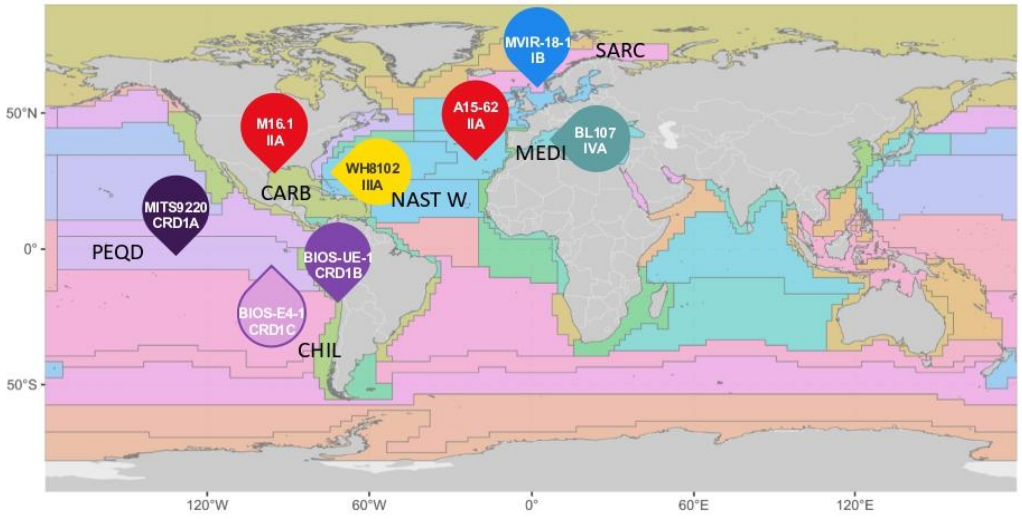

Supplementary Figure 1. Isolation sites of the *Synechococcus* strains used in this study. Isolation site of each strain is indicated on the map by a bubble arrow colored according to their corresponding ESTUs indicated below the strain name. Longhurst provinces (Longhurst A., 2007, Ecological Geography of the Sea, Academic Press, London) are shown as a colored background shown in the insert. Only provinces from which at least one strain has been isolated are indicated on the map using the following abbreviations: PEQD (Pacific equatorial divergence, Pacific, Trade wind), CHIL (Chile-Peru, current coastal province, Pacific, Coastal), NAST W (Northwest Atlantic subtropical gyral, Atlantic, Westerly), CARB (Caribbean, Atlantic, Trade wind), MEDI (Mediterranean Sea, Atlantic, Westerly), SARC (Atlantic sub-Arctic, Atlantic, Polar).

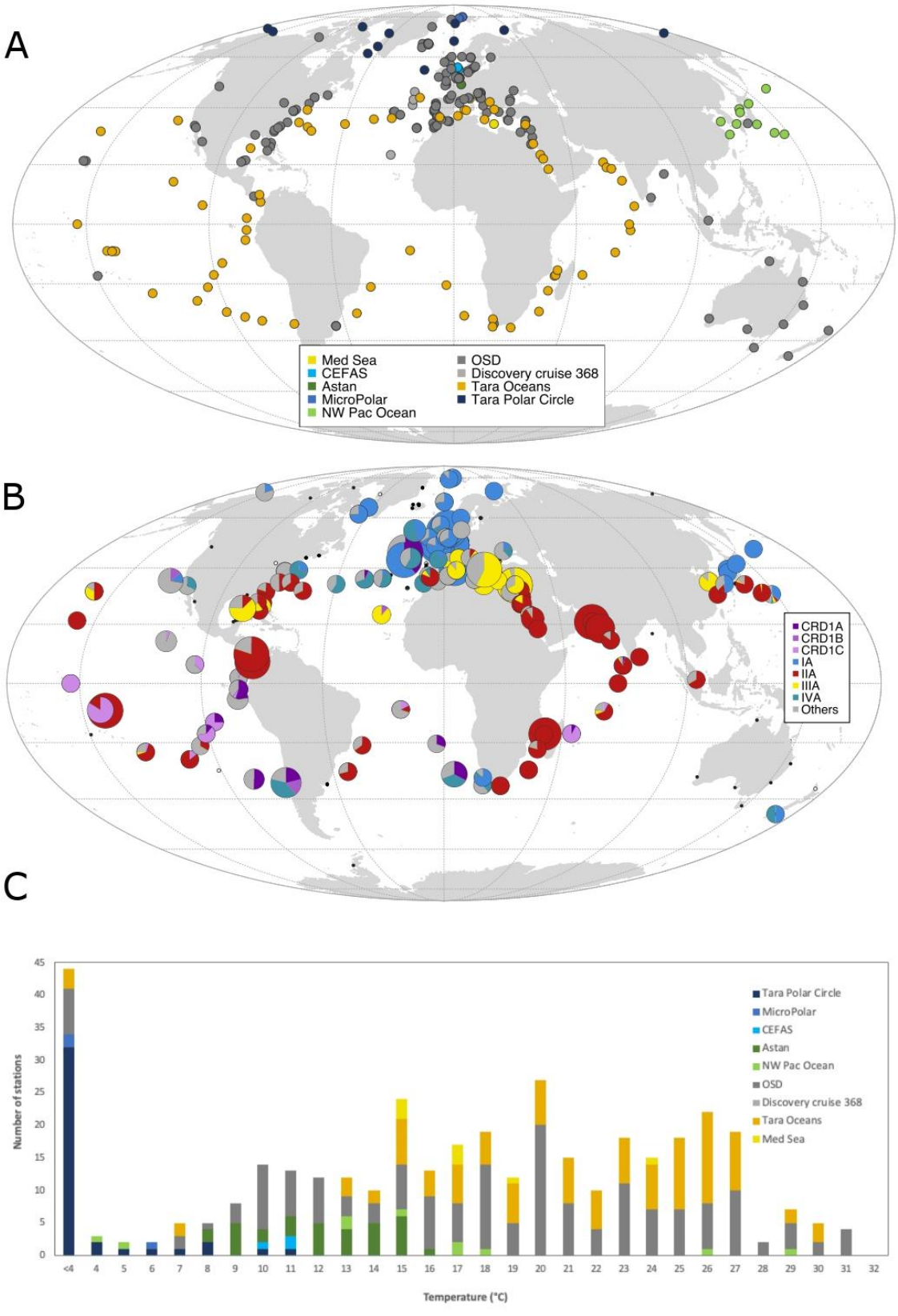

Supplementary Figure 2. Oceanwide environmental data used in this study to determine the environmental realized thermal niches of the main ESTUs from clades CRD1 and I to IV. **(A)** Map of the sampling sites, **(B)** Relative abundance of *Synechococcus* ESTUs IA to IVA and CRD1A to C. **(C)** Temperature distribution of the sampling sites. The inserts specify **(A,C)** the name of campaigns or datasets analyzed and **(B)** the *Synechococcus* ESTUs.

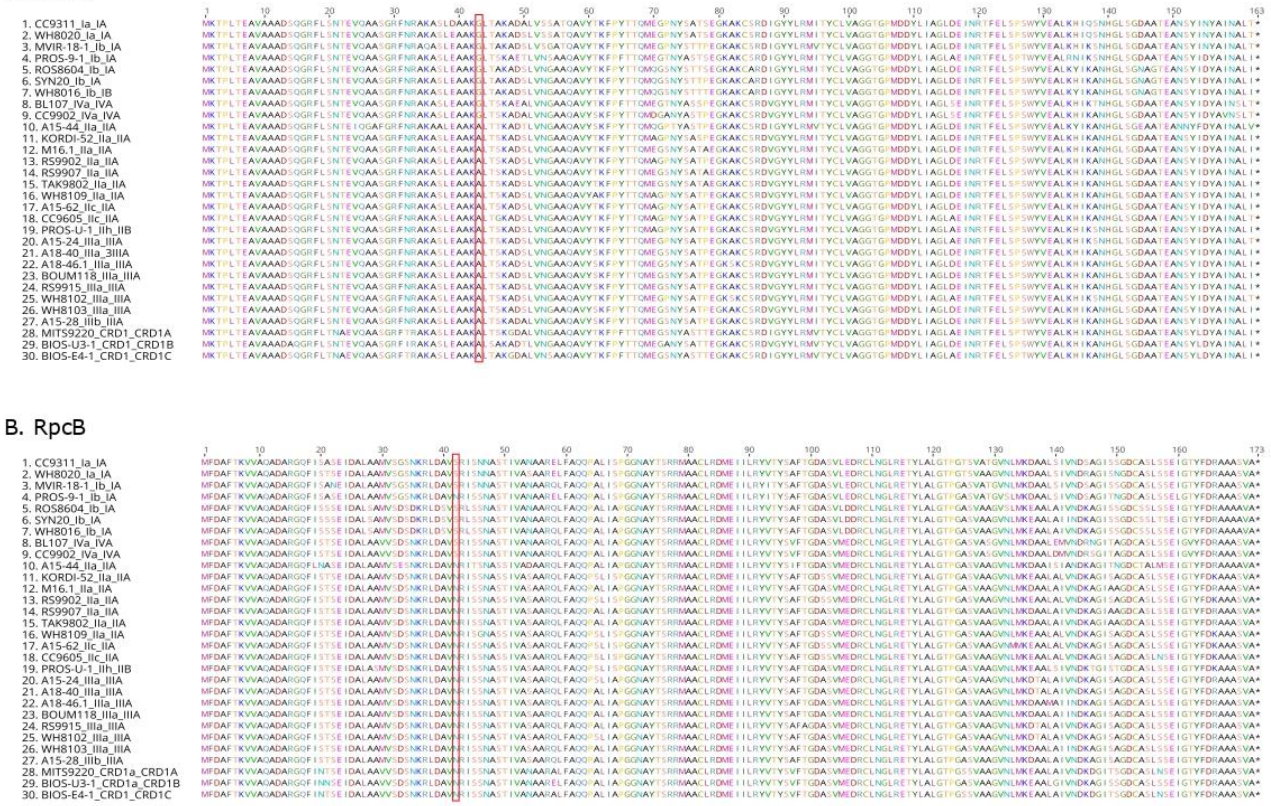

Supplementary Figure 3. Alignment of RpcA and RpcB, encoding phycocyanin α- and β-subunits, from CRD1 and clades I-IV *Synechococcus* strains. (A) RpcA. (B) RpcB. Substitutions potentially involved in thermotolerance are shown by a red rectangle in the alignment.

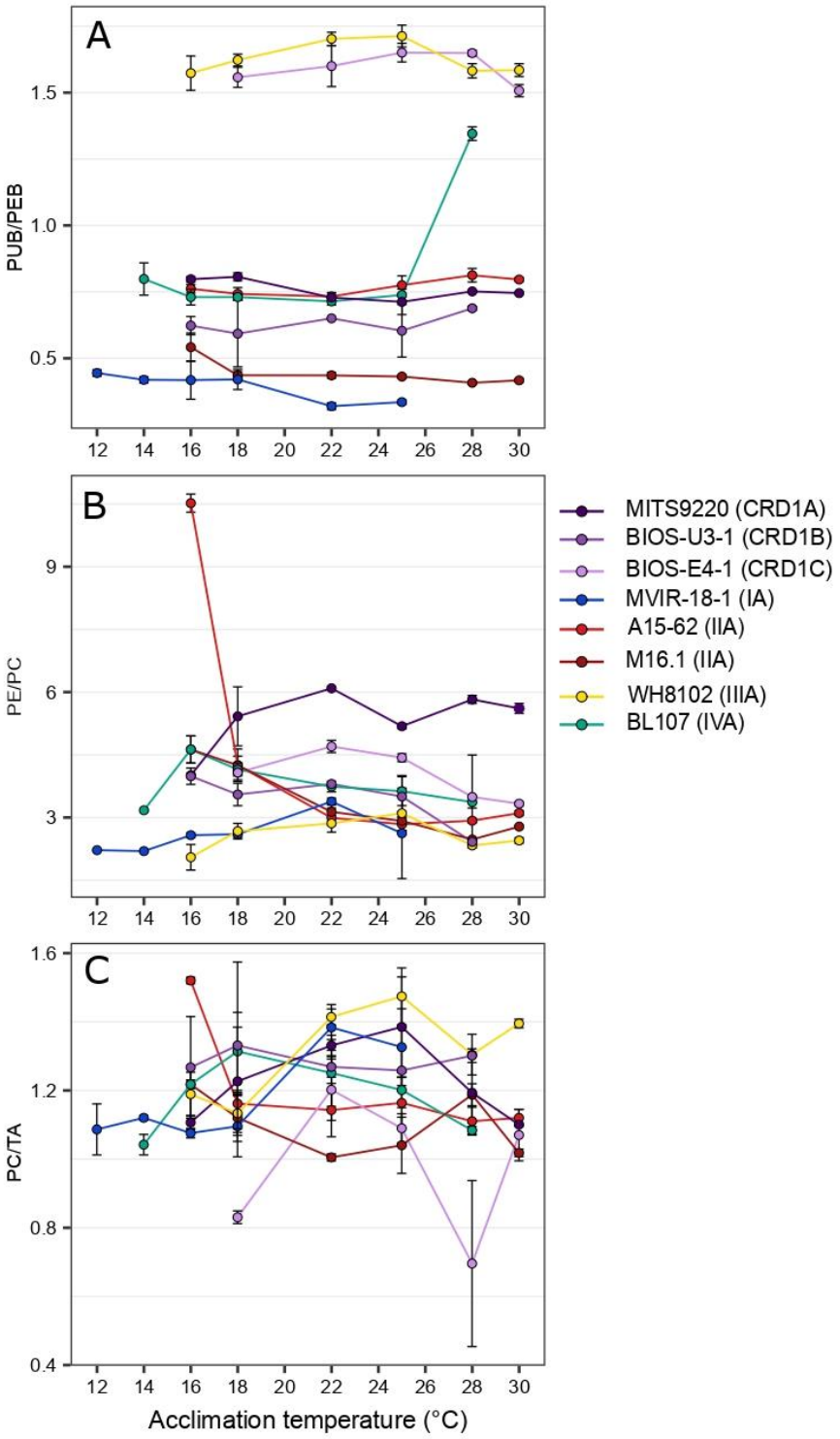

Supplementary Figure 4. Variation with growth temperature of phycobilins and phycobiliproteins fluorescence excitation and emission ratios. (A) Average PUB:PEB ratios. (B) Average phycoerythrin (PE) to phycocyanin (PC) ratios. (C) Average PC to terminal acceptor (TA) ratios. The insert indicates the strain names, their corresponding ESTU (sensu Farrant et al., 2016) and pigment type (sensu Humily et al., 2013) between brackets.

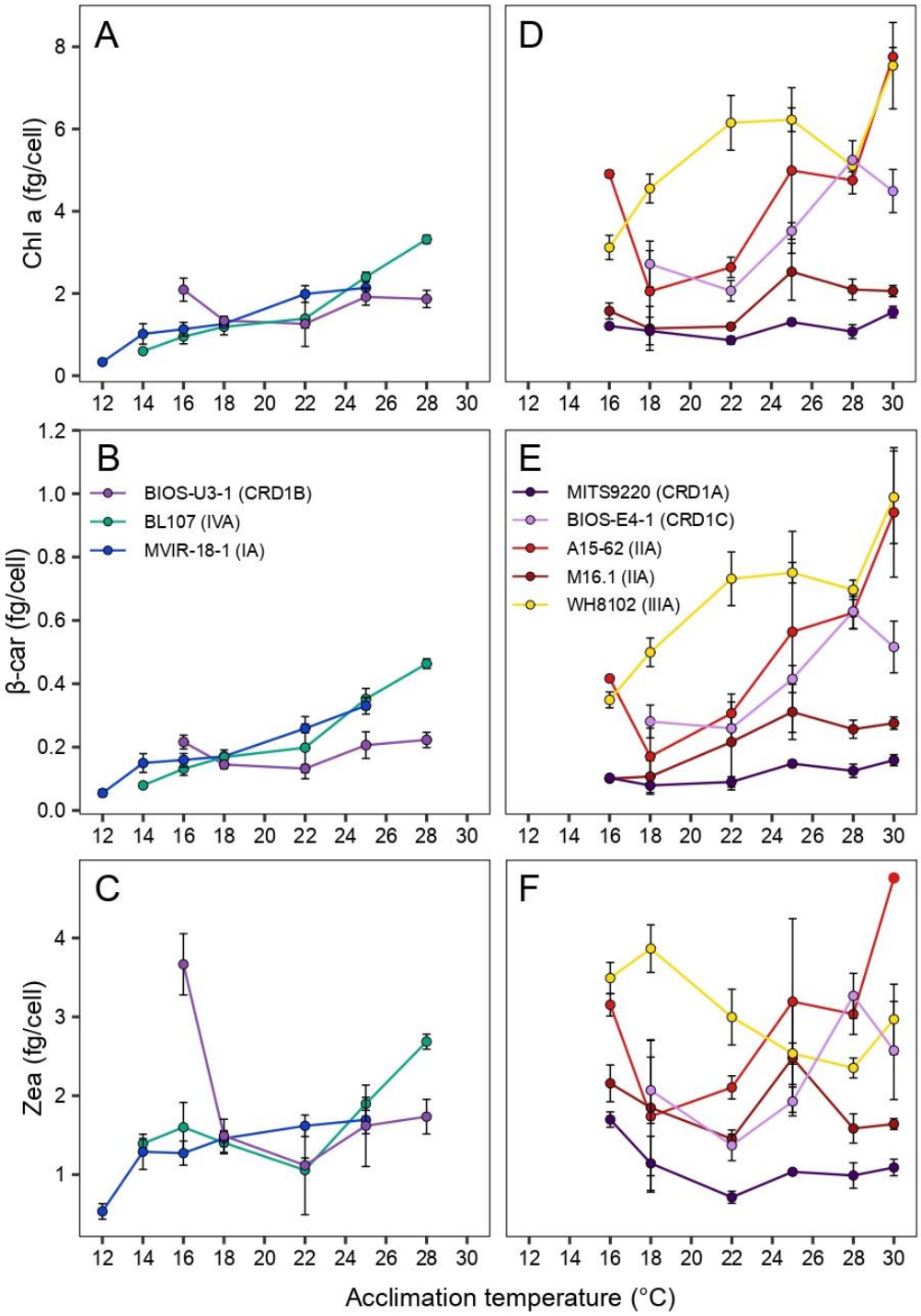

Supplementary Figure 5. Variation with growth temperature of the three main liposoluble pigments per cell for CRD1 vs. clade I and IV strains. (A, D) Chlorophyll (Chl) a content (fg/cell). **(B, E)** Zeaxanthin (Zea) content (fg/cell). **(C, F)** β-carotene (β-car) content (fg/cell). **(A-C)** CRD1-B strain BIOS-U3-1 vs. cold thermotypes. **(D-F)** CRD1-A strain MITS9220 and CRD1-C strain BIOS-E4-1 vs. warm thermotypes. Inserts indicate the strain names and their corresponding ESTU (*sensu* Farrant et al., 2016) between brackets.

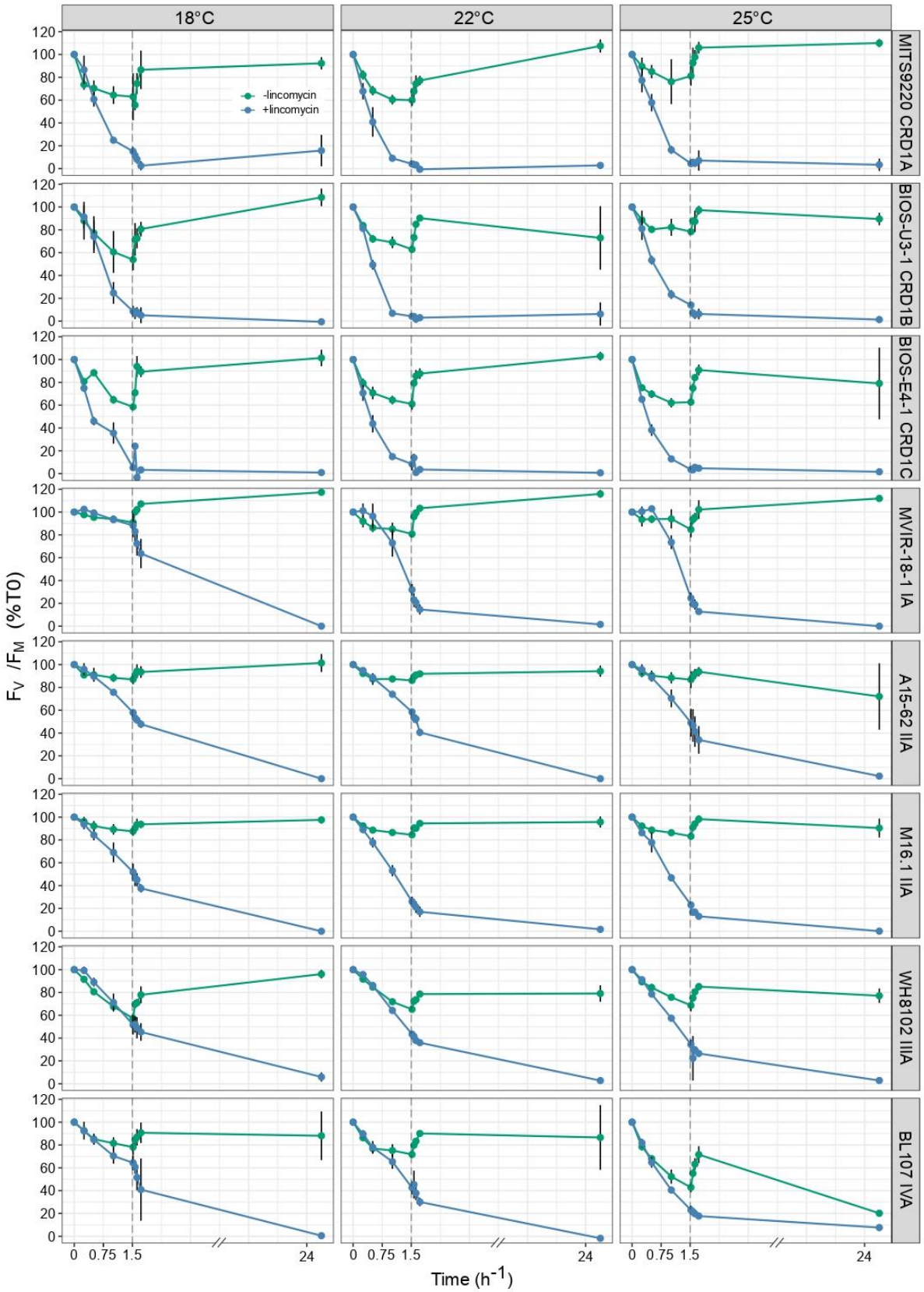

Supplementary Figure 6. Time course of photosystem II quantum yield (F_V/F_M) following light stress in the presence or absence of lincomycin for CRD1 and clade I-IV strains acclimated to different temperatures. Cultures acclimated to 75 µE m^{-2} s^{-1} were shifted to 375 µE m^{-2} s^{-1} at T0 for 90 min, then shifted back to the initial light conditions for 24h as indicated by a vertical dashed line on each figure. Strain names and their corresponding ESTU between brackets (*sensu* Farrant et al., 2016) are indicated on the right hand side, acclimation temperature are indicated on the top, whilst line colour indicates the lincomycin treatment (i.e. -/+ linco).

Chapitre II :

Mécanismes d'adaptation à la limitation en fer chez *Synechococcus*

Contexte de l'étude

Dans les eaux marines, le Fe sous sa forme libre dissoute (Fe') est présent en très petites quantités (de l'ordre du pico- au nanomolaire). Au sein du Fe', le Fe sous sa forme ferreux Fe^{2+} est plus facilement assimilable par le plancton, contrairement à sa forme oxydée ferrique, Fe^{3+} (Johnson et al., 1997; Morel et al., 2008). Ainsi, dès qu'il est biodisponible, il est immédiatement consommé, c'est pourquoi on observe un décalage entre la biodisponibilité en Fe et les besoins en Fer du plancton, se traduisant par la présence de zones HNLC (« high-nutrient low-chlorophyll ») dans de vastes régions de l'océan. Chez *Synechococcus*, il a été mis en évidence que les ESTUs des clades CRD1 et EnvB codominaient les populations au sein de ce genre dans une grande partie de l'Océan Pacifique, de 33°S à 35°N, ainsi que des zones plus restreintes des océans Atlantique et Indien, caractérisées par une limitation en fer (Farrant et al., 2016). Le Fe semble donc avoir joué un rôle majeur dans la diversification génétique des picocyanobactéries marines. Dans ce contexte, le second axe de ma thèse s'est intéressé à la caractérisation des mécanismes d'acclimatation et d'adaptation développés par ces organismes par des approches de physiologie et génomique comparative.

Une première approche a consisté, en collaboration avec l'équipe LOMIC de Banyuls-sur-mer, à tenter d'acclimater des souches représentatives d'écotypes -Fe (CRD1) et +Fe (contrôles) au milieu de référence pour ce type d'étude (AQUIL ; Price et al., 1989), ce qui s'est avéré très difficilement réalisable, en partie du fait de la non-axénie des souches utilisées. Afin de comparer la résistance à la carence des différents ecotypes de *Synechococcus*, notre choix s'est donc porté sur l'utilisation d'un chélateur du Fe, le DFOB (mésilate de déferoxamine), qui induit un changement drastique de la source de Fe, de Fe' à FeL, c-à-d le Fe complexé par des ligands. Parallèlement, la comparaison des génomes (WGS, SAGs, MAGs) de picocyanobactéries disponibles dans l'application Cyanorak *v2.1* (Garczarek et al., 2021; http://sb-roscoff.fr/cyanorak/), complété par près de 160 nouveaux génomes issus de Genbank, nous a permis d'identifier les gènes impliqués dans le métabolisme du Fe dans les différents écotypes de *Synechococcus*. Ces données ont également été complétées par une analyse environnementale de la distribution de ces gènes le long du transect *Tara* Oceans afin de vérifier la spécificité de certains de ces gènes aux niches pauvres ou au contraire riches en Fer en utilisant les

recrutements de lectures métagénomiques (‘reads’) réalisés dans le cadre d’une seconde étude (Doré et al., submitted, Annexe B). Dans cette dernière, l’utilisation d’une approche de réseau intégrant les informations de synténie des gènes dans les génomes de référence et de distribution *in situ* a de plus permis d’identifier non seulement des gènes spécifiques de niches mais des régions génomiques (ou CAGs pour ‘cluster of adjacent genes’), notamment dans les régions limitées en Fe, mais plus globalement dans des zones carencées en nutriments. La combinaison de ces différentes approches (expérimentale, génomique et métagénomique) a apporté de nouveaux éléments de réponse concernant les mécanismes d’acclimatation et d’adaptation mis en place par les écotypes -Fe et +Fe des *Synechococcus* marins soumis à une carence en Fe, complétant des études précédentes sur le sujet (Ahlgren et al., 2020; Garcia et al., 2020; Hogle et al., 2022; Rusch et al., 2010).

Contribution

Les tests préliminaires d’acclimation au milieu AQUIL ont été initié par l’équipe du LOMIC à Banyuls-sur-Mer. Compte tenu de la difficulté à acclimater les cultures de *Synechococcus* à ces conditions, j’ai repris et poursuivi ces expériences à Roscoff en testant de nouveaux milieux de culture et différentes conditions de carence en Fe. J’ai effectué et analysé l’ensemble des suivis de croissance présentés dans cette étude et orchestré les échantillonnages réalisés en collaboration avec les membres de mon équipe (récoltes et analyses des différents paramètres : HPLC, transcriptomes, extraction d’ARN, cytométrie, etc.). J’ai également contribué à la curation de Cyanorak (Garczarek et al., 2021, Annexe A), à l’identification de gènes cibles reliés au métabolisme du Fe à partir de données de la littérature et à leur analyse par génomique comparative et métagénomique (Ferrieux et al., en préparation ci-après ; (Doré et al., submitted, Annexe B).

II.1 – Expériences préliminaires de culture de *Synechococcus* CRD1 et de clades contrôles en milieu carencé en fer

A Roscoff, les cultures de *Synechococcus* sont maintenues en routine en PCR-S11 (Rippka et al., 2000), un milieu à base d'eau de mer reconstituée à partir de sels de la Mer Rouge (Red Sea salts, Houston, Texas, USA), modifié par l'ajout de $NaNO_3$ et comprenant 2 µM de Fe-EDTA (Fe complexé) sous forme de chlorure ferrique hexahydraté ($FeCl_3 \cdot 6H_2O$; Sigma-Aldrich, USA, cf. https://www.protocols.io/view/pcr-s11-red-sea-medium-bpvemn3e). Afin de mener des expériences de carence en nutriments, dans notre cas le Fe, il faut en tout premier lieu acclimater les cultures à un milieu dont les concentrations en sels, nutriments et métaux sont très précisément contrôlées. L'un des milieux communément utilisés pour ce type d'étude est le milieu AQUIL (Price et al., 1989) qui contient 8,32 µM de Fe et 100 µM d'EDTA final. Afin de limiter la pollution en métaux, l'ensemble des solutions stocks doit être passé sur des colonnes « chelex » qui vont chélater les métaux excédentaires (https://www.protocols.io/view/aquil-medium-preparation-price-et-al-1989-vixe4fn) et la préparation doit être réalisée en salle blanche, rendant la préparation de ce milieu très longue.

Une première tentative pour carencer les cellules en Fe, réalisée à Banyuls, a consisté à transférer les cultures des souches CRD1 et contrôles directement en milieu AQUIL contenant 540 nM de Fe, puis à les diluer 10 fois avec du milieu sans Fe pour atteindre 54 nM, puis 5.4 nM de Fe. Des suivis de croissance ont été effectués à chaque concentration en Fe (au total, plus de 200 suivis), afin d'essayer de mettre en évidence une diminution différente selon les écotypes du taux de croissance en fonction de la carence en Fe. Il s'est avéré que la croissance en milieu Aquil, même à 540 nM de Fe, induisait une réduction importante des taux de croissance par rapport au PCR-S11 (Fig. 16) et que l'acclimatation a des concentrations plus faibles était très peu reproductible, seuls certains replicats de deux souches, BIOS-E4-1 (CRD1C) et A15-62 (IIA), ayant atteint la concentration de 5,4 nM de Fe (Fig. 17). De plus, le fait de diluer directement les cultures ne permet pas de maitriser parfaitement la concentration en Fe, puisque du Fe résiduel est toujours présent dans la culture au moment du transfert.

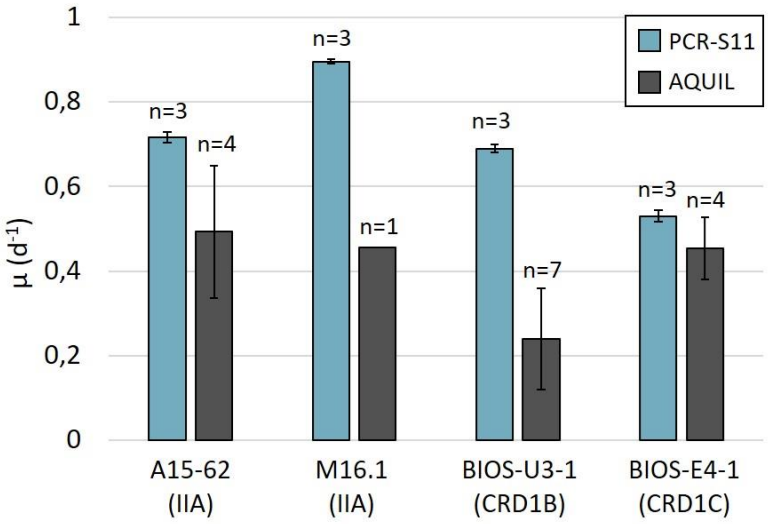

Figure 16 | Taux de croissance de cultures de *Synechococcus* en milieu de routine PCR-S11 *vs.* Aquil 540nM Fe au 2e repiquage.

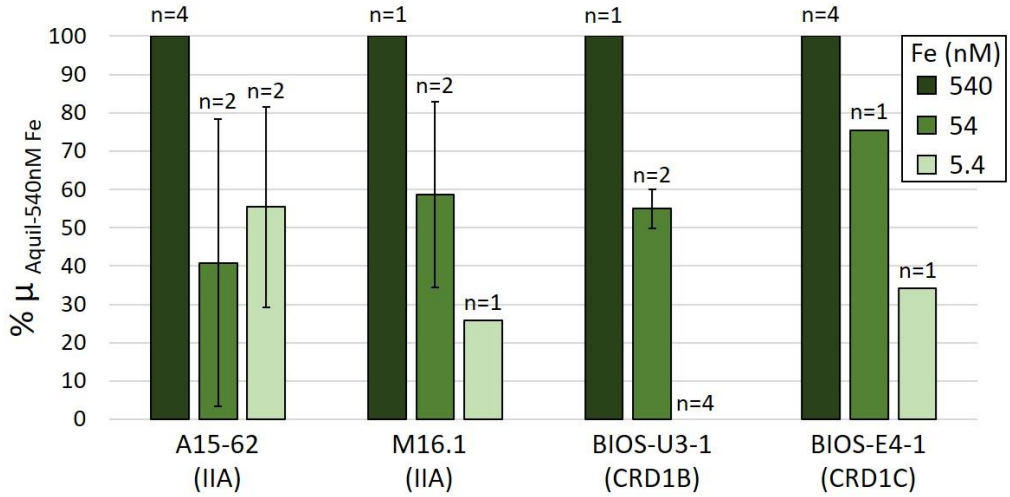

Figure 167 | Effet de la carence en Fe sur le taux de croissance des clades II *vs.* CRD1 en milieu Aquil (Price et al., 1989). Le taux de croissance aux différentes concentrations en Fe est exprimé en pourcentage du taux de croissance obtenu en condition initiale (Fe-repleted, c-à-d 540nM Fe). L'insert indique la concentration en Fe dans le milieu AQUIL.

Ces difficultés nous ont incitées à chercher une autre méthode d'acclimatation à la carence en fer. Conjointement avec Eva Bucciarelli du LEMAR de Brest, qui a l'expérience du milieu Aquil avec d'autres organismes phytoplanctoniques tels que les diatomées, nous avons réalisé deux milieux intermédiaires entre le PCR-S11 et l'AQUIL contenant les métaux traces utilisés dans le PCR-S11, les sels de l'AQUIL et deux concentrations en Fe-EDTA distinctes : 2 µM Fe-EDTA (comme dans le PCR-S11) et 8,32 µM Fe pour 100 µM

EDTA (comme dans l'AQUIL, cf. ANNEXE C). De plus, les études de carence en éléments traces utilisent communément des flacons Nalgene, qui peuvent être stérilisées à l'aide d'un micro-ondes (ce qui évite les contaminations en métaux qui peuvent survenir à l'autoclavage), et dont les bouchons empêchent les échanges gazeux avec l'extérieur, ce qui limite les contaminations potentielles en métaux mais pourrait également avoir un effet délétère sur la croissance de *Synechococcus*. Afin de tester ces différents milieux et l'influence du contenant, j'ai réalisé des suivis de croissance en milieu AQUIL/PCR-S11 2µM Fe-EDTA et AQUIL/PCR-S11 8,32 µM Fe-100 µM EDTA en flacons Nalgene fermées ou en flacons en polyéthylène à bouchons ventilés (environ 150 suivis). Différents paramètres ont été acquis de façon journalière : la quantité de cellules, la contamination bactérienne et le pH. Dans tous les cas, lorsque les cultures n'étaient pas axéniques, une augmentation rapide de la contamination en bactéries hétérotrophes, pouvant atteindre 75%, a été observée, ce qui suggère l'existence d'une compétition pour l'utilisation du Fe entre les bactéries et les *Synechococcus*. Par ailleurs, les cultures présentaient des phases exponentielles très courtes, probablement en partie liée à la limitation en carbone, particulièrement dans les flacons non ventilés. En effet, le pH, initialement à 7.8, augmentait fortement au cours des suivis (jusque 9 unités pH en milieu de phase exponentielle), un phénomène que j'ai essayé de controler par l'ajout d'une solution de $NaHCO_3$ (bicarbonate de sodium), qui permet une réduction du pH de quelques unités. Malgré tous les essais réalisés, la très grande variabilité observée entre les souches et les très forts taux de contamination n'ont pas permis de définir des conditions permettant de comparer la croissance des souches en milieu carencé en Fe. La souche la plus prometteuse s'est avérée être CC9311, une souche axénique du clade I que j'ai pu maintenir en milieu AQUIL non limité en Fe pendant plusieurs mois, mais qui en tant que thermotype froid, ne constituait pas le meilleur contrôle pour valider l'existence d'écotypes -Fe au sein des CRD1. Dans ce contexte, l'alternative finalement retenue pour l'article ci-après (Ferrieux et al., en prep) a été d'utiliser un chélateur du Fe', le DFOB, afin de simuler des conditions de carence en Fer en milieu PCR-S11.

II.2 - Bases moléculaires de l'adaptation à la limitation en fer dans le clade marin *Synechococcus* CRD1

Résumé de l'article en français

Le fer (Fe) limite la croissance du phytoplancton et la photosynthèse dans de vastes étendues de l'océan mondial, qui sont dominées par des écotypes spécifiques de *Prochlorococcus* (HLIII et HLIV) et de *Synechococcus* (CRD1, EnvB/CRD2). Alors que la plupart de ces lignées sont à ce jour non cultivées, plusieurs souches appartenant au clade CRD1, le clade majeur de *Synechococcus* dans les zones limitées en Fe, sont disponibles en culture et constituent de précieux modèles pour étudier les mécanismes d'adaptation à ces environnements. Au cours de cette étude, nous avons comparé la réponse à la carence en Fe inorganique non chélaté dissous (Fe'), provoquée par l'ajout d'une gamme de concentrations du chélateur desferrioxamine B (DFOB), sur des souches représentatives du clade CRD1 ainsi que des clades II et III, dominant dans d'autres niches écologiques chaudes et riches en Fe. Ces analyses ont montré que les trois souches CRD1 testées, mais aussi de manière plus inattendue la souche A15-62 du sous-clade IIc, étaient capables de croitre à une concentration beaucoup plus élevée de DFOB que les autres souches des clades II (M16.1, sous-clade IIa) et III (WH8102), cette dernière souche étant de loin la plus sensible à ce traitement. Ces expériences ont été complétées par la comparaison de 256 génomes de picocyanobactéries et l'analyse de la distribution globale dans le milieu naturel de gènes impliqués dans le métabolisme du Fe à partir des données de métagénomes de l'expédition *Tara* Oceans. Ces analyses ont montré que bien que les différentes sensibilités de ces organismes puissent en partie être liées à des différences de leur contenu en gènes impliqués dans le transport, l'assimilation et le stockage du Fe, les membres des lignées CRD1, EnvB et IIc ont adopté différentes stratégies pour faire face à la limitation en Fe. Dans l'ensemble, la découverte d'un écotype adapté à la faible carence en Fe au sein du clade II, le clade de *Synechococcus* dominant dans l'océan, pourrait avoir des conséquences importantes dans le contexte de l'expansion actuelle des zones limitées en Fe, causée par le changement global.

Insights into molecular bases of adaptation to iron limitation in the marine *Synechococcus* CRD1 clade

Mathilde Ferrieux[1], Jade Leconte[1], Ulysse Guyet[1], Audrey Guéneuguès[2], Léo Chasselin[2], Louison Dufour[1], Gregory Farrant[1], Morgane Ratin[1], Dominique Marie[1], Jukka Siltanen[3], Mark Hoebeke[3], Erwan Corre[3], François-Yves Bouget[2], Stéphane Blain[2], Frédéric Partensky[1] and Laurence Garczarek[1,4]

[1] Sorbonne Université, CNRS, UMR 7144 Adaptation and Diversity in the Marine Environment (AD2M), Station Biologique de Roscoff (SBR), Roscoff, France.

[2] Sorbonne Université, CNRS, UMR 7621 Laboratoire d'Océanographie Microbienne (LOMIC), Observatoire Océanologique de Banyuls/mer, Banyuls, France.

[3] CNRS, FR 2424, ABiMS Platform, Station Biologique de Roscoff (SBR), Roscoff, France

[4] CNRS Research Federation (FR2022) *Tara* Océans GO-SEE, Paris, France.

* Correspondence:
Corresponding Author: L. Garczarek

Keywords: Marine picocyanobacteria, *Synechococcus*, CRD1, EnvB, CRD2, iron limitation, HNLC areas

Abstract

Iron (Fe) is limiting phytoplankton growth and photosynthesis in wide expanses of the world ocean, which are dominated by specific ecotypes of both *Prochlorococcus* (HLIII and HLIV) and *Synechococcus* (CRD1, EnvB/CRD2). While most of these lineages are so far uncultivated, several strains belonging to CRD1, the major *Synechococcus* clade in low-Fe areas, are available in culture and constitute invaluable models to study the adaptation mechanisms to these environments. Here, we compared the response to starvation in dissolved unchelated inorganic Fe (Fe'), triggered by the addition of a range of concentrations of the strong chelator desferrioxamine B (DFOB), on representative strains of the CRD1 clade as well as clades II and III, dominating in other warm, Fe-replete ecological niches. These analyses showed that all three CRD1 strains tested, but also unexpectedly the subclade IIc strain A15-62, were able to grow at much higher concentration of DFOB than the other clades II (M16.1, subclade IIa) and III (WH8102) strains, the latter strain being by far the most sensitive to this treatment. Comparative genomics of 256 picocyanobacterial genomes and analysis of the global distribution of Fe-metabolism genes in the field using the *Tara* Oceans metagenome dataset showed that although the different sensitivities of these organisms can in part be related to differences in their gene complement involved in Fe uptake, assimilation and storage capabilities, CRD1, EnvB and IIc members have adopted different strategies to cope with Fe limitation. Altogether, the discovery of low-Fe adapted ecotype within the globally dominant clade II might have important consequences in context of the current expansion of low-Fe areas caused by global change.

Introduction

Oceans are particularly affected by the global change, which causes an increase in seawater temperature, but also an expansion of nutrient-poor areas, notably iron (Fe)-poor regions such as the tropical Pacific Ocean (Behrenfeld et al., 2009; Blain et al., 2008; Polovina et al., 2008; Tagliabue et al., 2017). Contrary to other oceanic areas, which are regularly replenished in nutrients by wind-transported aerosols or vertical mixing events during winter, most of the tropical Pacific remains Fe-limited year-round, raising the question of the capacity of local marine phytoplanktonic populations to adapt to these specific conditions. Indeed, while Fe is essential to the metabolism and growth of all living organisms, it is particularly critical for phytoplankton for which up to 50% of the cellular Fe occurs in the photosynthetic apparatus (Behrenfeld & Milligan, 2013). Furthermore, the dissolved unchelated inorganic iron (Fe') is only present in picomolar to nanomolar concentrations in the ocean, the most readily available form of Fe to phytoplankton being the soluble ferrous iron (Fe^{2+}) and to a least extent the oxidized ferric form (Fe^{3+}; Johnson et al., 1997; Morel et al., 2008). For these reasons, Fe depletion is thought to already impair phytoplankton growth in 35 to 50 % of the global ocean depending on phytoplanktonic groups, these Fe-poor areas being often referred to as 'high-nutrient low-chlorophyll' (HNLC) areas (Moore et al., 2002).

The vast majority of phytoplankton cells living in the upper lit layer of Fe-poor regions are of tiny size (<2-3 µm), these so-called 'picophytoplankters' being numerically dominated by two cyanobacterial genera, *Prochlorococcus* and *Synechococcus*, which together account for an estimated 24 % of global net marine primary productivity (8 and 16 %, respectively; (Flombaum et al., 2013; Partensky et al., 1999). In the last 20 years, extensive laboratory and environmental studies have shown that both of these ubiquitous genera encompass several 'ecotypes', i.e. genetically distinct populations occupying different ecological niches (Coleman et al., 2006). For *Prochlorococcus*, among the genetically distinct lineages thriving in the upper mixed layer, so-called high light (HL) clades (Moore et al., 1998), HLIII and HLIV co-occur specifically in warm Fe-limited areas (Johnson et al., 2006; Rusch et al., 2010; West et al., 2011), HLII members dominate in warm Fe-replete waters, while HLI preferentially thrive in temperate Fe-replete waters (Chandler et al., 2016; Johnson et al., 2006; Kent et al., 2019). Similarly, *Synechococcus*

clade CRD1 – first observed in the Costa Rica Dome – was recently found to dominate the *Synechococcus* populations specifically in Fe-depleted areas of the world Ocean in co-occurrence with EnvB (a.k.a CRD2 using ITS; (Ahlgren et al., 2020; Farrant et al., 2016; Sohm et al., 2015), while members of clades II and III were mainly found in warm N and P-poor waters, respectively, and clades I and IV in cold, nutrient-rich waters (Farrant et al., 2016; Kent et al., 2019; Zwirglmaier et al., 2008). Furthermore, global distribution patterns of *Synechococcus* populations using *Tara* Oceans metagenomes, have recently allowed Farrant et al. (2016) to define, within the CRD1 and EnvB clades, three distinct 'Ecologically Significant Taxonomic Units' (ESTUs), i.e. operational taxonomic units (OTUs) belonging to the same clade and occupying distinct oceanic niches: CRD1C/EnvBC preferentially thrives in warm waters, CRD1B/EnvBB in cold waters, while CRD1A/EnvBA members were found in both thermal niches. The occurrence of cold (ESTUs IA, IVA and CRD1B) and warm (ESTUs IIA, IIIA, CRD1A and CRD1C) *Synechococcus* 'thermotypes' was confirmed by showing that strains representative of these different lineages exhibit distinct thermal preferenda, a feature notably linked to difference in photophysiology (Breton et al., 2019; Doré et al., 2022; Ferrieux et al., 2022; Pittera et al., 2014), thermostability of their light-harvesting systems (Pittera et al., 2016), content in lipid desaturases (Pittera et al., 2017), and/or their ability to induce photoprotective light dissipation at colder temperatures using the orange carotenoid protein (OCP; Six et al., 2021). Thus, this suggests that both Fe availability and temperature have played a key role in the genetic diversification of marine picocyanobacterial lineages colonizing Fe-limited waters, even though the mechanisms involved in adaptation to low-Fe conditions largely remain to be deciphered.

Until now, physiological and molecular studies of the mechanisms involved in Fe acquisition and utilization have mainly concerned model freshwater or halotolerant cyanobacteria and have allowed to highlight several common characteristics of the response of cyanobacteria to Fe limitation. These notably include i) sensing intracellular Fe(II) pools and regulating the expression of a large number of genes, directly or indirectly affected by Fe limitation, using the ferric uptake regulator (Fur; Lee & Helmann, 2007; Riediger et al., 2021), ii) acquiring organic Fe through the uptake and/or synthesis of siderophores (Ito & Butler, 2005; Jiang et al., 2015), iii) reducing the cellular Fe

requirement in low-Fe conditions by decreasing the PSI (12-Fe atoms) to PSII (3-Fe atoms) ratio (Barber et al., 2006) and the number of phycobilisomes that require Fe-containing hemes for their biosynthesis (Frankenberg et al., 2001), and/or substituting Fe-containing proteins by an alternative protein lacking Fe (e.g. ferredoxin *vs.* flavodoxin; Leonhardt & Straus, 1992), iv) reducing oxidative damage that results from Fe deficiency (Michel et al., 2003; Park et al., 1999), as well as v) storing Fe in bacterioferritin and Dps complexes (Keren et al., 2004; Shcolnick & Keren, 2006).

However, much less is known on adaptation to Fe limitation in strictly marine cyanobacteria, despite the fact that picocyanobacteria numerically dominate phytoplanktonic communities in Fe-poor oceanic waters (Flombaum et al., 2013; Partensky et al., 1999). One of the rare studies on this topic compared the growth, photophysiology and proteomes of two *Synechococcus* strains isolated from different environmental niches (Mackey et al., 2015). In contrast to the paradigm that coastal phytoplankton is less able to adapt to Fe limitation than open ocean species, this study revealed that the coastal strain (*Synechococcus* sp. WH8020) was able to acclimate to changes in Fe concentration by modulating Fe uptake, Fe storage and the amount of photosynthetic proteins, whereas the oceanic one (WH8102) lacked these adaptive responses. Furthermore, Lis et al. (2015) showed that like for freshwater cyanobacteria, Fe' was the most bioavailable Fe form for the two marine *Synechococcus* strains, WH8102 and the model strain WH7803, with uptake rate much higher than those for Fe complexed with organic ligands (FeL) and that this uptake likely proceeds via a reductive Fe uptake pathway, functioning alone or in complement to siderophore-mediated uptake (Lis et al., 2015). However, none of the strains used in previous studies were isolated from a chronically low-Fe area, and therefore both may lack some specific adaptation to this harsh environment. Most other knowledge on adaptation to Fe- limitation in marine cyanobacteria are derived from meta-omic studies and led to the identification of a number of genes specifically present or absent in Fe-limited environments. For instance, analysis of metagenomes (Ahlgren et al., 2020; Garcia et al., 2020; Hogle et al., 2022; Kent et al., 2016; Rusch et al., 2010) or single cell genomes (Malmstrom et al., 2013), retrieved from populations specific of low-Fe areas (*Prochlorococcus* HLIII/IV and *Synechococcus* CRD1/2), suggests that adaptation to Fe limitation mainly relies on i) the reduction of their

Fe quota through the loss of several Fe-containing proteins, ii) the capacity for siderophore-mediated Fe uptake as well as iii) an expansion of the gene families involved in Fe storage, although the precise physiological mechanisms at work remain elusive.

In this paper, we compared the physiological and transcriptomic (work in progress; see below) responses of strains representative of different warm, oceanic niches limited by different nutrients to an abrupt change of Fe source from Fe' to FeL complexed by various concentrations of DFOB. This treatment led to very different responses between strains that were interpreted in the light of comparative genomics using 256 genomes and metagenomic analyses of the *Tara* Oceans dataset.

Material and Methods

Strains and growth conditions

The six *Synechococcus* spp. strains used for this study were retrieved from the Roscoff collection (https://roscoff-culture-collection.org/; Table 1). These include representative strains of the three known CRD1 ESTUs (CRD1A—C), one strain representative of ESTU IIIA, dominating in warm, P-limited waters as well as two strains belonging to the ESTU IIA, dominating in warm, N-limited waters. Strains were grown at 22°C under 75 µmol photons m^{-2} s^{-1} (hereafter µE m^{-2} s^{-1}) continuous light provided by a white-blue-green LED system (Alpheus, France) in temperature-controlled chambers. Cultures were maintained in 50 mL flasks (Sarstedt, Germany). The culture medium PCR-S11 (Rippka et al., 2000), supplemented with 1mM sodium nitrate, used for the experiment was prepared from seawater reconstituted using Red Sea Salts (Houston, TX, USA) and distilled water. The PCR-S11 recipe includes Fe as ferric chloride hexahydrate ($FeCl_3 \cdot 6H_2O$) complexed with EDTA at a final concentration of 2µM Fe-EDTA.

TABLE 1 | Characteristics of the *Synechococcus* strains used in this study

Strains name	MITS9220	BIOS-U3-1	BIOS-E4-1	A15-62	M16.1	WH8102
RCC # [1]	2571	2533	2534	2374	791	539
Subcluster [2]	5.1	5.1	5.1	5.1	5.1	5.1
Clade [2]	CRD1	CRD1	CRD1	II	II	III
Subclade[3]	n.a.	n.a.	n.a.	IIc	IIa	IIIa
ESTU [2]	CRD1A	CRD1B	CRD1C	IIA	IIA	IIIA
Pigment type [4]	3dA	3dA	3cA	3dB	3a	3c
Ocean	Pacific	Pacific	Pacific	Atlantic	Atlantic	Atlantic
Region	Equatorial Pacific	Chile upwelling	South East Pacific	Offshore Mauritania	Gulf of Mexico	Caribbean Sea
Isolation latitude	0°00’ N	34°00’ S	31°52’ S	17°37’ N	27°70’ N	22°48’ N
Isolation longitude	140°00’ W	73°22’ W	91°25’ W	20°57’ W	91°30’ W	65°36’ W

[1]Roscoff Culture Collection, [2]Farrant et al. (2016), [3]Mazard et al. (2012), [4]Humily et al. (2013).

Experimental set-up

In order to estimate the ability of these strains to grow using only FeL, a first set of experiment consisted in following growth of cultures submitted to various degrees of Fe’-depletion using a strong Fe chelator, desferrioxamine B (DFOB, as deferoxamine mesylate salt, Sigma-Aldrich), a compound that preferentially binds Fe^{3+}. The stock solution of DFOB was prepared at 8mM in milliQ water, filtered on 0.2 µm and stored at 4°C. DFOB was added to the PCRS-11 medium 24h before inoculation of the cultures at a final concentration of 50, 100, 200, 400, 800µM, 1.6mM or 2.4 mM, depending on its effect on strain growth (see results). When cell concentration reached ~ 5 x 10^6 cells mL^{-1}, cultures were transferred in 50mL Falcon tubes and centrifuged at 20°C, 9,000 x g for 7min using an Eppendorf 5804R (Eppendorf, France) in the presence of 0.01% (v/v) pluronic acid (Sigma-Aldrich, Germany). Pellets were resuspended at ~ 8 x 10^6 cells mL^{-1} in triplicate 50 mL flasks of either PCR-S11 only (control condition) or PCR-S11 supplemented with DFOB at the abovementioned concentrations.

Furthermore, based on growth rate of strains in the different DFOB concentrations, we selected a chelator concentration that affected the growth of most strains (see results) to be used for transcriptomic and pigment analyses by HPLC. These analyses were performed on all 6 strains submitted to 800 µM DFOB for 6h. Four liters of culture grown in PCR-S11 up to ~ 5 x 10^7 cell/ml were concentrated in presence of pluronic 0.01% (v/v) by a first centrifugation step at 20°C, 9,000 x g, during 10 min (Sorvall LYNX 6000, Thermo Fisher Scientific, USA) in 1 L Nalgene flasks followed by a second centrifugation step in 50

ml Flacon tubes at 20°C, 9,000 x g, during 7 min. Cells were resuspended in 50 ml PCR-S11 only (control) or PCR-S11 supplemented with DFOB or Fz, quantified by flow cytometry and then split into 460 ml triplicate cultures for each conditions at a concentration adjusted to 5 x 10^7 cell/ml. Cultures were then put in back into initial growth conditions (22°C, 75 µE) for 6h before harvesting cells for RNAseq and HPLC analyses.

Flow cytometry

Culture growth rates were determined by flow cytometry using 200 µl culture aliquots, collected twice a day during about one week. Cells were fixed using 0.25% (v/v) glutaraldehyde (grade II, Sigma Aldrich, USA) and stored at -80°C (Marie et al., 1999) until analysis using a Guava easyCyte flow cytometer (Luminex Corporation, USA) and growth rates were calculated as previously described (Ferrieux et al., 2022). Furthermore, the determination of cell number after concentration of the cultures by centrifugation was performed on living cells using a Novocyte Advanteon flow cytometer (Agilent).

Biovolume

Synechococcus cultures were acclimated at 22°C under 75 µE m^{-2} s^{-1}. For each strain, the width and length of 100 cells in triplicates were measured in exponential growth phase using an Eclipse 80i Nikon fluorescence microscope (Nikon, Japan). Cells were were excited in green light at λ=550nm at x100 objective with a Cy3 filter (Nikon, Japan) to observe their natural orange fluorescence. High resolution photographs were taken using a Spot camera (SPOT RT3, Diagnostic Instruments Inc., USA) and photographs were analyzed with SpotAdvanced software (Diagnostic Instruments Inc., USA) in order to estimate length (L) and width (W) of selected cells. Finally, biovolume (V in μm^{-3}) was estimated using the formula, assuming that *Synechococcus* cells have a Tic-Tac® shape:

$$V = (L - W) \times \pi \times (\frac{w}{2})^2 + [\frac{4}{3} \times \pi \times (\frac{w}{2})^3]$$

RNA extraction and sequencing

After 6h of incubation in PCR-S11 (control) or in PCR-S11 supplemented with DFOB 800 µM, two 150 mL aliquots of culture were harvested by centrifugation in presence of pluronic 0.01% (v/v) at 4°C, 9,000 x g for 7 min using an Eppendorf 5804R (Eppendorf, France). Pellets were resuspended in 2 mL Eppendorf tubes and centrifuged at 4°C, 14,000

x g for 2 min using an Eppendorf 5417R centrifuge. Supernatant was discarded and pellets were resuspended in 1 mL Qiazol (Qiagen, Valencia, CA, USA), immediately flash frozen and stored at -80°C until RNA extraction. The whole procedure took less than 15 min. RNA extraction was performed as described in Guyet et al. (2020). Briefly, frozen samples were thawed at 65°C, then incubated 5 more min at 65°C with regular vortexing and then centrifuged at 4°C, 16,000 x g for 10min (Eppendorf 5417R; Eppendorf, France). Total RNA was extracted with the Direct-Zol RNA MiniPrep kit (Zymo Research Corp, Proteigene, France) and DNA removed using the Qiagen RNase-free DNase Set (Qiagen). RNA quantification was done using a NanoDrop ND-1000 (Thermo Fisher Scientific, USA) and quality control was performed with the RNA 6000 Nano Kit on a BioAnalyzer 2100 (Agilent, USA). After being flash frozen in liquid nitrogen, RNA samples were stored at -80°C until sequencing.

Ribodepletion was performed from 200-300 ng of total RNA using the rRNA depletion kits, RiboCop (Lexogen) and Ribo-Zero Plant (Illumina). Libraries were then prepared using the Illumina TruSeq Stranded mRNA kit and sequenced as overlapping 150 bp paired-end reads on Illumina Novaseq SP System (Illumina, San Diego, CA, USA). Both ribodepletion and sequencing were performed at Fasteris (Plan-les-Ouates, Switzerland). 18.5 ± 4.7 × 106 paired-end reads were generated per sample.

HPLC analyses

After 6h of incubation in PCR-S11 (control) or in PCR-S11 supplemented with DFOB 800 µM, 50 mL of culture were harvested in triplicate and subjected to two centrifugation steps using an Eppendorf 5804R (Eppendorf, France), the first one at 4°C, 10,000 x g for 7min and then 5min after removing most of the supernatant. Cells were transferred in 2 mL Eppendorf and centrifuged at 4°C, 14,000 x g for 2min using an Eppendorf 5417R (Eppendorf, France) and the pellets were kept at -80°C until analyses. For pigment analyses, 400 µL of cold methanol 100% (HPLC grade, Thermo Fischer Scientific) was added to cell pellets and vortexed. Extracts were then centrifuged at 4°C, 14,000 x g for 10min (Eppendorf 5417R). Supernatants were kept and supplemented with 10% (v/v) Milli-Q water to prevent peak distorsion (Zapata & Garrido, 1991). Samples were analyzed using an HPLC 1100 Series System (Hewlett-Packard) as previously described (Pittera et al., 2014). The extraction was performed in dark and on ice to avoid pigments oxidation.

Pigment peaks were identified based on their retention times and peaks were measured as previously described (Six et al., 2005).

Comparative genomics and metagenomics

The 256 whole genome sequences (WGS), single amplified genomes (SAGs) and metagenome assembled genomes (MAGs) used as reference genomes in this study were retrieved either from the Cyanorak v2.1 information system (Garczarek, Guyet, Doré, Farrant, Hoebeke, Brillet-Guéguen, Bisch, Ferrieux, Siltanen, Corre, Le Corguillé, et al., 2021) or from Genbank (**Dataset 1**). Protein sequences retrieved from new genomes were clustered with proteins from Cyanorak v2.1 to assign them to pre-existing clusters of likely orthologous genes (CLOGs) using the OrthoFinder algorithm (Emms & Kelly, 2019). Result of this clustering was used to define phyletic patterns for a selection of genes involved in Fe metabolism (**Dataset 2**).

Whole genome recruitment of metagenomic reads from the *Tara* Oceans dataset on the 256 picocyanobacterial genome was performed and used to draw distribution maps of genes of interests using custom-designed R scripts, as previously described (Doré et al., submitted).

Results

Response to Fe deprivation induced by DFOB

In order to compare the response to an abrupt change of Fe source from Fe' to FeL of strains representative of the *Synechococcus* CRD1 ESTUs to that of clades II and III counterparts, dominating in warm, N or P-depleted areas, respectively, exponentially growing cultures were centrifuged and transferred into PCR-S11 supplemented with different concentrations of the strong chelator DFOB. Growth was followed for seven to ten days depending on culture growth rate. All three CRD1 strains exhibited a higher resistance to Fe' starvation than the clade II strain M16.1 and the clade III strain WH8102 (**Fig. 1**). The latter was by far the most sensitive strain with a complete loss of growth already at the lowest DFOB concentration tested (50 µM), M16.1 grew until 200 µM DFOB, while the three CRD1 strains could stand up to 800 µM DFOB, though with a strongly reduced growth rate. The least affected strain was the clade II strain A15-62, which

exhibited no significant reduction of its growth rate at 800 µM DFOB and needed a dose as high as 2.4 µM to have a quasi-complete inhibition of its growth.

Based on the previous results, the short-term effect of the addition of 800 µM DFOB for 6h on the liposoluble pigment content (**Fig. 1 and S1**) and on the transcriptome (work in progress) was also analyzed. Pigment content analyses by HPLC showed not significant effect of this treatment except for the clade III strain WH8102, for which a clear drop of Chl *a* but also β-car and Zea was observed but with not modification of the β-car/Chl *a* or Zea/Chl *a* ratios, suggesting that DFOB affected the whole photosynthetic apparatus.

Cell Biovolume

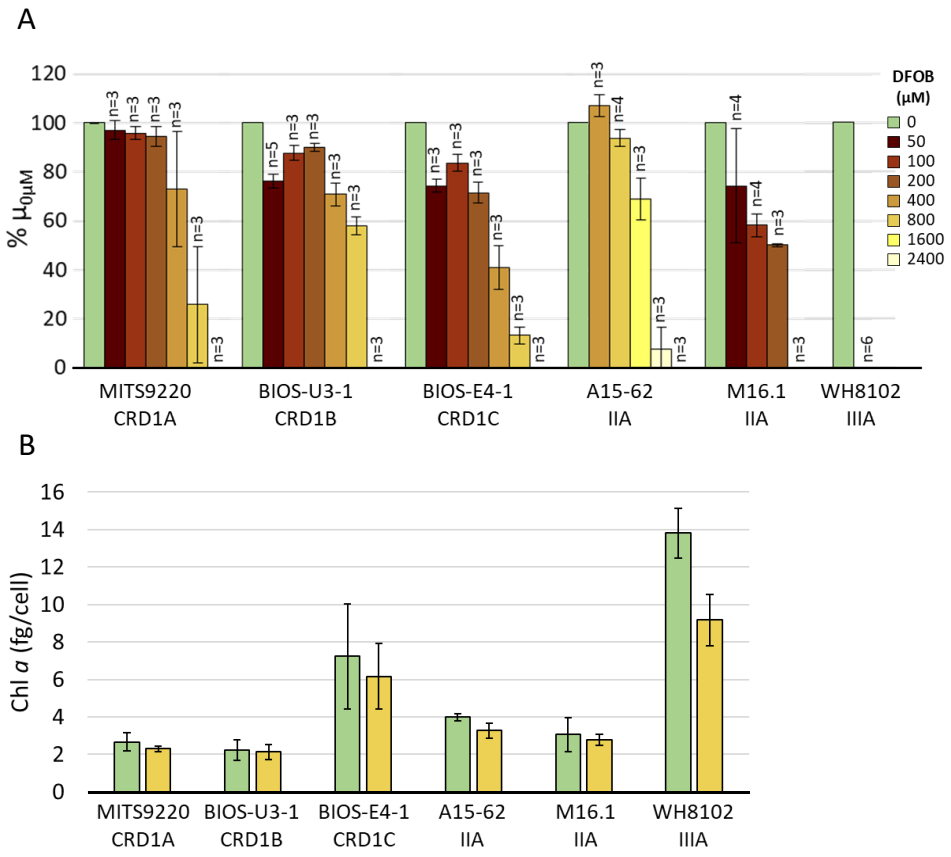

Figure 1. Effect of DFOB on the growth rate and chlorophyll a content of CRD1 vs clades II and III strains. (**A**) Growth rate at different DFOB concentration expressed as percentage of the growth rate obtained in the control condition (PCR-S11 only). The insert indicates the concentration of DFOB in µM. Each data point is the average of several biological replicates, whose number is indicated above each histogram. Note that for A15-62, intermediate DFOB concentrations between the control (0µM) and 400 µM have not been tested. (**B**) chlorophyll a content measured 6h after addition of 800 µM DFOB. Each data point is the average of three biological replicates. The corresponding ESTU (sensu Farrant et al., 2016) is indicated below each strain name.

To check whether adaptation to low-Fe conditions may affect cell size, we measured the biovolume of representative strains of the main *Synechococcus* lineages as well as the one from the model strain *Synechococcus* sp. WH7803. These analyses showed that this parameter exhibits wide variations with no clear relationship with genotype or ecotype (Table 2). Indeed, the CRD1 strains ranged from 0.29 to 0.57 μm^3, the biggest one, BIOS-E4-1 exhibiting the fourth largest biovolume among the 13 tested strains.

Table 2 | Biovolumes and genome sizes of representative strains of the main *Synechococcus* lineages as well as the model strain WH7803. All strains were grown a 75 $\mu E.m^{-2}.s^{-1}$ and 22°C.

Strain	Clade	Sub-clade	ESTU	Mean cell length (µm)	Mean cell width (µm)	Mean cell biovolume (µm3)	SD biovolume	Genome size (Mbp)	CDS number
MITS9220	CRD1	n.a.	CRD1A	1.02	0.67	0.29	0.03	2424175	3045
BIOS-U3-1	CRD1	n.a.	CRD1B	1.21	0.71	0.39	0.03	2710834	3434
BIOS-E4-1	CRD1	n.a.	CRD1C	1.35	0.81	0.57	0.10	3314220	4428
CC9311	I	Ia	IA	1.18	0.73	0.41	0.02	2606749	2931
MVIR-18-1	I	Ib	IA	1.02	0.62	0.25	0.01	2451974	3033
ROS8604	I	Ib	IA	1.86	1.00	1.22	0.05	2876904	3732
MVIR16-2	I	Ib	IA	1.26	0.91	0.64	0.03	n.a.	n.a.
M16.1	II	IIa	IIA	1.28	0.77	0.52	0.14	2112236	2501
A15-62	II	IIc	IIA	1.02	0.58	0.22	0.03	2294140	2791
WH8102	III	IIIa	IIIA	1.27	0.76	0.49	0.11	2434429	2780
BL107	IV	IVa	IVA	0.99	0.70	0.30	0.03	2285035	2505
WH7803	V	n.a.	VA	1.74	1.15	1.49	0.13	2366981	2577

Comparative and environmental genomics

The comparison of the gene content of 256 *Prochlorococcus* and marine *Synechococcus/Cyanobium* genomes (WGS, SAGs or MAGs) and their distribution in the *Tara* oceans metagenomic dataset allowed us to i) retrieve the set of genes involved in Fe uptake and metabolism, ii) highlight the specificities of CRD1 and EnvB clades co-dominating *Synechococcus* communities in low-Fe areas, complementing previous observations made by several groups (Ahlgren et al., 2020; Doré et al., submitted; Garcia et al., 2020; Hogle et al., 2022) and iii) better explain the abovementioned behavior of A15-62 and WH8102 with regard to Fe' depletion. For the transport of Fe^{3+},

picocyanobacterial genomes possess the FutBC transporter as well as one or two FutA subunits (Katoh et al., 2001; **Dataset 2**). Like most *Synechococcus* SC 5.1 strains, all CRD1 and all but one EnvB genomes possess one FutA-like subunit, potentially binding Fe^{3+} in the periplasmic space like *Synechocystis* sp. PCC 6803 FutA2 (Slr0513; Katoh et al., 2001; Kranzler et al., 2014) or the sole FutA of *Trichodesmium erythraeum* (Polyviou et al., 2018), while most clades III, V, VI, VIII and SC 5.2 and 5.3 strains additionally or alternatively (including WH8102; **Fig. S2B**) possess another FutA subunit, that we called FutA1 since it has a higher homology with *Synechocystis* FutA1 (Slr1295) than the FutA-like protein (**Fig. 2**). Like *Synechocystis* FutA1, this latter protein could have a regulatory role, notably to regulate iron uptake pathway. In agreement with its phyletic pattern, *futA1* is specifically found in the Mediterranean Sea and in the Gulf of Mexico, where clade III and SC 5.3 dominate (**Fig. 3A**). Most CRD1 genomes also possess a Fe^{2+} transport system widespread in bacteria (Gómez-Garzón et al., 2022), consisting in a large transmembrane nucleoside triphosphatase (NTPase) protein, FeoB, as well as an accessory cytoplasmic protein, FeoA, required for multimeric complex formation. Interestingly, besides CRD1, these genes were only found in a couple of clade I strains, explaining their presence at high latitude in the distribution map (**Fig. 3B**), as well as in clade VIII and SC 5.2, in which only *feoB* may be present. Furthermore, marine picocyanobacteria have a highly variable set of divalent metal transporters (**Dataset 2**), among which some were more specifically found in CRD1 and/or EnvB genomes (**Fig. 2**). Half of CRD1 WGS specifically possess a VIT (vacuolar iron transporter)-like Fe^{2+}/Mn^{2+} transporter (CK_00035628). Although this transporter has been shown to play important roles in Fe homeostasis in *Arabidopsis* (Kim et al., 2006), its homolog in *Synechococcus* is apparently very scarce in the ocean (**Fig. 3C**). CRD1 genomes also possess one or two members of the $Zn^{2+}/Fe^{2+}/Mn^{2+}$ transporter ZIP (Zrt/Irt-like protein) family (Barnett et al., 2012; Hu, 2021), CK_00008752 and/or CK_00055218, which are indeed enriched in low-Fe areas, while EnvB genomes and a few clade II genomes (including A15-62, **Fig. S2A**) systematically possess another member of this protein family (CK_00006138). By comparison, most other *Synechococcus* clades but clade I possess either none or only one member of this protein family. Of note, while most SC 5.1 strains possess a member of the natural resistance associated macrophage protein (NRAMP) family, a divalent metal (Cd, Co, Mn, Zn) transporter widely distributed among prokaryotes and eukaryotes (Agranoff et al., 2005; Cellier et al., 1995), this transporter is

specifically absent from CRD1 strains, in agreement with its very low abundance at the HNLC stations, e.g. at TARA_052 or TARA_100. Among this gene category, CRD1 and clade III strains are also strongly enriched in an ABC-type divalent metal transporter that we have called *znuA2-B2-C2* because of its relatedness to *Nostoc* sp. PCC 7120 ZnuABC (Napolitano et al., 2012), while the core *znuA1-B1-C1* genes that possess the zinc uptake regulator gene *zur* in their immediate vicinity (Barnett et al., 2012) are fairly distantly related from *Nostoc znuABC.* Although absence of a specific *zur* regulator in the *znuA2-B2-C2* operon might indicate that this transporter has a different metal specificity, the systematic presence of a putative Zn chaperone (COG0523, CK_00009118) and of a WD-repeat containing protein of unknown role (CK_00002334; Barnett et al., 2012) either next to the *znuC1-zur-znuB1-znuA1* gene cluster or next to the *znuA2-B2-C2* when present, tends to confirm its role in Zn transport. Although a surprisingly low fraction of the Mediterranean Sea population possesses these genes, this additional Zn transporter and associated proteins are present in a much larger proportion of the *Synechococcus* population suggests in typical HNLC areas, which are not only Fe-limited but potentially Zn-limited as well (Croot et al., 2011; Koch & Trimborn, 2019). Besides being transported into the cytoplasm by FutABC system, periplasmic Fe^{3+} can also be reduced into Fe^{2+} by a reductive Fe pathway. At this level, most *Synechococcus* genomes, including all CRD1 and one out of three EnvB genomes possess the *ctaC2-D2-E2* operon, encoding an alternative respiratory terminal oxidase (ARTO; **Dataset 2 and Fig. 2**), which based on the characterization of *Synechocystis* sp. PCC 6803 orthologs (Kranzler et al., 2014) and its distribution in the field (Doré et al., submitted) could constitute an important adaptation mechanism to low-Fe through the reduction of Fe^{3+} into Fe^{2+} prior to its transport through the plasma membrane. This reduction could also be performed outside the outer membrane by the major pilin protein, PilA1 (Lamb et al., 2014), which is seemingly enriched in CRD1 as well as in clades I and IIh but not in EnvB genomes, but which although widespread seems to be present in a larger part of the population in HNLC areas (**Dataset 2 and Fig. S3A**). Finally, although all marine picocyanobacteria lack siderophore synthesis genes, a number of genomes from different clades (II, III, IV, EnvA, EnvB, WPC1) possess a TonB-dependent siderophore transport system gathering a TonB-dependent receptor (FecA), an energy transducing complex (TonB-ExbB-ExbD), the TonB existing under two possible forms (CK_00041994 and CK_00051610), as well as an ABC-transporter to convey

periplasmic Fe^{3+} through the plasma membrane, which we renamed FecBDE (**Dataset2 and Fig. 2**) based on its homology with their orthologs in *Nostoc* sp. PCC 7120 (FecB2D2E2; Stevanovic et al., 2012). As previously shown by Ahlgren et al. (2020), CRD1 genomes totally lack this system while two out of three EnvB genome possess it. Accordingly, the distribution of this operon in the field (Doré et al., submitted) shows that it is most abundant at stations where EnvB (and/or EnvA, which seemingly also possess this system**;** **Dataset 2**) have a high relative abundance (e.g. TARA_070, 72, 133, etc.), while despite its presence in one genome of each clade III and WPC1, it is virtually absent from the Mediterranean Sea and the Gulf of Mexico (Doré et al., submitted).

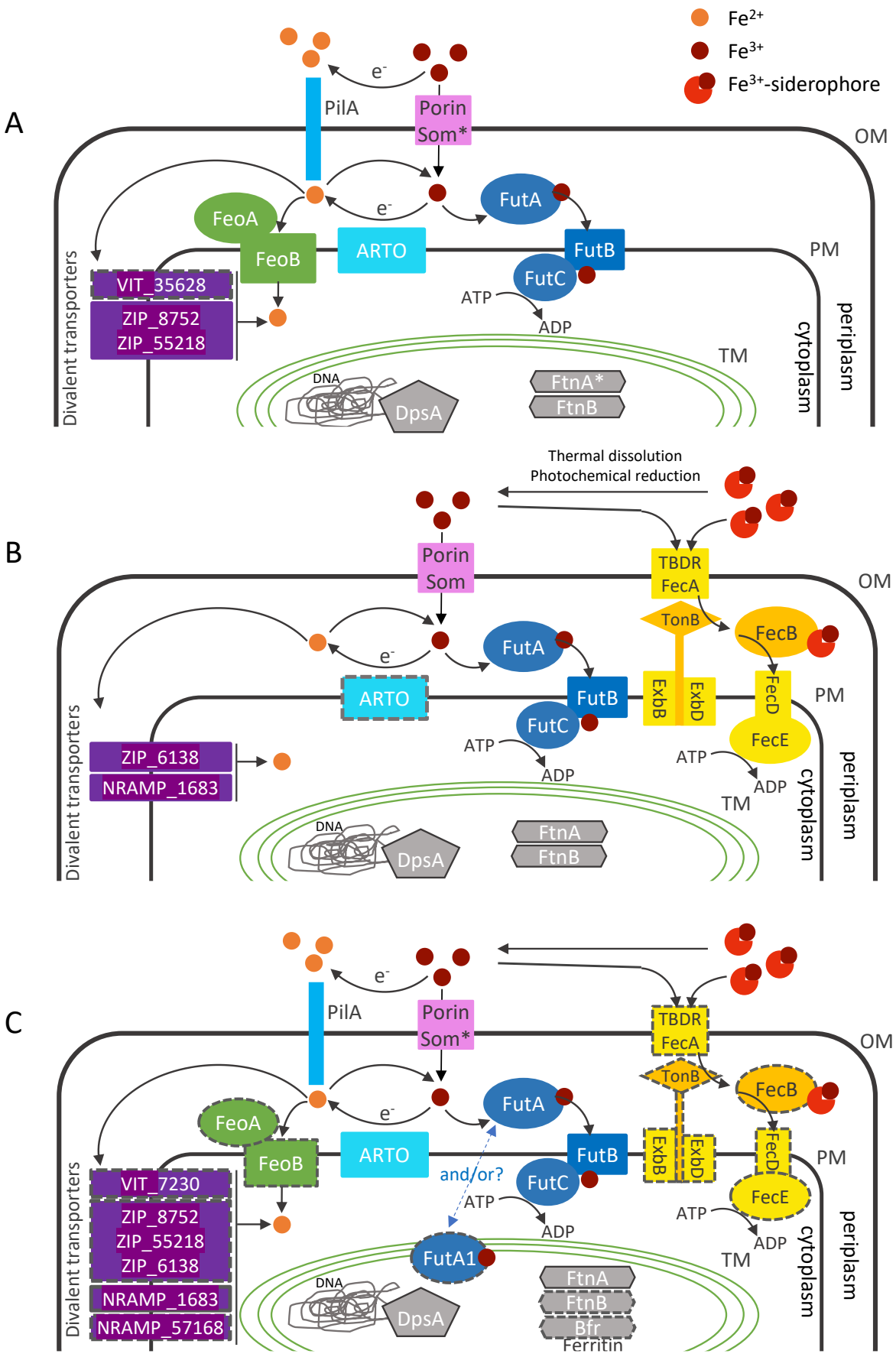
Fe2+
Fe3+
Fe3+-siderophore
A
e-
PilA
Porin
Som*
OM
FeoA
FeoB
ARTO
FutA
FutB
FutC
PM
VIT_35628
ZIP_8752
ZIP_55218
Divalent transporters
ATP
ADP
TM
periplasm
cytoplasm
DNA
DpsA
FtnA*
FtnB
B
Thermal dissolution
Photochemical reduction
Porin
Som
TBDR
FecA
TonB
FecB
ExbB
ExbD
FecD
FecE
ZIP_6138
NRAMP_1683
FtnA
FtnB
C
VIT_7230
NRAMP_57168
and/or?
FutA1
Bfr
Ferritin

Figure 2. Specific set of proteins involved in Fe uptake and storage in low-Fe adapted *Synechococcus* ecotypes. Proteins are shown with a continuous contour when they are found in most genomes of CRD1 (A), EnvB (B) or other *Synechococcus* clades (C), or with a discontinuous contour when present in less than 50% of the genomes of a given category. Free Fe^{3+} could be reduced in the immediate vicinity of the cells by the major pilin protein, PilA1 (light blue; Lamb et al., 2014). Alternatively, both free and siderophore-bound Fe^{3+} are transported across the outer membrane through a TonB-dependent transport system (TBDT; yellow) composed of a TonB-dependent receptor (TBDR or FecA) and an energy transducing complex, TonB-ExbB-ExbD. Siderophore- Fe^{3+} complexes are then conveyed by a periplasmic solute binding protein (FecB) to a plasma membrane ABC transporter consisting in the permease FecD and the ATPase FecE. Furthermore, Fe^{3+} can also be transported through the outer membrane by passive transport via non selective or Fe-selective porins (som, pink; Qiu et al., 2021), the majority would be absorbed by energy-coupled active transport through the TBDT (Jiang et al., 2015). Periplamic Fe^{3+} is then bound by the high-affinity Fe^{3+}-binding protein FutA2 (blue) and either transported into the cytoplasm by FutBC complex or reduced into Fe^{2+} in the periplam by the respiratory terminal oxidase, ARTO (orange, Kranzler et al., 2014). The FutA2 homolog FutA1 as well as FutC, both identified as intracellular proteins, were suggested to play a role in regulating the reductive iron uptake pathway (Kranzler et al., 2014). Fe^{2+} is then transported through the plasma membrane (PM) via either the FeoB (green) transporter after its activation by FeoA or by a divalent metal transporter of the ZIP, VIT and/or NRAMP family. The half-life of Fe^{2+} being very short, the remaining Fe^{2+} will be re-oxidized to Fe^{3+} by oxygen produced by photosynthesis. Stars indicate that genes encoding these proteins are present in multiples copies. Abbreviations: OM, outer membrane; PM, plasma membrane; TM, thylakoid membrane. Modified from Kranzler et al. (2014), Hogle et al. (2022), Jiang et al. (2015), Lamb et al. (2014) and Qiu et al. (2021).

As concerns Fe storage, although the ferritin FtnA is close to be core in marine picocyanobacteria, with the notable exception of WH8102 (**Fig. S2B**), CRD1 genomes often possess multiple copies (up to 6) of this gene and are also enriched in a second type of ferritin (FtnB), while EnvB genomes seemingly possess one gene copy of each type, and SC 5.2 and 5.3 possess, additionally to *ftnA* and often *ftnB,* a bacterioferritin (*bfr*, **Dataset 2, Fig. 2**). Most CRD1 and EnvB genomes also possess an Fe-detoxification protein (DpsA), absent from most clades II (except IIh), III and IV genomes, which based on its homology with *Synechococcus elongatus* PCC 7942 Synpcc7942_0109, could be involved either in protecting DNA from Fe-induced free radical damage and/or acting as a ferritin involved in metal homeostasis of the photosynthetic apparatus (Andrews et al., 2003; Durham & Bullerjahn, 2002). The distribution map of these genes indeed shows that *Synechococcus* populations thriving in typical HNLC as well as cold areas most often possess 3 copies of *ftnA* and one copy of each *ftnB* and *dpsA,* while only a small proportion of the populations dwelling in low-P areas and dominated by clades III, WPC1 and SC5.3 (Farrant et al., 2016) possess *dpsA* and even less *ftnA* and *bfr* (**Fig. 4A**).

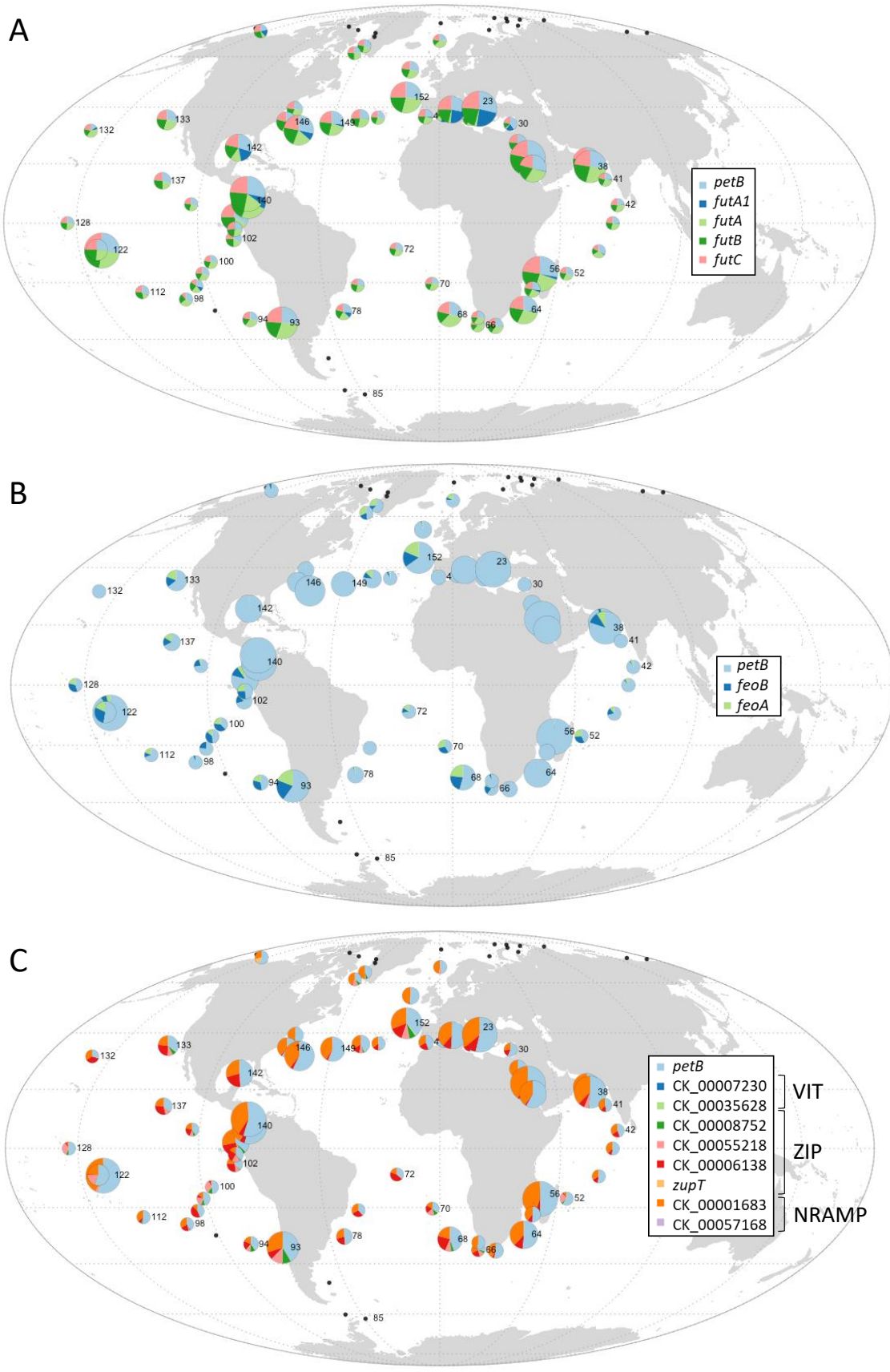

Figure 3. Global distribution map of *Synechococcus* genes involved in Fe transport. The size of the circle is proportional to relative abundance of each genus as estimated based on the *petB* gene and this gene was also used to estimate the relative abundance of other genes in the population. (**A**) *futABC* involved in Fe^{3+} transport, (**B**) *feoAB* involved in Fe^{2+} transport, (**C**) divalent metal transporters.

Another important category concerns Fe-containing proteins or proteins interacting with them that, in Fe-limited conditions, can be reduced or replaced by proteins containing another metallic cofactor. A first example concerns the alternative electron carriers Fe-containing cytochrome c_6 (PetJ) and Cu-containing plastocyanin (PetE; Durán et al., 2004). While *petE* is seemingly core in *Prochlorococcus* and *Synechococcus* SC 5.1, CRD1 but also most clades II, III and IV genomes most often lack one copy (*petJ2*) out of the three *petJ* copies, while EnvB seemingly only possess *petJ3* (**Dataset 2; Fig. S3B**). More strikingly, CRD1 and EnvB genomes are enriched in the Fe-free flavodoxin (Straus, 1994), most often having one of each *isiB1* and *isiB2* gene copies, able to substitute Fe-containing ferredoxins in Fe-limiting conditions. Yet, these genomes also encompass a fairly large set (up to 11) of ferredoxins but like *Prochlorococcus* lack CK_00008098, present in most other *Synechococcus* genomes and CK_00008099, present in less genomes (**Dataset 2)**. Both of these genes are indeed absent from low-Fe regions (**Fig. S3C**) Furthermore, all CRD1 and EnvB genomes also possess IsiA, a chlorophyll a-binding protein that forms a ring around PSI to compensate for the reduction of PBS under Fe limitation (Boekema et al., 2001), and which is missing in more than 50% of other *Synechococcus* genomes (e.g. only in two out of 10 clade III), except for clades II and XVI. Surprisingly in the field, *isiA* appears to be present in most environmental niches with the notable exception of the low-P areas (**Fig. S4A**). Also interesting is the phyletic and distribution patterns of *ftrC* and *ftrV* genes, which respectively encode the [4Fe–4S] cluster containing catalytic subunit and the variable subunit of the ferredoxin-thioredoxin reductase, an enzyme that receives electrons from ferredoxins and then reduces a thioredoxin through a disulfide–dithiol interchange system (Dai et al., 2004). While both genes are found in all Fe-replete areas, *ftrC* is found at similar relative abundance as the core gene *petB*, whereas *ftrV* is often present in two copies, since we did not find any *ftrV*-related gene in *Synechococcus* genomes that could have been recruited by our approach (**Fig. S4B**). In contrast, only a very low fraction of the population colonizing HNLC areas possess *ftrC* and *V* genes and most often a higher proportion of the former. This is in agreement with the fact that EnvB possess neither *ftrC* and *V* and CRD1 possess either none of these genes, both, or only a degenerated *ftrC* gene (in 3, 4 and 4 genomes, respectively; **Dataset 2**). So, we hypothesize that *Synechococcus* populations dwelling in HNLC areas might possess such a FtrC remnant, though whether it has retained any function related to electron transport

is unlikely since the sequence of degenerated *frtC* miss most of the cysteinyl sites necessary to bind the [4Fe–4S] cluster (Dai et al., 2004). Furthermore, like all *Prochlorococcus* and most strictly marine *Synechococcus,* CRD1 and EnvB genomes systematically possess the Ni-superoxide dismutase (*sodN*) and lack the Fe-SOD (*sodB*), the latter being more specifically present in clades V, VI and VIII. Although *sodX*, coding for a putative maturation peptidase, displays a quite similar phyletic pattern to *sodN*, surprisingly *sodT*, which has been proposed to supply nickel for SodN and that usually co-localizes with *sodN* (Dupont et al., 2012) is specifically lacking in CRD1 and clade VII genomes and is virtually absent from low-Fe areas, in which *sodX* is unexpectedly also absent (**Fig. S5A**). This suggests that these two proteins are dispensable in low-Fe areas. Also interesting is that two CRD1 and one EnvB genomes possess an alternative oxygen-independent protoporphyrinogen IX oxidase (*hemG*; Skotnicová et al., 2018), also present in most HLIII and IV SAGs/MAGs, while all other *Synechococcus* genomes possess the typical oxygen-dependent protoporphyrinogen IX oxidase (*hemJ;* **Dataset 2**). Accordingly, *hemG* is the dominant form of protoporphyrinogen IX oxidase in HNLC areas (**Fig. S5B**), a replacement which could potentially affect the regulation of heme synthesis in Fe-limited conditions (Dailey et al., 2012). Finally, one high light inducible protein (HLIP) is strongly amplified in CRD1 and EnvB genomes compared to other *Synechococcus* ecotypes and two additional copies are quasi-specific or CRD1 genomes. In much the same way, several CRD1 genomes possess a very high copy number (up to 92) of the Nif11-like leader peptide domain (Haft et al., 2010), although the possible link of this gene amplification process with adaptation to low-Fe condition is unclear yet (**Dataset 2**).

As concerns regulation, while the three members of the Fur-like regulator family potentially involved in the regulation of Fe and Zn metabolism, including Fur, the zinc-uptake regulator Zur and the putative peroxide-sensing regulator PerR (CK_00001492; Mikhaylina et al., 2022), are all core in marine *Synechococcus/Cyanobium* genomes, CRD1 are enriched in putative ferric citrate regulators (FecR), most genomes possessing one or two members of this family, while these regulators are seemingly absent in EnvB genomes (**Dataset 2**). Furthermore, CRD1 are also enriched in three members of the cyclic AMP receptor protein (CRP) regulators family CK_00002049, CK_00001390, CK_00002546, the latter two having several genes involved in Fe-metabolism (*ftnA*, *futABC*, *som*, *fur, isiB,*

etc.) in their immediate vicinity, suggesting that they could play a role in Fe acquisition. However, these enrichments are not fully retrieved in the field since both *fecR*-like genes are only present in very low abundance including in low-Fe regions while crp_1390 rather seems to be the dominant CRP form in low Fe-areas, crp_2546 being in contrast present in often less than one fourth of the *Synechococcus* populations dwelling in low-Fe areas (**Fig. 4**).

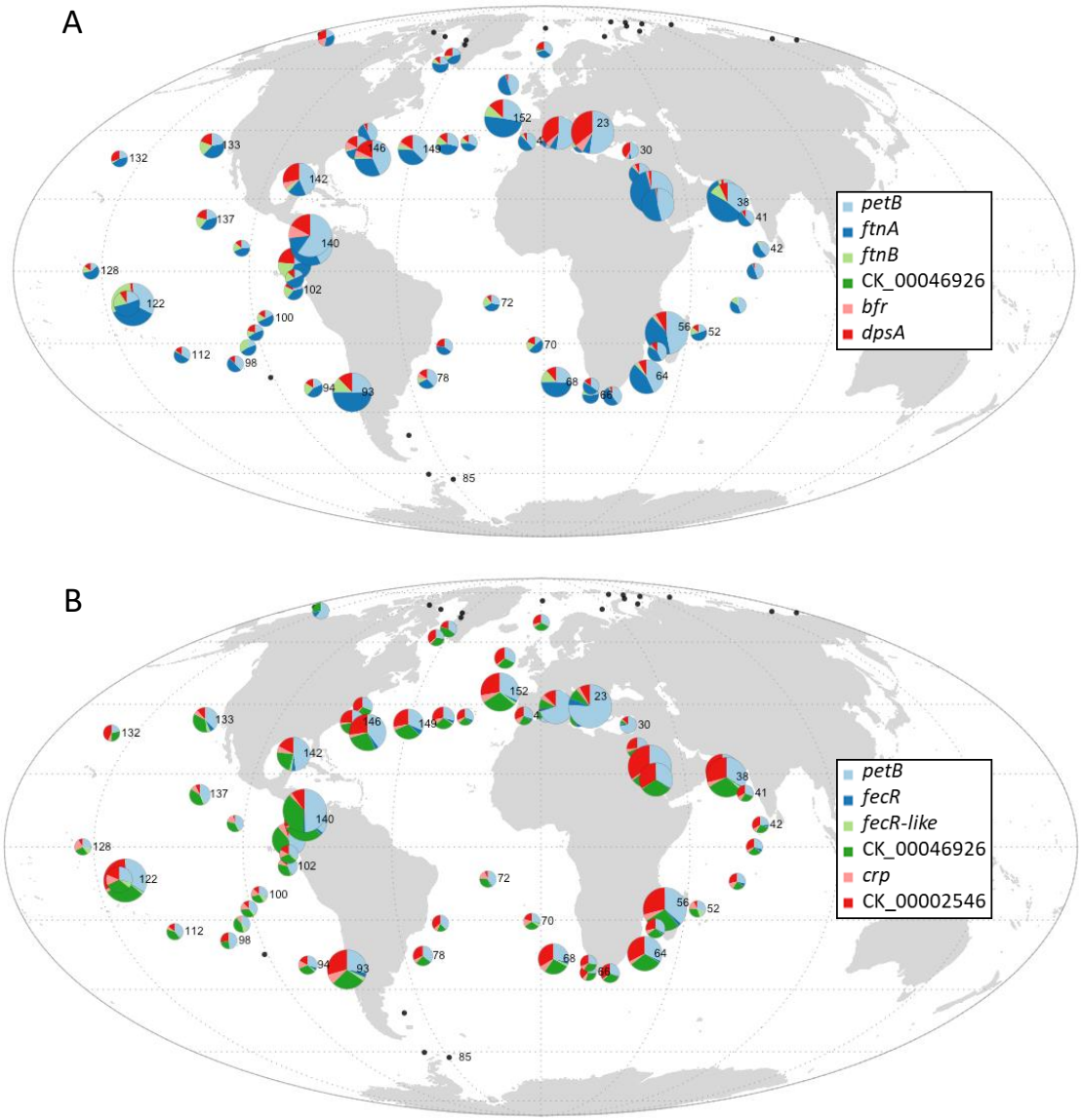

Figure 4. Global distribution map of *Synechococcus* genes involved in Fe transport. The size of the circle is proportional to relative abundance of each genus as estimated based on the *petB* gene and this gene was also used to estimate the relative abundance of other genes in the population. (**A**) genes encoding Fe-storage proteins, (**B**) genes encoding putative ferric citrate regulators (FecR-like) and cyclic AMP receptor proteins (Crp).

Discussion

Biogeographical analyses of *Prochlorococcus* and *Synechococcus* communities have demonstrated a clear relationship between phylogeny and environmental niches for both genera and notably in low-Fe areas, where the HLIII and IV clades dominate the *Prochlorococcus* populations, while CRD1 and EnvB constitute the major component of the *Synechococcus* communities (Ahlgren et al., 2020; Caputi et al., 2019; Farrant et al., 2016; Kent et al., 2019; Sohm et al., 2015). Among those, only CRD1 have representatives in culture, including at least one for each of the three previously identified ESTUs (Ahlgren et al., 2020; Farrant et al., 2016) making these isolates invaluable models to study adaptation of cyanobacteria to quasi-permanent Fe limitation. However, the fact that all CRD1 strains available in culture are not axenic and hardly grow in fully artificial medium such as Aquil (Price et al., 1989; data not shown) make it difficult to work with them in Fe-limiting conditions. For this reason, we chose here to induce Fe' limitation using Fe-siderophores DFOB, since this treatment applied on natural phytoplankton communities from Fe-replete regions was previously shown to induce an artificial Fe limitation similar to the one observed in HNLC areas (Hutchins et al., 1999). Additionally, Lis et al. (2015) showed that two marine *Synechococcus* strains, WH8102 and WH7803, assimilate DFOB at 10,000 times lower uptake rate per surface area than Fe'. So, we hypothesized that transferring cells in DFOB-supplemented medium could provoke an Fe starvation. Indeed, the measurements of the growth rate of the different *Synechococcus* strains in PCR-S11 medium supplemented with DFOB showed a progressive growth inhibition with increasing DFOB concentrations for most strains. However, different behaviors were observed between strains, those isolated from low-Fe environments, i.e. CRD1 representative strains, but also the clade II strain A15-62, being able to grow at much higher concentration of DFOB, suggesting that they are more efficient at using either the remaining traces of Fe' or the FeL. The very strong resistance to Fe starvation of A15-62 was somewhat unexpected since this genotype (clade II) and ecotype (ESTU IIA), corresponding to the most abundant *Synechococcus* genotype/ecotype worldwide, was so far shown to dominate in warm, Fe-replete, N-depleted conditions (Farrant et al., 2016; Kent et al., 2016; Sohm et al., 2015). This behavior might be related to a number of specificities compared to M16.1, which appears to be more representative of typical ESTU

IIA. First, although the presence of this clade has never been reported in low-Fe areas, A15-62 was isolated off the Mauritanian coast, which was also shown to be Fe limited in several studies (Moore et al., 2013; Ustick et al., 2021). Second, A15-62 was shown to have a significantly slower maximal growth rate than M16.1 at all temperatures tested, though still higher than all three CRD1 strains (Ferrieux et al., 2022). Third, M16.1 and A15-62 strains belong to different subclades *sensu* Mazard et al. (2012), M16.1 to the dominant subclade IIa and A15-62 to subclade IIc, these two subclades being phylogenetically distantly related based on the *petB* gene marker (Mazard et al., 2012). Fourth, A15-62 belongs to an OTU (OTU012) that, although assigned to ESTU IIA due to its low relative abundance along the *Tara* Oceans transect, seems to display a fairly different distribution pattern from the major OTU of ESTU IIA (OTU003), to which belongs M16.1, and to recruit a maximum of reads at station TARA_004 at the entrance of the Mediterranean Sea but also a relatively high number reads near the southeastern coast of Africa (TARA_057, TARA_064; (Farrant et al., 2016), the latter stations being Fe-limited (Ustick et al., 2021).

In order to better under understand the molecular basis of adaptation to Fe limitation in marine picocyanobacteria and more specifically in *Synechococcus*, we used a combination of comparative genomics and metagenomics using 256 WGS, SAGs or MAGs, representatives of the wide genetic and functional diversity occurring within this group. One of the key characteristics of CRD1 is that they possess a large set of genes involved in Fe^{2+} transport, including the FeoAB system as well as one VIT and two ZIP transporters, which are absent from most other genomes (**Fig. 2A**). As concerns the reductive Fe uptake pathway, which has been suggested to add flexibility in accessing different Fe substrates in most marine and freshwater cyanobacteria (Lis et al., 2015), all CRD1 possess the ARTO system that was recently found to be present in the whole *Prochlorococcus* and *Synechococcus* populations in low-Fe areas (Doré et al., submitted) as well as one to two copies of *pilA1*, thought to be involved in Fe^{3+} reduction (Lamb et al., 2014). Iron storage also seems to be a quite important adaptation mechanism for CRD1 with a strong amplification of the main ferritin family FtnA, the frequent occurrence of a second ferritin type (FtnB) present in only few other *Synechococcus* genomes, as well as the ferritin-like protein DpsA. Yet, the putative presence of two distinct DpsA pools, as proposed for the

freshwater *Synechococcus* sp. strain PCC 7942 (Durham & Bullerjahn, 2002), i.e. an insoluble fraction bound to the chromosome and a soluble fraction within the photosynthetic apparatus, remains to be demonstrated in these and other marine *Synechococcus.*

As for members of the EnvB clade, with the caveat that the three selected genomes are only partial (57 to 78 % completeness), they seemingly lack the FeoAB system, while their Fe^{2+} transporter set includes a ZIP, only present in a few other *Synechococcus* strains but not in CRD1, as well as a NRAMP transporter that is widespread in *Synechococcus* but again absent in CRD1 genomes (**Fig. 2B**). EnvB might also possess limited Fe^{3+} reduction capacities, since *pilA1* was absent from all EnvB genomes and the ARTO system was only present in one out of three EnvB genomes, though the fact that the quasi-totality of the *Synechococcus* population possess these genes in HNLC areas (Doré et al., submitted) suggests that natural EnvB populations, like CRD1, may actually possess this system. As previously mentioned by Ahlgren et al. (2020), another major difference with CRD1 members is the presence in most EnvB genomes of a TonB-dependent siderophore-mediated Fe uptake system, which abundance in the field is indeed correlated with the relative abundance of EnvB and/or EnvA (Doré et al., submitted). In terms of Fe storage EnvB seem to possess the same set of genes as CRD1 but with no evidence of an amplification of the ferritin FtnA family.

Interestingly, *Synechococcus* A15-62 shares more characteristics with EnvB than with CRD1, i.e. a quite low Fe^{2+} uptake capacity (no FeoAB, no VIT and only one ZIP transporter; **Fig. S2A**) and some Fe^{3+}-reduction capabilities provided by ARTO but not PilA1. Yet, compared to EnvB, A15-62 further lacks the TBDT system (like the typical clade II strain M16.1; **Fig. S2C**) and displays a lower Fe-storage capacity (no FtnB). The gene content of WH8102, which in contrast proved to be highly sensitive to Fe-depletion, was most similar to A15-62 but contains NRAMP_1683 as the sole divalent transporter and more generally Fe^{2+} transporter, a seemingly lower regulation capacity (no CRP regulator), no Fe storage protein as well as a FutA1 homolog (instead of the more distantly related FutA protein found in most other *Synechococcus*), which in *Synechocystis* sp. PCC 6803 was suggested to be involved in the regulation of the reductive Fe pathway via ARTO rather than in

scavenging periplasmic Fe^{3+} (Kranzler et al., 2014; **Fig. S2B**). Yet, given the absence of a second FutA subunit, the role of FutA1 would need to be confirmed in WH8102.

In summary, this comparative omic approach allowed us to highlight and/or confirm some specificities of CRD1 and EnvB ecotypes, which despite their frequent co-occurrence in HNLC waters, seem to exhibit different strategies to cope with these harsh conditions (Ahlgren et al., 2020), to better understand the very high sensitivity of WH8102 to Fe'-starvation, which seems to be related to the total absence of Fe-storage capacity. Yet, the molecular bases of the unexpected response of A15-62 with regard to DFOB addition are still unclear given that it is apparently less well equipped to face Fe limitation (**Fig. S2A and Figs. 2AB**). In this context, the ongoing transcriptomic analyses of cultures of all five studied strains incubated for six hours in presence of DFOB shoud help elucidating this enigma and possibly uncovering novel genes and/or pathways involved in Fe metabolism. In any case, it seems that adaptation to low-Fe conditions might not be an exclusive trait of *Synechococcus* clades CRD1 and EnvB and that some members of clade II, possibly all members of sub-clade IIc, might have a larger tolerance to Fe limitation than ESTU IIA, dominating in warm, N-depleted areas. This high diversification level within clade II is also supported by the fact that Farrant et al. (Farrant et al., 2016) already identified a minor ESTU, IIB, which was found to be restricted to fairly cold, mixed waters. The finding of a phytoplanktonic strain with an outstanding capacity to stand low-Fe conditions somehow mirrors the situation observed for *Ostreococcus* RCC802, a strain which was found to display a low-Fe requirement, seemingly associated to a marked cell biomass reduction (Botebol et al., 2017), as previously hypothesized for diatoms (Marchetti & Cassar, 2009). Although we showed here that there is no evidence for such a reduction within the CRD1 clade since BIOS-E4-1 displays a quite large biovolume (and the largest genome of all marine *Synechococcus*; (Doré et al., 2020), A15-62 appears to have the smallest biovolume of the whole range of *Synechococcus* strains analyzed in the present study (**Table 2**). The discovery of such low-Fe ecotype within clade II may have some importance consequences on the fate of *Synechococcus* communities in the future Ocean, where warm, Fe limited are expected to expand considerably (Polovina et al., 2008).

Acknowledgments

This work was supported by the French “Agence Nationale de la Recherche” Programs CINNAMON (ANR-17-CE02-0014-01) and EFFICACY (ANR-19-CE02-0019) as well as the European Union program Assemble+ (Horizon 2020, under grant agreement number 287589). We also thank the support and commitment of Priscillia Gourvil and Martin Gachenot from the Roscoff Culture Collection (http://roscoff-culture-collection.org/) and Hugo Doré for help with R scripts used in this study. We also thank the support and commitment of the *Tara* Oceans coordinators and consortium, Agnès b. and E. Bourgois, the Veolia Environment Foundation, Région Bretagne, Lorient Agglomeration, World Courier, Illumina, the EDF Foundation, FRB, the Prince Albert II de Monaco Foundation, the *Tara* schooner and its captains and crew.

References

Agranoff, D., Collins, L., Kehres, D., Harrison, T., Maguire, M., & Krishna, S. (2005). The Nramp orthologue of *Cryptococcus neoformans* is a pH-dependent transporter of manganese, iron, cobalt and nickel. *Biochemical Journal*, *385*(Pt 1), 225-232. https://doi.org/10.1042/BJ20040836

Ahlgren, N. A., Belisle, B. S., & Lee, M. D. (2020). Genomic mosaicism underlies the adaptation of marine *Synechococcus* ecotypes to distinct oceanic iron niches. *Environmental Microbiology*, *22*(5), 1801-1815. https://doi.org/10.1111/1462-2920.14893

Andrews, S. C., Robinson, A. K., & Rodríguez-Quiñones, F. (2003). Bacterial iron homeostasis. *FEMS Microbiology Reviews*, *27*(2-3), 215-237. https://doi.org/10.1016/S0168-6445(03)00055-X

Barber, J., Nield, J., Duncan, J., & Bibby, T. S. (2006). Accessory Chlorophyll Proteins in Cyanobacterial Photosystem I. In J. H. Golbeck (Éd.), *Photosystem I: The Light-Driven Plastocyanin:Ferredoxin Oxidoreductase* (p. 99-117). Springer Netherlands. https://doi.org/10.1007/978-1-4020-4256-0_9

Barnett, J. P., Millard, A., Ksibe, A. Z., Scanlan, D. J., Schmid, R., & Blindauer, C. A. (2012). Mining Genomes of Marine Cyanobacteria for Elements of Zinc Homeostasis. *Frontiers in Microbiology*, *3*. https://doi.org/10.3389/fmicb.2012.00142

Behrenfeld, M. J., & Milligan, A. J. (2013). Photophysiological Expressions of Iron Stress in Phytoplankton. *Annual Review of Marine Science*, *5*(1), 217-246. https://doi.org/10.1146/annurev-marine-121211-172356

Behrenfeld, M. J., Westberry, T. K., Boss, E. S., O'Malley, R. T., Siegel, D. A., Wiggert, J. D., Franz, B. A., McClain, C. R., Feldman, G. C., Doney, S. C., Moore, J. K., Dall'Olmo, G., Milligan, A. J., Lima, I., & Mahowald, N. (2009). Satellite-detected fluorescence reveals global physiology of ocean phytoplankton. *Biogeosciences*. https://doi.org/10.5194/bg-6-779-2009

Blain, S., Bonnet, S., & Guieu, C. (2008). Dissolved iron distribution in the tropical and sub tropical South Eastern Pacific. *Biogeosciences*, *5*(1), 269-280. https://doi.org/10.5194/bg-5-269-2008

Boekema, E. J., Hifney, A., Yakushevska, A. E., Piotrowski, M., Keegstra, W., Berry, S., Michel, K. P., Pistorius, E. K., & Kruip, J. (2001). A giant chlorophyll-protein complex induced by iron deficiency in cyanobacteria. *Nature*, *412*(6848), 745-748. https://doi.org/10.1038/35089104

Botebol, H., Lelandais, G., Six, C., Lesuisse, E., Meng, A., Bittner, L., Lecrom, S., Sutak, R., Lozano, J.-C., Schatt, P., Vergé, V., Blain, S., & Bouget, F.-Y. (2017). Acclimation of a low iron adapted *Ostreococcus* strain to iron limitation through cell biomass lowering. *Scientific Reports*, *7*(1), 327-327. https://doi.org/10.1038/s41598-017-00216-6

Breton, S., Jouhet, J., Guyet, U., Gros, V., Pittera, J., Demory, D., Partensky, F., Doré, H., Ratin, M., Maréchal, E., Nguyen, N. A., Garczarek, L., & Six, C. (2019). Unveiling membrane thermoregulation strategies in marine picocyanobacteria. *New Phytologist*, *225*(6), 2396-2410. https://doi.org/10.1111/nph.16239

Caputi, L., Carradec, Q., Eveillard, D., Kirilovsky, A., Pelletier, E., Pierella Karlusich, J. J., Rocha Jimenez Vieira, F., Villar, E., Chaffron, S., Malviya, S., Scalco, E., Acinas, S. G., Alberti, A., Aury, J. M., Benoiston, A. S., Bertrand, A., Biard, T., Bittner, L., Boccara, M., …

Iudicone, D. (2019). Community-level responses to iron availability in open ocean plankton ecosystems. *Global Biogeochemical Cycles*, *33*(3), 391-419. https://doi.org/10.1029/2018GB006022

Cellier, M., Privé, G., Belouchi, A., Kwan, T., Rodrigues, V., Chia, W., & Gros, P. (1995). Nramp defines a family of membrane proteins. *Proceedings of the National Academy of Sciences of the United States of America*, *92*(22), 10089-10093. https://doi.org/10.1073/pnas.92.22.10089

Chandler, J. W., Lin, Y., Gainer, P. J., Post, A. F., Johnson, Z. I., & Zinser, E. R. (2016). Variable but persistent coexistence of *Prochlorococcus* ecotypes along temperature gradients in the ocean's surface mixed layer. *Environmental microbiology reports*, *8*(2), 272-284. https://doi.org/10.1111/1758-2229.12378

Coleman, M. L., Sullivan, M. B., Martiny, A. C., Steglich, C., Barry, K., Delong, E. F., & Chisholm, S. W. (2006). Genomic islands and the ecology and evolution of *Prochlorococcus*. *Science*, *311*(5768), 1768-1770.

Croot, P. L., Baars, O., & Streu, P. (2011). The distribution of dissolved zinc in the Atlantic sector of the Southern Ocean. *Deep Sea Research Part II: Topical Studies in Oceanography*, *58*(25), 2707-2719. https://doi.org/10.1016/j.dsr2.2010.10.041

Dai, S., Johansson, K., Miginiac-Maslow, M., Schürmann, P., & Eklund, H. (2004). Structural Basis of Redox Signaling in Photosynthesis : Structure and Function of Ferredoxin:thioredoxin Reductase and Target Enzymes. *Photosynthesis Research*, *79*(3), 233-248. https://doi.org/10.1023/B:PRES.0000017194.34167.6d

Dailey, H. A., Dailey, T. A., Gerdes, S., Jahn, D., Jahn, M., O'Brian, M. R., & Warren, M. J. (2012). Prokaryotic Heme Biosynthesis : Multiple Pathways to a Common Essential Product. https://doi.org/10.1128/MMBR.00048-16

Doré, H., Farrant, G. K., Guyet, U., Haguait, J., Humily, F., Ratin, M., Pitt, F. D., Ostrowski, M., Six, C., Brillet-Guéguen, L., Hoebeke, M., Bisch, A., Le Corguillé, G., Corre, E., Labadie, K., Aury, J.-M., Wincker, P., Choi, D. H., Noh, J. H., … Garczarek, L. (2020). Evolutionary mechanisms of long-term genome diversification associated with niche partitioning in marine picocyanobacteria. *Frontiers in Microbiology*, *11*, 567431. https://doi.org/10.3389/fmicb.2020.567431

Doré, H., Guyet, U., Leconte, J., Farrant, G. K., Ratin, M., Pitt, F. D., Ostrowski, M., Ferrieux, M., Six, C., Brillet-Guéguen, L., Hoebeke, M., Siltanen, J., Le Corquillé, G., Corre, E., Labadie, K., Aury, J.-M., Wincker, P., Eveillard, D., Scanlan, D. J., … Garczarek, L. (submitted). Differential global distribution of marine picocyanobacteria gene clusters reveals distinct niche-related adaptive strategies. *PNAS*.

Doré, H., Leconte, Jade, Breton, Solène, Guyet, Ulysse, Demory, David, Hoebeke, Mark, Corre, Erwan, Ratin, Morgane, Pitt, Francès D., Ostrowski, Martin, Scanlan, David J., Partensky, Frédéric, Six, Christophe, & Garczarek, Laurence. (2022). Global phylogeography of marine *Synechococcus* in coastal areas unveils strikingly different communities than in open ocean. *BioRxiv*.

Dupont, C. L., Johnson, D. A., Phillippy, K., Paulsen, I. T., Brahamsha, B., & Palenik, B. (2012). Genetic Identification of a High-Affinity Ni Transporter and the Transcriptional Response to Ni Deprivation in *Synechococcus* sp. Strain WH8102. *Applied and Environmental Microbiology*, *78*(22), 7822-7832. https://doi.org/10.1128/AEM.01739-12

Durán, R. V., Hervás, M., De la Rosa, M. A., & Navarro, J. A. (2004). The Efficient Functioning of Photosynthesis and Respiration in *Synechocystis* sp. PCC 6803 Strictly Requires the Presence of either Cytochrome c_6 or Plastocyanin*. *Journal of Biological Chemistry*, *279*(8), 7229-7233. https://doi.org/10.1074/jbc.M311565200

Durham, K. A., & Bullerjahn, G. S. (2002). Immunocytochemical localization of the stress-induced DpsA protein in the cyanobacterium *Synechococcus* sp. Strain PCC 7942. *Journal of Basic Microbiology*, *42*(6), 367-372. https://doi.org/10.1002/1521-4028(200212)42:6<367::AID-JOBM367>3.0.CO;2-T

Emms, D. M., & Kelly, S. (2019). OrthoFinder : Phylogenetic orthology inference for comparative genomics. *Genome Biology*, *20*(1), 238. https://doi.org/10.1186/s13059-019-1832-y

Farrant, G. K., Doré, H., Cornejo-Castillo, F. M., Partensky, F., Ratin, M., Ostrowski, M., Pitt, F. D., Wincker, P., Scanlan, D. J., Iudicone, D., Acinas, S. G., & Garczarek, L. (2016). Delineating ecologically significant taxonomic units from global patterns of marine picocyanobacteria. *Proceedings of the National Academy of Sciences*, *113*(24), E3365-E3374. https://doi.org/10.1073/pnas.1524865113

Ferrieux, M., Dufour, L., Doré, H., Ratin, M., Guéneuguès, A., Chasselin, L., Marie, D., Rigaut-Jalabert, F., Le Gall, F., Sciandra, T., Monier, G., Hoebeke, M., Corre, E., Xia, X., Liu, H., Scanlan, D. J., Partensky, F., & Garczarek, L. (2022). Comparative Thermophysiology of Marine *Synechococcus* CRD1 Strains Isolated From Different Thermal Niches in Iron-Depleted Areas. *Frontiers in Microbiology*, *13*. https://www.frontiersin.org/article/10.3389/fmicb.2022.893413

Flombaum, P., Gallegos, J. L., Gordillo, R. a, Rincón, J., Zabala, L. L., Jiao, N., Karl, D. M., Li, W. K. W., Lomas, M. W., Veneziano, D., Vera, C. S., Vrugt, J. a, & Martiny, A. C. (2013). Present and future global distributions of the marine Cyanobacteria *Prochlorococcus* and *Synechococcus*. *Proceedings of the National Academy of Sciences of the United States of America*, *110*(24), 9824-9829. https://doi.org/10.1073/pnas.1307701110

Frankenberg, N., Mukougawa, K., Kohchi, T., & Lagarias, J. C. (2001). Functional genomic analysis of the HY2 family of ferredoxin-dependent bilin reductases from oxygenic photosynthetic organisms. *The Plant Cell*, *13*(4), 965-978. https://doi.org/10.1105/tpc.13.4.965

Garcia, C. A., Hagstrom, G. I., Larkin, A. A., Ustick, L. J., Levin, S. A., Lomas, M. W., & Martiny, A. C. (2020). Linking regional shifts in microbial genome adaptation with surface ocean biogeochemistry. *Philosophical Transactions of the Royal Society B: Biological Sciences*, *375*(1798), 20190254. https://doi.org/10.1098/rstb.2019.0254

Garczarek, L., Guyet, U., Doré, H., Farrant, G. K., Hoebeke, M., Brillet-Guéguen, L., Bisch, A., Ferrieux, M., Siltanen, J., Corre, E., Le Corguillé, G., Ratin, M., Pitt, F. D., Ostrowski, M., Conan, M., Siegel, A., Labadie, K., Aury, J.-M., Wincker, P., … Partensky, F. (2021). Cyanorak v2.1 : A scalable information system dedicated to the visualization and expert curation of marine and brackish picocyanobacteria genomes. *Nucleic Acids Research*, *49*(D1), D667-D676. https://doi.org/10.1093/nar/gkaa958

Gómez-Garzón, C., Barrick, J. E., & Payne, S. M. (2022). Disentangling the Evolutionary History of Feo, the Major Ferrous Iron Transport System in Bacteria. *mBio*, *13*(1), e03512-21. https://doi.org/10.1128/mbio.03512-21

Guyet, U., Nguyen, N. A., Doré, H., Haguait, J., Pittera, J., Conan, M., Ratin, M., Corre, E., Le Corguillé, G., Brillet-Guéguen, L., Hoebeke, M., Six, C., Steglich, C., Siegel, A., Eveillard, D., Partensky, F., & Garczarek, L. (2020). Synergic effects of temperature and irradiance on the physiology of the marine *Synechococcus* strain WH7803. *Frontiers in Microbiology*, *11*, 1707. https://doi.org/10.3389/fmicb.2020.01707

Haft, D. H., Basu, M. K., & Mitchell, D. A. (2010). Expansion of ribosomally produced natural products : A nitrile hydratase- and Nif11-related precursor family. *BMC Biology*, *8*, 70. https://doi.org/10.1186/1741-7007-8-70

Hogle, S. L., Hackl, T., Bundy, R. M., Park, J., Satinsky, B., Hiltunen, T., Biller, S., Berube, P. M., & Chisholm, S. W. (2022). Siderophores as an iron source for picocyanobacteria in deep chlorophyll maximum layers of the oligotrophic ocean. *The ISME Journal*, 1-11. https://doi.org/10.1038/s41396-022-01215-w

Hu, J. (2021). Toward unzipping the ZIP metal transporters : Structure, evolution, and implications on drug discovery against cancer. *The FEBS Journal*, *288*(20), 5805-5825. https://doi.org/10.1111/febs.15658

Hutchins, D. A., Witter, A. E., Butler, A., & Luther, G. W. (1999). Competition among marine phytoplankton for different chelated iron species. *Nature*, *400*(6747), 858-861. https://doi.org/10.1038/23680

Ito, Y., & Butler, A. (2005). Structure of synechobactins, new siderophores of the marine cyanobacterium *Synechococcus* sp. PCC 7002. *Limnology and Oceanography*, *50*(6), 1918-1923. https://doi.org/10.4319/lo.2005.50.6.1918

Jiang, H.-B., Lou, W.-J., Ke, W.-T., Song, W.-Y., Price, N. M., & Qiu, B.-S. (2015). New insights into iron acquisition by cyanobacteria : An essential role for ExbB-ExbD complex in inorganic iron uptake. *The ISME Journal*, *9*(2), 297-309. https://doi.org/10.1038/ismej.2014.123

Johnson, K. S., Gordon, R. M., & Coale, K. H. (1997). What controls dissolved iron concentrations in the world ocean? *Marine Chemistry*, *57*(3), 137-161. https://doi.org/10.1016/S0304-4203(97)00043-1

Johnson, Z. I., Zinser, E. R., Coe, A., McNulty, N. P., Woodward, E. M. S., & Chisholm, S. W. (2006). Niche partitioning among *Prochlorococcus* ecotypes along ocean-scale environmental gradients. *Science*. https://doi.org/10.1126/science.1118052

Katoh, H., Hagino, N., Grossman, A. R., & Ogawa, T. (2001). Genes essential to iron transport in the cyanobacterium *Synechocystis* sp. Strain PCC 6803. *Journal of Bacteriology*, *183*(9), 2779-2784. https://doi.org/10.1128/JB.183.9.2779-2784.2001

Kent, A. G., Baer, S. E., Mouginot, C., Huang, J. S., Larkin, A. A., Lomas, M. W., & Martiny, A. C. (2018). Parallel phylogeography of *Prochlorococcus* and *Synechococcus*. *The ISME Journal*, *13*(2), 430-441. https://doi.org/10.1038/s41396-018-0287-6

Kent, A. G., Dupont, C. L., Yooseph, S., & Martiny, A. C. (2016). Global biogeography of *Prochlorococcus* genome diversity in the surface ocean. *The ISME Journal*, *10*(8), 1856-1865. https://doi.org/10.1038/ismej.2015.265

Keren, N., Aurora, R., & Pakrasi, H. B. (2004). Critical Roles of Bacterioferritins in Iron Storage and Proliferation of Cyanobacteria. *Plant Physiology*, *135*(3), 1666-1673. https://doi.org/10.1104/pp.104.042770

Kim, S. A., Punshon, T., Lanzirotti, A., Li, L., Alonso, J. M., Ecker, J. R., Kaplan, J., & Guerinot, M. L. (2006). Localization of

iron in *Arabidopsis* seed requires the vacuolar membrane transporter VIT1. *Science (New York, N.Y.)*, *314*(5803), 1295-1298. https://doi.org/10.1126/science.1132563

Koch, F., & Trimborn, S. (2019). Limitation by Fe, Zn, Co, and B12 Results in Similar Physiological Responses in Two Antarctic Phytoplankton Species. *Frontiers in Marine Science*, *6*. https://www.frontiersin.org/article/10.3389/fmars.2019.00514

Kranzler, C., Lis, H., Finkel, O. M., Schmetterer, G., Shaked, Y., & Keren, N. (2014). Coordinated transporter activity shapes high-affinity iron acquisition in cyanobacteria. *The ISME Journal*, *8*(2), 409-417. https://doi.org/10.1038/ismej.2013.161

Lamb, J. J., Hill, R. E., Eaton-Rye, J. J., & Hohmann-Marriott, M. F. (2014). Functional Role of PilA in Iron Acquisition in the Cyanobacterium *Synechocystis* sp. PCC 6803. *PLOS ONE*, *9*(8), e105761. https://doi.org/10.1371/journal.pone.0105761

Lee, J.-W., & Helmann, J. D. (2007). Functional specialization within the Fur family of metalloregulators. *Biometals: An International Journal on the Role of Metal Ions in Biology, Biochemistry, and Medicine*, *20*(3-4), 485-499. https://doi.org/10.1007/s10534-006-9070-7

Leonhardt, K., & Straus, N. A. (1992). An iron stress operon involved in photosynthetic electron transport in the marine cyanobacterium *Synechococcus* sp. PCC 7002. *Journal of General Microbiology*, *138 Pt 8*, 1613-1621. https://doi.org/10.1099/00221287-138-8-1613

Lis, H., Kranzler, C., Keren, N., & Shaked, Y. (2015). A Comparative Study of Iron Uptake Rates and Mechanisms amongst Marine and Fresh Water Cyanobacteria : Prevalence of Reductive Iron Uptake. *Life*, *5*(1), 841-860. https://doi.org/10.3390/life5010841

Mackey, K. R. M., Post, A. F., McIlvin, M. R., Cutter, G. A., John, S. G., & Saito, M. A. (2015). Divergent responses of Atlantic coastal and oceanic *Synechococcus* to iron limitation. *Proceedings of the National Academy of Sciences*, *112*(32), 9944-9949. https://doi.org/10.1073/pnas.1509448112

Malmstrom, R. R., Rodrigue, S., Huang, K. H., Kelly, L., Kern, S. E., Thompson, A., Roggensack, S., Berube, P. M., Henn, M. R., & Chisholm, S. W. (2013). Ecology of uncultured *Prochlorococcus* clades revealed through single-cell genomics and biogeographic analysis. *The ISME Journal*, *7*(1), 184-198. https://doi.org/10.1038/ismej.2012.89

Marchetti, A., & Cassar, N. (2009). Diatom elemental and morphological changes in response to iron limitation : A brief review with potential paleoceanographic applications. *Geobiology*, *7*(4), 419-431. https://doi.org/10.1111/j.1472-4669.2009.00207.x

Marie, D., Brussaard, C. P. D., Partensky, F., & Vaulot, D. (1999). Flow cytometric analysis of phytoplankton, bacteria and viruses. In J. P. Robinson (Éd.), *Current protocols in cytometry: Vol. 11.11* (p. 1-15). John Wiley & Sons.

Mazard, S., Ostrowski, M., Partensky, F., & Scanlan, D. J. (2012). Multi-locus sequence analysis, taxonomic resolution and biogeography of marine *Synechococcus* : Taxonomic resolution and biogeography of marine *Synechococcus*. *Environmental Microbiology*, *14*(2), 372-386. https://doi.org/10.1111/j.1462-2920.2011.02514.x

Michel, K.-P., Berry, S., Hifney, A., Kruip, J., & Pistorius, E. K. (2003). Adaptation to iron deficiency : A comparison between the cyanobacterium *Synechococcus elongatus* PCC 7942 wild-type and a DpsA-free mutant. *Photosynthesis Research*, *75*(1), 71-84.

https://doi.org/10.1023/A:1022459919040

Mikhaylina, A., Ksibe, A. Z., Wilkinson, R. C., Smith, D., Marks, E., Coverdale, J. P. C., Fülöp, V., Scanlan, D. J., & Blindauer, C. A. (2022). A single sensor controls large variations in zinc quotas in a marine cyanobacterium. *Nature Chemical Biology*, 1-9. https://doi.org/10.1038/s41589-022-01051-1

Moore, C. M., Mills, M. M., Arrigo, K. R., Berman-Frank, I., Bopp, L., Boyd, P. W., Galbraith, E. D., Geider, R. J., Guieu, C., Jaccard, S. L., Jickells, T. D., La Roche, J., Lenton, T. M., Mahowald, N. M., Marañón, E., Marinov, I., Moore, J. K., Nakatsuka, T., Oschlies, A., … Ulloa, O. (2013). Processes and patterns of oceanic nutrient limitation. *Nature Geoscience*, *6*(9), 701-710. https://doi.org/10.1038/ngeo1765

Moore, J. K., Doney, S. C., Glover, D. M., & Fung, I. Y. (2002). Iron cycling and nutrient-limitation patterns in surface waters of the World Ocean. *Deep Sea Research Part II: Topical Studies in Oceanography*, *49*(1–3), 463-507. https://doi.org/10.1016/S0967-0645(01)00109-6

Moore, L. R., Rocap, G., & Chisholm, S. W. (1998). Physiology and molecular phylogeny of coexisting *Prochlorococcus* ecotypes. *Nature*, *393*(6684), 464-467. https://doi.org/10.1038/30965

Morel, F. M. M., Kustka, A. B., & Shaked, Y. (2008). The role of unchelated Fe in the iron nutrition of phytoplankton. *Limnology and Oceanography*, *53*(1), 400-404. https://doi.org/10.4319/lo.2008.53.1.0400

Napolitano, M., Rubio, M. Á., Santamaría-Gómez, J., Olmedo-Verd, E., Robinson, N. J., & Luque, I. (2012). Characterization of the Response to Zinc Deficiency in the Cyanobacterium Anabaena sp. Strain PCC 7120. *Journal of Bacteriology*, *194*(10), 2426-2436. https://doi.org/10.1128/JB.00090-12

Park, Y. I., Sandström, S., Gustafsson, P., & Oquist, G. (1999). Expression of the isiA gene is essential for the survival of the cyanobacterium *Synechococcus* sp. PCC 7942 by protecting photosystem II from excess light under iron limitation. *Molecular Microbiology*, *32*(1), 123-129. https://doi.org/10.1046/j.1365-2958.1999.01332.x

Partensky, F., Blanchot, J., & Vaulot, D. (1999). Differential distribution and ecology of *Prochlorococcus* and *Synechococcus* in oceanic waters : A review. In L. Charpy & A. W. D. Larkum (Éds.), *Marine Cyanobacteria* (p. 457-475). Bulletin de l'Institut Océanographique de Monaco. Numéro spécial 19.

Pittera, J., Humily, F., Thorel, M., Grulois, D., Garczarek, L., & Six, C. (2014). Connecting thermal physiology and latitudinal niche partitioning in marine *Synechococcus*. *The ISME Journal*, *8*(6), 1221-1236. https://doi.org/10.1038/ismej.2013.228

Pittera, J., Jouhet, J., Breton, S., Garczarek, L., Partensky, F., Maréchal, É., Nguyen, N. A., Doré, H., Ratin, M., Pitt, F. D., Scanlan, D. J., & Six, C. (2018). Thermoacclimation and genome adaptation of the membrane lipidome in marine *Synechococcus*. *Environmental Microbiology*, *20*(2), 612-631. https://doi.org/10.1111/1462-2920.13985

Pittera, J., Partensky, F., & Six, C. (2017). Adaptive thermostability of light-harvesting complexes in marine picocyanobacteria. *The ISME Journal*, *11*(1), 112-124. https://doi.org/10.1038/ismej.2016.102

Polovina, J. J., Howell, E. A., & Abecassis, M. (2008). Ocean's least productive waters are expanding. *Geophysical Research Letters*, *35*(3). https://doi.org/10.1029/2007GL031745

Polyviou, D., Machelett, M. M., Hitchcock, A., Baylay, A. J., MacMillan, F., Moore, C.

M., Bibby, T. S., & Tews, I. (2018). Structural and functional characterization of IdiA/FutA (Tery_3377), an iron-binding protein from the ocean diazotroph *Trichodesmium erythraeum*. *Journal of Biological Chemistry*, *293*(47), 18099-18109. https://doi.org/10.1074/jbc.RA118.001929

Price, N. M., Harrison, G. I., Hering, J. G., Hudson, R. J., Nirel, P. M. V., Palenik, B., & Morel, F. M. M. (1989). Preparation and Chemistry of the Artificial Algal Culture Medium Aquil. *Biological Oceanography*, *6*(5-6), 443-461. https://doi.org/10.1080/01965581.1988.10749544

Riediger, M., Hernández-Prieto, M. A., Song, K., Hess, W. R., & Futschik, M. E. (2021). Genome-wide identification and characterization of Fur-binding sites in the cyanobacteria *Synechocystis* sp. PCC 6803 and PCC 6714. *DNA Research*, *28*(6), dsab023. https://doi.org/10.1093/dnares/dsab023

Rippka, R., Coursin, T., Hess, W., Lichtle, C., Scanlan, D. J., Palinska, K. A., Iteman, I., Partensky, F., Houmard, J., & Herdman, M. (2000). *Prochlorococcus marinus* Chisholm et al. 1992 subsp. *Pastoris* subsp. Nov. Strain PCC 9511, the first axenic chlorophyll a_2/b_2-containing cyanobacterium (Oxyphotobacteria). *International Journal of Systematic and Evolutionary Microbiology*, *50*(5), 1833-1847. https://doi.org/10.1099/00207713-50-5-1833

Rusch, D. B., Martiny, A. C., Dupont, C. L., Halpern, A. L., & Venter, J. C. (2010). Characterization of *Prochlorococcus* clades from iron-depleted oceanic regions. *Proceedings of the National Academy of Sciences*, *107*(37), 16184-16189. https://doi.org/10.1073/pnas.1009513107

Shcolnick, S., & Keren, N. (2006). Metal Homeostasis in Cyanobacteria and Chloroplasts. Balancing Benefits and Risks to the Photosynthetic Apparatus. *Plant Physiology*, *141*(3), 805-810. https://doi.org/10.1104/pp.106.079251

Six, C., Ratin, M., Marie, D., & Corre, E. (2021). Marine *Synechococcus* picocyanobacteria : Light utilization across latitudes. *Proceedings of the National Academy of Sciences*, *118*(38), Article 38. https://doi.org/10.1073/pnas.2111300118

Six, C., Thomas, J. C., Thion, L., Lemoine, Y., Zal, F., & Curie, M. (2005). Two Novel Phycoerythrin-Associated Linker Proteins in the Marine. *Journal of Bacteriology*, *187*(5), 1685-1694. https://doi.org/10.1128/JB.187.5.1685

Skotnicová, P., Sobotka, R., Shepherd, M., Hájek, J., Hrouzek, P., & Tichý, M. (2018). The cyanobacterial protoporphyrinogen oxidase HemJ is a new b-type heme protein functionally coupled with coproporphyrinogen III oxidase. *The Journal of Biological Chemistry*, *293*(32), 12394-12404. https://doi.org/10.1074/jbc.RA118.003441

Sohm, J. A., Ahlgren, N. A., Thomson, Z. J., Williams, C., Moffett, J. W., Saito, M. A., Webb, E. A., & Rocap, G. (2015). Co-occurring *Synechococcus* ecotypes occupy four major oceanic regimes defined by temperature, macronutrients and iron. *The ISME Journal*, *10*(2), 333-345. https://doi.org/10.1038/ismej.2015.115

Stevanovic, M., Hahn, A., Nicolaisen, K., Mirus, O., & Schleiff, E. (2012). The components of the putative iron transport system in the cyanobacterium Anabaena sp. PCC 7120. *Environmental Microbiology*, *14*(7), 1655-1670. https://doi.org/10.1111/j.1462-2920.2011.02619.x

Straus, N. A. (s. d.). Iron Deprivation : Physiology and Gene Regulation. In *The Molecular Biology of*

Cyanobacteria. https://doi.org/10.1007/0-306-48205-3_25

Tagliabue, A., Bowie, A. R., Boyd, P. W., Buck, K. N., Johnson, K. S., & Saito, M. A. (2017). The integral role of iron in ocean biogeochemistry. *Nature*, *543*(7643), 51-59. https://doi.org/10.1038/nature21058

Ustick, L. J., Larkin, A. A., Garcia, C. A., Garcia, N. S., Brock, M. L., Lee, J. A., Wiseman, N. A., Moore, J. K., & Martiny, A. C. (2021). Metagenomic analysis reveals global-scale patterns of ocean nutrient limitation. *Science*, *372*(6539), 287-291. https://doi.org/10.1126/science.abe6301

West, N. J., Lebaron, P., Strutton, P. G., & Suzuki, M. T. (2011). A novel clade of *Prochlorococcus* found in high nutrient low chlorophyll waters in the South and Equatorial Pacific Ocean. *The ISME Journal*, *5*(6), 933-944. https://doi.org/10.1038/ismej.2010.186

Zapata, M., & Garrido, J. L. (1991). Influence of injection conditions in reversed-phase high-performance liquid chromatography of chlorophylls and carotenoids. *Chromatographia*, *31*(11), 589-594. https://doi.org/10.1007/BF02279480

Zwirglmaier, K., Jardillier, L., Ostrowski, M., Mazard, S., Garczarek, L., Vaulot, D., Not, F., Massana, R., Ulloa, O., & Scanlan, D. J. (2008). Global phylogeography of marine *Synechococcus* and *Prochlorococcus* reveals a distinct partitioning of lineages among oceanic biomes. *Environmental Microbiology*, *10*(1), 147-161. https://doi.org/10.1111/j.1462-2920.2007.01440.x

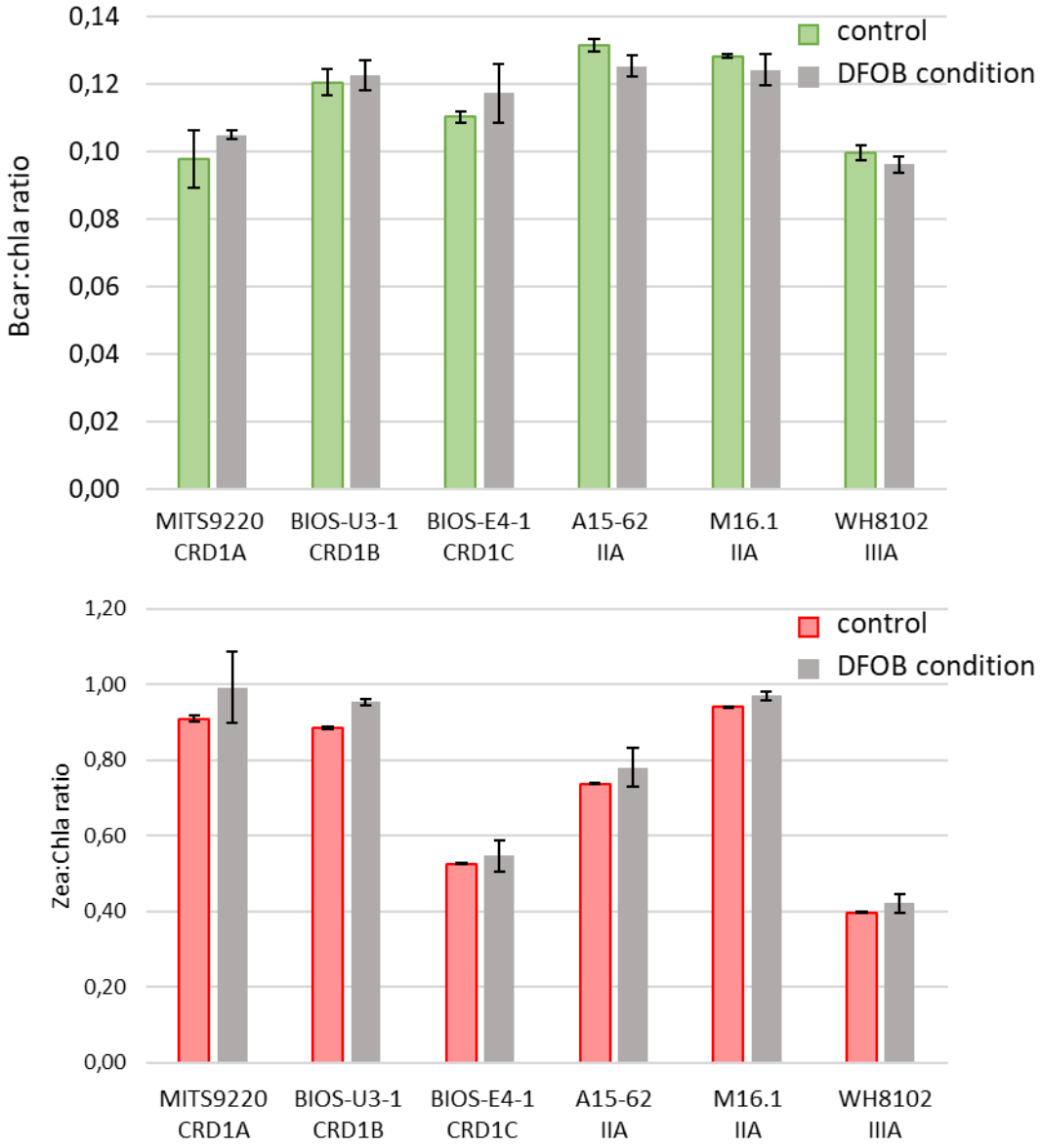

Fig. S1: Effect of DFOB addition (800 µM, 6h) on cellular mass liposoluble pigment ratios of CRD1 vs clades II and III strains. (**A**) b-carotene (b-car) to chlorophyll a (Chla) ratio, (**B**) Zeaxanthin (Zea) to Chla ratio. The corresponding ESTU (*sensu* Farrant et al., 2016) is indicated below each strain name. Each data point is the average of three biological replicates.

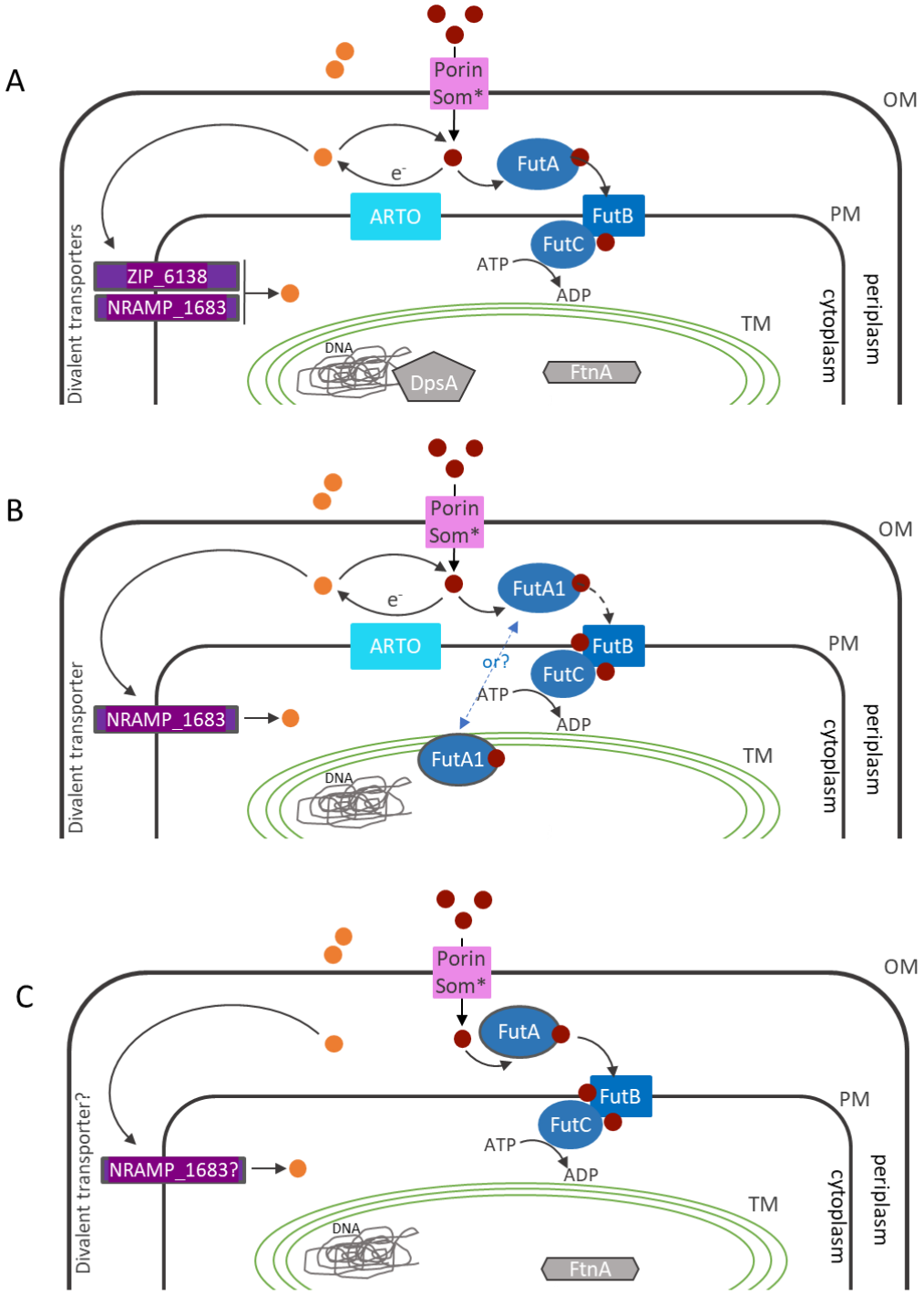

Fig. S2: Same as Figure 2 but for *Synechococcus* spp. A15-62 (A), WH8102 (B) and M16.1 (C). Note that the NRAMP_1683 gene of M16.1 is frameshifted and thus is probably inactive.

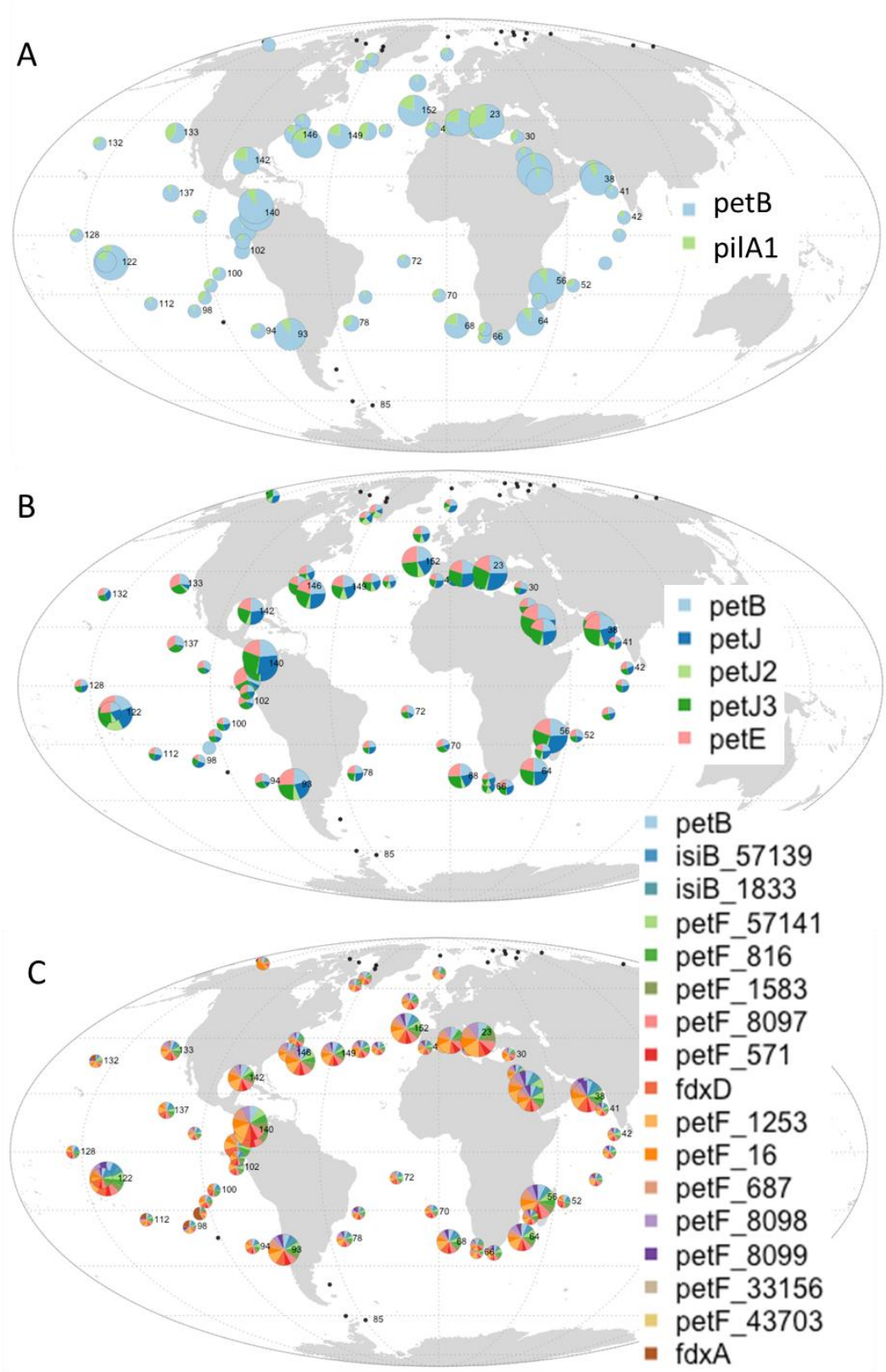

Fig. S3: Same as Figure 3 but for (**A**) *pilA1*, encoding the major pilin protein, potentially involved in the the reduction of Fe^{3+}, (**B**) *petJ,* encoding Fe-containing cytochrome c_6 and *petE*, the Cu-containing plastocyanin, (**C**) *isiB1* and *2*, encoding the Fe-free flavodoxin and genes encoding Fe-containing ferredoxins.

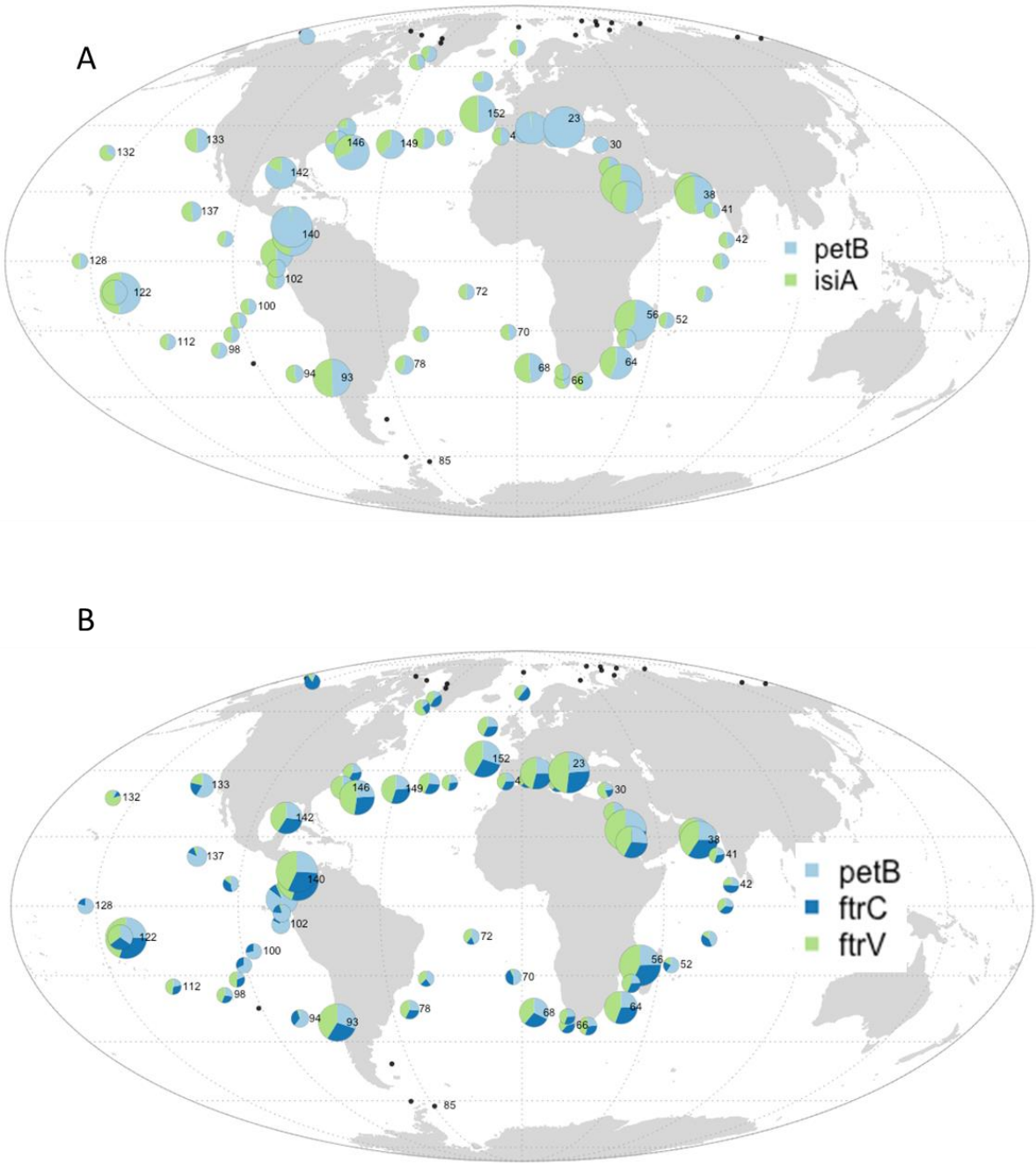

Fig. S4: Same as Figure 3 but for (**A**) *isiA*, encoding an Fe-stress induced chlorophyll a-binding protein, (**B**) *ftrC* and *ftrV* genes, encoding the catalytic and variable subunits of the ferredoxin-thioredoxin reductase, respectively.

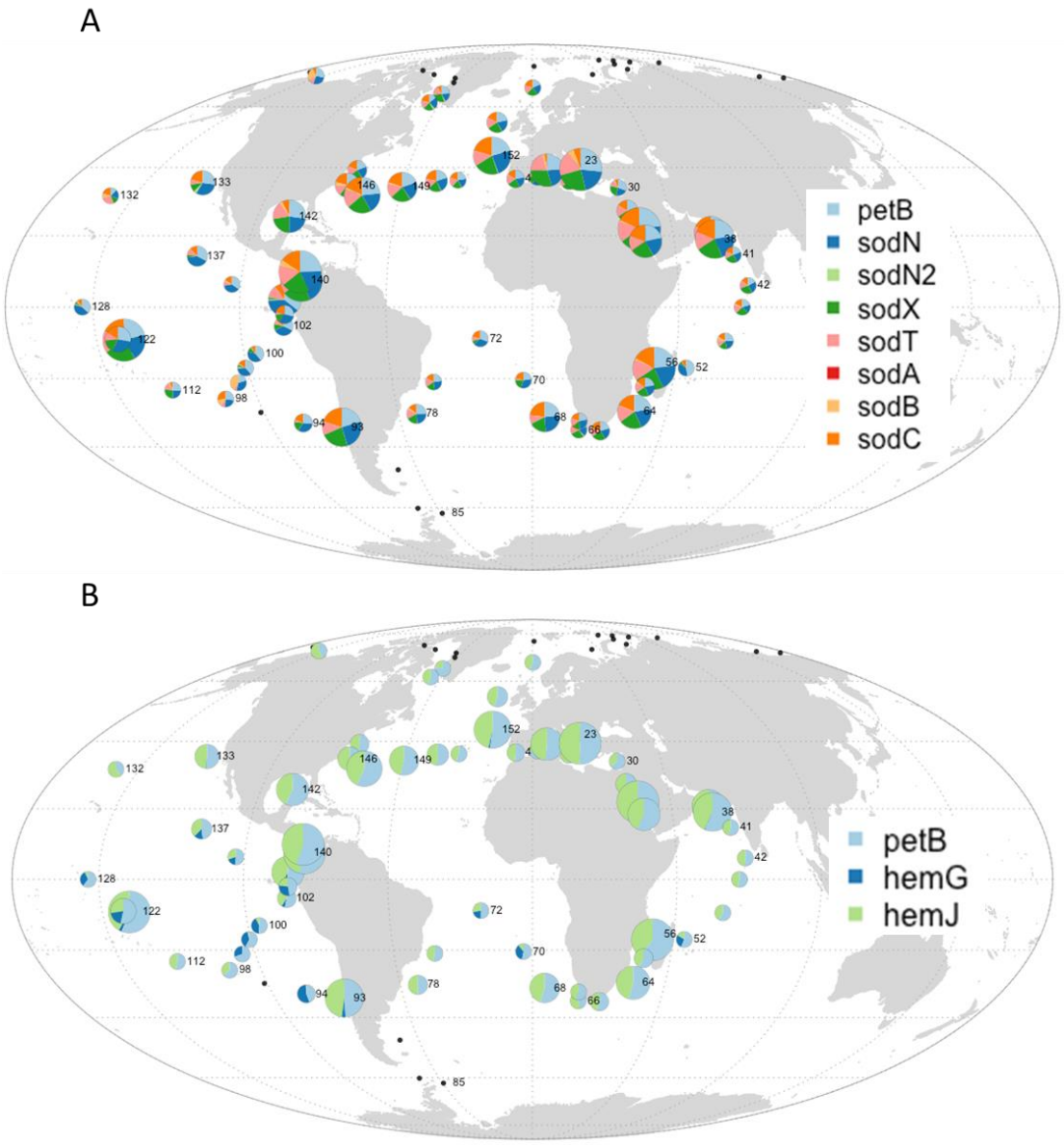

Fig. S5: Same as Figure 3 but for (**A**) *sod* genes, encoding different forms of superoxide dismutas, (**B**) *ftrC* and *ftrV* genes, encoding the catalytic and variable subunits of the ferredoxin-thioredoxin reductase, respectively.

II.3 – Identification de régions génomiques impliquées dans l'adaptation à la carence en Fe.

Alors que l'approche utilisée dans la partie précédente a consisté à rechercher à partir de la littérature des gènes connus chez les picocyanobactéries (ou d'autres organismes) pour être impliqués dans l'adaptation à la carence en Fe, nous avons également utilisé dans le cadre d'une autre étude à laquelle j'ai participé plus marginalement (Doré et al., submitted, cf. Annexe B) une approche sans a priori afin d'identifier les génes spécifiquement présents (ou absents) dans une niche écologique donnée et notamment la niche pauvre en Fe. Pour cela, une approche de réseau, la WGCNA (pour 'weighted correlation network analysis'), appliquée à la matrice d'abondance des gènes par station, nous a permis de générer des groupes de gènes (ou modules) qui présentent un profil de distribution similaire le long du transect *Tara* Oceans. Ces modules ont ensuite été corrélés aux paramètres environnementaux et à l'abondance relative en ESTU afin d'identifier les gènes spécifiques de niches et/ou d'ecotypes de picocyanobactéries. En ce qui concerne plus spécifiquement les zones limitées en fer, un module de *Synechococcus* (module yellow) et un autre de *Prochlorococcus* (brown) se sont avérés très fortement anti-corrélés à la disponibilité en Fer. Le premier etait fortement corrélé à l'abondance relative des ESTUs CRD1A et EnvBA (et dans une moindre mesure CRD1C et EnvAA) alors que le module brown etait corrélé à la présence d'HLIIIA/IVA ainsi que de LLIB (Doré et al., Fig. 2). Ces résultats montrent que les communautés colonisant ces niches sont non seulement génétiquement distinctes sur la base d'un gène marqueur unique mais possèdent également des répertoires de gènes spécifiques, potentiellement impliqués dans leur adaptation à ces conditions environnementales particulières.

De plus, afin de mieux comprendre la fonction de ces gènes spécifiques de niche et notamment des nombreux gènes codant pour des protéines hypothétiques conservées, ces données ont été intégrées aux connaissances sur l'organisation (synténie) des gènes dans les génomes de référence par une approche en réseau, en utilisant les matrices d'adjacence des gènes dans les génomes de référence au sein de chaque module. Cette intégration a permis d'identifier des clusters de gènes, appelés CAGs (pour 'clusters of adjacent genes'), qui sont à la fois adjacents dans certains génomes de référence et qui présentent une distribution et une abondance similaires *in-situ,* et qui sont donc potentiellement impliqués dans la même voie métabolique.

En accord avec la stratégie adaptative consistant à réduire la consommation en fer, plusieurs CAGs comprenant des gènes codant pour des protéines interagissant avec le Fe se sont en effet révélés anti-corrélés aux régions HNLC dans les deux genres. Cela inclut un CAG codant pour les trois sous-unités du complexe (photo)respiratoire succinate déshydrogénase (ShdABC), qui contient un cluster Fe-S, ainsi que plusieurs CAGs codant pour des protéines contenant du Fe et impliquées dans le métabolisme de l'azote et/ou du phosphore. C'est notamment le cas de CAGs impliqués dans la biosynthèse de la guanidinase, la nitrilase et la pyrimidine, ou encore le transport et l'assimilation des phosphonates et des nitrates et des nitrites, cette dernière région génomique n'étant accessoire que chez *Prochlorococcus*. De plus, les *Synechococcus* des zones riches en Fe, notamment de la mer Méditerranée et de l'océan Indien, possèdent également un grand CAG impliqué dans la biosynthèse des capsules de polysaccharides. Il a récemment été montré chez *Klebsiella* que ces structures extracellulaires, connues pour fournir une protection contre le stress biotique ou abiotique, fournirait un avantage adaptatif en conditions de carence en nutriments (Buffet et al., 2021). Cependant, alors que ces auteurs ont suggéré que les capsules pourraient jouer un rôle dans l'absorption du Fe, la forte réduction de l'abondance relative des gènes *kps* dans les zones à faible teneur en Fe et leur absence dans les souches CRD1 suggèrent plutôt que ces capsules pourraient en fait être trop énergivores pour les picocyanobactéries colonisant les régions HNLC, alors qu'elles pourraient avoir un rôle important et précédemment inconnu dans l'adaptation à la limitation en phosphore ou en azote.

A l'inverse, un certain nombre de CAGs ont été retrouvés spécifiquement dans les populations de picocyanobactéries colonisant les environnements pauvres en Fe. C'est notamment le cas d'un CAG de *Prochlorococcus* qui comprend notamment une leucine déshydrogénase (*leudH)*, capable de produire de l'ammonium à partir d'acides aminés ramifiés et d'un autre CAG comprenant les gènes *natFGH,* impliqués dans le système de transport des acides aminés polaires. Etant donné l'absence dans les populations de *Prochlorococcus* des zones HNLC de gènes impliqués dans l'assimilation des nitrates et des nitrites et la présence d'un second transporteur d'ammonium (*amt2*), ces données suggèrent que les principales sources d'azote pour les populations colonisant ces régions seraient l'ammonium et les acides aminés. En ce qui concerne plus directement le métabolisme du fer, les populations de *Prochlorococcus* et *Synechococcus* des zones HNLC sont également

enrichies en un CAG codant pour un transporteur de sidérophore TonB-dépendant (*fecA*, *tonB-exbBD, fecBDE*) et possèdent la plupart du temps un CAG contenant l'opéron *ctaC2-D2-E2* (Annexe B. Fig. 7), codant pour le complexe ARTO, impliqué dans la réduction du Fe^{3+} en Fe^{2+} et retrouvé dans 85% des génomes de référence de *Synechococcus* (dont les CRD1) mais seulement dans quelques souches de *Prochlorococcus.* Etant donné cette distribution, ce système pourrait constituer un mécanisme essentiel d'adaptation à la carence en fer chez *Prochlorococcus*.

Cet article, actuellement soumis, est accessible dans son intégralité en Annexe B.

Chapitre III :

Rôle des cyanobactéries marines du genre *Synechococcus* dans la production de DMS

Contexte de l'étude

Le diméthylsufure (DMS, $(CH_3)_2S$) est un composé organique soufré volatile qui contribue à 18% dans l'hémisphère Nord et jusqu'à 45% dans l'hémisphère Sud de la quantité totale de S atmosphérique (Mahajan et al., 2015). Ses produits d'oxydation forment dans l'atmosphère des noyaux de condensation des nuages (CCN) qui contribuent à la formation de gouttelettes nuageuses (Charlson et al., 1987). Les CCN contribuent aussi à une augmentation de l'albédo, ce qui a conduit certains chercheurs à suggérer qu'il serait possible d'atténuer en partie le réchauffement climatique grâce à une augmentation du DMS atmosphérique : c'est le principe de l'hypothèse CLAW (Charlson et al., 1987). L'océan à lui seul contribuerait à 98% des flux de DMS vers l'atmosphère (Gondwe et al., 2003). Le précurseur du DMS, le diméthylsulfoniopropionate (DMSP, $(CH_3)_2SCH_2CH_2COOH$) et son produit d'oxydation, le diméthylsulfoxyde (DMSO, $(CH_3)_2SO$) sont produits et dégradés par les micro-organismes. Ainsi, le cycle du DMS dépend directement de la biologie et va influencer la structure des populations marines (Hay, 2009). Les concentrations en DMS/P/O et les flux océan/atmosphère résultent d'une interaction complexe entre physique, biologie et chimie qui sont pour l'instant peu connues (Stefels et al., 2007). Cependant, il a été mis en évidence certaines spécificités du DMSP, qui aurait notamment une fonction cryoprotectrice notamment chez les algues polaires et qui, d'une manière plus large, jouerait un rôle antioxydant (Sunda et al., 2002). La quantité de DMSP/O cellulaire varie d'une espèce phytoplanctonique à une autre. Ainsi les prasinophytes, haptophytes et dinoflagellés sont de forts producteurs de DMSP, tandis que les cyanobactéries marines (telles que *Synechococcus*) et les diatomées sont de faibles producteurs de DMSP (Stefels et al., 2007). Il a cependant été montré qu'en condition de limitation en macronutriments et en Fe, les diatomées étaient capables de d'augmenter leur DMSP intracellulaire à des valeurs proches des forts producteurs (Bucciarelli et al., 2013; Bucciarelli & Sunda, 2003). Ainsi, dans le contexte d'une expansion des zones limitées en Fe dans l'océan mondial, on peut se demander i) si les cyanobactéries, autre groupe considéré comme faible producteur de DMSP, sont capables de produire du DMS et en quelle quantité, et ii) si la biodisponibilité en fer pourrait jouer sur leur capacité de production du DMSP des *Synechococcus* marins. Ce chapitre présente les résultats d'une étude réalisée en collaboration entre le LEMAR (Brest) et mon équipe

dans le cadre du programme « FeDRe » (INSU Ocean Atmosphère LEFE) qui visait à répondre à la première question. Bien que j'aie aussi réalisé des tests préliminaires pour tenter de répondre à la seconde question, les difficultés que j'ai rencontrées pour faire pousser les souches de *Synechococcus* en carence en fer m'ont empêché de mener à bien cette seconde étude.

Contribution

Pour tester la capacité de *Synechococcus* de produire du DMS, des souches axéniques m'ont été fournies par Morgane Ratin (équipe ECOMAP Roscoff) et David J. Scanlan (Université de Warwick, Royaume Uni). La présence de bactéries hétérotrophes pouvant perturber les résultats car elles sont susceptibles de produire du DMS, je me suis d'abord assurée de l'axénie des cultures, en les suivant au microscope et au cytomètre en flux. J'ai ensuite mis en place le protocole expérimental et organisé la récolte des échantillons avec Eva Bucciarelli (LEMAR) et les membres de mon équipe. J'ai ensuite activement participé au traitement des échantillons de cytométrie en flux et à l'analyse des données.

Marine *Synechococcus* ability to produce DMS via DMSO reduction

Résumé de l'article en français

Le diméthylsulfure (DMS) est un composé soufré volatile qui participe à la formation des nuages, à l'albédo de la Terre et au refroidissement climatique. L'océan contribue jusqu'à 98% aux flux de DMS vers l'atmosphère. Son précurseur océanique, le diméthylsulfoniopropionate (DMSP), et son produit d'oxydation, le diméthylsulfoxyde (DMSO), sont produits et dégradés par les micro-organismes marins. Historiquement, les cyanobactéries marines seraient de faibles producteurs de DMSP et leur rôle dans le cycle du DMS n'est donc pas considéré comme significatif. Cependant, nous montrons dans cette étude que trois souches marines de *Synechococcus* (CC9311, WH8102, WH7803) sont capables de réduire le DMSO en DMS. Ce processus suit une courbe de type Michaelis-Menten, cohérente avec un processus enzymatique, tel que décrit précédemment pour d'autres groupes phytoplanctoniques. La constante de Michaelis-Menten Km est du même ordre de grandeur pour toutes les espèces testées jusqu'à présent, *Synechococcus* se situant dans la gamme haute et la vitesse de réaction maximale Vmax étant 10 à 100 fois plus élevée. La recherche de gènes candidats pour la capacité à réduire le DMSO n'a révélé aucun homologue de DMSO réductases retrouvées typiquement chez les bactéries. Cependant, tous les *Synechococcus* marins possèdent des homologues de la méthionine sulfoxide réductase qui pourraient avoir une fonction de réduction du DMSO, comme cela a été suggéré précédemment pour les diatomées. Chez *Synechococcus,* les constantes de vitesse de réduction du DMSO à de faibles concentrations de DMSO (~24 j^{-1}) sont 4 à 30 fois plus élevées que celles des autres groupes phytoplanctoniques et que les constantes de vitesse *in situ*. Cette capacité peut être liée à la protection antioxydante et indique que les cyanobactéries participeraient activement au cycle du DMS dans l'eau de mer.

Marine *Synechococcus* can produce dimethylsulfide via an unusual dimethyl sulfoxide reduction pathway

Eva Bucciarelli[1], Mathilde Ferrieux[2], Morgane Ratin[2], Frédéric Partensky[2] and Laurence Garczarek[2]

[1] Université de Brest, CNRS, IFREMER, UMR 6539, Laboratoire des sciences de l'environnement marin (LEMAR), Observatoire des Sciences de l'Univers-Institut Universitaire Européen de la Mer, Plouzané, France.

[2] Sorbonne Université, CNRS, UMR 7144 Adaptation and Diversity in the Marine Environment (AD2M), Station Biologique de Roscoff (SBR), Roscoff, France.

* Correspondence:
Corresponding Author: E. Bucciarelli: Eva.Bucciarelli@univ-brest.fr

Abstract

Dimethylsulfide (DMS) is a volatile sulfur compound that participates in cloud formation, Earth planetary albedo and climate cooling. The ocean contributes to up to 98% of the DMS fluxes to the atmosphere. The oceanic precursor of DMS, dimethylsulfoniopropionate (DMSP), and their oxidation product dimethylsulfoxide (DMSO) are produced and degraded by marine microorganisms. Cyanobacteria are low DMSP-producers, and their role in the DMS cycle is not considered to be significant. However, we show in this study that three marine *Synechococcus* strains (CC9311, WH8102, WH7803) are able to reduce DMSO to DMS. This process follows a Michaelis-Menten type curve, consistent with an enzymatic process as described previously for other phytoplanktonic groups. The Michaelis-Menten constant Km is on the same order of magnitude for all species tested so far, with *Synechococcus* being in the upper range, while the maximum reaction rate Vmax is 10-100-fold higher. The search for candidate genes for the ability to reduce DMSO revealed no homolog of typical bacterial DMSO reductases. However, all marine *Synechococcus* possess methionine sulfoxide reductase homologs which could have a DMSO reduction function, as previously suggested for diatoms. DMSO reduction rate constants at low DMSO concentrations (~24 d^{-1}) are 4-30 times higher than those of other phytoplanktonic groups and than *in situ* rate constants. This ability may be related to antioxidant protection, and indicates that cyanobacteria actively participate in DMS cycling in seawater.

Introduction

Dimethylsulfide (DMS, $(CH_3)_2S$) is a volatile organic sulfur compound that contributes to 18% (Northern Hemisphere) and up to 45% (Southern Hemisphere) of the total atmospheric sulfur burden (Mahajan et al., 2015). Its oxidation products in the atmosphere are cloud condensation nuclei (CCN) that are supposed to participate in cloud droplet formation and the planetary albedo (Charlson et al., 1987). Increases in atmospheric DMS concentrations might thus increase albedo, and partly alleviate climate warming. Thirty years have passed since this hypothesis has been postulated (Charlson et al., 1987). However, the significance of the possible links between atmospheric DMS oxidation products, CCN and albedo is still strongly debated (Lana et al., 2012; Mahajan et al., 2015; Quinn & Bates, 2011). The ocean contributes to up to 98% of the DMS fluxes to the atmosphere (Gondwe et al., 2003). The oceanic precursor of DMS, dimethylsulfoniopropionate (DMSP, $(CH_3)_2SCH_2CH_2COOH$), and their oxidation product dimethylsulfoxide (DMSO, $(CH_3)_2SO$) are produced and degraded by marine microorganisms. DMS, DMSP and DMSO (DMS/P/O) are rapidly cycled through the oceanic food web (Stefels, 2007). DMS/P/O can decrease viral infection (Evans et al. 2006) or induce parasitoid activation (Garcés et al., 2013) of phytoplankton, and are potent chemical signals for plankton (Seymour et al., 2010) and higher predators (Nevitt, 2011). As such, they can strongly influence the structure of marine populations, communities and ecosystems (Hay, 2009). DMS/P/O may thus have important consequences at different environmental scales, from marine ecosystems structure to climate regulation. Many uncertainties remain however in the various processes that control the biogeochemical cycle of DMS. Oceanic DMS/P/O concentrations and ocean/atmosphere fluxes result from complex physical, biological, and chemical interactions that are not well constrained (Stefels, 2007). It is generally considered that prasinophytes, haptophytes, chrysophytes, and dinoflagellates are high DMSP-producers, while diatoms and cyanobacteria are low DMSP-producers (Stefels, 2007). As a result, the high DMSP-producers that possess the DMSP lyase that can cleave DMSP into DMS, are considered the main contributors to DMS production. However, the discovery of a DMSO-reducing enzyme in phototrophs may add a new twist to the story (Spiese et al., 2009; Spiese & Tatarkov, 2014). The existence of DMSO reductases in heterotrophic bacteria has been

known for a long time (see McCrindle et al., 2005 for review), but it has been largely overlooked in phytoplankton. (Fuse et al., 1995) were the first to report the ability of 5 phytoplanktonic species to produce DMS from added DMSO, but this ability was not quantified. This was further investigated in Spiese et al. (2009) and Spiese & Tatarkov, (2014), which indicated DMSO reduction by 8 other species. Michaelis Menten kinetics experiments were performed for 4 of them, revealing an enzymatic process (Spiese et al., 2009). Very few studies however have estimated the significance of DMSO reduction in biogeochemistry. Rates of DMS production from DMSO reduction have been measured *in situ* only 4 times to our knowledge. Depending on the considered environment, these rates were found to be comparable to rates of DMS produced from DMSP cleavage in sea-ice brines and Antarctic polynia waters (Asher et al., 2011), and two- or ten-fold lower in coastal Antarctic waters (Asher et al., 2017) and NE Subarctic Pacific (Asher et al., 2017), respectively. The latter study nonetheless points out that DMSO reduction can still provide a significant source of DMS in this HNLC region (Asher et al., 2017), and the most recent study in this region revealed that DMSO reduction rates could exceed dissolved DMSP cleavage at nearly all stations (Herr et al., 2021). Overall these few studies indicate that in situ DMSO reduction may be an important overlooked process in DMS production.

Further understanding of the factors influencing DMSO reduction by marine phytoplankton is necessary to better constrain the relative contribution of phytoplankton to DMS/P/O dynamics. In particular, six different phytoplanktonic groups were tested, but cyanobacteria were absent from these experiments. Cyanobacteria, however, may play a role in DMS/P/O cycling. *Trichodesmium*, although a low DMSP-producer, is able to up-regulate its intracellular DMSP concentration when Fe-limited (Bucciarelli et al., 2013b). The ubiquitous marine cyanobacterium *Synechococcus* is able to actively take up DMSP (Malmstrom et al., 2005; Vila-Costa et al., 2006). This is important not only because it demonstrates that phototrophs can efficiently compete with heterotrophs for dissolved organic sulfur (DOS) acquisition, but also because it may divert part of the DOS (and consequently DMS) from emission into the atmosphere (Vila-Costa et al., 2006). *Synechococcus* is the second most abundant photosynthetic organism in the ocean and contributes for an estimated 16 % of primary productivity (Flombaum et al., 2013).

Given the seemingly widespread occurrence of DMSO reduction ability in autotrophic and heterotrophic microorganisms, and the importance of marine

Synechococcus in oceanic primary production, we explored the ability of three axenic marine strains (CC9311, WH8102, WH7803) to produce DMS from DMSO.

Material and methods

Strains and growth conditions

As bacteria are able to produce DMS, we selected three axenic *Synechococcus* spp. strains that were retrieved from the Roscoff Culture Collection (https://roscoff-culture-collection.org/; Table 1). Cultures were grown in PCR-S11 medium (Rippka et al., 2000b) supplemented with 1 mM sodium nitrate in 400 mL flasks (Sarstedt, Germany). Cultures were maintained in temperature-controlled chambers at 22°C under continuous 75 µmol photons m^{-2} s^{-1} provided by a white-blue-green LED system (Alpheus, France).

Table 1: Characteristics of the *Synechococcus* strains used in this study

Strains name	CC9311	WH8102	WH7803
RCC # [1]	1086	539	752
Subcluster [2]	5.1	5.1	5.1
Clade [2]	I	III	V
Pigment type [4]	3dA	3c	3a
Axeny	Yes	Yes	Yes
Biovolume (µm^{-3})	0.41 ± 0.02	0.46 ± 0.11	1.49 ± 0.13
Ocean	Pacific	Atlantic	Atlantic
Region	California current	Caribbean Sea	Sargasso Sea
Isolation latitude	31°54' N	22°48' N	33°45' N
Isolation longitude	124°10' W	65°36' W	67°30' W

[1]Roscoff Culture Collection, [2]Farrant *et al.* (2016), [3]Mazard *et al.* (2012), [4]Humily *et al.* (2013).

Flow cytometry and microscopic analyses

In order to enumerate *Synechococcus* cells in pre-cultures and experimental samples, 200 µl aliquots were fixed using 0.25% (v/v) glutaraldehyde (grade II, Sigma Aldrich, USA) and stored at -80°C until analysis. Cell concentrations were determined using a Guava easyCyte flow cytometer based on natural fluorescence (Marie et al., 1999b). Axenicity was verified both by flow cytometry using a Novocyte Advanteon instrument (Agilent, USA) after labelling the samples for 15 min with SYBR™ Green II (Thermo Fisher Scientific, USA) as described in Marie et al. (1999), and by fluorescence

microscopy (Eclipse 80i, Nikon, Japan). All three strains proved bacteria-free all along the experiments. Cell biovolumes of the three strains used in this study were determined using the same microscope after illuminating cells at λ=550 nm (Cy3 filter, Nikon, Japan), exciting *Synechococcus* phycoerythrin. For each strain, the width (W) and length (L) of 300 cells were measured and biovolume (in μm^{-3}) was estimated using the following formula, assuming that *Synechococcus* cells exhibit a short-rod shape, i.e. a cylinder complemented by two half spheres:

$$V = (L - W) \times \pi \times (\frac{w}{2})^2 + [\frac{4}{3} \times \pi \times (\frac{w}{2})^3]$$

Dimethylsulfide analyses

On the day of the experiments, 8 times 5 mL of each triplicate cultures were subsampled in 8 10 mL vials. Increasing concentrations of DMSO were added to the vials (0, 1.5, 3, 5, 10, 25, 50, 100 µM). The vials were sealed and placed back in the incubator for 1 h. All manipulations were conducted in a sterile laminar flow hood using sterile techniques. Vials and septa were sterilized by overnight heating at 120°C.

The DMS released 1 hour after addition of DMSO was measured by sparging 5 mL of cultures with He (35 ml min^{-1}) and trapping the resulting gas flux in liquid N_2 within a Teflon loop to preconcentrate the samples. After 5 minutes of purge and trap, DMS was desorbed by warming the Teflon loop with hot water and was injected in a Shimadzu 2010-Plus Gas Chromatograph (GC) equipped with a sulfur-selective flame photometric detector (air / H_2: 70 mL min^{-1} / 60 mL min^{-1}) and fitted with an Equity 1 capillary column (3.2 mm i.d., 30 m long, Supelco, T = 180 °C, carrier gas: He, 6.7 ml min^{-1}). Detector and injection port temperatures were set at 250 °C. DMS was calibrated using DMSP standards that were prepared the day before by adding increasing concentrations of 10-6 M DMSP to 5 mL of 5 M NaOH. Six to 7 standards spanning 0-1000 pmol of DMSP were run (R^2 > 0.99).

Blanks were measured by analyzing DMS released from PCR-S11 medium alone, and prepared in the exact same way as the samples (same DMSO additions in triplicate vials, analyses run after 1h in the incubator). All culture values presented below were corrected for blanks. DMS is expressed in nmol per liter of medium, and for the sake of comparison with previous studies, per biovolume (i.e., mmol L_{cell}^{-1}).

Comparative genomics and metagenomics

50 *Synechococcus* and 6 *Cyanobium* genomes, retrieved from the Cyanorak *v2.1* database, covering quite well the large genomic diversity occurring within these genera (Garczarek et al., 2021), were used to search for proteins involved in the DMS/O/P metabolism based on characterized proteins from the literature using BLASTP. Interpro (Blum et al., 2020) was also used to compare the protein domains of the query and best hits within Cyanorak. Clusters of likely orthologous genes (CLOGs) within Cyanorak were used to define phyletic patterns within the 56 *Synechococcus/Cyanobium* genomes for genes with significant matches. Whole genome recruitment of metagenomic reads from the *Tara* Oceans dataset on the 56 *Synechococcus/Cyanobium* genomes was performed and used to draw distribution maps of genes of interests using custom-designed R scripts, as previously described (Doré et al., submitted)

Results and Discussion

Synechococcus can produce DMS through DMSO reduction

All three *Synechococcus* species have the ability to produce DMS after DMSO addition (Fig. 1a, 1b). Their production in nmol of DMS per liter of medium per hour is significantly higher than the abiotic DMS production by the sterile medium (Fig. 1a). Abiotic DMS production determined in the medium amounted 0.01 ± 0.01 % of added DMSO (n=21) for 1 hour incubation, while DMS production by *Synechococcus* (minus abiotic contribution) amounted 0.03 – 1.94 % of added DMSO, depending on the species. Biotic increase in DMS concentrations could not be attributed to another process than DMSO reduction, as these species have no detectable intracellular DMSP concentration (this study, data not shown) and do not exhibit any DMSP lyase activity (Malmstrom et al., 2005; Sheehan & Petrou, 2020). This increase after addition of DMSO followed a Michaelis-Menten type curve, consistent with an enzymatic process as described in Spiese et al. (2009) and Spiese & Tatarkov (2014). The kinetic parameters of the Michaelis-Menten equation are presented in Table 2, along with available data for other phototrophs (Fuse et al., 1995; Spiese et al., 2009). The Michaelis-Menten constant Km is on the same order of magnitude for all species, with *Synechococcus* being in the upper range. Similar Km values may indicate similar DMSO-reductases or DMSO-reductase like

enzymes with similar affinities for DMSO, contrary to what has been measured for DMSP-lyases like enzymes so far (Yost & Mitchelmore, 2012).

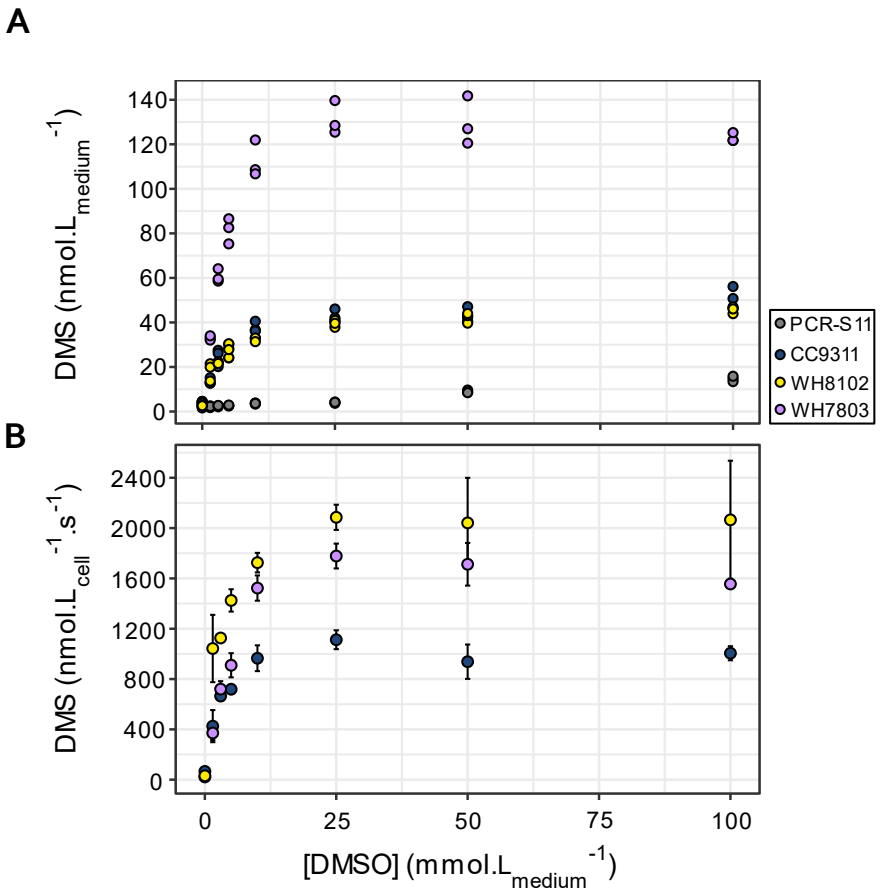

Figure 1. Production of DMS A) in the culture medium (in nmol L_{medium}^{-1}) and B) per cell volume (in nmol $L_{cell}^{-1}.s^{-1}$), in triplicate cultures of *Synechococcus* CC9311, WH7803 and WH8102, over 1 hour incubation, vs increasing concentrations of added DMSO (mmol L_{medium}^{-1}). In the lower panel **B**), data were corrected from abiotic DMS production by sterile medium (mean ±standard deviation, n=3).

The maximum reaction rate Vmax is 10-100 fold higher for *Synechococcus* than for the other species. Nine other phototrophs are also able to reduce DMSO to DMS (Fuse et al., 1995; Spiese et al., 2009). Although enzyme kinetics experiments following a Michaelis-Menten kinetics were not performed for these species, they exhibited DMS production upon addition of 1-2 mmol^{-1} DMSO. Assuming linearly increasing activities in the non-saturating substrate range, we estimated DMS production by *Synechococcus* at 1 mmol L^{-1} DMSO by equation (1) :

$$\text{DMS production at 1mM} = \frac{\text{DMS production at 1.5mM} - \text{DMS production in control}}{1.5} \qquad (1)$$

These estimates indicate that *Synechococcus* produced DMS 2-70 times more rapidly than the other phototrophs, except for *T. oceanica* (Table 2). The apparent first-order rate constant at low substrate concentration, defined as Vmax/Km (Cleland, 1975), is strikingly similar for the 3 *Synechococcus*. It also indicates their high ability at producing DMS from low DMSO concentrations, compared to the other species.

Table 2 : DMS production and Michaelis-Menten kinetics for the Synechococcus species tested in this study, and the autotrophs tested in 1 (Spiese et al., 2009) and 2 (Fuse et al., 1995).

		DMS production ($nmol.L_{cell}^{-1}.s^{-1}$) from DMSO	Michaelis-Menten kinetics			
Group	Species	reduction*	K_m ($mmol.L^{-1}$)	V_{max} ($nmol.L_{cells}^{-1}.s^{-1}$)	V_{max}/K_m (d^{-1})	Reference
Cyanobacteria	*Synechococcus* CC9311	~0.24	3.9 ± 0.1	1071 ± 38	24 ± 1	This study
	Synechococcus WH7803	~0.23	6.7 ± 0.2	1852 ± 74	24 ± 2	
	Synechococcus WH8102	~0.67	7.7 ± 0.3	2137 ± 84	24 ± 2	
Baccilarophyceae	*Thalassiosira oceanica*	1.5 ± 0.2	n.d.	n.d.	n.d.	1
	Thalassiosira pseudonana 1335	~0.02	2.0 ± 0.7	17 ± 2	0.8 ± 0.3	1
	Thalassiosira pseudonana 1014	~0.04	2.7 ± 1.2	55 ± 9	1.7 ± 1.0	1
	Thalassiosira weissflogii	Yes	n.d.	n.d.	n.d.	2
Hpatophyceae	*Emiliana huxleyi*	~0.10	n.d.	n.d.	n.d.	1
	Isochrysis galbana 1323	~0.03	0.96 ± 0.32	29 ± 2	2.6 ± 1.0	1
	Crocosphaera roscoffensis	Yes	n.d.	n.d.	n.d.	2
Dinophyceae	*Prorocentrum minimum*	~0.12	n.d.	n.d.	n.d.	1
	Amphidinium carterae 1314	~0.11	1.6 ± 0.4	118 ± 6	6.4 ± 1.9	1
Crytophyceae	*Rhodomonas lens*	0.006 ± 0.002	n.d.	n.d.	n.d.	1
Raphydophyceae	*Chattonella antiqua*	Yes	n.d.	n.d.	n.d.	2
	Heterosigma akashiwo	Yes	n.d.	n.d.	n.d.	2
Chlorophyceae	*Dunaliella sp.*	Yes	n.d.	n.d.	n.d.	2

In order to find candidate genes that might explain the ability for these strains to produce DMS from DMSO, we explored the genomes of the 56 *Synechococcus/Cyanobium* of the Cyanorak database, which notably includes the three strains used in the present study for the presence of a putative DMSO reductase using characterized DMSO reductases as baits. Like for *Thalassiora pseudonana* (Spiese et al., 2009), there was no homolog of typical DMSO reductases. We notably searched for the *dmsA-B-C* genes coding for the three chains of the DMSO reductase in *Escherichia coli,* a membrane-bound, [Fe-S] molybdoenzyme, which catalyzes reduction of DMSO to DMS and also reduces a

wide variety of S- and N-oxide compounds (Weiner et al., 1992). The closest homolog of DmsA was the nitrate reductase (NarB), DmsB hit a 3Fe-4S ferredoxin while DmsC had no significant hit. Absence of obvious candidates for DMSO reduction suggest that marine *Synechococcus* might use a different and yet unknown pathway for this function. As for *T. pseudonana*, the most probable candidates for the DMSO reductase function are members of the MsrA family, which are usually thought to reduce *S*-methionine sulfoxide in peptides. Yet in *Saccharomyces cerevisiae* MRX1, a MsrA homolog, was suggested to reduce DMSO and its inactivation inhibited the production of DMSO (Bamforth, 1980; Hansen, 1999). All marine *Synechococcus* possess two MsrA homologs (CK_00000160 and CK_00001078) and two MsrB homologs (CK_00000040 and CK_00008118) and one or several of those could have a DMSO reduction function, although this hypothesis would need to be checked experimentally.

Oceanographic relevance

To our knowledge, only four publications have reported in situ DMSO reduction rates, in Antarctic sea brines, polynya and coastal waters (Asher et al., 2011, 2017) and in the Northeast Subarctic Pacific (Asher et al., 2017; Herr et al., 2021). When reported, DMSO reduction rate constant varied from 0.07 d-1 to 2.82 d-1 in the Northeast Subarctic Pacific, and equalled 1.6 d-1 in Antarctic coastal waters. These rates, which are equivalent to DMSP cleavage rate constant (Herr et al., 2021), are similar to Vmax/Km (i.e., the apparent first-order rate constant of an enzymatic reduction at low DMSO concentration, Table 1) for *T. pseudonana*, I*. galbana* and *A. carterae*. This is consistent with in situ DMSO reduction rates correlating with phytoplanktonic communities and suggests that phytoplanktonic DMSO reduction may play a significant role in DMS cycling (Herr et al., 2021).

Synechococcus are not dominant in the subpolar and polar regions. They are mostly abundant in the Indian and western Pacific Oceans, and at mid latitudes (Flombaum et al., 2013c). Moderate to high DMS concentrations are measured in (sub)tropical waters, e.g. the subtropical Indian Ocean and the tropical and subtropical Pacific Ocean, contributing to hot spots of DMS emission in these regions (Cui et al., 2015; Lana et al., 2011). High values of Vmax/Km measured in our study for *Synechococcus* could

help explain at least part of these DMS concentrations and high fluxes to the atmosphere. This contribution may be all the more important as DMSO reducing ability seems to be related to an antioxidant function. DMSO (and DMS and DMSP) can indeed react with reactive oxygen species (ROS, e.g., hydroxyl radical) within the cell with the same as, or greater efficiency than conventional antioxidants such as glutathione and ascorbate peroxidase (W. Sunda et al., 2002b). Tropical and subtropical oligotrophic open ocean waters, where *Synechococcus* thrive, experience high solar radiation and low nutrient concentrations. These conditions increase oxidative stress and intracellular DMS/P/O contents in some phytoplankton (Bucciarelli & Sunda, 2003b; Keller et al., 1999; Kinsey et al., 2015; W. Sunda et al., 2002b), including the cyanobacteria Thrichodesmium (Bucciarelli et al., 2013b). Nutrient limitation also up-regulates enzymatic DMSP lysis (Sunda et al., 2007) and DMSO reduction (Spiese & Tatarkov, 2014). This may increase antioxidant protection as DMS is a better antioxidant than DMSP or DMSO (Sunda et al., 2002; Sunda et al., 2007). DMS could be intracellularly re-oxidized to DMSO by ROS, creating a very efficient catalytic cycle between DMSO and DMS to remove ROS (Spiese et al., 2009; Sunda et al., 2002). *Synechococcus* can also actively take up DMSP (Malmstrom et al., 2005; Vila-Costa et al., 2006). This should produce intracellular DMSO when DMSP reacts with ROS, fueling their intracellular antioxidant systems through DMSO reduction.

Together with DMSP uptake (*Synechococcus*, Malmstrom et al., 2005; Vila-Costa et al., 2006) and intracellular DMSP regulation (*Trichodesmium*, Bucciarelli et al., 2013), DMSO reducing ability indicates that cyanobacteria can actively participate in DMS-P-O cycling in seawater. Future experiments should further investigate if nutrient limitation and high irradiance levels, both co-occuring in oligotrophic regions, may increase the already high DMSO reduction rate constant of *Synechococcus* as would be expected for antioxidant systems. If confirmed significant compared to other in situ processes, the role of cyanobacteria in the biogeochemical cycle of DMS may have to be re-evaluated.

Acknowledgements

This work was supported by the French programs INSU-OA LEFE 'FeDre' and "Agence Nationale de la Recherche 'CINNAMON' (ANR-17-CE02-0014-01). We also would like to thank Priscillia Gourvil and Martin Gachenot from the Roscoff Culture Collection (http://roscoff-culture-collection.org/) and Dave J. Scanlan for maintaining the *Synechococcus* strains used in this study and Morgane Ratin for her help with axenic strains and culture media.

References

Asher, E. C., Dacey, J. W. H., Mills, M. M., Arrigo, K. R., & Tortell, P. D. (2011). High concentrations and turnover rates of DMS, DMSP and DMSO in Antarctic sea ice : DMS DYNAMICS IN ANTARCTIC SEA ICE. *Geophysical Research Letters*, *38*(23), n/a-n/a. https://doi.org/10.1029/2011GL049712

Asher, E. C., Dacey, J. W. H., Stukel, M., Long, M. C., & Tortell, P. D. (2017). Processes driving seasonal variability in DMS, DMSP, and DMSO concentrations and turnover in coastal Antarctic waters. *Limnology and Oceanography*, 104-124. https://doi.org/10.1002/lno.10379

Asher, E., Dacey, J. W., Ianson, D., Peña, A., & Tortell, P. D. (2017). Concentrations and cycling of DMS, DMSP, and DMSO in coastal and offshore waters of the Subarctic Pacific during summer, 2010-2011. *Journal of Geophysical Research: Oceans*, *122*(4), 3269-3286. https://doi.org/10.1002/2016JC012465

Bamforth. (1980). *Dimethyl sulphoxide reductase of* Saccharomyces spp.

Blum, M., Chang, H.-Y., Chuguransky, S., Grego, T., Kandasaamy, S., Mitchell, A., Nuka, G., Paysan-Lafosse, T., Qureshi, M., Raj, S., Richardson, L., Salazar, G., Williams, L., Bork, P., Bridge, A., Gough, J., Haft, D., Letunic, I., Marchler-Bauer, A., & Finn, R. (2020). The InterPro protein families and domains database : 20 years on. *Nucleic Acids Research*, *49*. https://doi.org/10.1093/nar/gkaa977

Bucciarelli, E., Ridame, C., Sunda, W. G., Dimier-Hugueney, C., Cheize, M., & Belviso, S. (2013). Increased intracellular concentrations of DMSP and DMSO in iron-limited oceanic phytoplankton *Thalassiosira oceanica* and *Trichodesmium erythraeum*. *Limnology and Oceanography*, *58*(5), 1667-1679. https://doi.org/10.4319/lo.2013.58.5.1667

Bucciarelli, E., & Sunda, W. G. (2003). Influence of CO_2, nitrate, phosphate, and silicate limitation on intracellular dimethylsulfoniopropionate in batch cultures of the coastal diatom *Thalassiosira pseudonana*. *Limnology and Oceanography*, *48*(6), 2256-2265. https://doi.org/10.4319/lo.2003.48.6.2256

Charlson, R. J., Lovelock, J. E., Andreae, M. O., & Warren, S. G. (1987). Oceanic phytoplankton, atmospheric sulphur, cloud albedo and climate. https://www.nature.com/articles/326655a0

Cleland, W. W. (1975). What limits the rate of an enzyme-catalyzed reaction. *Accounts of Chemical Research*, *8*(5), 145-151. https://doi.org/10.1021/ar50089a001

Cui, Y., Suzuki, S., Omori, Y., Wong, S.-K., Ijichi, M., Kaneko, R., Kameyama, S., Tanimoto, H., & Hamasaki, K. (2015). Abundance and Distribution of Dimethylsulfoniopropionate Degradation Genes and the Corresponding Bacterial Community Structure at Dimethyl Sulfide Hot Spots in the Tropical and Subtropical Pacific Ocean. *Applied and Environmental Microbiology*, *81*(12), 4184-4194. https://doi.org/10.1128/AEM.03873-14

Farrant, G. K., Doré, H., Cornejo-Castillo, F. M., Partensky, F., Ratin, M., Ostrowski, M., Pitt, F. D., Wincker, P., Scanlan, D. J., Iudicone, D., Acinas, S. G., & Garczarek, L. (2016). Delineating ecologically significant taxonomic units from global patterns of marine picocyanobacteria. *Proceedings of the National Academy of Sciences*, *113*(24), E3365-E3374. https://doi.org/10.1073/pnas.1524865113

Flombaum, P., Gallegos, J. L., Gordillo, R. A., Rincón, J., Zabala, L. L., Jiao, N., Karl, D. M., Li, W. K. W., Lomas, M. W., Veneziano, D., Vera, C. S., Vrugt, J. A.,

& Martiny, A. C. (2013). Present and future global distributions of the marine Cyanobacteria *Prochlorococcus* and *Synechococcus*. *Proceedings of the National Academy of Sciences of the United States of America*, *110*(24), 9824-9829. https://doi.org/10.1073/pnas.1307701110

Fuse, H., Takimura, O., Kamimura, K., Murakami, K., Yamaoka, Y., & Yoshikatsu, M. (1995). Transformation of Dimethyl Sulfide and Related Compounds by Cultures and Cell Extracts of Marine Phytoplankton. Shibaura Institute of Technology. https://shibaura.pure.elsevier.com/en/publications/transformation-of-dimethyl-sulfide-and-related-compounds-by-cultu-2/fingerprints/

Garcés, E., Alacid, E., Reñé, A., Petrou, K., & Simó, R. (2013). Host-released dimethylsulphide activates the dinoflagellate parasitoid *Parvilucifera sinerae*. *The ISME Journal*, *7*(5), 1065-1068. https://doi.org/10.1038/ismej.2012.173

Garczarek, L., Guyet, U., Doré, H., Farrant, G. K., Hoebeke, M., Brillet-Guéguen, L., Bisch, A., Ferrieux, M., Siltanen, J., Corre, E., Le Corguillé, G., Ratin, M., Pitt, F. D., Ostrowski, M., Conan, M., Siegel, A., Labadie, K., Aury, J. M., Wincker, P., … Partensky, F. (2021). Cyanorak v2.1 : A scalable information system dedicated to the visualization and expert curation of marine and brackish picocyanobacteria genomes. *Nucleic acids research*, *49*(D1), D667-D676. https://doi.org/10.1093/nar/gkaa958

Gondwe, M., Krol, M., Gieskes, W., Klaassen, W., & de Baar, H. (2003). The contribution of ocean-leaving DMS to the global atmospheric burdens of DMS, MSA, SO_2, and NSS $SO_4^=$. *Global Biogeochemical Cycles*, *17*(2). https://doi.org/10.1029/2002GB001937

Hansen, J. (1999). Inactivation of MXR1 Abolishes Formation of Dimethyl Sulfide from Dimethyl Sulfoxide in *Saccharomyces cerevisiae*. *Applied and Environmental Microbiology*, *65*(9), 3915-3919.

Hay, M. E. (2009). Marine chemical ecology : Chemical signals and cues structure marine populations, communities, and ecosystems. *Annual Review of Marine Science*, *1*, 193-212. https://doi.org/10.1146/annurev.marine.010908.163708

Herr, A. E., Dacey, J. W. H., Kiene, R. P., McCulloch, R. D., Schuback, N., & Tortell, P. D. (2021). Potential roles of dimethysulfoxide in regional sulfur cycling and phytoplankton physiological ecology in the NE Subarctic Pacific. *Limnology and Oceanography*, *66*(1), 76-94. https://doi.org/10.1002/lno.11589

Humily, F., Partensky, F., Six, C., Farrant, G. K., Ratin, M., Marie, D., & Garczarek, L. (2013). A gene island with two possible configurations is involved in chromatic acclimation in marine *Synechococcus*. *PLoS ONE*, *8*(12), e84459. https://doi.org/10.1371/journal.pone.0084459

Keller, M. D., Kiene, R. P., Matrai, P. A., & Bellows, W. K. (1999). Production of glycine betaine and dimethylsulfoniopropionate in marine phytoplankton. II. N-limited chemostat cultures. *Marine Biology*, *135*(2), 249-257. https://doi.org/10.1007/s002270050622

Kinsey, J. D., Kieber, D., & Neale, P. (2015). Effects of iron limitation and UV radiation on *Phaeocystis antarctica* growth and dimethylsulfoniopropionate, dimethylsulfoxide and acrylate concentrations. https://hero.epa.gov/hero/index.cfm/reference/details/reference_id/4131220

Lana, A., Bell, T., Simó, R., Vallina, S., Ballabrera-Poy, J., Kettle, A., Dachs, J., Bopp, L., Saltzman, E., Stefels, J., Johnson, J., & Liss, P. (2011). An

updated climatology of surface dimethlysulfide concentrations and emission fluxes in the global ocean. *Global Biogeochemical Cycles*, *25*(1), n/a-n/a. https://doi.org/10.1029/2010GB003850

Lana, A., Simó, R., Vallina, S. M., & Dachs, J. (2012). Potential for a biogenic influence on cloud microphysics over the ocean : A correlation study with satellite-derived data. *Atmospheric Chemistry and Physics*, *12*(17), 7977-7993. https://doi.org/10.5194/acp-12-7977-2012

Mahajan, A. S., Fadnavis, S., Thomas, M. A., Pozzoli, L., Gupta, S., Royer, S.-J., Saiz-Lopez, A., & Simó, R. (2015). Quantifying the impacts of an updated global dimethylsulfide (DMS) climatology on cloud microphysics and aerosol radiative forcing. https://www.academia.edu/51408582/Quantifying_the_impacts_of_an_updated_global_dimethylsulfide_DMS_climatology_on_cloud_microphysics_and_aerosol_radiative_forcing

Malmstrom, R. R., Kiene, R. P., Vila, M., & Kirchman, D. L. (2005). Dimethylsulfoniopropionate (DMSP) assimilation by *Synechococcus* in the Gulf of Mexico and northwest Atlantic Ocean. *Limnology and Oceanography*, *50*(6), 1924-1931. https://doi.org/10.4319/lo.2005.50.6.1924

Marie, D., Brussaard, C. P. D., Partensky, F., & Vaulot, D. (1999). Flow cytometric analysis of phytoplankton, bacteria and viruses. In J. P. Robinson (Éd.), *Current protocols in cytometry: Vol. 11.11* (p. 1-15). John Wiley & Sons.

Mazard, S., Ostrowski, M., Partensky, F., & Scanlan, D. J. (2012). Multi-locus sequence analysis, taxonomic resolution and biogeography of marine *Synechococcus* : Taxonomic resolution and biogeography of marine *Synechococcus*. *Environmental Microbiology*, *14*(2), 372-386. https://doi.org/10.1111/j.1462-2920.2011.02514.x

McCrindle, S. L., Kappler, U., & McEwan, A. G. (2005). Microbial dimethylsulfoxide and trimethylamine-N-oxide respiration. *Advances in Microbial Physiology*, *50*, 147-198. https://doi.org/10.1016/S0065-2911(05)50004-3

Nevitt, G. A. (2011). The neuroecology of dimethyl sulfide : A global-climate regulator turned marine infochemical. *Integrative and Comparative Biology*, *51*(5), 819-825. https://doi.org/10.1093/icb/icr093

Quinn, P. K., & Bates, T. S. (2011). The case against climate regulation via oceanic phytoplankton sulphur emissions. https://www.nature.com/articles/nature10580

Rippka, R., Coursin, T., Hess, W., Lichtle, C., Scanlan, D. J., Palinska, K. A., Iteman, I., Partensky, F., Houmard, J., & Herdman, M. (2000). *Prochlorococcus marinus* Chisholm et al. 1992 subsp. *Pastoris* subsp. Nov. Strain PCC 9511, the first axenic chlorophyll a_2/b_2-containing cyanobacterium (Oxyphotobacteria). *International Journal of Systematic and Evolutionary Microbiology*, *50*(5), 1833-1847. https://doi.org/10.1099/00207713-50-5-1833

Seymour, J. R., Simó, R., Ahmed, T., & Stocker, R. (2010). Chemoattraction to dimethylsulfoniopropionate throughout the marine microbial food web. *Science (New York, N.Y.)*, *329*(5989), 342-345. https://doi.org/10.1126/science.1188418

Sheehan, C., & Petrou, K. (2020). Dimethylated sulfur production in batch cultures of Southern Ocean phytoplankton. *Biogeochemistry*, *147*. https://doi.org/10.1007/s10533-019-00628-8

Spiese, C. E., Kieber, D. J., Nomura, C. T., & Kiene, R. P. (2009). Reduction of dimethylsulfoxide to dimethylsulfide by marine phytoplankton. *Limnology and Oceanography*, *54*(2), 560-570.

https://doi.org/10.4319/lo.2009.54.2.0560

Spiese, C. E., & Tatarkov, E. A. (2014). Dimethylsulfoxide reduction activity is linked to nutrient stress in Thalassiosira pseudonana NCMA 1335. *Marine Ecology Progress Series*, *507*, 31-38. https://doi.org/10.3354/meps10842

Stefels, J. (2007). Sulfur in the marine environment. https://link.springer.com/chapter/10.1007/978-1-4020-5887-5_4

Sunda, W. G., Hardison, R., Kiene, R. P., Bucciarelli, E., & Harada, H. (2007). The effect of nitrogen limitation on cellular DMSP and DMS release in marine phytoplankton : Climate feedback implications. *Aquatic Sciences*, *69*(3), 341-351. https://doi.org/10.1007/s00027-007-0887-0

Sunda, W., Kieber, D. J., Kiene, R. P., & Huntsman, S. (2002). An antioxidant function for DMSP and DMS in marine algae. *Nature*, *418*(6895), 317-320. https://doi.org/10.1038/nature00851

Vila-Costa, M., Simó, R., Harada, H., Gasol, J. M., Slezak, D., & Kiene, R. P. (2006). Dimethylsulfoniopropionate uptake by marine phytoplankton. *Science (New York, N.Y.)*, *314*(5799), 652-654. https://doi.org/10.1126/science.1131043

Weiner, J. H., Rothery, R. A., Sambasivarao, D., & Trieber, C. A. (1992). Molecular analysis of dimethylsulfoxide reductase : A complex iron-sulfur molybdoenzyme of *Escherichia coli*. *Biochimica et Biophysica Acta (BBA) - Bioenergetics*, *1102*(1), 1-18. https://doi.org/10.1016/0005-2728(92)90059-B

Yost, D., & Mitchelmore, C. (2012). Substrate Kinetics of DMSP-lyases in Various Cultured *Symbiodinium* Strains. *Bulletin of Marine Science*, *88*. https://doi.org/10.5343/bms.2011.1046

Conclusion générale & perspectives

Les océans recouvrent 70% de la surface de la planète et sont particulièrement affectés par le changement climatique. Les modèles biogéochimiques actuels prédisent que le plancton de « petite taille » devrait tirer avantage ou du moins s'adapter plus rapidement aux futures conditions océaniques (Flombaum et al., 2020; Fu et al., 2016). C'est pourquoi il existe de plus en plus d'études s'intéressant aux mécanismes d'adaptation mis en place par ces organismes en réponse aux variations des facteurs impactés par le changement climatique, tels que la disponibilité en nutriments, l'utilisation de la lumière ou encore la température. Dans ce contexte il est intéressant de se demander si les populations phytoplanctoniques seraient capables de s'adapter à court et à long termes à de tels changements. C'est pourquoi, de par leur abondance et leur diversité les picocyanobactéries marines figurent parmi les modèles d'étude les plus pertinents en écologie microbienne pour apporter des réponses aux grandes questions environnementales (Coleman & Chisholm, 2007). En effet, ils occupent une large gamme de conditions environnementales et les principaux paramètres responsables de leur distribution et les niches occupées par les différents écotypes ont récemment été affinées (Doré et al., 2022; Farrant et al., 2016; Garcia et al., 2020; Sohm et al., 2015). Dans ce contexte, mon travail de thèse a consisté à caractériser d'un point de vue physiologique et génomique des membres du clade CRD1, le taxon dominant de *Synechococcus* dans les zones limitées en Fe, en comparant des souches représentatives des différents ESTUs au sein de ce clade avec celles de clades I à IV déjà bien étudiées. En effet, ce n'est que récemment que des études ont porté sur la caractérisation du clade CRD1 et essentiellement d'un point de vue métagénomique (Ahlgren et al., 2020). Ce travail de thèse a donc permis de i) valider l'existence de thermotypes au sein de ce clade, ii) mettre en évidence des spécificités du clade CRD1 par rapport aux autres clades dominants dans le milieu marin et iii) réveler un certain nombre de processus potentiellement impliqués dans l'adaptation à la carence en Fe et à la température chez ces organismes. Ces résultats soulèvent de nouvelles hypothèses et pistes de recherche à explorer dans le futur.

Les picocyanobactéries marines : des organismes modèles mais parfois difficiles à cultiver pour étudier la réponse aux variations environnementales

A l'heure actuelle, un grand nombre de souches de cyanobactéries marines ont été isolées et sont disponibles en culture, avec notamment plus de 450 souches dans la collection de culture de Roscoff. Les cyanobactéries marines présentent également un avantage de par leur simplicité par rapport aux cyanobactéries d'eau douce qui présentent une machinerie métabolique plus complexe. Malheureusement ces organismes sont aussi plus compliqués à cultiver. En effet, l'isolement et la caractérisation physiologique de cultures monoclonales sont des processus longs mais indispensables pour identifier les mécanismes adaptatifs. Les premières tentatives d'isolement et de purification de cultures de cyanobactéries marines dateraient du début du XXe siècle (Pringsheim, 1913) tandis que pour les cyanobactéries marines, cela aurait débuté au milieu des années 1950 grâce notamment à M. M. Allen, puis à J. Waterbury et R.Y. Stanier (Rippka, 1988). Il est en effet plus difficile de cultiver certaines cyanobactéries marines, notamment du fait de la composition des milieux de culture. Durant ma thèse, j'ai utilisé un milieu utilisé en routine à Roscoff, le PCR-S11 (Rippka et al., 2000), mais qui ne permet pas d'effectuer des expériences sur des métaux traces tels que le Fe puisque l'utilisation d'eau de mer naturelle ou reconstituée à partir de Red Sea Salts, apporte différents minéraux dont la concentration est inconnue. Pour les études concernant les sels nutritifs, on utilise en général des milieux artificiels tels que le milieu AQUIL (Price et al., 1989) dont la concentration en sels, nutriments et métaux traces est précisément connue. Cependant, le Fe étant présent en abondance dans le milieu environnant et sous différentes espèces, les contaminations sont fréquentes et il est difficile d'estimer sa biodisponibilité pour les cellules (Tagliabue et al., 2017). C'est pourquoi il est nécessaire de manipuler en condition ultra-propre, en salle blanche. Au cours de ma thèse, malgré de nombreuses tentatives d'acclimatation à ce milieu, je n'ai pas réussi à obtenir de croissance reproductible des souches CRD1. Il aurait été intéressant de tester d'autres milieux de culture artificiels, tels que le PCR-Tu2 (Rippka et al., 2000) ou l'AMP1, ou encore des milieux réalisés à partir d'eau de mer ultra-oligotrophe, tels que le Pro99 (Ahlgren et al., 2020; Moore et al., 2007). En effet, Ahlgren et collaborateurs ont utilisé le milieu Pro99, préparé à base d'eau de Mer des Sargasses, modifié avec 100 µM EDTA et 1 µM de $FeCl_3$ correspondant à 39 nM de Fe' (Ahlgren et al., 2020) et ont apparemment réussi à

mesurer des taux de croissance en fonction de la carence en Fe chez deux souches de CRD1 (GEYO et UW179) et une souche du clade III, WH8102 (non-axénique), en condition +Fe uniquement. Au cours de ma thèse, les différentes tentatives de cultures de souches de *Synechococcus* en milieu AQUIL semble avoir abouti à une compétition entre les *Synechococcus* et les bactéries hétérotrophes à l'avantage de ces dernières puisque les taux de contamination pouvaient atteindre 85% en fin de suivi. De plus, j'ai observé une forte diminution de la durée de la phase exponentielle de croissance de *Synechococcus* avec un nombre de cellules maximum en phase stationnaire très inférieur à celui obtenu en milieu PCR-S11. Ainsi, la seule souche que j'ai pu cultiver de façon reproductible en milieu AQUIL (non limité en fer) est la souche axénique CC9311 (clade I), dans le cadre du projet FeDre, visant à vérifier si les cyanobactéries marines étaient capables de produire du DMS (Chapitre 3). Par contre, aucune des souches de CRD1 n'étant axéniques, je n'ai pas réussi à les acclimater à ce milieu qui m'aurait permis de réaliser des expériences en conditions de limitation en Fe. Il serait donc intéressant pour la poursuite de ces expériences de commencer par axéniser des cultures de CRD1 afin de s'abstraire de la présence des bactéries hétérotrophes. Cela permettrait notamment de mesurer l'incorporation du Fe par exemple en utilisant l'isotope ^{55}Fe radiomarqué afin d'estimer la quantité de Fe consommée par souche. Toujours en utilisant des isotopes du Fe, il aurait été intéressant de visualiser le transport du Fe au sein des cellules via la technique d'imagerie NanoSIMS (Nanoscale Secondary Ion Mass Spectrometry) qui pourrait permettre de visualiser les voies de transport du Fe au sein de la cellule comme cela a pu être réalisé chez le blé (Sheraz et al., 2021). Toujours en utilisant le NanoSIMS et en couplant cette approche à la microscopie, il serait également possible de rechercher la présence de structures cellulaires contenant du Fe, comme cela a déjà été réalisé chez *Chlamydomonas reinhardtii* (Penen et al., 2016). Chez cet organisme, ces vésicules sont localisées partout dans la cellule et s'accumulent au niveau des plaques d'amidon du pyrénoïde. Par analogie, il est possible que des structures vésiculaires semblables existent chez les cyanobactéries par exemple dans les carboxysomes, qui remplissent des fonctions similaires à celles des pyrénoïdes. J'ai pu montrer dans le chapitre II que les différents écotypes de *Synechococcus* se distinguent notamment par leur capacité à stocker le Fe, certains synthétisant des ferritines, des bactérioferritines et/ou des complexes DpsA tandis que d'autres, comme la souche WH8102, ne semblent avoir aucun

système de stockage du Fe. Cependant, il est possible que la taille des cellules soit trop petite pour permettre la détection de telles structures. Dans ce contexte, il est intéressant de noter que les cyanobactéries marines et d'eau douce sont capables de former des vésicules extracellulaires (Biller et al., 2014, 2022). Ces vésicules sont composées d'une double couche lipidique et contiennent des protéines, lipides, ADN et des métabolites. Il a été suggéré que ces structures pourraient avoir un rôle dans la communication cellulaire, la formation de biofilm, le transfert horizontal de gènes, la communication entre phage et hôte ou encore l'échange de nutriments (Biller et al., 2014; Muñoz-Marín et al., 2020). Ce dernier point serait à creuser dans le contexte de l'adaptation à la limitation en Fe.

Microdiversité

Il a été montré que le SC 5.1 représente la lignée de *Synechococcus* la plus abondante dans le milieu pélagique (Farrant et al. 2016 ; Sohm et al. 2016) et la plus diversifiée du point de vue taxonomique avec une vingtaine de clades (Ahlgren & Rocap, 2012; Dufresne et al., 2008; Scanlan et al., 2009). En effet, plusieurs facteurs indépendants ont permis sa diversification, et notamment le gradient latitudinal de température (Pittera et al., 2014). D'une manière générale, la plupart des clades de *Synechococcus* marins sont retrouvés dans les eaux chaudes, tropicales et intertropicales, méso- à oligotrophes, et notamment les deux clades majeurs II et III (Mella-Flores et al., 2011; Zwirglmaier et al., 2008), tandis que les clades I et IV ont développé des adaptations spécifiques leur permettant de coloniser les zones côtières tempérées-froides à subpolaires, riches en nutriments. Plusieurs études de physiologie comparative ont permis de mettre en évidence certains processus adaptatifs permettant aux différents clades d'être compétitifs au sein de leurs niches thermiques respectives, et de définir des thermotypes en étudiant les *preferenda* et limites de croissance des souches vis-à-vis de la température (niche thermale fondamentale ; Breton et al., 2019; Doré et al., 2022; Pittera et al., 2014). Au cours de ma thèse, j'ai utilisé une approche similaire pour montrer qu'il existait également des thermotypes distincts au sein du clade CRD1. En effet, la souche MITS9220 de l'ESTU CRD1A correspond à un thermotype chaud, la souche BIOS-U3-1 de l'ESTU CRD1B, un thermotype tempéré-froid et enfin BIOS-E4-1 de l'ESTU CRD1C correspond à un thermotype sténotherme tempéré-chaud. J'ai également mis en évidence que les niches

fondamentales de ces souches sont cohérentes avec les niches environnementales réalisées de l'ESTU correspondant, déterminées grâce à un très large jeu de données de metabarcoding et métagénomiques. Cependant, il semble que l'adaptation au froid de la souche BIOS-U3-1 soit relativement récente puisqu'elle ne présente pas les caractéristiques génomiques identifiées chez les thermotypes froids typiques (clades I et IV). En revanche, nous avons mis en évidence des spécificités des CRD1 par rapport aux clades témoins tels qu'un taux de croissance et un rendement quantique du PSII faible mais des taux de réparation de la protéine D1 du PSII plus grande, ce qui suggère que l'adaptation à la carence en Fe des membres de ce clade, et du clade EnvB, est probablement plus ancienne que l'adaptation au froid. Les expériences de carence en Fe grâce à l'utilisation d'un chélateur du Fe ont également permis de mettre en évidence un gradient de sensibilité à la carence en Fe. J'ai utilisé deux représentants de l'ESTU IIA ayant des comportements relativement similaires vis-à-vis de la température mais bien distincts vis-à-vis du Fe. En effet la souche A15-62 s'est avéré être un « super écotype » -Fe tandis que la souche M16.1 a réagi tel qu'attendu, c'est-à-dire très sensible à la carence en Fe. Au cours de ce travail de thèse, j'ai mis en évidence des spécificités des CRD1 par rapport aux autres clades mais pas de réelles différences entre les souches de CRD1 vis-à-vis du Fe. Tandis que vis-vis de la température, on a pu déterminer des limites thermiques distinctes. Ainsi il est fort probable qu'il existe au sein des CRD1 une microdiversité plus grande que celle estimée lors de leur définition par Farrant et al (2016) et que de futures analyses permettent de subdiviser encore certains ESTUs en écotypes distincts. De plus, pour l'heure il n'existe qu'un seul représentant de chaque ESTU CRD1 en culture. De nouvelles analyses incluant plus de souches pourraient permettre de préciser ces différences. C'est pourquoi il est important de maintenir un effort sur l'isolement de cultures lors de campagnes océanographiques. Cela a d'ailleurs été l'un des objectifs de la campagne TONGA, à laquelle j'ai participé fin 2019 et qui a eu lieu dans le Sud-Ouest Pacifique, une zone pauvre en Fe caractérisée par l'apport de nutriments issus du volcanisme sous-marin (arc volcanique Tonga – Kermadec) et pour laquelle des cultures de *Synechococcus* sont actuellement en cours de caractérisation. La caractérisation physiologique des souches isolées devrait permettre de préciser les niches fondamentales de ces souches. Par ailleurs, le séquençage de gènes marqueurs des cultures isolées et des populations naturelles par metabarcoding ainsi que l'assemblage de génomes (MAGs) à

partir de reads environnementaux permettront de mieux appréhender la diversité génétique et fonctionnelle des populations de *Synechococcus* le long du transect de la campagne Tonga.

Biogéographie

A partir des données de métagénomique de *Tara* Oceans, Farrant et collaborateurs ont pu observer l'abondance relative des ESTUs le long du transect, et mettre en évidence une co-dominance des clades CRD1 et EnvB dans les eaux HNLC (Farrant et al., 2016). En regardant de plus près les assemblages de communautés de *Synechococcus* et *Prochlorococcus* au niveau des Îles Marquises (stations TARA_122, TARA_123, TARA_124 et TARA_125), ces chercheurs ont observé une modification des populations en fonction de la disponibilité en nutriments. En effet, cette zone est caractérisée par un « effet d'île », c'est-à-dire une fertilisation locale des eaux environnantes, entraînant des blooms de phytoplancton (Caputi et al., 2019). Ainsi, à la station 122 située en amont des Îles Marquises et typique des eaux HLNC, on a une dominance du clade CRD1 puis à la station 123 dans des eaux riches en Fe, proches des Marquises, on a un shift complet de population avec une majorité de clade II (Caputi et al., 2019). Les deux autres stations se caractérisent par un effet décroissant de l'effet d'île (Farrant et al., 2016). A l'échelle du clade, Ahlgren et al. avaient également observé la coexistence du clade II et CRD1 cette fois-ci au niveau du Dôme du Costa Rica, une zone géographique co-limitée en Fe et Mn (Ahlgren et al., 2014). Les picocyanobactéries réagissent donc rapidement aux forçages physico-chimiques grâce à leur temps de génération court (~1 jour), et pourraient donc servir de biosenseurs des changements rapides de l'écosystème, notamment ceux dus au changement climatique en cours. En 1961, Hutchinson a émis une hypothèse selon laquelle des espèces, ou dans notre cas des ESTUs, peuvent coexister dans une même niche grâce à l'hétérogénéité de cette niche dans le temps (c'est-à-dire qu'en fonction de la saison, ce ne sont pas les mêmes individus qui dominent) et dans l'espace (on peut avoir coexistence de différentes niches au même endroit, par exemple du fait d'une co-limitation en nutriments). On peut également attribuer ces différences à un transport passif des individus en dehors de leur niche respective. Ainsi, il est possible de détecter une population, mais cela ne présage pas de sa capacité à se maintenir au cours de temps. La plupart des données utilisées lors de ma thèse pour estimer la diversité génétique

concernaient des campagnes pour lesquelles un seul prélèvement a été effectué en un lieu et à un temps donné. Dans ce contexte, il pourrait être intéressant d'observer la variabilité temporelle en un site d'échantillonnage de la diversité de ces organismes, notamment en utilisant les séries temporelles disponibles, tels que fait cela a été fait par Caracciolo et collaborateurs (Caracciolo et al., 2022). Enfin, les expérimentations au laboratoire font abstraction des interactions biotiques, telles que la prédation ou encore la régulation des populations de cyanobactéries par des cyanophages qui participent au maintien de la diversité (Huang et al., 2012). Pour mieux comprendre les interactions au sein d'une niche précise, il serait intéressant de mener des expériences de co-cultures, p.ex. afin d'étudier la compétition entre écotypes -Fe et +Fe.

La modélisation est également un bon outil pour prédire l'évolution des communautés planctoniques. Il existe des modèles de prédiction prenant en compte les différentes valeurs cardinales de croissance des cultures (T_{min}, T_{max}, T_{opt}, μ, etc.) et les estimations de températures de surface de la période actuelle jusqu'à la fin du siècle. Dans ce contexte, il pourrait être intéressant de voir si les clades CRD1 seraient capables de persister malgré une hausse de la température. Celle-ci entraîne la dénaturation des métabolites clés tels que la Rubisco (Salvucci & Crafts-Brandner, 2004), la thermolabilité du PSII ou encore la fluidité des membranes (Breton et al., 2019; Pittera et al., 2016). L'adaptation des *Synechococcus* va se traduire par une modification de la gamme de tolérance thermique et de la température optimale de croissance. Une adaptation des cellules à des changements de température est possible si celle-ci se produit progressivement. En effet, la forme assymétrique des courbes de croissance laisse présager qu'une adaptation à une baisse des températures serait évolutivement plus aisée qu'à une hausse des températures. En plus des modèles théoriques, il serait intéressant de suivre la dynamique d'adaptation des communautés de *Synechococcus* à petite échelle de temps et dans des environnements où l'on s'attend à ce que la température fluctue rapidement.

Avènement de la métaomique pour comprendre les mécanismes d'adaptation

Au début de ma thèse, le set de génomes de picocyanobactéries disponible dans la base de données Cyanorak n'était que de 97 génomes, dont seulement trois représentants du clade CRD1 et aucun des clades environnementaux EnvA ou EnvB. Par

la suite, nous avons rajouté 156 génomes supplémentaires (tous les WGS et les meilleurs SAGs et MAGs disponibles au NCBI), comprenant notamment une dizaine de CRD1 mais aussi quelques génomes d'EnvB et EnvA. Ceci a permis à notre équipe de recruter les reads de picocyanobactéries du jeu de données de métagénomique de *Tara* Oceans (Doré et al., submitted). Ce travail a permis d'identifier un set de gènes impliqués dans le métabolisme du Fe, mais également mettre en évidence des spécificités des CRD1 et EnvB codominant dans les environnements pauvres en Fe, complétant ainsi quelques études récentes (Ahlgren et al., 2020; Doré et al., 2022; Garcia et al., 2020; Hogle et al., 2022). Bien que l'on ait pu identifier un certain nombre de gènes ou clusters de gènes spécifiques de la carence en Fe, la fonction de la plupart d'entre eux reste à préciser. Nous avons notamment pu mettre en évidence que la stratégie des CRD1 reposait principalement sur le fait de limiter la consommation d'énergie dans les environnements pauvres en Fe. Par exemple, les CRD1 ne synthétisent pas de capsules polysaccharidiques extracellulaires jouant un rôle protecteur contre les stress biotiques et abiotiques (Buffet et al., 2021). Leur absence chez les CRD1 est étonnante puisque ces capsules apporteraient un avantage clair en termes de fitness en conditions de limitation en nutriments chez *Klebsiella*, en augmentant à la fois les taux de croissance et les concentrations maximales au plateau. En s'intéressant aux substitutions d'acides aminés des sous-unités α (RpcA) et β (RpcB) de la phycocyanine qui diffèrent entre les clades froids/chauds typiques et influencent la thermotolérance des phycobiliprotéines (cf. Chapitre I), on a vu que les trois CRD1 présentaient des substitutions d'acides aminés des clades chauds. Or l'ESTU CRD1B correspond à un thermotype froid. A l'inverse, si l'on regarde les désaturases des acides gras, on voit que les CRD1 présentent des désaturases spécifiques des écotypes froids. D'une manière générale, les CRD1 présentent un set de gènes de désaturases différent de tous les autres clades, il semble donc que ce clade a une forte capacité à réguler la fluidité de sa membrane par rapport aux thermotypes froids/chauds typiques. De plus, l'opéron *ocp* impliqué dans la protection du PSII contre la photoinactivation est absent des CRD1. Ce résultat vient appuyer l'hypothèse formulée par Six et al (2021) selon laquelle la présence de l'opéron *ocp* serait d'avantage lié à une adaptation au froid qu'à une carence en nutriments.

Durant ma thèse, j'ai généré des transcriptomes de différentes souches de CRD1 et de souches contrôles en simulant une carence en fer par l'ajout d'un chélateur. Le

séquençage de ces transcriptomes est toujours en cours au moment de la rédaction de ce manuscrit mais les résultats devraient nous aider à mettre en évidence des gènes sous-exprimés ou surexprimés en réponse au stress et aider à l'interprétation des données de génomique comparative et de métagénomique. Pour une approche holistique de la réponse au stress -Fe, il serait intéressant de compléter l'approche transcriptomique par une approche protéomique. Par exemple, on a pu voir qu'une des stratégies mise en place par les CRD1 était la synthèse de protéines alternatives pauvres en Fe. En effet, les protéines composées de clusters [2Fe-2S] et [4Fe-4S] telles que les ferredoxines sont en partie remplacées par des flavodoxines. Par ailleurs, la complémentation de ces données par des approches de mutagénèse et de biochimie, permettrait la caractérisation fonctionnelle de certains gènes d'intérêt, parmi lesquels certains pourraient jouer un rôle majeur dans la survie de ces organismes à la carence en Fe.

References

Adir, N. (2005). Elucidation of the molecular structures of components of the phycobilisome : Reconstructing a giant. *Photosynthesis Research*, *85*(1), Art. 1. https://doi.org/10.1007/s11120-004-2143-y

Agranoff, D., Collins, L., Kehres, D., Harrison, T., Maguire, M., & Krishna, S. (2005). The Nramp orthologue of *Cryptococcus neoformans* is a pH-dependent transporter of manganese, iron, cobalt and nickel. *Biochemical Journal*, *385*(Pt 1), 225-232. https://doi.org/10.1042/BJ20040836

Ahlgren, N. A., Belisle, B. S., & Lee, M. D. (2020). Genomic mosaicism underlies the adaptation of marine *Synechococcus* ecotypes to distinct oceanic iron niches. *Environmental Microbiology*, *22*(5), Art. 5. https://doi.org/10.1111/1462-2920.14893

Ahlgren, N. A., & Rocap, G. (2006). Culture isolation and culture-independent clone libraries reveal new marine *Synechococcus* ecotypes with distinctive light and N physiologies. *Applied and Environmental Microbiology*. https://doi.org/10.1128/AEM.00358-06

Ahlgren, N. A., & Rocap, G. (2012). Diversity and distribution of marine *Synechococcus* : Multiple gene phylogenies for consensus classification and development of qPCR assays for sensitive measurement of clades in the ocean. *Frontiers in Microbiology*, *3*, 213-213. https://doi.org/10.3389/fmicb.2012.00213

Allahverdiyeva, Y., Ermakova, M., Eisenhut, M., Zhang, P., Richaud, P., Hagemann, M., Cournac, L., & Aro, E. M. (2011). Interplay between flavodiiron proteins and photorespiration in *Synechocystis* sp. PCC 6803. *Journal of Biological Chemistry*, *286*(27), Art. 27. https://doi.org/10.1074/jbc.M111.223289

Allahverdiyeva, Y., Mustila, H., Ermakova, M., Bersanini, L., Richaud, P., Ajlani, G., Battchikova, N., Cournac, L., & Aro, E.-M. (2013). Flavodiiron proteins Flv1 and Flv3 enable cyanobacterial growth and photosynthesis under fluctuating light. *Proceedings of the National Academy*

of Sciences of the United States of America, *110*(10), Art. 10. https://doi.org/10.1073/pnas.1221194110

Andrews, S. C., Robinson, A. K., & Rodríguez-Quiñones, F. (2003). Bacterial iron homeostasis. *FEMS Microbiology Reviews*, *27*(2-3), 215-237. https://doi.org/10.1016/S0168-6445(03)00055-X

Asada, K. (1994). *Causes of Photooxidative Stress and Amelioration of Defense Systems in Plants*. CRC Press.

Ashby, M. K., & Mullineaux, C. W. (1999). The role of ApcD and ApcF in energy transfer from phycobilisomes to PS I and PS II in a cyanobacterium. *Photosynthesis Research*, *61*(2), 169-179. https://doi.org/10.1023/A:1006217201666

Azam, F., Fenchel, T., Field, J., Gray, J., Meyer-Reil, L., & Thingstad, F. (1983). The Ecological Role of Water-Column Microbes in the Sea. *Marine Ecology Progress Series*, *10*, 257-263. https://doi.org/10.3354/meps010257

Badarau, A., Firbank, S. J., Waldron, K. J., Yanagisawa, S., Robinson, N. J., Banfield, M. J., & Dennison, C. (2008). FutA2 Is a Ferric Binding Protein from *Synechocystis* PCC 6803. *Journal of Biological Chemistry*, *283*(18), 12520-12527. https://doi.org/10.1074/jbc.M709907200

Bailey, S., Melis, A., Mackey, K. R., Cardol, P., Finazzi, G., van Dijken, G., Berg, G. M., Arrigo, K., Shrager, J., & Grossman, A. (2008). Alternative photosynthetic electron flow to oxygen in marine *Synechococcus*. *Biochimica et Biophysica Acta*, *1777*(3), Art. 3.

Barber, J., Nield, J., Duncan, J., & Bibby, T. S. (2006). Accessory Chlorophyll Proteins in Cyanobacterial Photosystem I. In J. H. Golbeck (Éd.), *Photosystem I: The Light-Driven Plastocyanin:Ferredoxin Oxidoreductase* (p. 99-117). Springer Netherlands. https://doi.org/10.1007/978-1-4020-4256-0_9

Barnett, J. P., Millard, A., Ksibe, A. Z., Scanlan, D. J., Schmid, R., & Blindauer, C. A. (2012). Mining Genomes of Marine Cyanobacteria for Elements of Zinc Homeostasis. *Frontiers in Microbiology*, *3*. https://doi.org/10.3389/fmicb.2012.00142

Basu, S., Gledhill, M., Beer, D. de, Matondkar, S. G. P., & Shaked, Y. (2019). Colonies of marine cyanobacteria *Trichodesmium* interact with associated bacteria to acquire iron from dust. *Communications Biology*, *2*(1), Art. 1. https://doi.org/10.1038/s42003-019-0534-z

Behrenfeld, M. J., Bale, A. J., Kolber, Z. S., Aiken, J., & Falkowski, P. G. (1996). Confirmation of iron limitation of phytoplankton photosynthesis in the equatorial Pacific Ocean. *Nature*, *383*(6600), Art. 6600. https://doi.org/10.1038/383508a0

Behrenfeld, M. J., & Kolber, Z. S. (1999). Widespread iron limitation of phytoplankton in the south pacific ocean. *Science*. https://doi.org/10.1126/science.283.5403.840

Behrenfeld, M. J., & Milligan, A. J. (2013). Photophysiological Expressions of Iron Stress in Phytoplankton. *Annual Review of Marine Science*, *5*(1), Art. 1. https://doi.org/10.1146/annurev-marine-121211-172356

Behrenfeld, M. J., Westberry, T. K., Boss, E. S., O'Malley, R. T., Siegel, D. A., Wiggert, J. D., Franz, B. A., McClain, C. R., Feldman, G. C., Doney, S. C., Moore, J. K., Dall'Olmo, G., Milligan, A. J., Lima, I., & Mahowald, N. (2009). Satellite-detected fluorescence reveals global physiology of ocean phytoplankton. *Biogeosciences*. https://doi.org/10.5194/bg-6-779-2009

Bersanini, L., Battchikova, N., Jokel, M., Rehman, A., Vass, I., Allahverdiyeva, Y., & Aro, E. M. (2014). Flavodiiron protein Flv2/Flv4-related photoprotective mechanism dissipates excitation pressure of PSII in cooperation with phycobilisomes in cyanobacteria. *Plant Physiology*. https://doi.org/10.1104/pp.113.231969

Berube, P. M., Biller, S. J., Kent, A. G., Berta-Thompson, J. W., Roggensack, S. E., Roache-Johnson, K. H., Ackerman, M., Moore, L. R., Meisel, J. D., Sher, D., Thompson, L. R., Campbell, L.,

Martiny, A. C., & Chisholm, S. W. (2015). Physiology and evolution of nitrate acquisition in *Prochlorococcus*. *ISME Journal*. https://doi.org/10.1038/ismej.2014.211

Berube, P. M., Rasmussen, A., Braakman, R., Stepanauskas, R., & Chisholm, S. W. (2019). Emergence of trait variability through the lens of nitrogen assimilation in *Prochlorococcus*. *eLife*, *8*, e41043-e41043. https://doi.org/10.7554/eLife.41043

Biller, S. J., Berube, P. M., Lindell, D., & Chisholm, S. W. (2015). *Prochlorococcus* : The structure and function of collective diversity. *Nature Reviews Microbiology*. https://doi.org/10.1038/nrmicro3378

Biller, S. J., Coe, A., Arellano, A. A., Dooley, K., Gong, J. S., Yeager, E. A., Becker, J. W., & Chisholm, S. W. (2022). *Environmental and taxonomic drivers of bacterial extracellular vesicle production in marine ecosystems* (p. 2022.01.18.476865). bioRxiv. https://doi.org/10.1101/2022.01.18.476865

Biller, S. J., Schubotz, F., Roggensack, S. E., Thompson, A. W., Summons, R. E., & Chisholm, S. W. (2014). Bacterial vesicles in marine ecosystems. *Science*, *343*(6167), Art. 6167. https://doi.org/10.1126/science.1243457

Blain, S., Bonnet, S., & Guieu, C. (2008). Dissolved iron distribution in the tropical and sub tropical South Eastern Pacific. *Biogeosciences*, *5*(1), 269-280. https://doi.org/10.5194/bg-5-269-2008

Blain, S., Guieu, C., Claustre, H., Leblanc, K., Moutin, T., Quèguiner, B., Ras, J., & Sarthou, G. (2004). Availability of iron and major nutrients for phytoplankton in the northeast Atlantic Ocean. *Limnology and Oceanography*, *49*(6), 2095-2104. https://doi.org/10.4319/lo.2004.49.6.2095

Blot, N., Mella-Flores, D., Six, C., Le Corguillé, G., Boutte, C., Peyrat, A., Monnier, A., Ratin, M., Gourvil, P., Campbell, D. A., & Garczarek, L. (2011). Light history influences the response of the marine cyanobacterium *Synechococcus* sp. WH7803 to oxidative stress. *Plant Physiology*, *156*(4), Art. 4. https://doi.org/10.1104/pp.111.174714

Boekema, E. J., Hifney, A., Yakushevska, A. E., Piotrowski, M., Keegstra, W., Berry, S., Michel, K. P., Pistorius, E. K., & Kruip, J. (2001). A giant chlorophyll-protein complex induced by iron deficiency in cyanobacteria. *Nature*, *412*(6848), 745-748. https://doi.org/10.1038/35089104

Bonnet, S., & Guieu, C. (2004). Dissolution of atmospheric iron in seawater. *Geophysical Research Letters*, *31*(3). https://doi.org/10.1029/2003GL018423

Botebol, H., Lelandais, G., Six, C., Lesuisse, E., Meng, A., Bittner, L., Lecrom, S., Sutak, R., Lozano, J.-C., Schatt, P., Vergé, V., Blain, S., & Bouget, F.-Y. (2017). Acclimation of a low iron adapted *Ostreococcus* strain to iron limitation through cell biomass lowering. *Scientific Reports*, *7*(1), Art. 1. https://doi.org/10.1038/s41598-017-00216-6

Boulay, C., Wilson, A., D'Haene, S., & Kirilovsky, D. (2010). Identification of a protein required for recovery of full antenna capacity in OCP-related photoprotective mechanism in cyanobacteria. *Proceedings of the National Academy of Sciences*, *107*(25), Art. 25. https://doi.org/10.1073/pnas.1002912107

Bouman, H. A., Ulloa, O., Scanlan, D. J., Zwirglmaier, K., Li, W. K. W., Platt, T., Stuart, V., Barlow, R., Leth, O., Clementson, L., Lutz, V., Fukasawa, M., Watanabe, S., & Sathyendranath, S. (2006). Oceanographic basis of the global surface distribution of *Prochlorococcus* ecotypes. *Science*. https://doi.org/10.1126/science.1122692

Boyd, P. W., Jickells, T., Law, C. S., Blain, S., Boyle, E. A., Buesseler, K. O., Coale, K. H., Cullen, J. J., de Baar, H. J. W., Follows, M., Harvey, M., Lancelot, C., Levasseur, M., Owens, N. P. J., Pollard, R., Rivkin, R. B., Sarmiento, J., Schoemann, V., Smetacek, V., … Watson, A. J. (2007). Mesoscale Iron Enrichment Experiments 1993-2005 : Synthesis and Future Directions. *Science*, *315*(5812), 612-617. https://doi.org/10.1126/science.1131669

Boyd, P. W., Law, C. S., Hutchins, D. A., Abraham, E. R., Croot, P. L., Ellwood, M., Frew, R. D., Hadfield, M., Hall, J., Handy, S., Hare, C., Higgins, J., Hill, P., Hunter, K. A., LeBlanc, K., Maldonado, M. T., McKay, R. M., Mioni, C., Oliver, M., … Wilhelm, S. W. (2005). FeCycle :

Attempting an iron biogeochemical budget from a mesoscale SF6 tracer experiment in unperturbed low iron waters. *Global Biogeochemical Cycles*, *19*(4). https://doi.org/10.1029/2005GB002494

Bradley, J. M., Svistunenko, D. A., Pullin, J., Hill, N., Stuart, R. K., Palenik, B., Wilson, M. T., Hemmings, A. M., Moore, G. R., & Le Brun, N. E. (2019). Reaction of O_2 with a diiron protein generates a mixed-valent Fe^{2+}/Fe^{3+} center and peroxide. *Proceedings of the National Academy of Sciences*, *116*(6), 2058-2067. https://doi.org/10.1073/pnas.1809913116

Bressac, M., Wagener, T., Leblond, N., Tovar-Sánchez, A., Ridame, C., Taillandier, V., Albani, S., Guasco, S., Dufour, A., Jacquet, S. H. M., Dulac, F., Desboeufs, K., & Guieu, C. (2021). Subsurface iron accumulation and rapid aluminum removal in the Mediterranean following African dust deposition. *Biogeosciences*, *18*(24), 6435-6453. https://doi.org/10.5194/bg-18-6435-2021

Breton, S., Jouhet, J., Guyet, U., Gros, V., Pittera, J., Demory, D., Partensky, F., Doré, H., Ratin, M., Maréchal, E., Nguyen, N. A., Garczarek, L., & Six, C. (2019). Unveiling membrane thermoregulation strategies in marine picocyanobacteria. *New Phytologist*, *225*(6), Art. 6. https://doi.org/10.1111/nph.16239

Broecker, W. S., & Henderson, G. M. (1998). The sequence of events surrounding Termination II and their implications for the cause of glacial-interglacial CO2 changes. *Paleoceanography*, *13*(4), 352-364. https://doi.org/10.1029/98PA00920

Bucciarelli, E., Ridame, C., Sunda, W. G., Dimier-Hugueney, C., Cheize, M., & Belviso, S. (2013). Increased intracellular concentrations of DMSP and DMSO in iron-limited oceanic phytoplankton *Thalassiosira oceanica* and *Trichodesmium erythraeum*. *Limnology and Oceanography*, *58*(5), 1667-1679. https://doi.org/10.4319/lo.2013.58.5.1667

Buffet, A., Rocha, E. P. C., & Rendueles, O. (2021). Nutrient conditions are primary drivers of bacterial capsule maintenance in *Klebsiella*. *Proceedings of the Royal Society B: Biological Sciences*, *288*(1946), Art. 1946. https://doi.org/10.1098/rspb.2020.2876

Cabello-Yeves, P. J., Picazo, A., Camacho, A., Callieri, C., Rosselli, R., Roda-Garcia, J. J., Coutinho, F. H., & Rodriguez-Valera, F. (2018). Ecological and genomic features of two widespread freshwater picocyanobacteria : Genomes of widespread freshwater picocyanobacteria. *Environmental Microbiology*, *20*(10), Art. 10. https://doi.org/10.1111/1462-2920.14377

Cabello-Yeves, P. J., Zemskaya, T. I., Rosselli, R., Coutinho, F. H., Zakharenko, A. S., Blinov, V. V., & Rodriguez-Valera, F. (2018). Genomes of novel microbial lineages assembled from the sub-ice waters of Lake Baikal. *Applied and Environmental Microbiology*, *84*(1), Art. 1.

Cai, H., Wang, K., Huang, S., Jiao, N., & Chen, F. (2010). Distinct patterns of picocyanobacterial communities in winter and summer in the Chesapeake Bay. *Applied and Environmental Microbiology*, *76*(9), Art. 9. https://doi.org/10.1128/AEM.02868-09

Canfield, D. E. (1998). A new model for Proterozoic ocean chemistry. *Nature*, *396*(6710), Art. 6710. https://doi.org/10.1038/24839

Caputi, L., Carradec, Q., Eveillard, D., Kirilovsky, A., Pelletier, E., Pierella Karlusich, J. J., Rocha Jimenez Vieira, F., Villar, E., Chaffron, S., Malviya, S., Scalco, E., Acinas, S. G., Alberti, A., Aury, J. M., Benoiston, A. S., Bertrand, A., Biard, T., Bittner, L., Boccara, M., … Iudicone, D. (2019). Community-level responses to iron availability in open ocean plankton ecosystems. *Global Biogeochemical Cycles*, *33*(3), Art. 3. https://doi.org/10.1029/2018GB006022

Caracciolo, M., Rigaut-Jalabert, F., Romac, S., Mahé, F., Forsans, S., Gac, J.-P., Arsenieff, L., Manno, M., Chaffron, S., Cariou, T., Hoebeke, M., Bozec, Y., Goberville, E., Le Gall, F., Guilloux, L., Baudoux, A.-C., de Vargas, C., Not, F., Thiébaut, E., … Simon, N. (2022). Seasonal dynamics of marine protist communities in tidally mixed coastal waters. *Molecular Ecology*, *n/a*(n/a). https://doi.org/10.1111/mec.16539

Cellier, M., Privé, G., Belouchi, A., Kwan, T., Rodrigues, V., Chia, W., & Gros, P. (1995). Nramp defines a family of membrane proteins. *Proceedings of the National Academy of Sciences*

of the United States of America, *92*(22), 10089-10093. https://doi.org/10.1073/pnas.92.22.10089

Chadd, H. E., Newman, J., Mann, N. H., & Carr, N. G. (1996). Identification of iron superoxide dismutase and a copper/zinc superoxide dismutase enzyme activity within the marine cyanobacterium *Synechococcus* sp. WH 7803. *FEMS Microbiology Letters*, *138*(2-3), 161-165. https://doi.org/10.1111/j.1574-6968.1996.tb08150.x

Chandler, J. W., Lin, Y., Gainer, P. J., Post, A. F., Johnson, Z. I., & Zinser, E. R. (2016). Variable but persistent coexistence of *Prochlorococcus* ecotypes along temperature gradients in the ocean's surface mixed layer. *Environmental microbiology reports*, *8*(2), Art. 2. https://doi.org/10.1111/1758-2229.12378

Chappell, P. D., & Webb, E. A. (2010). A molecular assessment of the iron stress response in the two phylogenetic clades of *Trichodesmium*. *Environmental Microbiology*, *12*(1), 13-27. https://doi.org/10.1111/j.1462-2920.2009.02026.x

Chen, F., Wang, K., Kan, J., Bachoon, D. S., Lu, J., Lau, S., & Campbell, L. (2004). Phylogenetic diversity of *Synechococcus* in the Chesapeake Bay revealed by Ribulose-1,5-bisphosphate carboxylase-oxygenase (RuBisCO) large subunit gene (*rbcL*) sequences. *Aquatic Microbial Ecology*, *36*(2), Art. 2. https://doi.org/10.3354/ame036153

Chen, F., Wang, K., Kan, J., Suzuki, M. T., & Wommack, K. E. (2006). Diverse and Unique Picocyanobacteria in Chesapeake Bay, Revealed by 16S-23S rRNA Internal Transcribed Spacer Sequences. *Applied and Environmental Microbiology*, *72*(3), Art. 3. https://doi.org/10.1128/AEM.72.3.2239-2243.2006

Chen, J.-H., Tang, M., Jin, X.-Q., Li, H., Chen, L.-S., Wang, Q.-L., Sun, A.-Z., Yi, Y., & Guo, F.-Q. (2022). Regulation of Calvin–Benson cycle enzymes under high temperature stress. *ABIOTECH*, *3*(1), 65-77. https://doi.org/10.1007/s42994-022-00068-3

Chisholm, S. W., Frankel, S. L., Goericke, R., Olson, R. J., Palenik, B., Waterbury, J. B., West-Johnsrud, L., & Zettler, E. R. (1992). *Prochlorococcus marinus* nov. Gen. Nov. Sp. : An

oxyphototrophic marine prokaryote containing divinyl chlorophyll *a* and *b*. *Archives of Microbiology*, *157*(3), Art. 3. https://doi.org/10.1007/BF00245165

Chisholm, S. W., Olson, R. J., & Yentsch, C. M. (1988). Flow cytometry in oceanography : Status and prospects. *Eos, Transactions American Geophysical Union*. https://doi.org/10.1029/88EO00156

Choi, D. H., Noh, J. H., & Shim, J. (2013). Seasonal changes in picocyanobacterial diversity as revealed by pyrosequencing in temperate waters of the East China Sea and the East Sea. *Aquatic Microbial Ecology*, *71*(1), Art. 1. https://doi.org/10.3354/ame01669

Coale, K. H., Johnson, K. S., Chavez, F. P., Buesseler, K. O., Barber, R. T., Brzezinski, M. A., Cochlan, W. P., Millero, F. J., Falkowski, P. G., Bauer, J. E., Wanninkhof, R. H., Kudela, R. M., Altabet, M. A., Hales, B. E., Takahashi, T., Landry, M. R., Bidigare, R. R., Wang, X., Chase, Z., … Johnson, Z. I. (2004). Southern Ocean Iron Enrichment Experiment : Carbon Cycling in High- and Low-Si Waters. *Science*, *304*(5669), 408-414. https://doi.org/10.1126/science.1089778

Coleman, M. L., & Chisholm, S. W. (2007). Code and context : *Prochlorococcus* as a model for cross-scale biology. *Trends in Microbiology*, *15*(9), Art. 9. https://doi.org/10.1016/j.tim.2007.07.001

Coleman, M. L., Sullivan, M. B., Martiny, A. C., Steglich, C., Barry, K., Delong, E. F., & Chisholm, S. W. (2006). Genomic islands and the ecology and evolution of *Prochlorococcus*. *Science*, *311*(5768), Art. 5768.

Cossins, A., Friedlander, M., & Prosser, C. (1977). Correlations between behavioral temperature adaptations of goldfish and viscosity and fatty-acid composition of their synaptic-membranes. *Journal of Comparative Physiology*, *120*, 109-121. https://doi.org/10.1007/BF00619309

Croot, P. L., Baars, O., & Streu, P. (2011). The distribution of dissolved zinc in the Atlantic sector of the Southern Ocean. *Deep Sea Research Part II: Topical Studies in Oceanography*, *58*(25), 2707-2719. https://doi.org/10.1016/j.dsr2.2010.10.041

Dai, S., Johansson, K., Miginiac-Maslow, M., Schürmann, P., & Eklund, H. (2004). Structural Basis of Redox Signaling in Photosynthesis : Structure and Function of Ferredoxin:thioredoxin Reductase and Target Enzymes. *Photosynthesis Research*, *79*(3), 233-248. https://doi.org/10.1023/B:PRES.0000017194.34167.6d

Dailey, H. A., Dailey, T. A., Gerdes, S., Jahn, D., Jahn, M., O'Brian, M. R., & Warren, M. J. (2012). *Prokaryotic Heme Biosynthesis : Multiple Pathways to a Common Essential Product*. https://doi.org/10.1128/MMBR.00048-16

Delmont, T. O., & Eren, A. M. (2018). Linking pangenomes and metagenomes : The *Prochlorococcus* metapangenome. *PeerJ*, *6*, e4320. https://doi.org/10.7717/peerj.4320

Dill, K. A., Ghosh, K., & Schmit, J. D. (2011). Physical limits of cells and proteomes. *Proceedings of the National Academy of Sciences of the United States of America*. https://doi.org/10.1073/pnas.1114477108

Doré, H., Farrant, G. K., Guyet, U., Haguait, J., Humily, F., Ratin, M., Pitt, F. D., Ostrowski, M., Six, C., Brillet-Guéguen, L., Hoebeke, M., Bisch, A., Le Corguillé, G., Corre, E., Labadie, K., Aury, J.-M., Wincker, P., Choi, D. H., Noh, J. H., … Garczarek, L. (2020). Evolutionary mechanisms of long-term genome diversification associated with niche partitioning in marine picocyanobacteria. *Frontiers in Microbiology*, *11*, 567431. https://doi.org/10.3389/fmicb.2020.567431

Doré, H., Guyet, U., Leconte, J., Farrant, G. K., Ratin, M., Pitt, F. D., Ostrowski, M., Ferrieux, M., Six, C., Brillet-Guéguen, L., Hoebeke, M., Siltanen, J., Le Corquillé, G., Corre, E., Labadie, K., Aury, J.-M., Wincker, P., Eveillard, D., Scanlan, D. J., … Garczarek, L. (submitted). Differential global distribution of marine picocyanobacteria gene clusters reveals distinct niche-related adaptive strategies. *PNAS*.

Doré, H., Leconte, Jade, Breton, Solène, Guyet, Ulysse, Demory, David, Hoebeke, Mark, Corre, Erwan, Ratin, Morgane, Pitt, Francès D., Ostrowski, Martin, Scanlan, David J., Partensky, Frédéric, Six, Christophe, & Garczarek, Laurence. (2022). Global phylogeography of marine *Synechococcus* in coastal areas unveils strikingly different communities than in open ocean. *BioRxiv*.

Duce, R. A., & Tindale, N. W. (1991). Atmospheric transport of iron and its deposition in the ocean. *Limnology and Oceanography*, *36*(8), 1715-1726. https://doi.org/10.4319/lo.1991.36.8.1715

Dufresne, A., Garczarek, L., & Partensky, F. (2005). Accelerated evolution associated with genome reduction in a free-living prokaryote. *Genome Biology*, *6*, R14.

Dufresne, A., Ostrowski, M., Scanlan, D. J., Garczarek, L., Mazard, S., Palenik, B. P., Paulsen, I. T., de Marsac, N. T., Wincker, P., Dossat, C., Ferriera, S., Johnson, J., Post, A. F., Hess, W. R., & Partensky, F. (2008). Unraveling the genomic mosaic of a ubiquitous genus of marine cyanobacteria. *Genome Biology*, *9*(5), Art. 5. https://doi.org/10.1186/gb-2008-9-5-r90

Dupont, C. L., Johnson, D. A., Phillippy, K., Paulsen, I. T., Brahamsha, B., & Palenik, B. (2012). Genetic Identification of a High-Affinity Ni Transporter and the Transcriptional Response to Ni Deprivation in *Synechococcus* sp. Strain WH8102. *Applied and Environmental Microbiology*, *78*(22), Art. 22. https://doi.org/10.1128/AEM.01739-12

Durán, R. V., Hervás, M., De la Rosa, M. A., & Navarro, J. A. (2004). The Efficient Functioning of Photosynthesis and Respiration in *Synechocystis* sp. PCC 6803 Strictly Requires the Presence of either Cytochrome c_6 or Plastocyanin*. *Journal of Biological Chemistry*, *279*(8), 7229-7233. https://doi.org/10.1074/jbc.M311565200

Durham, K. A., & Bullerjahn, G. S. (2002). Immunocytochemical localization of the stress-induced DpsA protein in the cyanobacterium *Synechococcus* sp. Strain PCC 7942. *Journal of Basic Microbiology*, *42*(6), 367-372. https://doi.org/10.1002/1521-4028(200212)42:6<367::AID-JOBM367>3.0.CO;2-T

Ellis, R. J. (1979). The most abundant protein in the world. *Trends in Biochemical Sciences*, *4*(11), 241-244. https://doi.org/10.1016/0968-0004(79)90212-3

Emms, D. M., & Kelly, S. (2019). OrthoFinder : Phylogenetic orthology inference for comparative genomics. *Genome Biology*, *20*(1), 238. https://doi.org/10.1186/s13059-019-1832-y

Erdner, D. D. L., & Anderson, D. M. D. (1999). Ferredoxin and flavodoxin as biochemical indicators of iron limitation during open-ocean iron enrichment. *Limnology and Oceanography*, *44*(7), Art. 7. https://doi.org/10.4319/lo.1999.44.7.1609

Everroad, C., Six, C., Partensky, F., Thomas, J.-C., Holtzendorff, J., & Wood, A. M. (2006). Biochemical bases of Type IV chromatic adaptation in marine *Synechococcus* spp. *Journal of Bacteriology*, *188*(9), Art. 9. https://doi.org/10.1128/JB.188.9.3345-3356.2006

Falkowski, P. G. (1997). Evolution of the nitrogen cycle and its influence on the biological sequestration of CO_2 in the ocean. *Nature*, *387*, 272-275. https://doi.org/10.1038/387272a0

Falkowski, P. G. (2006). Evolution—Tracing oxygen's imprint on Earth's metabolic evolution. *Science*, *311*(5768), Art. 5768. https://doi.org/10.1126/science.1125937

Farrant, G. K., Doré, H., Cornejo-Castillo, F. M., Partensky, F., Ratin, M., Ostrowski, M., Pitt, F. D., Wincker, P., Scanlan, D. J., Iudicone, D., Acinas, S. G., & Garczarek, L. (2016). Delineating ecologically significant taxonomic units from global patterns of marine picocyanobacteria. *Proceedings of the National Academy of Sciences*, *113*(24), E3365-E3374. https://doi.org/10.1073/pnas.1524865113

Ferrieux, M., Dufour, L., Doré, H., Ratin, M., Guéneuguès, A., Chasselin, L., Marie, D., Rigaut-Jalabert, F., Le Gall, F., Sciandra, T., Monier, G., Hoebeke, M., Corre, E., Xia, X., Liu, H., Scanlan, D. J., Partensky, F., & Garczarek, L. (2022). Comparative Thermophysiology of Marine *Synechococcus* CRD1 Strains Isolated From Different Thermal Niches in Iron-Depleted Areas. *Frontiers in Microbiology*, *13*. https://www.frontiersin.org/article/10.3389/fmicb.2022.893413

Field, C. B., Behrenfeld, M. J., Randerson, J. T., & Falkowski, P. (1998). Primary production of the biosphere : Integrating terrestrial and oceanic components. *Science*, *281*(5374), Art. 5374.

Fillat, M. F. (2014). The FUR (ferric uptake regulator) superfamily : Diversity and versatility of key transcriptional regulators. *Archives of Biochemistry and Biophysics*, *546*, 41-52. https://doi.org/10.1016/j.abb.2014.01.029

Flombaum, P., Gallegos, J. L., Gordillo, R. A., Rincón, J., Zabala, L. L., Jiao, N., Karl, D. M., Li, W. K. W., Lomas, M. W., Veneziano, D., Vera, C. S., Vrugt, J. A., & Martiny, A. C. (2013). Present and future global distributions of the marine Cyanobacteria *Prochlorococcus* and *Synechococcus*. *Proceedings of the National Academy of Sciences of the United States of America*, *110*(24), 9824-9829. https://doi.org/10.1073/pnas.1307701110

Flombaum, P., Wang, W.-L., Primeau, F. W., & Martiny, A. C. (2020). Global picophytoplankton niche partitioning predicts overall positive response to ocean warming. *Nature Geoscience*, *13*(2), Art. 2. https://doi.org/10.1038/s41561-019-0524-2

Frankenberg, N., Mukougawa, K., Kohchi, T., & Lagarias, J. C. (2001). Functional genomic analysis of the HY2 family of ferredoxin-dependent bilin reductases from oxygenic photosynthetic organisms. *The Plant Cell*, *13*(4), Art. 4. https://doi.org/10.1105/tpc.13.4.965

Fu, W., Randerson, J. T., & Moore, J. K. (2016). Climate change impacts on net primary production (NPP) and export production (EP) regulated by increasing stratification and phytoplankton communitystructure in the CMIP5 models. *Biogeosciences*, *13*(18), 5151-5170. https://doi.org/10.5194/bg-13-5151-2016

Fujita, Y., Murakami, A., Aizawa, K., & Ohki, K. (1994). Short-term and Long-term Adaptation of the Photosynthetic Apparatus : Homeostatic Properties of Thylakoids. In D. A. Bryant (Éd.), *The Molecular Biology of Cyanobacteria* (p. 677-692). Springer Netherlands. https://doi.org/10.1007/978-94-011-0227-8_22

Garcia, C. A., Hagstrom, G. I., Larkin, A. A., Ustick, L. J., Levin, S. A., Lomas, M. W., & Martiny, A. C. (2020). Linking regional shifts in microbial genome adaptation with surface ocean

biogeochemistry. *Philosophical Transactions of the Royal Society B: Biological Sciences*, *375*(1798), Art. 1798. https://doi.org/10.1098/rstb.2019.0254

Garczarek, L., Dufresne, A., Blot, N., Cockshutt, A. M., Peyrat, A., Campbell, D. A., Joubin, L., & Six, C. (2008). Function and evolution of the *psbA* gene family in marine *Synechococcus* : *Synechococcus* sp. WH7803 as a case study. *The ISME Journal*, *2*(9), Art. 9. https://doi.org/10.1038/ismej.2008.46

Garczarek, L., Guyet, U., Doré, H., Farrant, G. K., Hoebeke, M., Brillet-Guéguen, L., Bisch, A., Ferrieux, M., Siltanen, J., Corre, E., Le Corguillé, G., Ratin, M., Pitt, F. D., Ostrowski, M., Conan, M., Siegel, A., Labadie, K., Aury, J. M., Wincker, P., … Partensky, F. (2021). Cyanorak v2.1 : A scalable information system dedicated to the visualization and expert curation of marine and brackish picocyanobacteria genomes. *Nucleic acids research*, *49*(D1), Art. D1. https://doi.org/10.1093/nar/gkaa958

Garczarek, L., Guyet, U., Doré, H., Farrant, G. K., Hoebeke, M., Brillet-Guéguen, L., Bisch, A., Ferrieux, M., Siltanen, J., Corre, E., Le Corguillé, G., Ratin, M., Pitt, F. D., Ostrowski, M., Conan, M., Siegel, A., Labadie, K., Aury, J.-M., Wincker, P., … Partensky, F. (2021). Cyanorak v2.1 : A scalable information system dedicated to the visualization and expert curation of marine and brackish picocyanobacteria genomes. *Nucleic Acids Research*, *49*(D1), D667-D676. https://doi.org/10.1093/nar/gkaa958

Glazer, A. N. (1985). Light harvesting by phycobilisomes. *Annual review of biophysics and biophysical chemistry*, *14*(64), Art. 64. https://doi.org/10.1146/annurev.bb.14.060185.000403

Gledhill, M., & van den Berg, C. M. G. (1994). Determination of complexation of iron(III) with natural organic complexing ligands in seawater using cathodic stripping voltammetry. *Marine Chemistry*, *47*(1), 41-54. https://doi.org/10.1016/0304-4203(94)90012-4

Gómez-Garzón, C., Barrick, J. E., & Payne, S. M. (2022). Disentangling the Evolutionary History of Feo, the Major Ferrous Iron Transport System in Bacteria. *mBio*, *13*(1), e03512-21. https://doi.org/10.1128/mbio.03512-21

Grébert, T., Doré, H., Partensky, F., Farrant, G. K., Boss, E. S., Picheral, M., Guidi, L., Pesant, S., Scanlan, D. J., Wincker, P., Acinas, S. G., Kehoe, D. M., & Garczarek, L. (2018). Light color acclimation is a key process in the global ocean distribution of *Synechococcus* cyanobacteria. *Proceedings of the National Academy of Sciences*, *115*(9), Art. 9. https://doi.org/10.1073/pnas.1717069115

Grébert, T., Garczarek, L., Daubin, V., Humily, F., Marie, D., Ratin, M., Devailly, A., Farrant, G. K., Mary, I., Mella-Flores, D., Tanguy, G., Labadie, K., Wincker, P., Kehoe, D. M., & Partensky, F. (2022). Diversity and Evolution of Pigment Types in Marine *Synechococcus* Cyanobacteria. *Genome Biology and Evolution*, *14*(4), Art. 4. https://doi.org/10.1093/gbe/evac035

Grébert, T., Nguyen, A. A., Pokhrel, S., Joseph, K. L., Ratin, M., Dufour, L., Chen, B., Haney, A. M., Karty, J. A., Trinidad, J. C., Garczarek, L., Schluchter, W. M., Kehoe, D. M., & Partensky, F. (2021). Molecular bases of an alternative dual-enzyme system for light color acclimation of marine *Synechococcus* cyanobacteria. *Proceedings of the National Academy of Sciences*, *118*(9), Art. 9. https://doi.org/10.1073/pnas.2019715118

Greenwood, D. R., & Wing, S. L. (1995). Eocene continental climates and latitudinal temperature gradients. *Geology*, *23*(11), 1044-1048. https://doi.org/10.1130/0091-7613(1995)023<1044:ECCALT>2.3.CO;2

Guidi, L., Chaffron, S., Bittner, L., Eveillard, D., Larhlimi, A., Roux, S., Darzi, Y., Audic, S., Berline, L., Brum, J., Coelho, L. P., Espinoza, J. C. I., Malviya, S., Sunagawa, S., Dimier, C., Kandels-Lewis, S., Picheral, M., Poulain, J., Searson, S., … Gorsky, G. (2016). Plankton networks driving carbon export in the oligotrophic ocean. *Nature*, *532*(7600), Art. 7600. https://doi.org/10.1038/nature16942

Guieu, C., & Martin, J. M. (2002). The Level and Fate of Metals in the Danube River Plume. *Estuarine, Coastal and Shelf Science*, *54*(3), 501-512. https://doi.org/10.1006/ecss.2000.0660

Gutiérrez-Rodríguez, A., Slack, G., Daniels, E. F., Selph, K. E., Palenik, B., & Landry, M. R. (2014). Fine spatial structure of genetically distinct picocyanobacterial populations across environmental gradients in the Costa Rica Dome. *Limnology and Oceanography*, *59*(3), Art. 3. https://doi.org/10.4319/lo.2014.59.3.0705

Guyet, U., Nguyen, N. A., Doré, H., Haguait, J., Pittera, J., Conan, M., Ratin, M., Corre, E., Le Corguillé, G., Brillet-Guéguen, L., Hoebeke, M., Six, C., Steglich, C., Siegel, A., Eveillard, D., Partensky, F., & Garczarek, L. (2020). Synergic effects of temperature and irradiance on the physiology of the marine *Synechococcus* strain WH7803. *Frontiers in Microbiology*, *11*, 1707. https://doi.org/10.3389/fmicb.2020.01707

Hackl, T., Laurenceau, R., Ankenbrand, M. J., Bliem, C., Cariani, Z., Thomas, E., Dooley, K. D., Arellano, A. A., Hogle, S. L., Berube, P., Leventhal, G. E., Luo, E., Eppley, J., Zayed, A. A., Beaulaurier, J., Stepanauskas, R., Sullivan, M. B., DeLong, E. F., Biller, S. J., & Chisholm, S. W. (2020). Novel integrative elements and genomic plasticity in ocean ecosystems. *BioRxiv*, 2020.12.28.424599. https://doi.org/10.1101/2020.12.28.424599

Haft, D. H., Basu, M. K., & Mitchell, D. A. (2010). Expansion of ribosomally produced natural products : A nitrile hydratase- and Nif11-related precursor family. *BMC Biology*, *8*, 70. https://doi.org/10.1186/1741-7007-8-70

Halliwell, B., & Gutteridge, J. M. C. (1992). Biologically relevant metal ion-dependent hydroxyl radical generation An update. *FEBS Letters*, *307*(1), 108-112. https://doi.org/10.1016/0014-5793(92)80911-Y

Haro-Moreno, J. M., López-Pérez, M., de la Torre, J. R., Picazo, A., Camacho, A., & Rodriguez-Valera, F. (2018). Fine metagenomic profile of the Mediterranean stratified and mixed

water columns revealed by assembly and recruitment. *Microbiome*, *6*(1), Art. 1. https://doi.org/10.1186/s40168-018-0513-5

Havaux, M., Guedeney, G., Hagemann, M., Yeremenko, N., Matthijs, H. C. P., & Jeanjean, R. (2005a). The chlorophyll-binding protein IsiA is inducible by high light and protects the cyanobacterium *Synechocystis* PCC6803 from photooxidative stress. *FEBS Letters*, *579*, 2289-2293. https://doi.org/10.1016/j.febslet.2005.03.021

Havaux, M., Guedeney, G., Hagemann, M., Yeremenko, N., Matthijs, H. C. P., & Jeanjean, R. (2005b). The chlorophyll-binding protein IsiA is inducible by high light and protects the cyanobacterium *Synechocystis* PCC6803 from photooxidative stress. *FEBS Letters*, *579*(11), 2289-2293. https://doi.org/10.1016/j.febslet.2005.03.021

Haverkamp, T., Acinas, S. G., Doeleman, M., Stomp, M., Huisman, J., & Stal, L. J. (2008). Diversity and phylogeny of Baltic Sea picocyanobacteria inferred from their ITS and phycobiliprotein operons. *Environmental Microbiology*, *10*, 174-188. https://doi.org/10.1111/j.1462-2920.2007.01442.x

He, Q., Dolganov, N., Bjo, O., Grossman, A. R., Natl, P., & Sci, A. (2001). The high light-inducible polypeptides in *Synechocystis* PCC6803. *Journal of Biological Chemistry*, *276*(1), Art. 1. https://doi.org/10.1074/jbc.M008686200

Herdman, M., Castenholz, R. W., Waterbury, J. B., & Rippka, R. (2001). Form-genus XIII. *Synechococcus*. In D. Boone & R. Castenholz (Éds.), *Bergey's Manual of Systematics of Archaea and Bacteria Volume 1* (2nd Ed., p. 508-512). Springer-Verlag.

Hirayama, O., Nakamura, K., Hamada, S., & Kobayasi, Y. (1994). Singlet oxygen quenching ability of naturally occurring carotenoids. *Lipids*, *29*(2), Art. 2. https://doi.org/10.1007/BF02537155

Hirayama, S., Ueda, R., & Sugata, K. (1995). Effect of hydroxyl radical on intact microalgal photosynthesis. *Energy Conversion and Management*, *36*(6), 685-688. https://doi.org/10.1016/0196-8904(95)00098-X

Hogle, S. L., Hackl, T., Bundy, R. M., Park, J., Satinsky, B., Hiltunen, T., Biller, S., Berube, P. M., & Chisholm, S. W. (2022). Siderophores as an iron source for picocyanobacteria in deep chlorophyll maximum layers of the oligotrophic ocean. *The ISME Journal*, 1-11. https://doi.org/10.1038/s41396-022-01215-w

Holtrop, T., Huisman, J., Stomp, M., Biersteker, L., Aerts, J., Grébert, T., Partensky, F., Garczarek, L., & van der Woerd, H. J. (2021). Vibrational modes of water predict spectral niches for photosynthesis in lakes and oceans. *Nature Ecology and Evolution*, *5*, 55-66. https://doi.org/10.1038/s41559-020-01330-x

Horner-Devine, A. R., Hetland, R. D., & MacDonald, D. G. (2015). Mixing and Transport in Coastal River Plumes. *Annual Review of Fluid Mechanics*, *47*(1), 569-594. https://doi.org/10.1146/annurev-fluid-010313-141408

Hu, J. (2021). Toward unzipping the ZIP metal transporters : Structure, evolution, and implications on drug discovery against cancer. *The FEBS Journal*, *288*(20), 5805-5825. https://doi.org/10.1111/febs.15658

Huang, L., McCluskey, M. P., Ni, H., & LaRossa, R. A. (2002). Global gene expression profiles of the cyanobacterium *Synechocystis* sp. Strain PCC 6803 in response to irradiation with UV-B and white light. *J. Bacteriol.*, *184*(24), Art. 24. https://doi.org/10.1128/JB.184.24.6845-6858.2002

Huang, S., Wilhelm, S. W., Harvey, H. R., Taylor, K., Jiao, N., & Chen, F. (2012). Novel lineages of *Prochlorococcus* and *Synechococcus* in the global oceans. *The ISME Journal*, *6*(2), 285-297. https://doi.org/10.1038/ismej.2011.106

Hudson, R. J. M., & Morel, F. M. M. (1990). Iron transport in marine phytoplankton : Kinetics of cellular and medium coordination reactions. *Limnology and Oceanography*, *35*(5), 1002-1020. https://doi.org/10.4319/lo.1990.35.5.1002

Humily, F., Partensky, F., Six, C., Farrant, G. K., Ratin, M., Marie, D., & Garczarek, L. (2013). A gene island with two possible configurations is involved in chromatic acclimation in marine *Synechococcus*. *PLoS ONE*, *8*(12), Art. 12. https://doi.org/10.1371/journal.pone.0084459

Hunter-Cevera, K., Neubert, M., Olson, R., Shalapyonok, A., Sosik, H., & Solow, A. (2016). Physiological and ecological drivers of early spring blooms of a coastal phytoplankter. *Science*, *354*(6310), Art. 6310. https://doi.org/10.1126/science.aaf8536

Hutchins, D. A., & Bruland, K. W. (1998). Iron-limited diatom growth and Si:N uptake ratios in a coastal upwelling regime. *Nature*, *393*(6685), Art. 6685. https://doi.org/10.1038/31203

Hutchins, D. A., Witter, A. E., Butler, A., & Luther, G. W. (1999). Competition among marine phytoplankton for different chelated iron species. *Nature*, *400*(6747), Art. 6747. https://doi.org/10.1038/23680

Hutchinson, G. E. (1957). Concluding Remarks. *Cold Spring Harbor Symposia on Quantitative Biology*, *22*, 415-427. https://doi.org/10.1101/SQB.1957.022.01.039

Ito, Y., & Butler, A. (2005). Structure of synechobactins, new siderophores of the marine cyanobacterium *Synechococcus* sp. PCC 7002. *Limnology and Oceanography*, *50*(6), 1918-1923. https://doi.org/10.4319/lo.2005.50.6.1918

Jiang, H.-B., Lou, W.-J., Ke, W.-T., Song, W.-Y., Price, N. M., & Qiu, B.-S. (2015). New insights into iron acquisition by cyanobacteria : An essential role for ExbB-ExbD complex in inorganic iron uptake. *The ISME Journal*, *9*(2), 297-309. https://doi.org/10.1038/ismej.2014.123

Jiang, H.-B., Lu, X.-H., Deng, B., Liu, L.-M., & Qiu, B.-S. (2020). Adaptive Mechanisms of the Model Photosynthetic Organisms, Cyanobacteria, to Iron Deficiency. In Q. Wang (Éd.), *Microbial Photosynthesis* (p. 197-244). Springer. https://doi.org/10.1007/978-981-15-3110-1_11

Jickells, T. D., An, Z. S., Andersen, K. K., Baker, A. R., Bergametti, G., Brooks, N., Cao, J. J., Boyd, P. W., Duce, R. A., Hunter, K. A., Kawahata, H., Kubilay, N., laRoche, J., Liss, P. S., Mahowald, N., Prospero, J. M., Ridgwell, A. J., Tegen, I., & Torres, R. (2005). Global Iron Connections

Between Desert Dust, Ocean Biogeochemistry, and Climate. *Science*, *308*(5718), 67-71. https://doi.org/10.1126/science.1105959

Johnson, K. S., Gordon, R. M., & Coale, K. H. (1997). What controls dissolved iron concentrations in the world ocean? *Marine Chemistry*, *57*(3), 137-161. https://doi.org/10.1016/S0304-4203(97)00043-1

Johnson, P. W., & Sieburth, J. M. N. (1979). Chroococcoid cyanobacteria in the sea : A ubiquitous and diverse phototrophic biomass. *Limnology and Oceanography*, *24*(5), Art. 5. https://doi.org/10.4319/lo.1979.24.5.0928

Johnson, Z. I., Zinser, E. R., Coe, A., McNulty, N. P., Woodward, E. M. S., & Chisholm, S. W. (2006). Niche partitioning among *Prochlorococcus* ecotypes along ocean-scale environmental gradients. *Science*. https://doi.org/10.1126/science.1118052

Kämpf, J., & Chapman, P. (2016). *Upwelling Systems of the World*. Springer International Publishing. https://doi.org/10.1007/978-3-319-42524-5

Kashtan, N., Roggensack, S. E., Rodrigue, S., Thompson, J. W., Biller, S. J., Coe, A., Ding, H., Marttinen, P., Malmstrom, R. R., Stocker, R., Follows, M. J., Stepanauskas, R., & Chisholm, S. W. (2014). Single-cell genomics reveals hundreds of coexisting subpopulations in wild *Prochlorococcus*. *Science (New York, N.Y.)*, *344*(6182), Art. 6182. https://doi.org/10.1126/science.1248575

Katoh, H., Hagino, N., Grossman, A. R., & Ogawa, T. (2001). Genes essential to iron transport in the cyanobacterium *Synechocystis* sp. Strain PCC 6803. *Journal of Bacteriology*, *183*(9), 2779-2784. https://doi.org/10.1128/JB.183.9.2779-2784.2001

Katoh, H., Hagino, N., & Ogawa, T. (2001). Iron-Binding Activity of FutA1 Subunit of an ABC-type Iron Transporter in the Cyanobacterium *Synechocystis* sp. Strain PCC 6803. *Plant and Cell Physiology*, *42*(8), 823-827. https://doi.org/10.1093/pcp/pce106

Kent, A. G., Baer, S. E., Mouginot, C., Huang, J. S., Larkin, A. A., Lomas, M. W., & Martiny, A. C. (2019). Parallel phylogeography of *Prochlorococcus* and *Synechococcus*. *The ISME Journal*, *13*(2), 430-441. https://doi.org/10.1038/s41396-018-0287-6

Kent, A. G., Dupont, C. L., Yooseph, S., & Martiny, A. C. (2016). Global biogeography of *Prochlorococcus* genome diversity in the surface ocean. *The ISME Journal*, *10*(8), Art. 8. https://doi.org/10.1038/ismej.2015.265

Keren, N., Aurora, R., & Pakrasi, H. B. (2004). Critical Roles of Bacterioferritins in Iron Storage and Proliferation of Cyanobacteria. *Plant Physiology*, *135*(3), 1666-1673. https://doi.org/10.1104/pp.104.042770

Kettler, G. C., Martiny, A. C., Huang, K., Zucker, J., Coleman, M. L., Rodrigue, S., Chen, F., Lapidus, A., Ferriera, S., Johnson, J., Steglich, C., Church, G. M., Richardson, P., & Chisholm, S. W. (2007). Patterns and implications of gene gain and loss in the Evolution of *Prochlorococcus*. *PLOS Genetics*, *3*(12), Art. 12. https://doi.org/10.1371/journal.pgen.0030231

Kim, S. A., Punshon, T., Lanzirotti, A., Li, L., Alonso, J. M., Ecker, J. R., Kaplan, J., & Guerinot, M. L. (2006). Localization of iron in *Arabidopsis* seed requires the vacuolar membrane transporter VIT1. *Science (New York, N.Y.)*, *314*(5803), 1295-1298. https://doi.org/10.1126/science.1132563

Kirilovsky, D., & Kerfeld, C. A. (2012). The orange carotenoid protein in photoprotection of photosystem II in cyanobacteria. *Biochimica et Biophysica Acta (BBA) - Bioenergetics*, *1817*(1), Art. 1. https://doi.org/10.1016/j.bbabio.2011.04.013

Knox, J. P., & Dodge, A. D. (1985). Singlet oxygen and plants. *Phytochemistry*, *24*(5), 889-896. https://doi.org/10.1016/S0031-9422(00)83147-7

Koch, F., & Trimborn, S. (2019). Limitation by Fe, Zn, Co, and B12 Results in Similar Physiological Responses in Two Antarctic Phytoplankton Species. *Frontiers in Marine Science*, *6*. https://www.frontiersin.org/article/10.3389/fmars.2019.00514

Koeppel, A. F., Wertheim, J. O., Barone, L., Gentile, N., Krizanc, D., & Cohan, F. M. (2013). Speedy speciation in a bacterial microcosm : New species can arise as frequently as adaptations within a species. *The ISME Journal*, *7*(6), Art. 6. https://doi.org/10.1038/ismej.2013.3

Kolber, Z., & Falkowski, P. G. (1993). Use of active fluorescence to estimate phytoplankton photosynthesis in situ. *Limnology and Oceanography*, *38*(8), 1646-1665. https://doi.org/10.4319/lo.1993.38.8.1646

Kranzler, C., Lis, H., Finkel, O. M., Schmetterer, G., Shaked, Y., & Keren, N. (2014). Coordinated transporter activity shapes high-affinity iron acquisition in cyanobacteria. *The ISME Journal*, *8*(2), Art. 2. https://doi.org/10.1038/ismej.2013.161

La Roche, J., van der Staay, G. W. M., Partensky, F., Ducret, A., Aebersold, R., Li, R., Golden, S. S., Hiller, R. G., Wrench, P. M., Larkum, A. W. D., & Green, B. R. (1996). Independent evolution of the prochlorophyte and green plant chlorophyll *a*/*b* light-harvesting proteins. *Proceedings of the National Academy of Sciences of the United States of America*, *93*(26), Art. 26.

Lam, P. J., & Bishop, J. K. B. (2008). The continental margin is a key source of iron to the HNLC North Pacific Ocean. *Geophysical Research Letters*, *35*(7). https://doi.org/10.1029/2008GL033294

Lamb, J. J., Hill, R. E., Eaton-Rye, J. J., & Hohmann-Marriott, M. F. (2014). Functional Role of PilA in Iron Acquisition in the Cyanobacterium *Synechocystis* sp. PCC 6803. *PLOS ONE*, *9*(8), e105761. https://doi.org/10.1371/journal.pone.0105761

Larkin, A. A., Blinebry, S. K., Howes, C., Lin, Y., Loftus, S. E., Schmaus, C. A., Zinser, E. R., & Johnson, Z. I. (2016). Niche partitioning and biogeography of high light adapted *Prochlorococcus* across taxonomic ranks in the North Pacific. *The ISME Journal*, *10*, 1555-1567-1555-1567. https://doi.org/10.1038/ismej.2015.244

Larkin, A. A., & Martiny, A. C. (2017). Microdiversity shapes the traits, niche space, and biogeography of microbial taxa : The ecological function of microdiversity. *Environmental Microbiology Reports*, *9*(2), Art. 2. https://doi.org/10.1111/1758-2229.12523

Larsson, J., Nylander, J. A., & Bergman, B. (2011). Genome fluctuations in cyanobacteria reflect evolutionary, developmental and adaptive traits. *BMC Evolutionary Biology*, *11*(1), Art. 1. https://doi.org/10.1186/1471-2148-11-187

Latifi, A., Jeanjean, R., Lemeille, S., Havaux, M., & Zhang, C.-C. (2005). *Iron Starvation Leads to Oxidative Stress in* Anabaena *sp. Strain PCC 7120*. https://journals.asm.org/doi/full/10.1128/JB.187.18.6596-6598.2005

Latifi, A., Ruiz, M., & Zhang, C. C. (2009). Oxidative stress in cyanobacteria. *FEMS Microbiol. Rev.*, *33*(2), Art. 2. https://doi.org/10.1111/j.1574-6976.2008.00134.x

Lavin, P., González, B., Santibáñez, J. F., Scanlan, D. J., & Ulloa, O. (2010). Novel lineages of Prochlorococcus thrive within the oxygen minimum zone of the eastern tropical South Pacific : Picocyanobacteria in oxygen minimum zones. *Environmental Microbiology Reports*, *2*(6), Art. 6. https://doi.org/10.1111/j.1758-2229.2010.00167.x

Le Brun, N. E., Crow, A., Murphy, M. E. P., Mauk, A. G., & Moore, G. R. (2010). Iron core mineralisation in prokaryotic ferritins. *Biochimica et Biophysica Acta (BBA) - General Subjects*, *1800*(8), 732-744. https://doi.org/10.1016/j.bbagen.2010.04.002

Lee, J.-W., & Helmann, J. D. (2007). Functional specialization within the Fur family of metalloregulators. *Biometals: An International Journal on the Role of Metal Ions in Biology, Biochemistry, and Medicine*, *20*(3-4), 485-499. https://doi.org/10.1007/s10534-006-9070-7

Lee, M. D., Ahlgren, N. A., Kling, J. D., Walworth, N. G., Rocap, G., Saito, M. A., Hutchins, D. A., & Webb, E. A. (2019). Marine *Synechococcus* isolates representing globally abundant genomic lineages demonstrate a unique evolutionary path of genome reduction without

a decrease in GC content. *Environmental Microbiology*, *21*(5), Art. 5. https://doi.org/10.1111/1462-2920.14552

Leonhardt, K., & Straus, N. A. (1992). An iron stress operon involved in photosynthetic electron transport in the marine cyanobacterium *Synechococcus* sp. PCC 7002. *Journal of General Microbiology*, *138 Pt 8*, 1613-1621. https://doi.org/10.1099/00221287-138-8-1613

Lindell, D., Sullivan, M. B., Johnson, Z. I., Tolonen, A. C., Rohwer, F., & Chisholm, S. W. (2004). Transfer of photosynthesis genes to and from *Prochlorococcus* viruses. *Proceedings of the National Academy of Sciences of the United States of America*, *101*(30), 11013-11018. https://doi.org/10.1073/pnas.0401526101

Lis, H., Kranzler, C., Keren, N., & Shaked, Y. (2015). A Comparative Study of Iron Uptake Rates and Mechanisms amongst Marine and Fresh Water Cyanobacteria : Prevalence of Reductive Iron Uptake. *Life*, *5*(1), Art. 1. https://doi.org/10.3390/life5010841

Los, D., & Mironov, K. (2015). Modes of Fatty Acid Desaturation in Cyanobacteria : An Update. *Life*, *5*(1), Art. 1. https://doi.org/10.3390/life5010554

Mackey, K. R. M., Paytan, A., Caldeira, K., Grossman, A. R., Moran, D., McIlvin, M., & Saito, M. A. (2013). Effect of temperature on photosynthesis and growth in marine *Synechococcus* spp. *Plant Physiology*, *163*(2), Art. 2. https://doi.org/10.1104/pp.113.221937

Mackey, K. R. M., Post, A. F., McIlvin, M. R., Cutter, G. A., John, S. G., & Saito, M. A. (2015). Divergent responses of Atlantic coastal and oceanic *Synechococcus* to iron limitation. *Proceedings of the National Academy of Sciences*, *112*(32), Art. 32. https://doi.org/10.1073/pnas.1509448112

Mahowald, N. M., Baker, A. R., Bergametti, G., Brooks, N., Duce, R. A., Jickells, T. D., Kubilay, N., Prospero, J. M., & Tegen, I. (2005). Atmospheric global dust cycle and iron inputs to the ocean. *Global Biogeochemical Cycles*, *19*(4). https://doi.org/10.1029/2004GB002402

Maldonado, M. T., Strzepek, R. F., Sander, S., & Boyd, P. W. (2005). Acquisition of iron bound to strong organic complexes, with different Fe binding groups and photochemical

reactivities, by plankton communities in Fe-limited subantarctic waters. *Global Biogeochemical Cycles*, *19*(4). https://doi.org/10.1029/2005GB002481

Malmstrom, R. R., Coe, A., Kettler, G. C., Martiny, A. C., Frias-Lopez, J., Zinser, E. R., & Chisholm, S. W. (2010). Temporal dynamics of *Prochlorococcus* ecotypes in the Atlantic and Pacific oceans. *The ISME Journal*, *4*(10), Art. 10. https://doi.org/10.1038/ismej.2010.60

Malmstrom, R. R., Rodrigue, S., Huang, K. H., Kelly, L., Kern, S. E., Thompson, A., Roggensack, S., Berube, P. M., Henn, M. R., & Chisholm, S. W. (2013). Ecology of uncultured *Prochlorococcus* clades revealed through single-cell genomics and biogeographic analysis. *The ISME Journal*, *7*(1), Art. 1. https://doi.org/10.1038/ismej.2012.89

Marchetti, A., & Cassar, N. (2009). Diatom elemental and morphological changes in response to iron limitation : A brief review with potential paleoceanographic applications. *Geobiology*, *7*(4), 419-431. https://doi.org/10.1111/j.1472-4669.2009.00207.x

Marie, D., Brussaard, C. P. D., Partensky, F., & Vaulot, D. (1999). Flow cytometric analysis of phytoplankton, bacteria and viruses. In J. P. Robinson (Éd.), *Current protocols in cytometry: Vol. 11.11* (p. 1-15). John Wiley & Sons.

Martin, J. H., Coale, K. H., Johnson, K. S., Fitzwater, S. E., Gordon, R. M., Tanner, S. J., Hunter, C. N., Elrod, V. A., Nowicki, J. L., Coley, T. L., Barber, R. T., Lindley, S., Watson, A. J., Van Scoy, K., Law, C. S., Liddicoat, M. I., Ling, R., Stanton, T., Stockel, J., … Tindale, N. W. (1994). Testing the iron hypothesis in ecosystems of the equatorial Pacific Ocean. *Nature*. https://doi.org/10.1038/371123a0

Martin, J. H., & Fitzwater, S. E. (1988). Iron deficiency limits phytoplankton growth in the north-east Pacific subarctic. *Nature*, *331*(6154), Art. 6154. https://doi.org/10.1038/331341a0

Martinez, A., Tyson, G. W., & Delong, E. F. (2010). Widespread known and novel phosphonate utilization pathways in marine bacteria revealed by functional screening and metagenomic analyses. *Environmental Microbiology*, *12*(1), Art. 1. https://doi.org/10.1111/j.1462-2920.2009.02062.x

Martiny, A. C., Coleman, M. L., & Chisholm, S. W. (2006). Phosphate acquisition genes in *Prochlorococcus* ecotypes : Evidence for genome-wide adaptation. *Proceedings of the National Academy of Sciences of the United States of America*, *103*(33), Art. 33. https://doi.org/10.1073/pnas.0601301103

Martiny, A. C., Kathuria, S., & Berube, P. M. (2009). Widespread metabolic potential for nitrite and nitrate assimilation among *Prochlorococcus* ecotypes. *Proceedings of the National Academy of Sciences*, *106*(26), Art. 26. https://doi.org/10.1073/pnas.0902532106

Martiny, A. C., Tai, A. P. K., Veneziano, D., Primeau, F., & Chisholm, S. W. (2009). Taxonomic resolution, ecotypes and the biogeography of *Prochlorococcus*. *Environmental Microbiology*, *11*(4), Art. 4. https://doi.org/10.1111/j.1462-2920.2008.01803.x

Martiny, J. B. H., Jones, S. E., Lennon, J. T., & Martiny, A. C. (2015). Microbiomes in light of traits : A phylogenetic perspective. *Science (New York, N.Y.)*, *350*(6261), Art. 6261. https://doi.org/10.1126/science.aac9323

Mazard, S., Ostrowski, M., Partensky, F., & Scanlan, D. J. (2012). Multi-locus sequence analysis, taxonomic resolution and biogeography of marine *Synechococcus* : Taxonomic resolution and biogeography of marine *Synechococcus*. *Environmental Microbiology*, *14*(2), Art. 2. https://doi.org/10.1111/j.1462-2920.2011.02514.x

Mella-Flores, D., Mazard, S., Humily, F., Partensky, F., Mahé, F., Bariat, L., Courties, C., Marie, D., Ras, J., Mauriac, R., Jeanthon, C., Mahdi Bendif, E., Ostrowski, M., Scanlan, D. J., & Garczarek, L. (2011). Is the distribution of *Prochlorococcus* and *Synechococcus* ecotypes in the Mediterranean Sea affected by global warming? *Biogeosciences*, *8*(9), Art. 9. https://doi.org/10.5194/bg-8-2785-2011

Mella-Flores, D., Six, C., Ratin, M., Partensky, F., Boutte, C., Le Corguillé, G., Marie, D., Blot, N., Gourvil, P., Kolowrat, C., & Garczarek, L. (2012). *Prochlorococcus* and *Synechococcus* have evolved different adaptive mechanisms to cope with light and UV stress. *Frontiers in Microbiology*, *3*. https://doi.org/10.3389/fmicb.2012.00285

Mengel, K., & Kirkby, E. A. (1987). *Principles of Plant Nutrition*. Springer Science & Business Media.

Michel, K.-P., Berry, S., Hifney, A., Kruip, J., & Pistorius, E. K. (2003). Adaptation to iron deficiency : A comparison between the cyanobacterium *Synechococcus elongatus* PCC 7942 wild-type and a DpsA-free mutant. *Photosynthesis Research*, *75*(1), 71-84. https://doi.org/10.1023/A:1022459919040

Mikami, K., & Murata, N. (2003). Membrane fluidity and the perception of environmental signals in cyanobacteria and plants. *Progress in Lipid Research*, *42*(6), Art. 6. https://doi.org/10.1016/S0163-7827(03)00036-5

Mikhaylina, A., Ksibe, A. Z., Wilkinson, R. C., Smith, D., Marks, E., Coverdale, J. P. C., Fülöp, V., Scanlan, D. J., & Blindauer, C. A. (2022). A single sensor controls large variations in zinc quotas in a marine cyanobacterium. *Nature Chemical Biology*, 1-9. https://doi.org/10.1038/s41589-022-01051-1

Moore, C. M., Mills, M. M., Arrigo, K. R., Berman-Frank, I., Bopp, L., Boyd, P. W., Galbraith, E. D., Geider, R. J., Guieu, C., Jaccard, S. L., Jickells, T. D., La Roche, J., Lenton, T. M., Mahowald, N. M., Marañón, E., Marinov, I., Moore, J. K., Nakatsuka, T., Oschlies, A., … Ulloa, O. (2013). Processes and patterns of oceanic nutrient limitation. *Nature Geoscience*, *6*(9), Art. 9. https://doi.org/10.1038/ngeo1765

Moore, J. K., Doney, S. C., Glover, D. M., & Fung, I. Y. (2002). Iron cycling and nutrient-limitation patterns in surface waters of the World Ocean. *Deep Sea Research Part II: Topical Studies in Oceanography*, *49*(1-3), 463-507. https://doi.org/10.1016/S0967-0645(01)00109-6

Moore, L. R., & Chisholm, S. W. (1999). Photophysiology of the marine cyanobacterium Prochlorococcus : Ecotypic differences among cultured isolates. *Limnology and Oceanography*, *44*(3), Art. 3. https://doi.org/10.4319/lo.1999.44.3.0628

Moore, L. R., Coe, A., Zinser, E. R., Saito, M. A., Sullivan, M. B., Lindell, D., Frois-Moniz, K., Waterbury, J., & Chisholm, S. W. (2007). Culturing the marine cyanobacterium

Prochlorococcus : Prochlorococcus culturing. *Limnology and Oceanography: Methods*, *5*(10), Art. 10. https://doi.org/10.4319/lom.2007.5.353

Moore, L. R., Rocap, G., & Chisholm, S. W. (1998). Physiology and molecular phylogeny of coexisting Prochlorococcus ecotypes. *Nature*, *393*(6684), 464-467. https://doi.org/10.1038/30965

Morel, F. M. M., Kustka, A. B., & Shaked, Y. (2008). The role of unchelated Fe in the iron nutrition of phytoplankton. *Limnology and Oceanography*, *53*(1), 400-404. https://doi.org/10.4319/lo.2008.53.1.0400

Morrissey, J., & Bowler, C. (2012). Iron Utilization in Marine Cyanobacteria and Eukaryotic Algae. *Frontiers in Microbiology*, *3*. https://doi.org/10.3389/fmicb.2012.00043

Mullineaux, C. W. (2014). Electron transport and light-harvesting switches in cyanobacteria. *Frontiers in Plant Science*. https://doi.org/10.3389/fpls.2014.00007

Muñoz-Marín, M. C., Gómez-Baena, G., López-Lozano, A., Moreno-Cabezuelo, J. A., Díez, J., & García-Fernández, J. M. (2020). Mixotrophy in marine picocyanobacteria : Use of organic compounds by Prochlorococcus and Synechococcus. *The ISME Journal*, *14*(5), Art. 5. https://doi.org/10.1038/s41396-020-0603-9

Murata, N., Takahashi, S., Nishiyama, Y., & Allakhverdiev, S. I. (2007). Photoinhibition of photosystem II under environmental stress. *Biochimica et Biophysica Acta - Bioenergetics*. https://doi.org/10.1016/j.bbabio.2006.11.019

Napolitano, M., Rubio, M. Á., Santamaría-Gómez, J., Olmedo-Verd, E., Robinson, N. J., & Luque, I. (2012). Characterization of the Response to Zinc Deficiency in the Cyanobacterium *Anabaena* sp. Strain PCC 7120. *Journal of Bacteriology*, *194*(10), 2426-2436. https://doi.org/10.1128/JB.00090-12

Nishiyama, Y., Allakhverdiev, S. I., & Murata, N. (2006). A new paradigm for the action of reactive oxygen species in the photoinhibition of photosystem II. *Biochimica et Biophysica Acta (BBA) - Bioenergetics*, *1757*(7), Art. 7. https://doi.org/10.1016/j.bbabio.2006.05.013

Pachiadaki, M. G., Brown, J. M., Brown, J., Bezuidt, O., Berube, P. M., Biller, S. J., Poulton, N. J., Burkart, M. D., Clair, J. J. L., Chisholm, S. W., & Stepanauskas, R. (2019). Charting the Complexity of the Marine Microbiome through Single-Cell Genomics. *Cell*, *179*(7), Art. 7. https://doi.org/10.1016/j.cell.2019.11.017

Palenik, B. (2001). Chromatic adaptation in marine *Synechococcus* strains. *Applied and Environmental Microbiology*, *67*(2), Art. 2.

Pankowski, A., & McMinn, A. (2009). Iron availability regulates growth, photosynthesis, and production of ferredoxin and flavodoxin in Antarctic sea ice diatoms. *Aquatic Biology*, *4*(3), 273-288. https://doi.org/10.3354/ab00116

Park, Y. I., Sandström, S., Gustafsson, P., & Oquist, G. (1999). Expression of the isiA gene is essential for the survival of the cyanobacterium *Synechococcus* sp. PCC 7942 by protecting photosystem II from excess light under iron limitation. *Molecular Microbiology*, *32*(1), 123-129. https://doi.org/10.1046/j.1365-2958.1999.01332.x

Partensky, F., Blanchot, J., & Vaulot, D. (1999). Differential distribution and ecology of *Prochlorococcus* and *Synechococcus* in oceanic waters : A review. In L. Charpy & A. W. D. Larkum (Éds.), *Marine Cyanobacteria* (p. 457-475). Bulletin de l'Institut Océanographique de Monaco. Numéro spécial 19.

Partensky, F., & Garczarek, L. (2010). *Prochlorococcus* : Advantages and Limits of Minimalism. *Annual Review of Marine Science*, *2*(1), Art. 1. https://doi.org/10.1146/annurev-marine-120308-081034

Partensky, F., & Garczarek, L. (2011). Arms race in a drop of seawater. *Nature*, *474*, 582-583.

Partensky, F., & Garczarek, L. (2017). *Chapter 7. The colour of water. In : The ocean revealed. Part II. What is the ocean? A. Euzen, F. Gaill, D. Lacroix & P. Cury (Eds). CNRS Editions. pp.62-63.*

Paulsen, M. L., Doré, H., Garczarek, L., Seuthe, L., Müller, O., Sandaa, R.-A., Bratbak, G., & Larsen, A. (2016). *Synechococcus* in the Atlantic gateway to the Arctic Ocean. *Frontiers in Marine Science*, *3*. https://doi.org/10.3389/fmars.2016.00191

Pehowich, D. J., Macdonald, P. M., McElhaney, R. N., Cossins, A. R., & Wang, L. C. H. (1988, juin 28). *Calorimetric and spectroscopic studies of lipid thermotropic phase behavior in liver inner mitochondrial membranes from a mammalian hibernator* (world) [Research-article]. ACS Publications; American Chemical Society. https://doi.org/10.1021/bi00413a008

Penen, F., Malherbe, J., Isaure, M.-P., Dobritzsch, D., Bertalan, I., Gontier, E., Le Coustumer, P., & Schaumlöffel, D. (2016). Chemical bioimaging for the subcellular localization of trace elements by high contrast TEM, TEM/X-EDS, and NanoSIMS. *Journal of Trace Elements in Medicine and Biology*, *37*, 62-68. https://doi.org/10.1016/j.jtemb.2016.04.014

Penno, S., Lindell, D., & Post, A. F. (2006). Diversity of *Synechococcus* and *Prochlorococcus* populations determined from DNA sequences of the N-regulatory gene ntcA. *Environmental Microbiology*, *8*(7), 1200-1211. https://doi.org/10.1111/j.1462-2920.2006.01010.x

Pittera, J., Humily, F., Thorel, M., Grulois, D., Garczarek, L., & Six, C. (2014). Connecting thermal physiology and latitudinal niche partitioning in marine *Synechococcus*. *The ISME Journal*, *8*(6), Art. 6. https://doi.org/10.1038/ismej.2013.228

Pittera, J., Jouhet, J., Breton, S., Garczarek, L., Partensky, F., Maréchal, É., An Nguyen, N., Doré, H., Ratin, M., Pitt, F. D., Scanlan, D. J., & Six, C. (2017). Thermoacclimation and genome adaptation of the membrane lipidome in marine *Synechococcus*. *Environmental Microbiology*. https://doi.org/10.1111/1462-2920.13985

Pittera, J., Partensky, F., & Six, C. (2016). Adaptive thermostability of light-harvesting complexes in marine picocyanobacteria. *The ISME Journal*, Art. 1.

Polovina, J. J., Howell, E. A., & Abecassis, M. (2008). Ocean's least productive waters are expanding. *Geophysical Research Letters*, *35*(3). https://doi.org/10.1029/2007GL031745

Polyviou, D., Machelett, M. M., Hitchcock, A., Baylay, A. J., MacMillan, F., Moore, C. M., Bibby, T. S., & Tews, I. (2018). Structural and functional characterization of IdiA/FutA (Tery_3377), an iron-binding protein from the ocean diazotroph *Trichodesmium erythraeum*. *Journal of Biological Chemistry*, *293*(47), 18099-18109. https://doi.org/10.1074/jbc.RA118.001929

Price, N. M., Harrison, G. I., Hering, J. G., Hudson, R. J., Nirel, P. M. V., Palenik, B., & Morel, F. M. M. (1989). Preparation and Chemistry of the Artificial Algal Culture Medium Aquil. *Biological Oceanography*, *6*(5-6), 443-461. https://doi.org/10.1080/01965581.1988.10749544

Qiu, G.-W., Jiang, H.-B., Lis, H., Li, Z.-K., Deng, B., Shang, J.-L., Sun, C.-Y., Keren, N., & Qiu, B.-S. (2021). A unique porin meditates iron-selective transport through cyanobacterial outer membranes. *Environmental Microbiology*, *23*(1), 376-390. https://doi.org/10.1111/1462-2920.15324

Raiswell, R. (2013). Rusty meltwaters. *Nature Geoscience*, *6*(4), Art. 4. https://doi.org/10.1038/ngeo1776

Ras, M., Steyer, J.-P., & Bernard, O. (2013). Temperature effect on microalgae : A crucial factor for outdoor production. *Reviews in Environmental Science and Bio/Technology*, *12*(2), 153-164. https://doi.org/10.1007/s11157-013-9310-6

Rastogi, R. P., Richa, Kumar, A., Tyagi, M. B., & Sinha, R. P. (2010). Molecular mechanisms of ultraviolet radiation-induced DNA damage and repair. *J. Nucleic Acids*, 592980-592980. https://doi.org/10.4061/2010/592980

Raven, J. A., & Falkowski, P. G. (1999). Oceanic sinks for atmospheric CO_2. *Plant, Cell and Environment*, *22*(6), 741-755.

Riediger, M., Hernández-Prieto, M. A., Song, K., Hess, W. R., & Futschik, M. E. (2021). Genome-wide identification and characterization of Fur-binding sites in the cyanobacteria *Synechocystis* sp. PCC 6803 and PCC 6714. *DNA Research*, *28*(6), dsab023. https://doi.org/10.1093/dnares/dsab023

Rippka, R. (1988). Isolation and purification of cyanobacteria. *Methods in Enzymology*, *167*, 3-27. https://doi.org/10.1016/0076-6879(88)67004-2

Rippka, R., Coursin, T., Hess, W., Lichtle, C., Scanlan, D. J., Palinska, K. A., Iteman, I., Partensky, F., Houmard, J., & Herdman, M. (2000). *Prochlorococcus marinus* Chisholm et al. 1992 subsp. *Pastoris* subsp. Nov. Strain PCC 9511, the first axenic chlorophyll a_2/b_2-containing cyanobacterium (Oxyphotobacteria). *International Journal of Systematic and Evolutionary Microbiology*, *50*(5), Art. 5. https://doi.org/10.1099/00207713-50-5-1833

Roach, T., & Krieger-Liszkay, A. (2012). The role of the PsbS protein in the protection of photosystems I and II against high light in *Arabidopsis thaliana*. *Biochimica et Biophysica Acta (BBA) - Bioenergetics*, *1817*(12), 2158-2165. https://doi.org/10.1016/j.bbabio.2012.09.011

Rocap, G., Distel, D. L., Waterbury, J. B., & Chisholm, S. W. (2002). Resolution of *Prochlorococcus* and *Synechococcus* Ecotypes by Using 16S-23S Ribosomal DNA Internal Transcribed Spacer Sequences. *Applied and Environmental Microbiology*, *68*(3), Art. 3. https://doi.org/10.1128/AEM.68.3.1180-1191.2002

Rose, A. L., Salmon, T. P., Lukondeh, T., Neilan, B. A., & Waite, T. D. (2005). Use of Superoxide as an Electron Shuttle for Iron Acquisition by the Marine Cyanobacterium *Lyngbya majuscula*. *Environmental Science & Technology*, *39*(10), 3708-3715. https://doi.org/10.1021/es048766c

Rusch, D. B., Martiny, A. C., Dupont, C. L., Halpern, A. L., & Venter, J. C. (2010). Characterization of *Prochlorococcus* clades from iron-depleted oceanic regions. *Proceedings of the National Academy of Sciences*, *107*(37), Art. 37. https://doi.org/10.1073/pnas.1009513107

Saito, M. A., Rocap, G., & Moffett, J. W. (2005). Production of cobalt binding ligands in a *Synechococcus* feature at the Costa Rica upwelling dome. *Limnology and Oceanography*. https://doi.org/10.4319/lo.2005.50.1.0279

Saito, M. A., Sigman, D. M., & Morel, F. M. M. (2003). The bioinorganic chemistry of the ancient ocean : The co-evolution of cyanobacterial metal requirements and biogeochemical cycles at the Archean–Proterozoic boundary? *Inorganica Chimica Acta*, *356*, 308-318. https://doi.org/10.1016/S0020-1693(03)00442-0

Salvucci, M. E., & Crafts-Brandner, S. J. (2004). Inhibition of photosynthesis by heat stress : The activation state of Rubisco as a limiting factor in photosynthesis. *Physiologia Plantarum*, *120*(2), 179-186. https://doi.org/10.1111/j.0031-9317.2004.0173.x

Sánchez-Baracaldo, P., Bianchini, G., Wilson, J. D., & Knoll, A. H. (2022). Cyanobacteria and biogeochemical cycles through Earth history. *Trends in Microbiology*, *30*(2), 143-157. https://doi.org/10.1016/j.tim.2021.05.008

Sander, J., Nowaczyk, M., Buchta, J., Dau, H., Vass, I., Deák, Z., Dorogi, M., Iwai, M., & Rögner, M. (2010). Functional Characterization and Quantification of the Alternative PsbA Copies in *Thermosynechococcus elongatus* and Their Role in Photoprotection. *Journal of Biological Chemistry*, *285*(39), 29851-29856. https://doi.org/10.1074/jbc.M110.127142

Sandström, S., Ivanov, A. G., Park, Y.-I., Öquist, G., & Gustafsson, P. (2002). Iron stress responses in the cyanobacterium *Synechococcus* sp. PCC7942. *Physiologia Plantarum*, *116*(2), 255-263. https://doi.org/10.1034/j.1399-3054.2002.1160216.x

Sanfilippo, J. E., Nguyen, A. A., Garczarek, L., Karty, J. A., Pokhrel, S., Strnat, J. A., Partensky, F., Schluchter, W. M., & Kehoe, D. M. (2019). Interplay between differentially expressed enzymes contributes to light color acclimation in marine *Synechococcus*. *Proceedings of the National Academy of Sciences*, *116*(13), Art. 13. https://doi.org/10.1073/pnas.1810491116

Scanlan, D. J. (2012). Marine Picocyanobacteria. In B. A. Whitton (Éd.), *Ecology of Cyanobacteria II: Their Diversity in Space and Time* (p. 503-533). Springer Netherlands. https://doi.org/10.1007/978-94-007-3855-3_20

Scanlan, D. J., Ostrowski, M., Mazard, S., Dufresne, A., Garczarek, L., Hess, W. R., Post, A. F., Hagemann, M., Paulsen, I., & Partensky, F. (2009). Ecological genomics of marine picocyanobacteria. *Microbiology and Molecular Biology Reviews*, *73*(2), Art. 2. https://doi.org/10.1128/MMBR.00035-08

Schwarz, R., & Forchhammer, K. 2005. (s. d.). Acclimation of unicellular cyanobacteria to macronutrient deficiency : Emergence of a complex network of cellular responses. *Microbiology*, *151*(8), 2503-2514. https://doi.org/10.1099/mic.0.27883-0

Shaked, Y., & Lis, H. (2012). Disassembling Iron Availability to Phytoplankton. *Frontiers in Microbiology*, *3*. https://www.frontiersin.org/article/10.3389/fmicb.2012.00123

Shcolnick, S., & Keren, N. (2006). Metal Homeostasis in Cyanobacteria and Chloroplasts. Balancing Benefits and Risks to the Photosynthetic Apparatus. *Plant Physiology*, *141*(3), 805-810. https://doi.org/10.1104/pp.106.079251

Shcolnick, S., Summerfield, T. C., Reytman, L., Sherman, L. A., & Keren, N. (2009). The Mechanism of Iron Homeostasis in the Unicellular Cyanobacterium *Synechocystis* sp. PCC 6803 and Its Relationship to Oxidative Stress. *Plant Physiology*, *150*(4), Art. 4. https://doi.org/10.1104/pp.109.141853

Sheraz, S., Wan, Y., Venter, E., Verma, S. K., Xiong, Q., Waites, J., Connorton, J. M., Shewry, P. R., Moore, K. L., & Balk, J. (2021). Subcellular dynamics studies of iron reveal how tissue-specific distribution patterns are established in developing wheat grains. *New Phytologist*, *231*(4), 1644-1657. https://doi.org/10.1111/nph.17440

Sherr, E. B., & Sherr, B. F. (2002). Significance of predation by protists in aquatic microbial food webs. *Antonie van Leeuwenhoek*, *81*(1), 293-308. https://doi.org/10.1023/A:1020591307260

Shih, P. M., Wu, D., Latifi, A., Axen, S. D., Fewer, D. P., Talla, E., Calteau, A., Cai, F., Tandeau de Marsac, N., Rippka, R., Herdman, M., Sivonen, K., Coursin, T., Laurent, T., Goodwin, L., Nolan, M., Davenport, K. W., Han, C. S., Rubin, E. M., … Kerfeld, C. A. (2013). Improving

the coverage of the cyanobacterial phylum using diversity-driven genome sequencing. *Proceedings of the National Academy of Sciences of the USA*, *110*(3), Art. 3.

Sidler, W. A. (1994). Phycobilisome and phycobiliprotein structure. In D. A. Bryant (Éd.), *The Molecular Biology of Cyanobacteria* (p. 139-216). Springer Netherlands. https://doi.org/10.1007/978-94-011-0227-8_7

Sieburth, J. McN., Smetacek, V., & Lenz, J. (1978). Pelagic ecosystem structure : Heterotrophic compartments of the plankton and their relationship to plankton size fractions 1. *Limnology and Oceanography*, *23*(6), 1256-1263. https://doi.org/10.4319/lo.1978.23.6.1256

Six, C., Ratin, M., Marie, D., & Corre, E. (2021). Marine *Synechococcus* picocyanobacteria : Light utilization across latitudes. *Proceedings of the National Academy of Sciences*, *118*(38), Art. 38. https://doi.org/10.1073/pnas.2111300118

Six, C., Thomas, J. C., Thion, L., Lemoine, Y., Zal, F., & Curie, M. (2005). Two Novel Phycoerythrin-Associated Linker Proteins in the Marine. *Journal of Bacteriology*, *187*(5), Art. 5. https://doi.org/10.1128/JB.187.5.1685

Six, C., Thomas, J.-C., Garczarek, L., Ostrowski, M., Dufresne, A., Blot, N., Scanlan, D. J., & Partensky, F. (2007). Diversity and evolution of phycobilisomes in marine *Synechococcus* spp. : A comparative genomics study. *Genome Biology*, *8*(12), Art. 12. https://doi.org/10.1186/gb-2007-8-12-r259

Skotnicová, P., Sobotka, R., Shepherd, M., Hájek, J., Hrouzek, P., & Tichý, M. (2018). The cyanobacterial protoporphyrinogen oxidase HemJ is a new b-type heme protein functionally coupled with coproporphyrinogen III oxidase. *The Journal of Biological Chemistry*, *293*(32), 12394-12404. https://doi.org/10.1074/jbc.RA118.003441

Sohm, J. A., Ahlgren, N. A., Thomson, Z. J., Williams, C., Moffett, J. W., Saito, M. A., Webb, E. A., & Rocap, G. (2015). Co-occurring *Synechococcus* ecotypes occupy four major oceanic

regimes defined by temperature, macronutrients and iron. *The ISME Journal*, *10*(2), Art. 2. https://doi.org/10.1038/ismej.2015.115

Soo, R. M., Hemp, J., Parks, D. H., Fischer, W. W., & Hugenholtz, P. (2017). On the origins of oxygenic photosynthesis and aerobic respiration in Cyanobacteria. *Science*, *355*(6332), Art. 6332. https://doi.org/10.1126/science.aal3794

Stefels, J., Steinke, M., Turner, S., Malin, G., & Belviso, S. (2007). Environmental constraints on the production and removal of the climatically active gas dimethylsulphide (DMS) and implications for ecosystem modelling. *Biogeochemistry*, *83*(1), 245-275. https://doi.org/10.1007/s10533-007-9091-5

Steglich, C., Futschik, M., Rector, T., Steen, R., & Chisholm, S. W. (2006). Genome-Wide Analysis of Light Sensing in *Prochlorococcus*. *Journal of Bacteriology*, *188*(22), Art. 22. https://doi.org/10.1128/JB.01097-06

Stevanovic, M., Hahn, A., Nicolaisen, K., Mirus, O., & Schleiff, E. (2012). The components of the putative iron transport system in the cyanobacterium *Anabaena* sp. PCC 7120. *Environmental Microbiology*, *14*(7), 1655-1670. https://doi.org/10.1111/j.1462-2920.2011.02619.x

Straus, N. A. (s. d.). Iron Deprivation : Physiology and Gene Regulation. In *The Molecular Biology of Cyanobacteria*. https://doi.org/10.1007/0-306-48205-3_25

Strzepek, R. F., Boyd, P. W., & Sunda, W. G. (2019). Photosynthetic adaptation to low iron, light, and temperature in Southern Ocean phytoplankton. *Proceedings of the National Academy of Sciences*, *116*(10), 4388-4393. https://doi.org/10.1073/pnas.1810886116

Sugiura, M., Nakamura, M., Koyama, K., & Boussac, A. (2015). Assembly of oxygen-evolving Photosystem II efficiently occurs with the apo-Cytb559 but the holo-Cytb559 accelerates the recovery of a functional enzyme upon photoinhibition. *Biochimica et Biophysica Acta (BBA) - Bioenergetics*, *1847*(2), 276-285. https://doi.org/10.1016/j.bbabio.2014.11.009

Sunagawa, S., Coelho, L. P., Chaffron, S., Kultima, J. R., Labadie, K., Salazar, G., Djahanschiri, B., Zeller, G., Mende, D. R., Alberti, A., Cornejo-Castillo, F. M., Costea, P. I., Cruaud, C., D'Ovidio, F., Engelen, S., Ferrera, I., Gasol, J. M., Guidi, L., Hildebrand, F., … Velayoudon, D. (2015). Structure and function of the global ocean microbiome. *Science*, *348*(6237), Art. 6237. https://doi.org/10.1126/science.1261359

Sutak, R., Camadro, J.-M., & Lesuisse, E. (2020). Iron Uptake Mechanisms in Marine Phytoplankton. *Frontiers in Microbiology*, *11*. https://www.frontiersin.org/article/10.3389/fmicb.2020.566691

Tagliabue, A., Bowie, A. R., Boyd, P. W., Buck, K. N., Johnson, K. S., & Saito, M. A. (2017). The integral role of iron in ocean biogeochemistry. *Nature*, *543*(7643), Art. 7643. https://doi.org/10.1038/nature21058

Tai, V., & Palenik, B. (2009). Temporal variation of *Synechococcus* clades at a coastal Pacific Ocean monitoring site. *The ISME Journal*, *3*(8), Art. 8. https://doi.org/10.1038/ismej.2009.35

Takahashi, S., & Murata, N. (2008). How do environmental stresses accelerate photoinhibition? *Trends in Plant Science*, *13*(4), 178-182. https://doi.org/10.1016/j.tplants.2008.01.005

Toledo, G., & Palenik, B. (1997). *Synechococcus* diversity in the California current as seen by RNA polymerase (*rpoC1*) gene sequences of isolated strains. *Applied and Environmental Microbiology*, *63*(11), Art. 11.

Triantaphylidès, C., Krischke, M., Hoeberichts, F. A., Ksas, B., Gresser, G., Havaux, M., Van Breusegem, F., & Mueller, M. J. (2008). Singlet Oxygen Is the Major Reactive Oxygen Species Involved in Photooxidative Damage to Plants. *Plant Physiology*, *148*(2), 960-968. https://doi.org/10.1104/pp.108.125690

Tsuda, A., Takeda, S., Saito, H., Nishioka, J., Nojiri, Y., Kudo, I., Kiyosawa, H., Shiomoto, A., Imai, K., Ono, T., Shimamoto, A., Tsumune, D., Yoshimura, T., Aono, T., Hinuma, A., Kinugasa, M., Suzuki, K., Sohrin, Y., Noiri, Y., … Saino, T. (2003). A Mesoscale Iron Enrichment in the

Western Subarctic Pacific Induces a Large Centric Diatom Bloom. *Science*, *300*(5621), 958-961. https://doi.org/10.1126/science.1082000

Tyystjärvi, E. (2008). Photoinhibition of Photosystem II and photodamage of the oxygen evolving manganese cluster. *Coordination Chemistry Reviews*. https://doi.org/10.1016/j.ccr.2007.08.021

Ulloa, O., Henríquez-Castillo, C., Ramírez-Flandes, S., Plominsky, A. M., Murillo, A. A., Morgan-Lang, C., Hallam, S. J., & Stepanauskas, R. (2021). The cyanobacterium *Prochlorococcus* has divergent light-harvesting antennae and may have evolved in a low-oxygen ocean. *Proceedings of the National Academy of Sciences*, *118*(11), Art. 11. https://doi.org/10.1073/pnas.2025638118

Ussher, S. J., Achterberg, E. P., Sarthou, G., Laan, P., de Baar, H. J. W., & Worsfold, P. J. (2010). Distribution of size fractionated dissolved iron in the Canary Basin. *Marine Environmental Research*, *70*(1), 46-55. https://doi.org/10.1016/j.marenvres.2010.03.001

Ustick, L. J., Larkin, A. A., Garcia, C. A., Garcia, N. S., Brock, M. L., Lee, J. A., Wiseman, N. A., Moore, J. K., & Martiny, A. C. (2021). Metagenomic analysis reveals global-scale patterns of ocean nutrient limitation. *Science*, *372*(6539), Art. 6539. https://doi.org/10.1126/science.abe6301

Varkey, D., Mazard, S., Ostrowski, M., Tetu, S. G., Haynes, P., & Paulsen, I. T. (2016). Effects of low temperature on tropical and temperate isolates of marine *Synechococcus*. *The ISME Journal*, *10*(5), Art. 5. https://doi.org/10.1038/ismej.2015.179

Vass, I. (2012). Molecular mechanisms of photodamage in the Photosystem II complex. *Biochimica et Biophysica Acta (BBA) - Bioenergetics*, *1817*(1), Art. 1. https://doi.org/10.1016/j.bbabio.2011.04.014

Vaulot, D., Eikrem, W., Viprey, M., & Moreau, H. (2008). The diversity of small eukaryotic phytoplankton (<3 μm) in marine ecosystems. *FEMS Microbiology Reviews*, *32*(5), Art. 5.

Villar, E., Farrant, G. K., Follows, M., Garczarek, L., Speich, S., Audic, S., Bittner, L., Blanke, B., Brum, J. R., Brunet, C., Casotti, R., Chase, A., Dolan, J. R., d'Ortenzio, F., Gattuso, J.-P., Grima, N., Guidi, L., Hill, C. N., Jahn, O., … Iudicone, D. (2015). Ocean plankton. Environmental characteristics of Agulhas rings affect interocean plankton transport. *Science (New York, N.Y.)*, *348*(6237), Art. 6237. https://doi.org/10.1126/science.1261447

Wandersman, C., & Delepelaire, P. (2004). Bacterial Iron Sources : From Siderophores to Hemophores. *Annual Review of Microbiology*, *58*(1), 611-647. https://doi.org/10.1146/annurev.micro.58.030603.123811

Waterbury, J. B. (1986). Biological and ecological characterization of the marine unicellular cyanobacterium *Synechococcus*. *Canadian Bulletin of Fisheries and Aquatic Sciences*, *214*, 71-120.

Waterbury, J. B., Watson, S. W., Guillard, R. R. L., & Brand, L. E. (1979). Widespread occurrence of a unicellular, marine, planktonic, cyanobacterium. *Nature*, *277*(5694), Art. 5694. https://doi.org/10.1038/277293a0

West, N. J., Lebaron, P., Strutton, P. G., & Suzuki, M. T. (2011). A novel clade of *Prochlorococcus* found in high nutrient low chlorophyll waters in the South and Equatorial Pacific Ocean. *The ISME Journal*, *5*(6), Art. 6. https://doi.org/10.1038/ismej.2010.186

Whitman, W. B., Coleman, D. C., & Wiebe, W. J. (1998). Prokaryotes : The unseen majority. *Proceedings of the National Academy of Sciences*, *95*(12), Art. 12. https://doi.org/10.1073/pnas.95.12.6578

Wilhelm, S. W., & Suttle, C. a. (1999). Viruses and Nutrient Cycles in the Sea aquatic food webs. *BioScience*, *49*(October), Art. October. https://doi.org/10.2307/1313569

Wilson, A., Ajlani, G., Verbavatz, J.-M., Vass, I., Kerfeld, C. A., & Kirilovsky, D. (2006). A Soluble Carotenoid Protein Involved in Phycobilisome-Related Energy Dissipation in Cyanobacteria. *The Plant Cell*, *18*(4), Art. 4. https://doi.org/10.1105/tpc.105.040121

Wilson, A., Boulay, C., Wilde, A., Kerfeld, C. A., & Kirilovsky, D. (2007). Light-Induced Energy Dissipation in Iron-Starved Cyanobacteria : Roles of OCP and IsiA Proteins. *The Plant Cell*, *19*(2), Art. 2. https://doi.org/10.1105/tpc.106.045351

Xia, X., Cheung, S., Endo, H., Suzuki, K., & Liu, H. (2019). Latitudinal and Vertical Variation of *Synechococcus* Assemblage Composition Along 170° W Transect From the South Pacific to the Arctic Ocean. *Microbial Ecology*, *77*(2), Art. 2. https://doi.org/10.1007/s00248-018-1308-8

Xia, X., Guo, W., Tan, S., & Liu, H. (2017). *Synechococcus* assemblages across the salinity gradient in a salt wedge estuary. *Frontiers in Microbiology*, *8*, 1254. https://doi.org/10.3389/fmicb.2017.01254

Xia, X., Partensky, F., Garczarek, L., Suzuki, K., Guo, C., Yan Cheung, S., & Liu, H. (2017). Phylogeography and pigment type diversity of *Synechococcus* cyanobacteria in surface waters of the northwestern pacific ocean. *Environmental Microbiology*, *19*(1), Art. 1. https://doi.org/10.1111/1462-2920.13541

Xia, X., Vidyarathna, N. K., Palenik, B., Lee, P., & Liu, H. (2015). Comparison of the seasonal variations of *Synechococcus* assemblage structures in estuarine waters and coastal waters of Hong Kong. *Applied and Environmental Microbiology*, *81*(21), Art. 21. https://doi.org/10.1128/AEM.01895-15

Yan, W., Wei, S., Wang, Q., Xiao, X., Zeng, Q., Jiao, N., & Zhang, R. (2021). Genome Rearrangement Shapes *Prochlorococcus* Ecological Adaptation. *Applied and Environmental Microbiology*, *84*(17), Art. 17. https://doi.org/10.1128/AEM.01178-18

Yeremenko, N., Kouřil, R., Ihalainen, J. A., D'Haene, S., van Oosterwijk, N., Andrizhiyevskaya, E. G., Keegstra, W., Dekker, H. L., Hagemann, M., Boekema, E. J., Matthijs, H. C. P., & Dekker, J. P. (2004). Supramolecular organization and dual function of the IsiA chlorophyll-binding protein in cyanobacteria. *Biochemistry*, *43*(32), Art. 32. https://doi.org/10.1021/bi048772l

Zapata, M., & Garrido, J. L. (1991). Influence of injection conditions in reversed-phase high-performance liquid chromatography of chlorophylls and carotenoids. *Chromatographia*, *31*(11), 589-594. https://doi.org/10.1007/BF02279480

Zhang, P., Allahverdiyeva, Y., Eisenhut, M., & Aro, E.-M. (2009). Flavodiiron Proteins in Oxygenic Photosynthetic Organisms : Photoprotection of Photosystem II by Flv2 and Flv4 in *Synechocystis* sp. PCC 6803. *PLOS ONE*, *4*(4), e5331. https://doi.org/10.1371/journal.pone.0005331

Zinser, E. R., Coe, A., Johnson, Z. I., Martiny, A. C., Fuller, N. J., Scanlan, D. J., & Chisholm, S. W. (2006). *Prochlorococcus* ecotype abundances in the North Atlantic Ocean as revealed by an improved quantitative PCR method. *Applied and Environmental Microbiology*, *72*(1), Art. 1. https://doi.org/10.1128/AEM.72.1.723-732.2006

Zwirglmaier, K., Heywood, J. L., Chamberlain, K., Woodward, E. M. S., Zubkov, M. V., & Scanlan, D. J. (2007). Basin-scale distribution patterns of picocyanobacterial lineages in the Atlantic Ocean. *Environmental Microbiology*, *9*(5), Art. 5. https://doi.org/10.1111/j.1462-2920.2007.01246.x

Zwirglmaier, K., Jardillier, L., Ostrowski, M., Mazard, S., Garczarek, L., Vaulot, D., Not, F., Massana, R., Ulloa, O., & Scanlan, D. J. (2008). Global phylogeography of marine *Synechococcus* and *Prochlorococcus* reveals a distinct partitioning of lineages among oceanic biomes. *Environmental Microbiology*, *10*(1), 147-161. https://doi.org/10.1111/j.1462-2920.2007.01440.x

Annexes

Annexe A : Cyanorak *v2.1* : a scalable information system dedicated to the visualization and expert curation of marine and brackish picocyanobacteria genomes

Garczarek L., Guyet U., Doré H., Farrant G.K., Hoebeke M., Brillet-Guéguen L., Bisch A., Ferrieux M., Siltanen K., Corre E., Le Corguillé G., Ratin M., Pitt F.D., Ostrowki M., Conan M., Siegel A., Labadie L., Aury J-M., Wincker P., Scanlan D.J. and Partensky F. (2020). Cyanorak v2.1 : a scalable information system dedicated to visualization and expert curation of marine and brackish picocyanobacteria genomes. Nucleic Acids Research, 2021, Vol. 49, Database issue D667–D676

Annexe B : Global phylogeography of marine *Synechococcus* in coastal areas reveals strikingly different communities than in the open ocean

Doré H., Leconte J., Guyet U., Breton S., Farrant G.K., Demory D., Ratin M., Hoebeke M., Corre E., Pitt F.D., Ostrowski M., Scanlan D.J., Partensky F., Six C. and Garczarek L. (submitted to PNAS).

Annexe C : Composition des milieux de cultures utilisés pour cultiver les souches de *Synechococcus* au cours de cette thèse

Annexe A : Cyanorak *v2.1* : a scalable information system dedicated to the visualization and expert curation of marine and brackish picocyanobacteria genomes

Published online 30 October 2020

Nucleic Acids Research, 2021, Vol. 49, Database issue ***D667–D676***
doi: 10.1093/nar/gkaa958

Cyanorak v2.1: a scalable information system dedicated to the visualization and expert curation of marine and brackish picocyanobacteria genomes

Laurence Garczarek[1,*,†], Ulysse Guyet[1,†], Hugo Doré[1], Gregory K. Farrant[1,2], Mark Hoebeke[2], Loraine Brillet-Guéguen[2,3], Antoine Bisch[1,2], Mathilde Ferrieux[1], Jukka Siltanen[2], Erwan Corre[2], Gildas Le Corguillé[2], Morgane Ratin[1], Frances D. Pitt[4], Martin Ostrowski[4], Maël Conan[5], Anne Siegel[6], Karine Labadie[7], Jean-Marc Aury[7], Patrick Wincker[8], David J. Scanlan[4] and Frédéric Partensky[1]

[1]Sorbonne Université & CNRS, UMR 7144 'Adaptation & Diversity in the Marine Environment' (AD2M), Station Biologique de Roscoff (SBR), 29680 Roscoff, France, [2]CNRS & Sorbonne Université, FR 2424, ABiMS Platform, Station Biologique de Roscoff (SBR), F-29680 Roscoff, France, [3]Sorbonne Université & CNRS, UMR 8227 'Integrative Biology of Marine Models' (LBI2M), Station Biologique de Roscoff (SBR), F-29680 Roscoff, France, [4]University of Warwick, School of Life Sciences, Coventry CV4 7AL, UK, [5]Université de Rennes 1, INSERM, EHESP, IRSET, F-35043 Rennes, France, [6]Université de Rennes 1, INRIA, CNRS, IRISA, F-35000 Rennes, France, [7]Genoscope, Institut de biologie François-Jacob, Commissariat à l'Energie Atomique (CEA), Université Paris-Saclay, F-91000 Evry, France and [8]Génomique Métabolique, Genoscope, Institut de biologie François Jacob, CEA, CNRS, Université d'Évry, Université Paris-Saclay, F-91000 Evry, France

Received July 23, 2020; Revised September 22, 2020; Editorial Decision October 07, 2020; Accepted October 28, 2020

ABSTRACT

Cyanorak v2.1 (http://www.sb-roscoff.fr/cyanorak) is an information system dedicated to visualizing, comparing and curating the genomes of *Prochlorococcus*, *Synechococcus* and *Cyanobium*, the most abundant photosynthetic microorganisms on Earth. The database encompasses sequences from 97 genomes, covering most of the wide genetic diversity known so far within these groups, and which were split into 25,834 clusters of likely orthologous groups (CLOGs). The user interface gives access to genomic characteristics, accession numbers as well as an interactive map showing strain isolation sites. The main entry to the database is through search for a term (gene name, product, etc.), resulting in a list of CLOGs and individual genes. Each CLOG benefits from a rich functional annotation including EggNOG, EC/K numbers, GO terms, TIGR Roles, custom-designed Cyanorak Roles as well as several protein motif predictions. Cyanorak also displays a phyletic profile, indicating the genotype and pigment type for each CLOG, and a genome viewer (Jbrowse) to visualize additional data on each genome such as predicted operons, genomic islands or transcriptomic data, when available. This information system also includes a BLAST search tool, comparative genomic context as well as various data export options. Altogether, Cyanorak v2.1 constitutes an invaluable, scalable tool for comparative genomics of ecologically relevant marine microorganisms.

INTRODUCTION

The regular decrease in sequencing costs associated with the rapid development of Next Genome Sequencing (NGS) technologies has led to the multiplication of microbial genomes (1,2), making possible extensive comparative genomics studies. Genomes are generally annotated using gene calling programs, such as e.g. RAST (3) or Prokka (4), which can provide fairly reliable annotations for the most conserved core genes involved in general metabolism (e.g. ribosomal proteins, Krebs or Calvin cycle enzymes, DNA

*To whom correspondence should be addressed. Tel: +33 298 292 538; Fax: +33 298 292 324; Email: laurence.garczarek@sb-roscoff.fr
†The authors wish it to be known that, in their opinion, the first two authors should be regarded as joint First Authors.
Present addresses:
Martin Ostrowski, Climate Change Cluster, University of Technology, Broadway, NSW 2007, Australia.
Hugo Doré, Institute for Collaborative Biotechnologies and Department of Ecology, Evolution, and Marine Biology, University of California, Santa Barbara, Santa Barbara, California, USA.

replication, tRNA, etc.) or more specific but well characterized functions shared by many sequenced organisms (chlorophyll biosynthesis, nitrogen fixation, etc.). However, these automatic annotations are much less reliable for the least conserved accessory genes, such as those encoding enzymes responsible for cell wall biosynthesis that are often multi-domain, with highly variable domain composition, or those coding for species- or even strain-specific functions (e.g. biosynthesis of secondary metabolites, carotenoids, etc.). Thus, even though an initial step of automatic annotation is mandatory, functional annotation of predicted coding sequences (CDS) still requires extensive expert human curation to be reliable, especially for non-model organisms. With the exponential increase of newly sequenced genomes, manually curating individual genomes is however a highly time-consuming and inefficient approach. A smart alternative is to curate several phylogenetically related genomes at a time, after gathering sequences into Clusters of Likely Orthologous Genes (CLOGs), i.e. genes that exhibit reciprocal best hits to one another and are hypothesized to have the same function in the different members of the dataset (5,6). This strategy, notably used in the NCBI's 'prokaryotic genome annotation pipeline' (7) for annotating new genomes or re-annotating older genomes before inclusion in the RefSeq database, allows propagating rich, functional annotations made at CLOG level to all proteins composing the CLOG and makes it possible to unify and standardize these annotations across all sequenced strains.

Here we present Cyanorak v2.1, an information system based on CLOGs that is dedicated to the annotation, comparison and visualization of picocyanobacterial genomes. Initially created in the mid-2000s by A. Dufresne and coauthors to compare the first 14 genomes of marine and brackish picocyanobacteria (8), the Cyanorak database has significantly increased since then and relies on a completely redesigned and tremendously enriched information system (v2.1) which, contrary to Cyanorak v1, is scalable, i.e. conceived to allow addition of more genomes. The current database encompasses 95 genomes and two metagenome-assembled genomes (MAGs), including 31 newly released *Synechococcus* and *Cyanobium* genomes (9), which have been closed using a custom-designed assembly and scaffolding pipeline (10). All strains whose genomes have been included in the Cyanorak v2.1 database belong to Cyanobacteria Subsection I, Cluster 5 *sensu* Herdman (11), a short-rod shaped group that forms a deep monophyletic branch within this ancient phylum (12). The common ancestor of all Cluster 5 members is thought to have diverged from other cyanobacteria about 1 Gy ago, during the Mesoproterozoic period (13). Members of Cluster 5 are also called 'α-cyanobacteria', based on the occurrence in their cytoplasm of specific α-type carboxysomes, phylogenetically and structurally closer to that of thiobacilli than to the β-type carboxysomes found in all other cyanobacteria, so-called 'β−cyanobacteria' (14). Cluster 5 itself is split into four major groups, including the monophyletic, strictly marine *Prochlorococcus* lineage and three deeply branching groups, called sub-clusters (SC) 5.1 through 5.3 (8,15,16). Based on the comparison of 81 non-redundant genomes, Doré and coworkers recently suggested to rename them *Ca.* Marinosynechococcus (SC 5.1), *Cyanobium* (SC 5.2) and *Ca.* Juxtasynechococcus (SC 5.3) (9). SC 5.1 is the most diversified of all these lineages, with about 10 phylogenetically distinct clades based on 16S rDNA phylogeny (16) and 11 to 16 using higher resolution markers (17,18). Members of these clades are all strictly marine except clade VIII that specifically gathers halotolerant strains. SC 5.2 also mostly encompasses halotolerant strains as well as one freshwater representative (*Cyanobium gracile* PCC 6307). While members of SC 5.3 were initially thought to be strictly marine (8,16), freshwater members of this group were recently discovered in various lakes (19,20). The current version of Cyanorak v2.1 encompasses representatives of most of the lineages (SC and clades) known to date in Cluster 5, with the exception of the newly described freshwater members of SC 5.3 as well as members of the yet-uncultured SC 5.1 clades EnvA and EnvB (18,21). Since all Cluster 5 members possess a similar morphology (spherical to rod shaped) and lifestyle (aquatic, non-diazotrophic oxyphototrophs; (11)) and form a monophyletic branch within the Cyanobacteria phylum, we assume that members of most CLOGs defined within this genetically homogeneous group exhibit the same function, though this may not be true when considering more distant organisms, notably cyanobacteria from other clusters that exhibit different lifestyles. Here, we describe the construction of the Cyanorak v2.1 database, the rich functional annotation available for each CLOG and the tools and plugins that were developed to explore the genomic diversity of this ecologically relevant group of organisms, which has recently become one of the main microbial models in marine ecology.

MATERIALS AND METHODS

Clustering of likely orthologous sequences and CLOG curation

Following the construction of a first series of CLOGs based on the 14 first sequenced picocyanobacterial genomes (8), Cyanorak v1 CLOG numbers have been cited in a number of publications from our group (see, e.g. (22–30)). In order to preserve at best these preexisting CLOG numbers after the addition of 83 new genomes either retrieved from Genbank or newly sequenced at our initiative (Figure 1; (9)), all CDS from the 97 genomes were first clustered using all-against-all BLASTP+ comparison (31) and the OrthoMCL clustering algorithm (32) with an e-value threshold of 10^{-5} and new CLOGs were then mapped to previously defined Cyanorak v1 CLOGs. New CLOGs containing all sequences from a v1 CLOG plus additional sequences from new genomes as well as manually curated CLOGs were assigned the previous v1 CLOG numbers. All other sequences were then tentatively assigned to preexisting CLOGs using HMMER (33) with an e-value threshold of 10^{-20} and remaining sequences were finally clustered using OrthoMCL to define new CLOGs or left as singletons in individual CLOGs if not clustered.

While Cyanorak v1 contained only CDS, these steps also allowed us to generate CLOGs for rRNAs, tRNAs, tmRNAs using all-against-all BLASTN+ and the OrthoMCL algorithm using the same threshold as for CDS (32). After this semi-automatic clustering step, a large number

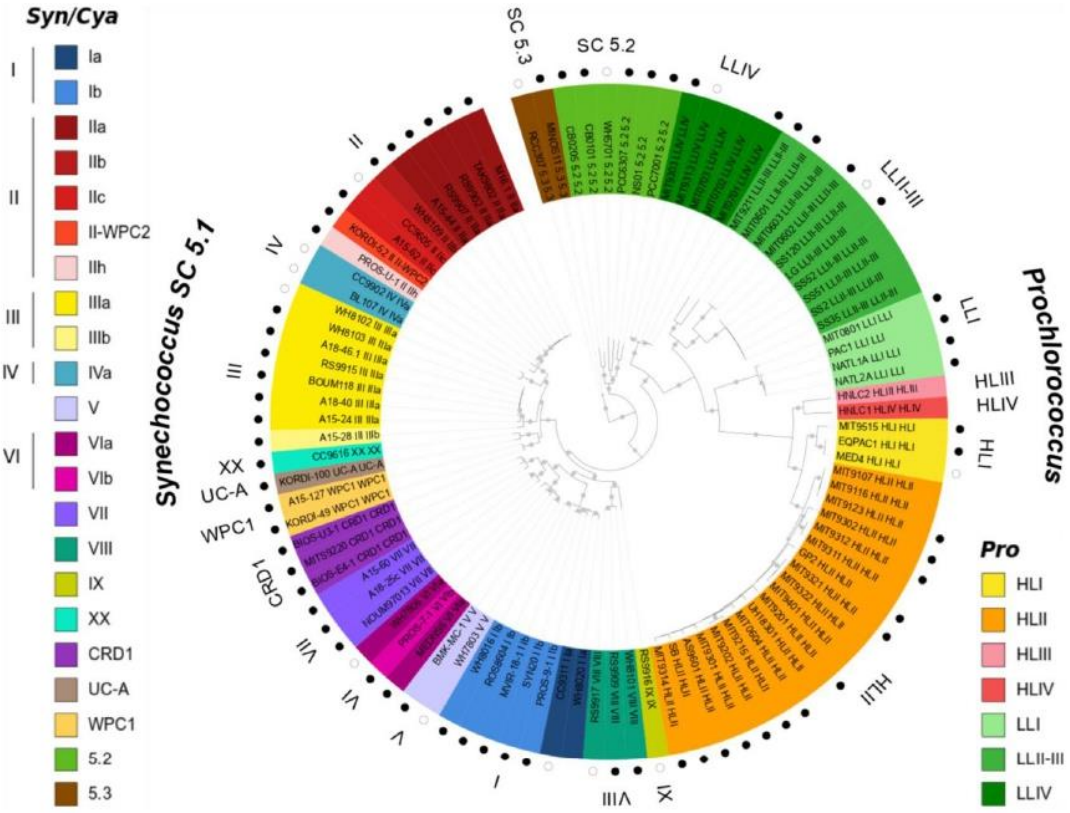

Figure 1. Maximum likelihood tree based on 579 core proteins showing the phylogenetic relatedness of the 97 genomes of the current Cyanorak v2.1 database. Grey dots indicate bootstrap support over 70%. Sequences were named after strain name followed by clade and subclade when available (subclade assignments as in 21) and the background colors correspond to the finest possible taxonomic resolution obtained for each strain using the *petB* marker gene (left hand side legend for *Synechococcus*, right hand side legend for *Prochlorococcus*). The 81 non-redundant, high quality genomes used by Doré *et al.* (9) for comparative genomics are indicated by a circle surrounding the tree and among them the 14 first genomes used in the previous version of Cyanorak (v1) are shown as empty circles.

of CLOGs (~4300, i.e. 17% of all CLOGs; Supplementary Figure S1) were further manually curated in order to (i) check and complement the functional description of CLOGs and (ii) verify that members of a given CLOG were truly orthologs, based on their phyletic pattern, alignments and phylogenetic trees. Paralogs were moved into different CLOGs when they grouped together into different branches as the *bona fide* orthologs. In order to refine assessment of the core genome (9), >1750 genes missed by gene prediction software tools, either because they were too short (e.g. *petM*, *psbM*) or partially overlapping with other genes notably in the case of long 3′-3′ overlaps (e.g. for *pyrB-ndbA or panB-hemN*), were also manually added to different genomes. Furthermore, many over-predictions of ORFs (e.g. short CDS of unknown function totally overlapping long annotated CDS) were eliminated, and this even from genomes retrieved from Genbank. Finally, many start positions were corrected from obviously too short or too long sequences, based on an alignment of all CLOG members and/or 5′-end extensions using TBLASTN searches.

Implementation of the Cyanorak v2.1 information system

The development of Cyanorak v2.1 was done in two steps. The first version (v2.0) of this information system included a history feature to keep track of every change and allowing to readily revert any change at a very granular level as well as enabling curators to check the journal of changes undergone by every gene or CLOG. This private version of the information system is still currently used for the manual curation of the database. However, in order to give the general public access to the curated data with the best possible response times, especially now that the number of genomes and MAG's in the database has risen to 97, a completely new version (v2.1) of the Cyanorak information system, devoid of the history feature, was recently developed and proved to be two to three times faster than v2.0. Two instances of the Cyanorak information system therefore co-exist on our server: (i) the restricted access, editable Cyanorak v2.0 version allowing expert curators to edit most fields of the 'CLOG' and 'gene' pages and (ii) the publicly accessible, non-editable Cyanorak v2.1 version, the latter corresponding to the state of the Cyanorak database at the time of publication of a comparative genomics study of the 81 non-redundant, high quality genomes of the database (9) and of an extensive transcriptomic analysis of the response of the *Synechococcus* sp. WH7803 strain to various environmental stresses (34). This public version will be regularly updated in the future, with concomitant changes in version number, when new whole genome sequences (WGS), single

amplified- and metagenome assembled- genomes (SAGs, MAGs) and/or transcriptomes either retrieved from public databases (e.g. Genbank) or generated by our group will be added to the Cyanorak database and described in the frame of forthcoming publications. A restricted access, editable instance based on the v2.1 implementation is currently being developed and should replace the current v2.0 instance in the near future for expert curation purposes.

On a technical level, the bulk of Cyanorak v2.1 has been implemented using the Java programming language, with an extensive use of the Spring framework. The data itself is stored in a relational database (PostgreSQL), and the link between the application and the database is done through an object relational mapper (Hibernate). A small set of Python auxiliary tools has also been developed, mostly to prepare the data for import, to post-process exported data or to perform specific batch updates.

RESULTS

General characteristics of the database

Built from 97 picocyanobacterial genomes, including 43 *Prochlorococcus* and 54 *Synechococcus/Cyanobium*, which are representative of the wide genetic and pigment diversity existing within these genera (Figure 1), Cyanorak v2.1 encompasses 252,176 genes that were split into 25,834 CLOGs. A plot of the distribution of the number of sequences per CLOG expectedly shows that the most frequent categories are CLOGs with one sequence, i.e. unique genes (15,283 CLOGs), and CLOGs with few (2-5) members (Supplementary Figure S1). Although most of these CLOGs (e.g. 91% of unique genes) are annotated as 'hypothetical' or 'conserved hypothetical' proteins, a number of them display a more precise functional annotation, since they share some similarities to genes or domains of known function, with among the most abundant: glycosyltransferases, restriction-modification system proteins, integrases, transposases, methyltransferases, NAD-dependent epimerases/dehydratases and tetratricopeptide repeat (TPR) family proteins. The next most abundant CLOG category (611 CLOGs) is the one containing 97 sequences, which corresponds to the picocyanobacterial core genome *sensu stricto*. As expected, this number is significantly lower than the picocyanobacterial strict core gene set (911 genes) estimated by Doré *et al.* (9) using the 81 non-redundant, high-quality genomes of the Cyanorak database. Yet, given that some of the 97 genomes or MAG's, especially those not included in this 81-genome set, are incomplete and/or contain frameshifted genes (in this case, the two or more gene fragments resulting from a frameshift have been put into the same CLOG), many CLOGs contain a number of genes that is close but not exactly equal to 97. So, the picocyanobacterial core genome *sensu lato* is likely much larger than 611 genes, and we estimated it using a relaxed definition of core genes (CLOG is considered as core of a taxonomic group if it is present in $\geq$90% of the strains within this group) to be 1,271 genes. A small number of CLOGs contain a large number of sequences, i.e. between 105 and 337 sequences. These CLOGs most often contain paralogous sequences that cannot be split into different CLOGs based on phylogenetic analyses. These notably include the identical multi-copy genes encoding the photosystem II core proteins D1.2 and D2, porins, AbrB-like transcriptional regulators and the high-affinity phosphate-binding protein PstS.

Cyanorak web interface and tools

The homepage of the Cyanorak v2.1 information system shortly describes the origin of the genomes used to build the CLOGs database, the history of its construction and the main references that used it. The top banner available from all pages encompasses several clickable menus, including the 'organisms page' that lists the different genomes of the database and their characteristics, a 'search page' with different options to access the CLOG or gene pages of interest, a 'BLAST scroll down menu', a JBrowse menu giving access to direct links to the viewer of each genome, as well as several other menus providing useful information about the database (Previous Versions, References, Links, About us, Help).

Organisms page. The 'organisms page' consists of two tables, the first one listing *Prochlorococcus* genomes and the other one *Synechococcus* and *Cyanobium* genomes. They provide taxonomy, pigment type, sequencing center as well as various genomic characteristics (size, GC%, status, accession numbers, number of CDS, etc.) for each genome included in the database. Next to each strain name is a clickable 'J' logo that gives access to the JBrowse page of the corresponding genome (see below). A distribution map of all of the strains drawn with OpenStreetMap® (https://www.openstreetmap.org/) is also available in this section (Figure 2), offering a flexible set of options to focus on individual strains or to select all or a subset of *Prochlorococcus* and *Synechococcus/Cyanobium* strains. Strains collected in nearby locations can also be shown with a single marker to enhance readability. In this section, each strain name in the Table can be clicked to get more detailed information (e.g. isolation site, isolator, environment ontology (ENVO) code, etc.) and also allows the user to export gene and protein sequences in FASTA format as well as whole genomes in Genbank format. In each of these files, the annotation of every gene corresponds to that found on CLOG pages (see below), which was given priority over the initial gene annotation, even if the genome was retrieved from Genbank.

Genomic Search tools. The main entry to the Cyanorak v.2.1 database content is through the 'genomic search' menu, with three possible options. The first one is a 'quick search' of any term mainly through 'cluster number', 'gene names' and 'product descriptions' fields, a term that can be searched either as an exact match or as a pattern in a more complex sentence. For instance, a search for 'dna' in 'pattern' configuration will provide a list of CDS clusters whose gene name annotation includes 'dna' (e.g. *dnaA*, *dnaB*, etc.) as well as a list of products whose description includes DNA (e.g. DNA gyrase, formamidopyrimidine-DNA glycolase, etc.). Search results are organized in three distinct tabs. The first one lists the matching clusters, the second one lists the matching CDS and the third one lists the matching RNA

Figure 2. Map of the isolation sites of the different sequenced strains included in the Cyanorak v2.1 database. Green markers indicate *Prochlorococcus* strains and orange markers *Synechococcus* strains. Each marker can be expanded to reveal a 'call-out' that shows the strain name, pigment type and taxonomy, as shown for the North West Pacific *Prochlorococcus marinus* SB. The Search Data boxes shown on the left hand side of the map allows to search for specific strain(s), genotype, etc.

entries. Each list gives the essential information about every match and provides links to access detailed descriptions of these entries. The 'advanced search' option allows the user to look into any field documented in the CLOG, CDS or RNA pages, including functional categories (e.g. EC or K number, InterPro entries, GO terms, etc.) and to select one, all or a specific set of strains. Finally, the 'phyletic pattern search' option is used to search for CLOGs, CDS and RNA that are shared by a selection of genomes and that can be either present or absent in other strains depending on the selected option. This search option is for instance most useful to identify genes specific to a particular strain combination such as all *Prochlorococcus*, a given clade or a given pigment type.

CLOG page. By clicking on a Cyanorak CLOG number (format: CK_XXXXXXXX) in the result list of any search (see above), the user is sent to a cluster page providing a full description of the function and phyletic pattern of the corresponding CLOG. An indication in the upper right corner of the CLOG page specifies whether the CLOG has been manually annotated, i.e. whether an expert has edited and validated its sequence content and functional annotation. The cluster page contains several fields, including from top to bottom: (i) the corresponding gene identifier in the Cyanorak v1 database (if any), generally corresponding to the last digits of the Cyanorak v2.1 CLOG number, (ii) a gene name and its synonyms (if any) as well as the product description, (iii) functional categories including COG (5) and EggNOG (6) identifiers and their description, CyOG number (as reported in (35)), Enzyme Commission (EC) and K numbers referring to the Kyoto Encyclopedia of Genes and Genomes (KEGG) database (www.kegg.jp), 'TIGR Roles' and custom-designed 'Cyanorak Roles' (see complete description at the end of the Help menu), the latter being largely derived from 'TIGR Roles' but providing more details on photosynthetic and other key cyanobacterial processes, as well as gene ontology (GO) terms and their description; (iv) results of protein domain and motif searches, including TIGRFAMs, PFAMs, ProSite patterns and profiles, as well as InterPro entries, (v) numbers of related CLOGs, i.e. possible paralogs and (vi) a phyletic pattern providing the distribution of the genes in the different genomes, classified by taxonomy (genus, clade and, for *Synechococcus* SC 5.1 strains only, subclades, according to (18)), and indicating the pigment type of the corresponding strain (Supplementary Figure S2, (26,36,37)). The bottom of the page lists ORF_IDs of the different members of the CLOG, with their initial annotation, a useful piece of information when the annotation was made either automatically or by other research groups.

On the top left of the 'cluster page' is a link to the 'genomic context', which displays the four genes upstream and downstream of the selected gene in all members of the CLOG. Two possible representations of the context are accessible through a toggle button: genes are shown either

all at the same size or in relative size (Figure 3A-B). To ease comparisons, the central gene is always represented in the forward direction whatever its original direction in the genome and the context is arranged accordingly. Each CLOG has a given (random) color and background (plain or stripped) and genome context can be regenerated around any gene of the current context by clicking on the ORF_ID of the corresponding gene, while clicking on a CLOG number opens the corresponding CLOG page.

Links at the bottom of the cluster page allow the user to export all sequences of the CLOG at once as an amino acid or nucleotide FASTA file. The descriptor of each sequence in the export is standardized and provides the genus abbreviated to the three first letters (Cya|Syn|Pro); strain name; SC, clade or subclade depending on the finest taxonomic level available for the strain as in (21); pigment type as in (36); Cyanorak ORF_ID; gene positions and strand in the genome; Cyanorak CLOG number and gene name if any (e.g. >Syn_A15–24_IIIa_3c|CK_Syn_A15–24_02629:2153016–2154431:1|CK_00000125|dnaB).

Gene page. By clicking on any gene in the cluster page or the relevant search result tab, the user accesses the 'gene page', which includes most fields previously described for the CLOG page. Specificities compared to the latter include (i) the source and location of the gene, namely the strain name, contig and gene location (position and strand) on the contig, generally consisting of the whole chromosome, (ii) a series of identifiers in Cyanorak and, if relevant, in other databases (Genbank, RefSeq, etc.) and (iii) the gene sequence in nucleotides and (for CDS) in amino acids. It must be stressed that this page contains the initial annotation of the gene (e.g. if the genome was retrieved from Genbank), and the latter often differs from the CLOG annotation which is typically much more extensive, especially if the cluster was manually curated. All genes included in Cyanorak (even when retrieved from public databases) were given, in addition to their initial ORF_ID, a unique Cyanorak ORF_ID with the standardized format CK_Genus_Strain_XXXXX (e.g. CK_Syn_PROS-U-1_00601) in order to normalize gene names and ease the identification of the genome source. Also noteworthy is that the genomes included in Cyanorak, even those that have been sequenced by other groups, have all been manually curated to some extent, including predictions of missing genes or removal of wrong predictions, and thus differ from their counterparts in other public databases (Genbank, RefSeq, etc.) not only regarding their annotation (made at CLOG level) but also their gene content.

BLAST. An indispensable complement to the Cyanorak database is the possibility for users to search any sequence in all genomes or proteomes of the database using two BLAST options available from a BLAST scroll down menu. This includes an implementation of the BLAST algorithm using the SequenceServer graphical interface (38) allowing to BLAST one or several nucleotide or protein sequence(s) against a selection of up to 97 genomes ('Blast a selection') or all genomes ('Blast all'). Results of a BLAST search returns the Cyanorak ORF_ID, the strain taxonomy (at the SC, clades and/or subclade level) and pigment type, the CLOG number as well as the CLOG gene name and product (e.g. CK_Syn_A15–24_00652_III_IIIa_3c CK_00001060!rpoC1!DNA-directed RNA polymerase complex, gamma subunit).

JBrowse page. Clicking on the 'J' logo next to each strain name in the JBrowse page (or 'Organisms' page) gives access to a JBrowse viewer (39) allowing the user to visualize the whole annotated genome and to zoom in to see the local context and detailed annotation of any gene, as derived from the 'CLOG page' (see above, Figure 4). Left clicking on a gene gives access to the detailed functional annotation of the corresponding gene, with hyperlinks to Cyanorak and external functional databases. The genes can be searched by annotation or Cyanorak ORF_ID. A 'select tracks' menu gives access to additional data associated with each genome, when available. These include strict and large core and accessory genomes, gained genes as well as genomic islands, as determined in a recent comparative genomic study of 81 non-redundant picocyanobacteria genomes (9). Also available are operon predictions using ProOpDB (40) and transcriptomic data. The latter can be visualized by bibliography, experiment, acclimation condition (e.g. low or high light) or stress conditions (e.g. exposure to low temperature or UV radiation). In the current version of Cyanorak, transcriptomic data are available for *Synechococcus* sp. WH7803 (29,34) and a number of other *Prochlorococcus* or *Synechococcus* strains studied by other groups, but in this case expression data are only displayed as log2(Fold Change).

Exports. Various exports are available from different pages of the Cyanorak v2.1 information system, including strain and genome characteristics from the organism page, annotated complete genomes from the individual strain pages, individual fasta protein and nucleotide sequences from gene pages and multifasta protein and nucleotide sequences from cluster pages.

DISCUSSION

As the most ancient photosynthetic organisms, cyanobacteria had a key role in the oxidation of the primitive Earth atmosphere (41) but also in the primary endosymbiosis, an event that led to the advent of green and red algae and ultimately to all eukaryotic oxygenic phototrophs (42). Besides their relevance in evolutionary biology, cyanobacteria are also of great interest in ecology, given their ubiquity and abundance in many ecosystems, including oceans and deserts (43) and the noxious impacts of their bloom-forming toxic representatives in freshwater environments (44). For all these reasons, but also thanks to their fairly small genomes sizes, ranging from 1.4 to 11.6 Mb, these microorganisms have been the subject of many sequencing projects (8,9,12,45), which in turn triggered the generation of a number of dedicated genome databases. The oldest of these databases is Cyanobase (http://genome.microbedb.jp/CyanoBase), initially created to provide access to the first sequenced cyanobacterial genome, the model freshwater strain *Synechocystis* sp. PCC6803 (46,47). This database has since then been extended to host many more recently sequenced freshwater and marine cyanobacterial genomes

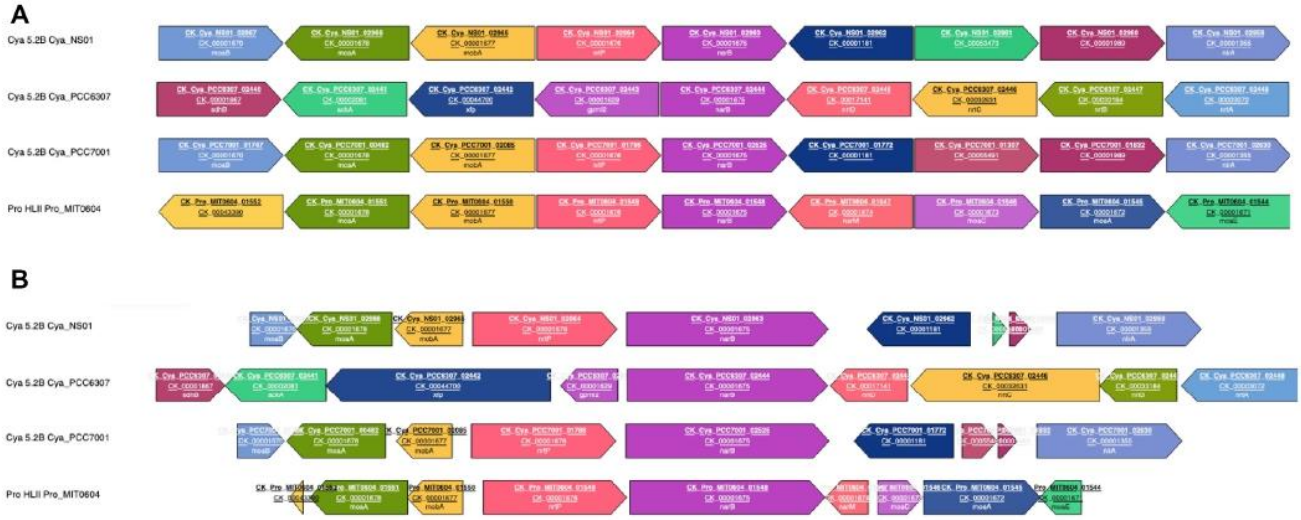

Figure 3. Genomic context of the *narB* gene encoding the nitrate reductase. (**A**) Genes represented at the same size. (**B**) Genes represented in relative size.

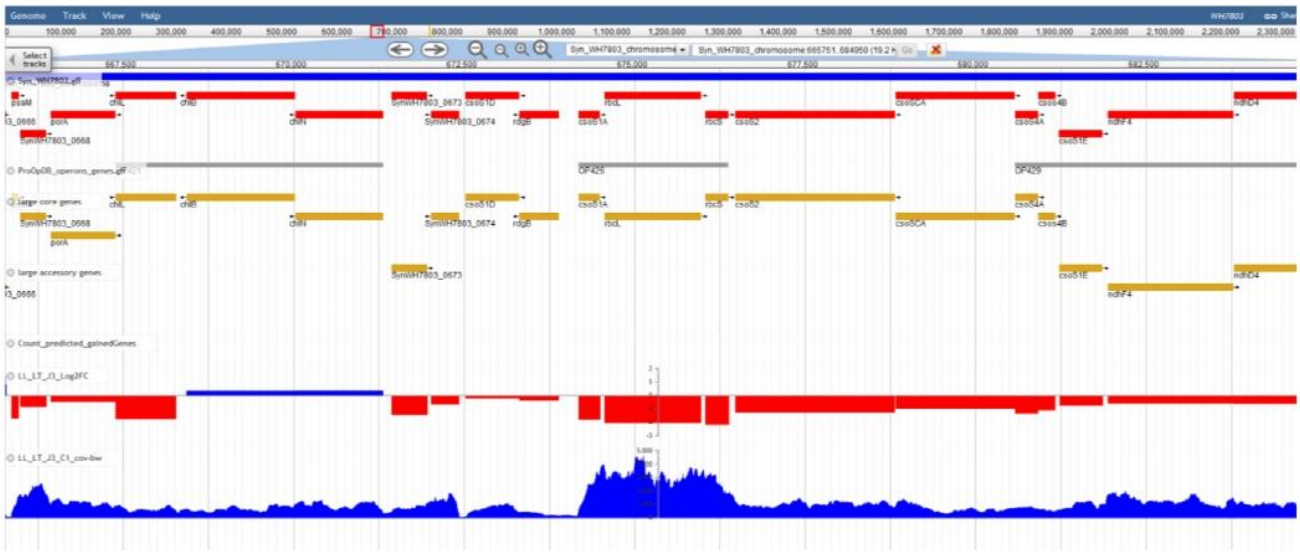

Figure 4. An example of genome visualization using the JBrowse plugin of Cyanorak v2.1.

(376 entries, including 86 complete genomes in April 2019), but has been 'under maintenance' since summer 2019. Although this database provides much useful genomic information, this is not a CLOG database and is therefore not designed to make extensive genomic comparisons. Also worth noting, CyanoClust (http://gclust.c.u-tokyo.ac.jp/CyanoClust/) is a database of homologous groups initially limited to cyanobacteria and plastids and which was more recently extended to heterotrophic bacteria and Archaea (48). It provides lists of orthologs generated by the program Gclust, but functional annotation is limited to the original product description and fasta sequence of individual members of each CLOG. The database that was most similar to Cyanorak v2.1, was the '*Prochlorococcus* portal' a.k.a. 'Proportal' (49). It was also based on CLOGs computed from a number of *Prochlorococcus* and marine *Synechococcus* genomes, with a strong focus on the former genus. Since 2018, this database has however been merged to the Joint Genome Institute Integrated Microbial Genomes and Microbiomes (JGI-IMG) and renamed 'IMG-Proportal' (http://img.jgi.doe.gov/cgi-bin/proportal/main.cgi). The latter site lists all publicly available genomic, transcriptomic, metagenomic and population data on *Prochlorococcus*, *Synechococcus* and their cyanophages, which can be analyzed using the IMG's data warehouse and comparative analysis tools (50), but the initial CLOG-centered organization of Proportal has been lost.

Compared to these databases, Cyanorak is more function-oriented and aims to provide rich and up-to-date functional annotations of CLOGs, with a preference for those derived from genes or proteins that were characterized in cyanobacteria. In contrast to most large

CLOG databases currently available, such as COG (5) or EggNOG (6) that encompass very distantly related organisms, Cyanorak is focused on *Prochlorococcus* and marine *Synechococcus/Cyanobium*, i.e. a monophyletic and homogenous group of microorganisms sharing a similar morphology and lifestyle, making more reliable the assumption that reciprocal best hits in different genomes truly correspond to orthologs. Thanks to this CLOG-based approach, the continuous expert curation efforts employed since the mid-2000's have allowed us to improve the annotation of all genomes of the Cyanorak database, even those initially retrieved from Genbank. Furthermore, a number of genes that were missing in these often automatically annotated genomes have been added, while many ORF over-predictions have been suppressed, so that both gene content and annotations differ between genomes in Cyanorak and their counterparts in large public databases.

Another important asset of Cyanorak is the variety of tools for exploring and exporting genomes from the database. For instance, one can search for CLOGs common or specific to a particular phylogenetic group of interest, an approach that can provide clues to identify genes encoding a specific function. For instance, searching Cyanorak for homologs of MpeZ, an enzyme involved in type IV chromatic acclimation (CA4), i.e. a reversible pigmentation change occurring in some *Synechococcus* strains when shifted from blue to green light (26), allowed us to identify a second type of chromatic acclimation, so-called CA4-B, which possess MpeW, a MpeZ homolog. Both the *mpeZ* and *mpeW* genes are located in a specific genomic island, but gene content, organization and genomic context differ between the CA4-A and CA4-B islands. Another interesting example concerns the chlorophyll (Chl) biosynthesis pathway. It is well known that *Prochlorococcus* lacks monovinyl-Chl *a*, which is replaced by divinyl-Chl *a,* even in reaction centers (51,52). Comparing the genomic context of the core *malQ* gene (encoding a glucanotransferase) between all genomes of the Cyanorak database shows that in marine *Synechococcus* this gene is always preceded by an enzyme that reduces divinyl-Chl *a* into mononyl-Chl *a*, but surprisingly there are two possible mutually exclusive reductase genes depending on strains, either *dvr* (53) in strains from clades I-IV, VII, CRD1, WPC1 XX and UC-A or *cvrA* (54) in all other *Synechococcus/Cyanobium* lineages (Supplementary Figure S3). Dvr and CvrA possess the same enzymatic function but share no sequence identity, and are thus analogs. In *Prochlorococcus* genomes, neither *dvr* nor *cvrA* are found upstream of *malQ*, and none of these genes is found elsewhere in the genome, explaining why these strains are all incapable of producing monovinyl-Chl *a*.

Cyanorak v2.1 is also a repository for a variety of transcriptomic data, the interpretation of which relies heavily on the quality of genome annotation. In Cyanorak, these data are connected to the genome database through a JBrowse interface, which also gives access to genomic features such as predicted operons, gained genes or the core or accessory nature of genes, which can be used to further refine the interpretation of gene expression data (see e.g. (34)).

FUTURE DEVELOPMENTS

The current version of the database includes rRNAs, tRNAs and tmRNAs, but still no small RNAs (sRNAs), so we plan to add such information in a forthcoming release, at least for the most conserved sRNAs. Another planned improvement of the database concerns the curation of gene starts. Although many gene starts have been corrected manually, amino acid alignments readily made from exports of CLOG pages show that a large number of those starts are still mis-predicted, leading to seemingly too short or too long sequences in a number of genomes. We will thus develop an application that allows to automatically correct likely wrong starts, at least when N-termini are not too variable. Finally, new fields will be added on the CLOG page, including for instance orthologs of each CLOG in relevant biological models, such as the freshwater cyanobacteria *Synechocystis* sp. PCC 6803 and *Synechococcus* sp. PCC 7942, the heterotrophic bacteria *Escherichia coli* and *Bacillus subtilis* or the higher plant *Arabidopsis thaliana*.

Future versions of the Cyanorak database will include genomes newly released from public data as well as a number of transcriptomes either generated by our team or by external users, providing that they follow instructions described in the Cyanorak help file. It must be stressed that the aim of Cyanorak is not to host all of the rapidly-growing number of incomplete SAGs and MAGs, apart from a few representative uncultivated lineages (e.g. *Synechococcus* EnvA/B, *Prochlorococcus* HLIII-VI). Thus, a pipeline is currently being developed to easily transfer the rich functional annotation of the Cyanorak genomes to these new partial genomic sequences and, more generally, to any picocyanobacterial environmental reads retrieved from metagenomes and metatranscriptomes. A few previous studies, where annotations made in Cyanorak were used to analyze omic data, have notably allowed us to (i) compare the nitrogen assimilation capacities of *Prochlorococcus* populations from inside and outside the Agulhas rings in the South Atlantic Ocean (55), (ii) highlight differences between *Prochlorococcus* and *Synechococcus* populations in their adaptation and acclimation responses to iron deficiency in the vicinity of the Marquesas island (56) and (iii) demonstrate through the global oceanic distribution of desaturase genes the key role of these enzymes involved in the modulation of membrane fluidity for the colonization of different thermal niches by distinct *Synechococcus* lineages (28). We envision that Cyanorak will become a reference genome database for the taxonomic and functional annotation of not only newly released genomes and transcriptomes of marine picocyanobacteria, but also the ever-increasing marine meta-omes, which given the natural abundance and ubiquity of these microorganisms in the marine environment constitute a significant part of all reads retrieved from the upper lit layer of marine waters.

DATA AVAILABILITY

The Cyanorak v2.1 information system is available at http://www.sb-roscoff.fr/cyanorak.

SUPPLEMENTARY DATA

Supplementary Data are available at NAR Online.

ACKNOWLEDGEMENTS

This paper is dedicated to the memory of our esteemed colleague Christophe Caron who was instrumental in launching the Cyanorak v2.1 project. We warmly thank Alexis Dufresne, who designed the first version (v1) of the database as well as Michelle G. Giglio and the Institute of Genome Science (IGS) staff for performing the initial automatic annotation of 32 *Synechococcus* and *Cyanobium* genomes using the IGS Manatee pipeline. We also thank Justine Pittera, Théophile Grébert, Garance Monier and Théo Sciandra for participating in the curation of the Cyanorak v2.1 database, the Roscoff Culture Collection and Sophie Mazard for maintaining and isolating some of the *Synechococcus* strains used in this study as well as the ABiMS platform for providing computational support for this work.

FUNDING

French 'Agence Nationale de la Recherche' Programs SAMOSA [ANR-13-ADAP-0010]; CINNAMON [ANR-17-CE2-0014-01]; IFB [ANR-11-INBS-0013]; Genoscope project METASYN, the Natural Environment Research Council [NE/I00985X/1]; European Union's Seventh Framework Programs FP7 MicroB3 [287589]; MaCuMBA [311975]. Funding for open access charge: Agence National de la recherche program CINNAMON [ANR-17-CE2-0014-01].
Conflict of interest statement. None declared.

REFERENCES

1. Nordberg,H., Cantor,M., Dusheyko,S., Hua,S., Poliakov,A., Shabalov,I., Smirnova,T., Grigoriev,I.V. and Dubchak,I. (2014) The genome portal of the Department of Energy Joint Genome Institute: 2014 updates. *Nucleic Acids Res.*, **42**, D26–D31.
2. Vallenet,D., Engelen,S., Mornico,D., Cruveiller,S., Fleury,L., Lajus,A., Rouy,Z., Roche,D., Salvignol,G., Scarpelli,C. *et al.* (2009) MicroScope: a platform for microbial genome annotation and comparative genomics. *Database*, **2009**, bap021.
3. Aziz,R.K.R.K., Bartels,D., Best,A.A., DeJongh,M., Disz,T., Edwards,R.A.R.A., Formsma,K., Gerdes,S., Glass,E.M.E.M., Kubal,M. *et al.* (2008) The RAST Server: rapid annotations using subsystems technology. *BMC Genomics*, **9**, 75.
4. Seemann,T. (2014) Prokka: rapid prokaryotic genome annotation. *Bioinformatics*, **30**, 2068–2069.
5. Galperin,M.Y., Makarova,K.S., Wolf,Y.I. and Koonin,E.V. (2015) Expanded microbial genome coverage and improved protein family annotation in the COG database. *Nucleic Acids Res.*, **43**, D261–D269.
6. Huerta-Cepas,J., Szklarczyk,D., Heller,D., Hernández-Plaza,A., Forslund,S.K., Cook,H., Mende,D.R., Letunic,I., Rattei,T., Jensen,L.J. *et al.* (2019) EggNOG 5.0: a hierarchical, functionally and phylogenetically annotated orthology resource based on 5090 organisms and 2502 viruses. *Nucleic Acids Res.*, **47**, D309–D314.
7. Tatusova,T., Dicuccio,M., Badretdin,A., Chetvernin,V., Nawrocki,E.P., Zaslavsky,L., Lomsadze,A., Pruitt,K.D., Borodovsky,M. and Ostell,J. (2016) NCBI prokaryotic genome annotation pipeline. *Nucleic Acids Res.*, **44**, 6614–6624.
8. Dufresne,A., Ostrowski,M., Scanlan,D.J.J., Garczarek,L., Mazard,S., Palenik,B.P.P., Paulsen,I.T.T., de Marsac,N.T.T., Wincker,P., Dossat,C. *et al.* (2008) Unraveling the genomic mosaic of a ubiquitous genus of marine cyanobacteria. *Genome Biol.*, **9**, R90.
9. Doré,H., Farrant,G.K., Guyet,U., Haguait,J., Humily,F., Ratin,M., Pitt,F.D., Ostrowski,M., Six,C., Brillet-Guéguen,L. *et al.* (2020) Evolutionary mechanisms of genome diversification in marine picocyanobacteria. *Front. Microbiol.*, **11**, 567431.
10. Farrant,G.K., Hoebeke,M., Partensky,F., Andres,G., Corre,E. and Garczarek,L. (2015) WiseScaffolder: an algorithm for the semi-automatic scaffolding of next generation sequencing data. *BMC Bioinformatics*, **16**, 281.
11. Herdman,M., Castenholz,R.W., Waterbury,J.B. and Rippka,R. (2001) Form-genus XIII. *Synechococcus.* In: Boone,D.R. and Castenholz,R.W. (eds). *Bergey's Manual of Systematic Bacteriology*. Springer-Verlag, NY, Vol. **1**, pp. 508–512.
12. Shih,P.M., Wu,D., Latifi,A., Axen,S.D., Fewer,D.P., Talla,E., Calteau,A., Cai,F., Tandeau de Marsac,N., Rippka,R. *et al.* (2013) Improving the coverage of the cyanobacterial phylum using diversity-driven genome sequencing. *Proc. Natl. Acad. Sci. U.S.A.*, **110**, 1053–1058.
13. Sánchez-Baracaldo,P. (2015) Origin of marine planktonic cyanobacteria. *Sci. Rep.*, **5**, 17418.
14. Badger,M.R. and Price,G.D. (2003) CO_2 concentrating mechanisms in cyanobacteria: molecular components, their diversity and evolution. *J. Exp. Bot.*, **54**, 609–622.
15. Huang,S., Wilhelm,S.W., Harvey,H.R., Taylor,K., Jiao,N. and Chen,F. (2012) Novel lineages of *Prochlorococcus* and *Synechococcus* in the global oceans. *ISME J.*, **6**, 285–297.
16. Scanlan,D.J., Ostrowski,M., Mazard,S., Dufresne,A., Garczarek,L., Hess,W.R., Post,A.F., Hagemann,M., Paulsen,I. and Partensky,F. (2009) Ecological genomics of marine picocyanobacteria. *Microbiol. Mol. Biol. Rev.*, **73**, 249–299.
17. Ahlgren,N.A. and Rocap,G. (2012) Diversity and distribution of marine *Synechococcus*: multiple gene phylogenies for consensus classification and development of qPCR assays for sensitive measurement of clades in the ocean. *Front. Microbiol.*, **3**, 213.
18. Mazard,S., Ostrowski,M., Partensky,F. and Scanlan,D.J. (2012) Multi-locus sequence analysis, taxonomic resolution and biogeography of marine *Synechococcus*. *Environ. Microbiol.*, **14**, 372–386.
19. Cabello-Yeves,P.J., Haro-Moreno,J.M., Martin-Cuadrado,A.B., Ghai,R., Picazo,A., Camacho,A. and Rodriguez-Valera,F. (2017) Novel *Synechococcus* genomes reconstructed from freshwater reservoirs. *Front. Microbiol.*, **8**, 1151.
20. Cabello-Yeves,P.J., Picazo,A., Camacho,A., Callieri,C., Rosselli,R., Roda-Garcia,J.J., Coutinho,F.H. and Rodriguez-Valera,F. (2018) Ecological and genomic features of two widespread freshwater picocyanobacteria. *Environ. Microbiol.*, **20**, 3757–3771.
21. Farrant,G.K., Doré,H., Cornejo-Castillo,F.M., Partensky,F., Ratin,M., Ostrowski,M., Pitt,F.D., Wincker,P., Scanlan,D.J., Iudicone,D. *et al.* (2016) Delineating ecologically significant taxonomic units from global patterns of marine picocyanobacteria. *Proc. Natl. Acad. Sci. U.S.A.*, **113**, E3365–E3374.
22. Partensky,F., Mella-Flores,D., Six,C., Garczarek,L. and Czjzek,M. (2018) Comparison of photosynthetic performances of marine picocyanobacteria with different configurations of the oxygen-evolving complex. *Photosynth. Res.*, **138**, 57–71.
23. Partensky,F. and Garczarek,L. (2010) *Prochlorococcus*: advantages and limits of minimalism. *Ann. Rev. Mar. Sci.*, **2**, 305–331.
24. Mella-Flores,D., Six,C., Ratin,M., Partensky,F., Boutte,C., Le Corguillé,G., Marie,D., Blot,N., Gourvil,P., Kolowrat,C. *et al.* (2012) *Prochlorococcus* and *Synechococcus* have evolved different adaptive mechanisms to cope with light and UV stress. *Front. Microbiol.*, **3**, 285.
25. Kolowrat,C., Partensky,F., Mella-Flores,D., Le Corguillé,G., Boutte,C., Blot,N., Ratin,M., Ferréol,M., Lecomte,X., Gourvil,P. *et al.* (2010) Ultraviolet stress delays chromosome replication in light/dark synchronized cells of the marine cyanobacterium *Prochlorococcus marinus* PCC9511. *BMC Microbiol.*, **10**, 204.
26. Humily,F., Partensky,F., Six,C., Farrant,G.K., Ratin,M., Marie,D. and Garczarek,L. (2013) A gene island with two possible configurations is involved in chromatic acclimation in marine *Synechococcus*. *PLoS One*, **8**, e84459.
27. Garczarek,L., Dufresne,A., Blot,N., Cockshutt,A.M., Peyrat,A., Campbell,D.A., Joubin,L. and Six,C. (2008) Function and evolution of the *psbA* gene family in marine *Synechococcus*: *Synechococcus* sp. WH7803 as a case study. *ISME J.*, **2**, 937–953.

28. Breton,S., Jouhet,J., Guyet,U., Gros,V., Pittera,J., Demory,D., Partensky,F., Doré,H., Ratin,M., Maréchal,E. *et al.* (2020) Unveiling membrane thermoregulation strategies in marine picocyanobacteria. *New Phytol.*, **225**, 2396–2410.
29. Blot,N., Mella-Flores,D., Six,C., Le Corguillé,G., Boutte,C., Peyrat,A., Monnier,A., Ratin,M., Gourvil,P., Campbell,D.A. *et al.* (2011) Light history influences the response of the marine cyanobacterium *Synechococcus* sp. WH7803 to oxidative stress. *Plant Physiol.*, **156**, 1934–1954.
30. Pittera,J., Jouhet,J., Breton,S., Garczarek,L., Partensky,F., Maréchal,É., Nguyen,N.A., Doré,H., Ratin,M., Pitt,F.D. *et al.* (2018) Thermoacclimation and genome adaptation of the membrane lipidome in marine *Synechococcus*. *Environ. Microbiol.*, **20**, 612–631.
31. Altschul,S., Gish,W. and Miller,W. (1990) Basic local alignment search tool. *J Mol Biol.*, **215**, 403–410.
32. Li,L., Stoeckert,C.J.J. and Roos,D.S. (2003) OrthoMCL: identification of ortholog groups for eukaryotic genomes. *Genome Res.*, **13**, 2178–2189.
33. Finn,R.D., Clements,J. and Eddy,S.R. (2011) HMMER web server: interactive sequence similarity searching. *Nucleic Acids Res.*, **39**, W29–W37.
34. Guyet,U., Nguyen,N.A., Doré,H., Haguait,J., Pittera,J., Conan,M., Ratin,M., Corre,E., Le Corguillé,G., Brillet-Guéguen,L. *et al.* (2020) Synergic effects of temperature and irradiance on the physiology of the marine *Synechococcus* strain WH7803. *Front. Microbiol*, **11**, 1707.
35. Mulkidjanian,A.Y., Koonin,E.V., Makarova,K.S., Mekhedov,S.L., Sorokin,A., Wolf,Y.I.I., Dufresne,A., Partensky,F., Burd,H., Kaznadzey,D. *et al.* (2006) The cyanobacterial genome core and the origin of photosynthesis. *Proc. Natl. Acad. Sci. U.S.A.*, **103**, 13126–13131.
36. Grébert,T., Doré,H., Partensky,F., Farrant,G.K., Boss,E.S., Picheral,M., Guidi,L., Pesant,S., Scanlan,D.J., Wincker,P. *et al.* (2018) Light color acclimation is a key process in the global ocean distribution of *Synechococcus* cyanobacteria. *Proc. Natl. Acad. Sci. U.S.A.*, **115**, E2010–E2019.
37. Moore,L.R. and Chisholm,S.W. (1999) Photophysiology of the marine cyanobacterium *Prochlorococcus*: Ecotypic differences among cultured isolates. *Limnol. Oceanogr.*, **44**, 628–638.
38. Priyam,A., Woodcroft,B.J., Rai,V., Moghul,I., Munagala,A., Ter,F., Chowdhary,H., Pieniak,I., Maynard,L.J., Gibbins,M.A. *et al.* (2019) Sequenceserver: a modern graphical user interface for custom BLAST databases. *Mol. Biol. Evol.*, **36**, 2922–2924.
39. Buels,R., Yao,E., Diesh,C.M., Hayes,R.D., Munoz-Torres,M., Helt,G., Goodstein,D.M., Elsik,C.G., Lewis,S.E., Stein,L. *et al.* (2016) JBrowse: a dynamic web platform for genome visualization and analysis. *Genome Biol.*, **17**, 66.
40. Taboada,B., Ciria,R., Martinez-Guerrero,C.E. and Merino,E. (2012) ProOpDB: prokaryotic operon database. *Nucleic Acids Res.*, **40**, D627–D631.
41. Lyons,T.W., Reinhard,C.T. and Planavsky,N.J. (2014) The rise of oxygen in Earth's early ocean and atmosphere. *Nature*, **506**, 307–315.
42. Archibald,J.M. (2012) The evolution of algae by secondary and tertiary endosymbiosis. *Adv. Bot. Res.*, **64**, 87–118.
43. Garcia-Pichel,F., Belnap,J., Neuer,S. and Schanz,F. (2003) Estimates of cyanobacterial biomass and its distribution. *Arch. Hydrobiol. Suppl. Algol. Stud.*, **109**, 213–228.
44. Huisman,J., Codd,G.A., Paerl,H.W., Ibelings,B.W., Verspagen,J.M.H. and Visser,P.M. (2018) Cyanobacterial blooms. *Nat. Rev. Microbiol.*, **16**, 471–483.
45. Kettler,G.C., Martiny,A.C., Huang,K., Zucker,J., Coleman,M.L., Rodrigue,S., Chen,F., Lapidus,A., Ferriera,S., Johnson,J. *et al.* (2007) Patterns and implications of gene gain and loss in the evolution of *Prochlorococcus*. *PLoS Genet.*, **3**, e231.
46. Nakamura,Y., Kaneko,T., Hirosawa,M., Miyajima,N. and Tabata,S. (1998) CyanoBase, a www database containing the complete nucleotide sequence of the genome of *Synechocystis* sp. strain PCC6803. *Nucleic Acids Res.*, **26**, 63–67.
47. Fujisawa,T., Narikawa,R., Maeda,S.I., Watanabe,S., Kanesaki,Y., Kobayashi,K., Nomata,J., Hanaoka,M., Watanabe,M., Ehira,S. *et al.* (2017) CyanoBase: a large-scale update on its 20th anniversary. *Nucleic Acids Res.*, **45**, D551–D554.
48. Sasaki,N.V. and Sato,N. (2010) CyanoClust: comparative genome resources of cyanobacteria and plastids. *Database*, **2010**, Bap025.
49. Kelly,L., Huang,K.H., Ding,H. and Chisholm,S.W. (2012) ProPortal: a resource for integrated systems biology of *Prochlorococcus* and its phage. *Nucleic Acids Res.*, **40**, D632–D640.
50. Markowitz,V.M., Chen,I.M.A., Palaniappan,K., Chu,K., Szeto,E., Pillay,M., Ratner,A., Huang,J., Woyke,T., Huntemann,M. *et al.* (2014) IMG 4 version of the integrated microbial genomes comparative analysis system. *Nucleic Acids Res.*, **42**, D560–D567.
51. Goericke,R. and Repeta,D.J. (1992) The pigments of *Prochlorococcusmarinus*: the presence of divinyl chlorophyll *a* and *b* in a marine prochlorophyte. *Limnol. Oceanogr.*, **37**, 425–433.
52. Ito,H. and Tanaka,A. (2011) Evolution of a divinyl chlorophyll-based photosystem in *Prochlorococcus*. *Proc. Natl. Acad. Sci. U.S.A.*, **108**, 18014–18019.
53. Nagata,N., Tanaka,R., Satoh,S. and Tanaka,A. (2005) Identification of a vinyl reductase gene for chlorophyll synthesis in *Arabidopsis thaliana* and implications for the evolution of *Prochlorococcus* species. *Plant Cell*, **17**, 233–240.
54. Islam,M.R., Aikawa,S., Midorikawa,T., Kashino,Y., Satoh,K. and Koike,H. (2008) *slr1923* of *Synechocystis* sp. PCC6803 is essential for conversion of 3,8-divinyl(proto)chlorophyll(ide) to 3-monovinyl(proto)chlorophyll(ide). *Plant Physiol.*, **148**, 1068–1081.
55. Villar,E., Farrant,G.K., Follows,M., Garczarek,L., Speich,S., Audic,S., Bittner,L., Blanke,B., Brum,J.R., Brunet,C. *et al.* (2015) Environmental characteristics of Agulhas rings affect interocean plankton transport. *Science*, **348**, 1261447.
56. Caputi,L., Carradec,Q., Eveillard,D., Kirilovsky,A., Pelletier,E., Pierella Karlusich,J.J., Rocha Jimenez Vieira,F., Villar,E., Chaffron,S., Malviya,S. *et al.* (2019) Community-Level responses to iron availability in open ocean plankton ecosystems. *Global Biogeochem. Cycles*, **33**, 391–419.

Annexe B : Differential global distribution of marine picocyanobacterial gene clusters reveals distinct niche-related adaptive strategies

PNAS
www.pnas.org

Main Manuscript for

Differential global distribution of marine picocyanobacteria gene clusters reveals distinct niche-related adaptive strategies

Hugo Doré[a,1], Ulysse Guyet [a,1], Jade Leconte[a], Gregory K. Farrant[a], Benjamin Alric[a], Morgane Ratin[a], Martin Ostrowski[b,2], Mathilde Ferrieux[a], Loraine Brillet-Guéguen[c,d], Mark Hoebeke[c], Jukka Siltanen[c], Gildas Le Corguillé[c], Erwan Corre[c], Patrick Wincker[f,g], David J. Scanlan[b], Damien Eveillard[h,g], Frédéric Partensky[a], and Laurence Garczarek[a,g,*]

[a]Sorbonne Université, CNRS, UMR 7144 Adaptation and Diversity in the Marine Environment (AD2M), Station Biologique de Roscoff (SBR), Roscoff, France; [b] School of Life Sciences, University of Warwick, Coventry CV4 7AL, UK; [c]CNRS, FR 2424, ABiMS Platform, Station Biologique de Roscoff (SBR), Roscoff, France; [d]Sorbonne Université, CNRS, UMR 8227, Integrative Biology of Marine Models (LBI2M), Station Biologique de Roscoff (SBR), Roscoff, France; [e]Genoscope, Institut de biologie François-Jacob, Commissariat à l'Energie Atomique (CEA), Université Paris-Saclay, Evry, France; [f]Génomique Métabolique, Genoscope, Institut de biologie François Jacob, CEA, CNRS, Université d'Evry, Université Paris-Saclay, Evry, France; [g]Research Federation (FR2022) *Tara* Océans GO-SEE, Paris, France; [h]Nantes Université, Centrale Nantes, CNRS, LS2N, UMR 6004, Nantes, France.

[1]H.D. and U.G. contributed equally to this work
[2]Current address: Climate Change Cluster, University of Technology, Broadway NSW 2007, Australia
[*]To whom correspondence should be addressed. Email: laurence.garczarek@sb-roscoff.fr. phone number: +33 2 98 29 25 38

Author Contributions: Paste the author contributions here.

Competing Interest Statement: The authors declare no competing interests.

Classification: Biological Sciences: Microbiology and Environmental Sciences

Keywords: *Prochlorococcus*, *Synechococcus*, niche partitioning, *Tara* Oceans, metagenomics

This PDF file includes:

Abstract

The ever-increasing number of available microbial genomes and metagenomes provide new opportunities to investigate the links between niche partitioning and genome evolution in the ocean, notably for the abundant and ubiquitous marine picocyanobacteria *Prochlorococcus* and *Synechococcus*. Here, by combining metagenome analyses of the *Tara* Oceans dataset with comparative genomics, including phyletic patterns and genomic context of individual genes from 256 reference genomes, we first showed that picocyanobacterial communities thriving in different niches possess distinct gene repertoires. We then managed to identify clusters of adjacent genes that display specific distribution patterns in the field (CAGs) and are thus potentially involved in the adaptation to particular environmental niches. Several CAGs are likely involved in the uptake or incorporation of complex organic forms of nutrients, such as guanidine, cyanate, cyanide, pyrimidine or phosphonates, which might be either directly used by cells, for e.g. the biosynthesis of proteins or DNA, or degraded into inorganic nitrogen and/or phosphorus forms. We also highlight the frequent presence of CAGs involved in polysaccharide capsule biosynthesis in *Synechococcus* populations thriving in both nitrogen- and phosphorus-depleted areas, which are absent in low-iron regions, suggesting that the complexes they encode may be too energy-consuming for picocyanobacteria thriving in these areas. In contrast, *Prochlorococcus* populations thriving in iron-depleted areas specifically possess an alternative respiratory terminal oxidase, potentially involved in the reduction of Fe(III) into Fe(II). Together, this study provides insights into how these key members of the phytoplankton community might behave in response to ongoing global change.

Significance Statement

Picocyanobacteria face various environmental conditions in the ocean and numerous studies have shown that genetically distinct ecotypes colonize different niches. Yet the functional basis of their adaptation remains poorly known, essentially due to the large number of genes of yet unknown function, many of which have little or no beneficial effect on fitness. Here, by combining comparative genomics and metagenomics approaches, we have identified not only single genes but also entire gene clusters, potentially involved in niche adaptation. Although being sometimes present in only one or a few sequenced strains, they occur in a large part of the population in

specific ecological niches and thus constitute precious targets for elucidating the biochemical function of yet unknown niche-related genes.

Main Text

Introduction

During the last two decades the sequencing of a large number of microbial genomes (more than 425,000 were available in Genbank in July 2022) has allowed tremendous advances in the delineation of core, accessory and unique gene repertoires within closely related organisms by building clusters of likely orthologous genes (CLOGs) based on sequence homology (1–4). Although this approach was tentatively used to identify the genetic basis of niche adaptation, relatively few genes were identified as being specific to particular ecotypes and thus potentially involved in niche adaptation (5–9). Various reasons may underpin this difficulty to identify niche-specific genes by a mere comparative genomics approach. These include the still fairly low number of genomes available given extensive known microbial genomic diversity (10), a lack of ecological representation due to cultivation biases, a limited knowledge of physiological traits of sequenced strains and/or the imprecise delineation of ecotypes and of the limits of their realized environmental niches *sensu* (11), especially for lineages present in low abundance in the field (12–14).

An alternative to comparative genomics to better decipher the link between niche partitioning and genome evolution consists of using the rapidly growing number of metagenomes. Besides triggering the generation of numerous metagenome-assembled genomes (MAGs), allowing to fill the gap for yet uncultured microbial taxa and/or ecotypes (15, 16), metagenome recruitment analyses using reference genomes have also allowed scientists to identify spatial or temporal niche-specific genes (17–19). In this context, due to their abundance and ubiquity in the field and the numerous available genomes, single amplified genomes (SAGs) and MAGs, marine picocyanobacteria constitute highly pertinent models for these metagenomic recruitment approaches. The *Prochlorococcus* and *Synechococcus* genera are indeed the two most abundant members of the phytoplankton community, *Prochlorococcus* being restricted to the 40°S-50°N latitudinal band, while *Synechococcus* distribution extends from the equator to subpolar waters (20, 21). Furthermore, physiological and environmental studies have allowed scientists to decipher their genetic diversity and their main physiological traits as well as to delineate ecotypes or Ecologically Significant Taxonomic Units (ESTUs), i.e., genetic groups within clades occupying a given ecological niche, notably using *Tara* oceans metagenomic data at the global scale (22). While

three major ESTU assemblages were identified for *Prochlorococcus* in surface waters, whose distribution was found to be mainly driven by temperature and iron (Fe) availability, eight distinct assemblages were identified for *Synechococcus* depending on three main environmental parameters (temperature, Fe and phosphate availability). Nevertheless, few studies have so far integrated our wide knowledge of ecotype distributions and the genetic and functional diversity of these organisms to identify niche- and/or ecotype-specific genes based on their relative abundance in the field (12, 23–26). Furthermore, most of these previous studies have focused on the abundance of individual genes, or more rarely, on a few genomic regions with known functions, e.g. involved in nitrogen or phosphorus uptake and assimilation (27, 28).

Here, by using a network approach to integrate metagenome analyses of the *Tara* Oceans dataset and synteny of individual accessory genes in 256 reference genomes, MAGs and SAGs, we managed to identify clusters of adjacent genes that display specific distribution patterns along the *Tara* Oceans transect. This led us to the unveil niche- and/or ecotype-specific genomic regions, including several previously unreported and sometimes only present in a few or even single genomes, potentially involved in the adaptation to the main ecological niches occurring in the marine environment (N, P and/or Fe-limited as well as cold *vs.* warm areas). Delineation of these gene clusters also led us to predict the putative functions of previously uncharacterized genes in these genomic regions based on genes functionally annotated in the same cluster. Altogether, this study provides unique insights into the functional basis of microbial niche partitioning and the molecular bases of fitness in key members of the phytoplankton community.

Results and Discussion

Different picocyanobacterial communities exhibit distinct gene repertoires

To analyze the distribution of *Prochlorococcus* and *Synechococcus* reads along the *Tara* Oceans transect, metagenomic reads corresponding to the bacterial size fraction were recruited against 256 picocyanobacterial reference genomes, including 178 whole genome sequences (WGS), and a selection of 48 SAGs and 30 MAGs, primarily representative of still uncultured lineages (e.g. *Prochlorococcus* HLIII-IV, *Synechococcus* EnvA or EnvB). This yielded a total of 1.07 billion recruited reads, of which 87.7% mapped onto *Prochlorococcus* genomes and 12.3% onto *Synechococcus* ones, which were then functionally assigned by mapping them on the manually curated Cyanorak *v2.1* CLOG database (29). In order to identify picocyanobacterial genes potentially involved in niche adaptation, we analyzed the distribution across the oceans of flexible genes (i.e., non-core

genes in Cyanorak *Prochlorococcus* and *Synechococcus* reference genomes). *Tara* Oceans stations were first clustered according to the relative abundance of flexible genes. This clustering resulted in three well-defined clusters for *Prochlorococcus* (left tree in Fig. 1A), which matched quite well those obtained when stations were clustered according to the relative abundance of *Prochlorococcus* ESTUs, as assessed using the high-resolution marker gene *petB,* encoding the cytochrome b_6 (right tree in Fig. 1A; see also (22)). Only a few discrepancies can be observed between the two trees, including stations TARA-070 that displayed one of the most disparate ESTU compositions and TARA-094, dominated by the rare HLID ESTU (Fig. 1A). For *Synechococcus*, there was also a good consistency between dendrograms obtained from flexible gene abundance and relative abundance of ESTUs (Fig. 1B). Of the eight assemblages of stations discriminated based on the relative abundance of ESTUs (Fig. 1B), most were retrieved in the clustering based on flexible gene abundance, except for a few intra-assemblage switches between stations, notably those dominated by ESTU IIA (Fig. 1B). Despite these few variations between *Synechococcus* trees, four major clusters can be clearly delineated in both trees, corresponding to four broadly defined ecological niches, namely i) cold, nutrient-rich, pelagic or coastal environments (blue and light red in Fig. 1B), ii) Fe-limited environments (purple and grey), iii) temperate, P-depleted, Fe-replete areas (yellow) and iv) warm, N-depleted, Fe-replete regions (dark red). This correspondence between taxonomic and functional information was also confirmed by the high congruence between distance matrices based on ESTU relative abundance and on CLOG relative abundance (p-value < 10^{-4}, mantel test r=0.84 and r=0.75 for *Synechococcus* and *Prochlorococcus,* respectively; dataset 1-4). Altogether, this indicates that distinct picocyanobacterial communities, as assessed based on a single taxonomic marker, also display different gene repertoires. As previously suggested for *Prochlorococcus* (30), this strong correlation between taxonomy and gene content strengthens the idea that, in both genera, the evolution of the accessory genome mainly occurs by vertical transmission, with a relatively low extent of lateral gene transfer.

Distribution of flexible genes is tightly linked to environmental parameters and ESTUs

In order to reduce the amount of data and better interpret the global distribution of picocyanobacterial gene content, a correlation network of genes was built for each genus based on relative abundance profiles of genes across *Tara* Oceans samples. Its analysis emphasized four main modules of genes for *Prochlorococcus* (Fig. S1A) and five main modules for *Synechococcus* (Fig. S1B), each gene module being abundant in a different set of stations. These modules were then associated with the available environmental parameters (Figs. 2A-B) and to the relative abundance of *Prochlorococcus* or *Synechococcus* ESTUs at each station (Figs. 2C-D). For instance, the *Prochlorococcus brown* module was strongly correlated with nutrient concentrations,

particularly nitrate and phosphate, and strongly anti-correlated with Fe availability (Fig. 2A). This module thus corresponds to genes preferentially found in Fe-limited high-nutrient low-chlorophyll (HNLC) areas. Indeed, the *brown* module *eigengenes* (Fig. S1A), representative of the abundance profiles of genes of this module at the different *Tara* Oceans stations, showed the highest abundances at stations TARA-100 to 125, localized in the South and North Pacific Ocean, as well as at TARA-052, a station located close to the northern coast of Madagascar and likely influenced by the Indonesian throughflow originating from the tropical Pacific Ocean (22, 31). Furthermore, the correlation of the *Prochlorococcus brown* module with the relative abundance of ESTUs at each station showed that it is also strongly associated with the presence of HLIIIA and HLIVA (Fig. 2C), previously shown to constitute the dominant *Prochlorococcus* ESTUs in low-Fe environments (22, 32, 33) but also the LLIB ESTU, found to dominate the LLI population in these low-Fe areas (22). Altogether, this example and analyses of all other *Prochlorococcus* and *Synechococcus* modules (SI Text1) show that the communities colonizing cold, Fe-, N- and/or P-depleted niches possess specific gene repertoires potentially involved in their adaptation to these peculiar environmental conditions.

Identification of individual genes potentially involved in niche partitioning

In order to identify flexible genes related to particular environmental conditions and to specific ESTU assemblages, we correlated relative abundance profiles of each gene to the *eigengene* vector of its corresponding module in order to identify the most representative genes of each module and thus the genes specifically present (or absent) in a given set of stations (Dataset 5, Figs. 3 and S2). Most genes retrieved this way encode proteins of unknown or hypothetical function (85.7% of 7,485 genes). Still, among the genes with a functional annotation (Dataset 6), a large fraction seems to have a function related to their realized environmental niche (Figs. 3 and S2). For instance, many genes involved in the transport and assimilation of nitrite and nitrate (*nirA*, *nirX*, *moaA-C, moaE, mobA, moeA, narB, M, nrtP;* all part of the same genomic island: Pro_GI004; (9)) as well as cyanate, an organic form of nitrogen (*cynA, B, D, S*; part of Pro_GI033), are enriched in the *Prochlorococcus blue* module, which is correlated with the HLIIA-D ESTU and to low inorganic N, P and Si levels and anti-correlated with Fe availability (Fig. 2A-C). This is consistent with previous studies showing that while few *Prochlorococcus* strains in culture possess the *nirA* gene and even less the *narB* gene, natural *Prochlorococcus* populations inhabiting N-poor areas do possess one or both of these genes (34–36). Similarly, numerous genes among the most representative genes of *Prochlorococcus brown, red* and *turquoise* modules are related to adaptation of HLIIIA/IVA, HLIA and LLIA ESTUs to Fe-limited, cold P-limited and cold, mixed waters,

respectively (Fig. 3), and comparable results were obtained for *Synechococcus,* although the niche delineation was fuzzier than for *Prochlorococcus* at the module level (Fig. S2). These results therefore constitute a proof of concept that this network analysis was able to retrieve niche-related genes from metagenomics data.

Identification of CAGs potentially involved in niche partitioning

In order to better understand the function of niche-related genes, notably the numerous ones encoding conserved hypothetical proteins, we then integrated these data with knowledge on the gene synteny in reference genomes using a network approach (Datasets 7 and 8). This led us to identify clusters of adjacent genes in reference genomes, several not previously reported in the literature, encompassing genes with similar distribution and abundance *in situ* and thus potentially involved in the same metabolic pathway (Figs. 4, S3 and S4; Dataset 6). Hereafter, these ecologically representative clusters of adjacent genes will be called 'CAGs'.

Regarding nitrogen, the well-known nitrate/nitrite gene cluster involved in uptake and assimilation of inorganic forms of nitrogen (see above) is present in most *Synechococcus* genomes (Dataset 6) and expectedly not restricted to a particular niche in natural *Synechococcus* populations, as shown by its quasi-absence from Weighted Correlation Network Analysis (WGCNA) modules. In *Prochlorococcus*, this cluster is separated into two CAGs, most genes being included in ProCAG_002, present in only 13 out of 118 *Prochlorococcus* genomes, while *nirA* and *nirX* form an independent CAG (ProCAG_001) due to their presence in many more genomes. Both CAGs are particularly enriched in *Prochlorococcus* populations thriving in low-N areas (Fig. S5A-B), as previously demonstrated by several authors (34–36). In *Prochlorococcus,* the quasi-core *ureA-G*/*urtB-E* genomic region was also found as a CAG (ProCAG_003) since it was comparatively impoverished in low-Fe compared to other regions (Fig. S5C-D) in agreement with its presence in only two out of six HLIII/IV genomes. In addition, we also uncovered several other *Prochlorococcus* and *Synechococcus* CAGs that seem to be involved in the transport and/or assimilation of more unusual and/or complex forms of nitrogen, including guanidine, cyanate, cyanide and possibly pyrimidine, which might either be degraded into elementary N, P or Fe molecules or possibly directly used by the cells for e.g. the biosynthesis of proteins or DNA. Indeed, we detected in both genera a CAG (ProCAG_004 and SynCAG_001 ; Figs. S6A-B, Dataset 6) that encompasses *speB2*, an ortholog of *Synechocystis* PCC 6803 *sll1077*, previously annotated as encoding an agmatinase (23, 37) and which was recently characterized as a guanidinase that degrades guanidine rather than agmatine to urea and ammonium (38). Interestingly *E. coli,* and likely other microorganisms as well, produce guanidine under nutrient-poor conditions, suggesting that guanidine metabolism

is biologically significant and prevalent in natural environments (38, 39). Furthermore, the *ykkC* riboswitch candidate, which was shown to specifically sense guanidine and to control the expression of a variety of genes involved in either guanidine metabolism or nitrate, sulfate, or bicarbonate transport, is located immediately upstream of this CAG in *Synechococcus* reference genomes, all genes of this cluster being predicted by RegPrecise 3.0 to be regulated by this riboswitch (Fig. S6C; (39, 40)). The presence of *hypA* and *B* homologs within this CAG furthermore suggests that, in the presence of guanidine, the latter could be involved in the insertion of Ni_2^+, or another metal cofactor, in the active site of guanidinase. Additionally, we speculate that the next three genes encoding an ABC transporter, similar to the TauABC taurine transporter in *E. coli* (Fig. S6C), could be involved in guanidine transport in low-N areas. Of note, the presence of a gene encoding a putative Rieske Fe-sulfur protein (CK_00002251), downstream of this gene cluster in most *Synechococcus*/*Cyanobium* genomes possessing this CAG, seems to constitute a specificity compared to its homologs in *Synechocystis* sp. PCC 6803 and might explain why this CAG is absent from picocyanobacteria thriving in low-Fe areas, while it is present in a large proportion of the population in most other oceanic areas (Figs. S6A-B).

As concerns compounds containing a cyano radical (C≡N), the cyanate transporter genes (*cynABD*) are scarce in both *Prochlorococcus* (present only in two HLI and five HLII genomes) and *Synechococcus* genomes (mostly in clade III strains; (9, 41, 42)). In the field, a small proportion of the *Prochlorococcus* community possesses the corresponding CAG (ProCAG_005; Fig. S7A-B), also including the conserved hypothetical gene CK_00055128, in warm, Fe-replete waters, while these genes were not included in a module, and thus not in a CAG, in *Synechococcus* (Dataset 6; Fig. S7C). Interestingly, we also uncovered a 7-gene CAG (ProCAG_006 and SynCAG_002), encompassing a putative nitrilase gene (*nitC*), which also suggests that most *Synechococcus* cells and a more variable proportion of the *Prochlorococcus* population could use nitriles or cyanides in warm, Fe-replete waters and more particularly in low-N areas such as the Indian Ocean (Fig. 5A-B). The whole operon (*nitHBCDEFG;* Fig. 5C), called Nit1C, was shown to be upregulated in the presence of cyanide and to trigger an increase in the rate of ammonia accumulation in the heterotrophic bacterium *Pseudomonas fluorescens* (43), suggesting that like cyanate, cyanide could constitute an alternative nitrogen source in marine picocyanobacteria as well. Yet, given the potential toxicity of these C≡N-containing compounds, we cannot exclude that these CAGs could also be devoted to cell detoxification (39, 41), as it is the case for arsenate and chromate (44, 45), which act as analogs of phosphate and sulfate respectively, and are toxic to marine phytoplankton (46).

Also noteworthy is the presence of a CAG encompassing *asnB, pyrB2* and *pydC* (ProCAG_007, SynCAG_003, Fig. S8), which could contribute to an alternative pyrimidine biosynthesis pathway and thus provide another way for cells to recycle complex nitrogen forms. While this CAG is found in only one fifth of HLII genomes and in quite specific locations for *Prochlorococcus*, notably in the Red Sea, it is found in most *Synechococcus* cells in warm, Fe-replete, N and P-depleted niches, consistent with its phyletic pattern showing its absence only from most clade I, IV, CRD1 and EnvB genomes (Fig. S8; Dataset 6). More generally, most N-uptake and assimilation genes in both genera were specifically absent from Fe-depleted areas, including the *nirA/narB* CAG for *Prochlorococcus,* as mentioned by Kent et al. (30) as well as guanidinase and nitrilase CAGs. In contrast, picocyanobacterial populations present in low-Fe areas possess, in addition to the core ammonium transporter *amt1,* a second transporter *amt2*, also present in cold areas for *Synechococcus* (Fig. S9). Additionally, *Prochlorococcus* populations thriving in HNLC areas also possess two amino acid-related CAGs that are quasi-core in *Synechococcus*, the first one involved in polar amino acids N-II transport system (ProCAG_008; *natF-G-H-bgtA;* (47); Fig. S10A-B) and the second one (*leuDH*, *soxA*, CK_00001744, ProCAG_009, Fig. S10C-D) that notably encompasses a leucine dehydrogenase, able to produce ammonium from branched-chain amino acids. Thus, the primary nitrogen sources for picocyanobacterial populations dwelling in Fe-limited areas seem to be ammonium and amino acids.

Adaptation to phosphorus depletion has been well documented in marine picocyanobacteria showing that while in P-replete waters *Prochlorococcus* and *Synechococcus* essentially rely on inorganic phosphate acquired by core transporters (PstABC), strains isolated from low-P regions and natural populations thriving in these areas additionally contain a number of accessory genes related to P metabolism, located in specific genomic islands (9, 25–28, 48). Here, we indeed found that virtually the whole *Prochlorococcus* population in the Mediterranean Sea, the Gulf of Mexico and the Western North Atlantic Ocean, which are known to be P-limited (26, 49), contained the *phoBR* operon (ProCAG_010, Fig. S11A-B) that encodes a two-component system response regulator, as well as the ProCAG_011, including the alkaline phosphatase *phoA*. By comparison, in *Synechococcus,* we only identified the *phoBR* CAG (SynCAG_005, Fig. S11C) that is systematically present in warm waters whatever their limiting nutrient, in agreement with its phyletic pattern in reference genomes showing its specific absence from cold thermotypes (clades I and IV, Dataset 6). Furthermore, although our analysis did not retrieve them within CAGs due to the variability of the content and order of genes in this genomic region, even within each genus, several other P-related genes were enriched in low-P areas but interestingly partially differed between *Prochlorococcus* and *Synechococcus* (Figs. S11, 3, S2 and Dataset 6). While the genes putatively

encoding a chromate transporter (ChrA) and an arsenate efflux pump ArsB were present in both genera in different proportions, a putative transcriptional phosphate regulator related to PtrA (CK_00056804; (50)) was specific to *Prochlorococcus*. *Synechococcus* in contrast harbors a large variety of alkaline phosphatases (PhoX, CK_00005263 and CK_00040198) as well as the phosphate transporter SphX (Fig. S11).

A second alternative P form are phosphonates, i.e. reduced organophosphorus compounds containing C–P bonds, which constitute up to 25% of the high-molecular-weight dissolved organic P pool in the open ocean (51). Indeed, the quasi-totality of the *Prochlorococcus* population of the most P-limited areas of the ocean possess, additionally to the core phosphonate ABC transporter (*phnD1-C1-E1*), a second previously unreported putative phosphonate transporter (*phnC2-D2-E2-E3;* ProCAG_012; Fig. 6A), while these genes are only present in a few *Prochlorococcus* (including MIT9314) and no *Synechococcus* genomes. Furthermore, as previously mentioned in several studies (52–54), a fairly low proportion of *Prochlorococcus* populations thriving in low-P areas also possess a gene cluster encompassing the *phnYZ* operon, involved in C-P bond cleavage, the putative phosphite dehydrogenase *ptxD* as well as the phosphite and methylphosphonate transporter *ptxABC* (ProCAG_0013, Dataset 6, and Fig. 6B, (54–56)). Compared to these previous studies that mainly reported the presence of these genes in *Prochlorococcus* cells from the North Atlantic Ocean, here we show that they actually occur in a much larger geographic area, including the Mediterranean Sea, the Gulf of Mexico and the ALOHA station (TARA_132) in the North Pacific, and are also present in an even larger proportion of the *Synechococcus* population (Fig. S12, Dataset 6). Interestingly, *Synechococcus* cells from the Mediterranean Sea, dominated by clade III, seem to lack *phnYZ,* in agreement with the phyletic pattern of these genes in reference genomes, showing the absence of this two-gene operon in the sole clade III strain that possesses the *ptxABDC* gene cluster. In contrast, the presence of the complete gene set (*ptxABDC-phnYZ*) in the North Atlantic and at the entrance of the Mediterranean Sea as well as in several clade II reference genomes rather suggests that it is primarily attributable to this specific clade. Altogether, our data indicate that at least part of the natural populations of both *Prochlorococcus* and *Synechococcus* would be able to assimilate phosphonate and phosphite as alternative P-sources in low-P areas using the *ptxABDC-phnYZ* operon. Yet, the fact that no picocyanobacterial genome except *P. marinus* RS01 (Fig. 6C) possesses both *phnC2-D2-E2-E3* and *phnYZ,* raises the question of how the phosphonate taken up by the *phnC2-D2-E2-E3* transporter is metabolized in these cells. Finally, although the Mediterranean Sea is not known to be N-limited, all reference clade III genomes possess a complete set of genes involved in the assimilation of organic nitrogen (Dataset 6),

suggesting that at least part of these organic nutrients might also be a source of organic phosphorus.

As for macronutrients, it has been hypothesized that the survival of marine picocyanobacteria in low-Fe regions was made possible through several strategies, including the elimination from the genomes of genes encoding proteins that contain Fe as a cofactor, the replacement of Fe by another metal cofactor, and the acquisition of genes involved in Fe uptake and storage (24, 25, 30, 33, 57). Accordingly, several CAGs encompassing genes encoding proteins interacting with Fe were found in the present study to be anti-correlated with HNLC regions in both genera. These include three subunits of the (photo)respiratory complex succinate deshydrogenase (SdhABC*,* ProCAG_014, SynCAG_006, Fig. S13; (58)) as well as Fe-containing proteins encoded in most of the abovementioned CAGs involved in N or P metabolism, such as the guanidinase CAG (Fig. S6), the NitC1 CAG (Fig. 5), the *pyrB2* CAG (Fig. S8), the phosphonate CAGs (Figs. 6 and S12) and the urea and inorganic nitrogen CAGs (Fig. S5). Most *Synechococcus* cells thriving in Fe-replete areas also possess the *sodT*/*sodX* CAG (SynCAG_007, Fig. S14A-B) involved in nickel transport and maturation of the Ni-superoxide dismutase (SodN), these three genes being in contrast core in *Prochlorococcus.* Additionally, *Synechococcus* from Fe-replete areas, notably from the Mediterranean Sea and the Indian Ocean, specifically possess two CAGs (Syn CAG_008 and 009; Fig. S14C-D), involved in the biosynthesis of a polysaccharide capsule that appear to be most similar to the *E. coli* groups 2 and 3 *kps* loci (59). These extracellular structures, known to provide protection against biotic or abiotic stress, were recently shown in *Klebsiella* to provide a clear fitness advantage in nutrient-poor conditions since they were associated with increased growth rates and population yields (60). Yet, while these authors suggested that capsules may play a role in Fe uptake, the significant reduction of the relative abundance of *kps* genes in low-Fe compared to Fe-replete areas (t-test p-value <0.05 for all genes of the Syn CAG_008 and 009 except CK_00002157; Fig. S14C) and their absence in CRD1 strains (Dataset 6) rather suggests that these capsules may be too energy-consuming for some picocyanobacteria thriving in this peculiar niche, while they may have a meaningful and previously overlooked role in their adaptation to low-P and low-N niches.

A number of CAGs were in contrast found to be enriched in populations dwelling in HNLC environments, dominated by *Prochlorococcus* HLIIIA/HLIVA/LLIB and *Synechococcus* CRD1A/EnvBA ESTUs (Fig. 2). For *Prochlorococcus,* this includes the abovementioned *natFGH* (ProCAG_008) and *leudH*/*soxA* (ProCAG_009) CAGs, involved in amino acid metabolism (Fig. S10), while a large proportion of the *Synechococcus* populations in these areas possess i) a large CAG involved in glycine betaine synthesis and transport (SynCAG_010, Fig. S15A-B; (9, 61)), almost

absent from low-N areas, ii) a CAG encompassing a flavodoxin and a thioredoxin reductase (SynCAG_011, Fig. S15C-D), mostly absent from low-P areas, as well as iii) the *nfeD-floT1-floT2* CAG (SynCAG_012, Fig. S16A-B) involved in the production of lipid rafts, potentially affecting cell shape and motility (9, 62). Both *Prochlorococcus* and *Synechococcus* thriving in low-Fe waters also possess the TonB-dependent siderophore uptake operon (*fecDCAB-tonB-exbBD*, Dataset 6). The latter gene cluster, which is found in a few picocyanobacterial genomes and was previously shown to be anti-correlated with dissolved Fe concentration (24, 25, 57), is indeed systematically present in a significant part of the *Prochlorococcus* and *Synechococcus* population in low-Fe areas (ProCAG_015 and SynCAG_013-014, Fig. S17). However, it is also present in a small fraction of the populations thriving in the Indian Ocean, consistent with its occurrence in two *Prochlorococcus* HLII and one *Synechococcus* clade II genomes (Dataset 6). The most striking result in this category is that the vast majority of *Prochlorococcus* cells thriving in low-Fe regions possess a CAG encompassing the *ctaC2-D2-E2* operon, also found in 85% of all *Synechococcus* reference genomes, including all CRD1 (Fig. 7; Dataset 6). This CAG encodes the alternative respiratory terminal oxidase ARTO, a protein complex that has been suggested to be part of a minimal respiratory chain in the cytoplasmic membrane, potentially providing an additional electron sink under Fe-deprived conditions (63, 64). Furthermore, a *Synechocystis* mutant in which the *ctaD2* and *ctaE2* genes had been inactivated was found to display markedly impaired Fe reduction and uptake rates as compared to wild-type cells, suggesting that ARTO is involved in the reduction of Fe(III) into Fe(II) prior to its transport through the plasma membrane via the Fe(II) transporter FeoB (65). Thus, the presence of the ARTO system appears to represent a major and previously unreported adaptation for *Prochlorococcus* populations thriving in low-Fe areas.

Besides genes involved in nutrient acquisition and metabolism, several *Prochlorococcus* and *Synechococcus* CAGs were found to be correlated with low-temperature waters. A closer examination of *Prochlorococcus* CAGs however, shows that their occurrence is not directly related to temperature adaptation but mainly explained by the prevalence at high latitude of either i) the HLIA ESTU (Fig. 2A, C and Fig. 4), the *red* module encompassing most of the above-mentioned CAGs involved in P-uptake and assimilation pathways, or ii) the LLIA ESTU, present in surface waters at vertically-mixed stations, the *turquoise* module mainly gathering *Prochlorococcus* LL-specific genes, such as Pro_CAG_017, involved in phycoerythrin-III biosynthesis (*ppeA*, *cpeFTZY*, *unk13*) or ProCAG_018, encoding the two subunits of exodeoxyribonuclease VII (XseA-B). As concerns *Synechococcus*, although a fairly high number of CAGs were identified in the *tan* module associated with ESTUs IA and IVA-C (Fig. 2B, D and Fig. S4), only very few are conserved in more than two reference strains and/or have a characterized function (Dataset 6). Among these, at least

one CAG is clearly related to adaptation to cold waters, the orange carotenoid protein (OCP) operon (*ocp-crtW-frp*; SynCAG_016). Indeed, this operon is involved in a photoprotective process (66) and was recently shown to provide cells with the ability to deal with oxidative stress under cold temperatures (67). In agreement with the latter study, our data shows that *Synechococcus* populations colonizing mixed waters at high latitudes or in upwelling areas all possess the *ocp* CAG (Fig. S18), highlighting the importance of this photoprotection system in *Synechococcus* populations colonizing cold and temperate areas. *Synechococcus* populations thriving in cold waters also appear to be enriched in CAGs involved in gene regulation. This includes transcriptional regulators involved in the regulation of the CA4-A form of the type IV chromatic acclimation process (*fciA-B;* SynCAG_017), consistent with the predominance of *Synechococcus* CA4-A cells in temperate or cold environments (68–70)(Dataset 6) as well as the *hidABC* operon (SynCAG_018), involved in the synthesis of a secondary metabolite (hierridin C; (71)). Altogether, the fairly low number of 'strong' CAGs associated with temperature supports the hypothesis that adaptation to cold temperature is not mediated by evolution of gene content but rather of protein sequences (8, 9, 30, 72).

In conclusion, our analysis of *Prochlorococcus* and *Synechococcus* gene distributions at the global scale using the deeply sequenced metagenomes collected along the *Tara* Oceans expedition transect revealed that each community has a specific gene repertoire, with different sets of accessory genes being highly correlated with distinct ESTUs and physicochemical parameters. As previously suggested for *Prochlorococcus* (30), this strong correlation between taxonomy and gene content strengthens the idea that, in both genera, genome evolution mainly occurs by vertical transmission and selective gene retention, with a fairly low extent of lateral gene transfer between clades. By combining information about gene synteny in 256 reference genomes with the distribution and abundance of these genes in the field, we further managed to delineate suites of adjacent genes likely involved in the same metabolic pathways that may have a crucial role in adaptation to specific niches. These analyses confirmed previous observations about the niche partitioning of individual genes and a few genomic regions involved in nutrient uptake and assimilation (24, 25, 27, 30, 34, 36). Most importantly, this network approach unveiled several novel genomic regions that could confer cells a fitness benefit in particular niches and also highlighted that some previously detected individual genes are part of larger genomic regions. It notably revealed the potential importance of the uptake and assimilation of organic forms of limiting nutrients, which might either be directly used by the cells, e.g. for the biosynthesis of proteins or DNA, or be degraded into inorganic N and/or P forms. Consistently, many CAGs potentially involved in the uptake and assimilation of complex compounds, such as guanidine,

C≡N-containing compounds or pyrimidine were present in both N- and P-depleted waters, and might constitute an advantage in areas of the world ocean co-limited in these nutrients (26). In contrast, most of these CAGs were specifically absent from N and/or P-rich, Fe-poor areas ((30); this study). Adaptation to Fe-limitation seemingly relies on specific adaptation mechanisms including reduction of Fe^{3+} to Fe^{2+} using ARTO, Fe storage, Fe scavenging using siderophores as well as reduction of the iron quota and of energy-consuming adaptation mechanisms, such as polysaccharide capsule biosynthesis. Altogether, this study provides unique insights into the functional basis of microbial niche partitioning and the molecular bases of fitness in key members of the phytoplankton community. A future challenge will clearly consist of biochemically characterizing the function of the different genes, including many unknown, gathered in the above-mentioned CAGs (Datasets 5 and 6), which are sometimes present only in a few or even a single strain but can occur in a large part or even the whole *Prochlorococcus* and/or *Synechococcus* population *in situ*, and which likely all contribute to the same complex and/or metabolic pathway.

Materials and Methods

Tara Oceans dataset

A total of 131 bacterial-size metagenomes (0.2-1.6 µm for stations TARA_004 to TARA_052 and 0.2-3µm for TARA_056 to TARA_152), collected in surface from 83 stations along the *Tara* Oceans expedition transect (73), were used in this study. Briefly, all metagenomes were sequenced as Illumina overlapping paired reads of 100-108 bp and paired reads were merged and trimmed based on quality, resulting in 100-215 bp fragments, as previously described (22). All metagenomes and corresponding environmental parameters were retrieved from PANGAEA (www.pangaea.de/) except for Fe and ammonium concentrations that were modeled and the Fe limitation index Φ_{sat} that was calculated from satellite data, as previously described (22).

Recruitment and taxonomic and functional assignment of metagenomic reads

Metagenomic reads were first recruited against 256 reference genomes, including the 97 genomes available in the information system Cyanorak *v2.1* (www.sb-roscoff.fr/cyanorak; (28)) as well as 84 additional WGS, 27 MAGs and 48 SAGs retrieved from Genbank (Dataset 9). Recruitment was made using MMseqs2 Release 11-e1a1c (76) with maximum sensitivity (mmseqs search -s 7.5) and limiting the results to one target sequence (mmseqs filterdb --extract-lines 1). Using the same MMseqs2 options, the resulting reads were then mapped to an extended database of 978 genomes, including all picocyanobacterial reference genomes complemented with 722

outgroup cyanobacterial genomes downloaded from NCBI. Reads mapping to outgroup sequences or having less than 90% of their sequence aligned were filtered out and the remaining reads were taxonomically assigned to either *Prochlorococcus* or *Synechococcus* according to their best hit. Reads were then functionally assigned to a cluster of likely orthologous genes (CLOGs) from the information system Cyanorak *v2.1* based on the position of their MMseqs2 match on the genome, the coordinates of which correspond to a particular gene in the database. More precisely, a read was functionally assigned to a gene if at least 75% of its size was aligned to the reading frame of this gene and if the percentage identity of the blast alignment was over 80%. Finally, read counts were aggregated by CLOG and normalized by dividing read counts by L-l+1, where L represents the average gene length of the CLOG and l the mean length of recruited reads. Only environmental samples that contained at least 2,500 and 1,700 distinct CLOGs for *Synechococcus* and *Prochlorococcus,* respectively, were kept, corresponding roughly to the average number of genes in a *Synechococcus* and a *Prochlorococcus* HL genome, respectively. After this filtration step, a CLOG was kept if it showed a gene-length normalized abundance higher than 1 (i.e., a gene coverage of 1) in at least 2 of the selected environmental samples. Then, large-core genes, as previously defined (9), were removed to keep only accessory genes. The resulting abundance profiles were used to perform co-occurrence analyses by weighted genes correlation network analysis, as detailed below (WGCNA, (74)).

Station clustering and ESTU analyses

In order to cluster stations displaying similar CLOG abundance patterns, the abundance of a given CLOG in a sample was divided by the total CLOG abundance in this sample to obtain relative abundance profiles per sample. Bray-Curtis similarities were calculated from these profiles and used to cluster *Tara* Oceans stations with the Ward's minimum variance method (75). The same normalization method was applied to picocyanobacterial ESTUs that were defined based on the *petB* marker gene at each station using a similar approach as in Farrant *et al.* (2016) but using a Ward's minimum variance method (75) to be consistent with the clustering of CLOG profiles. In order to check whether the Bray-Curtis distances between stations based on *petB* picocyanobacterial communities and based on gene content were significantly correlated, a mantel test was performed between the distance matrices, as implemented in the R package *vegan* v2.5 with 9,999 permutations (76).

Gene co-occurrence network analysis

A data-reduction approach based on WGCNA, as implemented in the R package WGCNA *v1.51* (77), was used to build a co-occurrence network of CLOGs based on their relative abundance in *Tara* Oceans stations and to delineate modules of CLOGs (i.e., subnetworks). The WGCNA adjacency matrix was calculated in 'signed' mode (i.e., considering correlated and anti-correlated CLOGs separately), by using the *Pearson* correlation between pairs of CLOGs (based on their relative abundance in every sample) and raising it to the power 12, which allowed to obtain a scale-free topology of the network. Modules were identified by setting the minimum number of genes in each module to 100 and 50 for *Synechococcus* and *Prochlorococcus,* respectively, and by forcing every gene to be included in a module. The *eigengene* of each module (representative of the relative abundance of genes of a given module at each *Tara* Oceans station) was then correlated to environmental parameters and to the relative abundance of ESTUs. Finally, genes in each module with the highest correlation to the *eigengene* (a measurement called 'membership'), were extracted in order to identify the most representative genes of each module.

Identification of differentially distributed clusters of adjacent genes (CAGs)

Results on individual niche-related genes identified by WGCNA were then integrated with knowledge on gene synteny in reference genomes (Datasets 7 and 8). For each WGCNA module, we defined CAGs by searching adjacent genes of the module in the 256 reference genomes. In order to be considered as belonging to the same CAG, two genes of the same module must be less than 6 genes apart in 80% of the genomes in which these two genes are present. This led us to identify clusters of adjacent genes in reference genomes, comprising genes displaying a similar distribution pattern, called CAGs. A network of CAGs was then built for each WGCNA module, taking into account the number of genomes in which these genes are adjacent (Figs. 4, S3 and S4). An unweighted, undirected graph was drawn for each module according to the Fruchterman-Reingold layout algorithm implemented in the R package igraph. This is a force-directed algorithm, meaning that node layout is determined by the forces pulling nodes together and pushing them apart. In other words, its purpose is to position the nodes of a graph so that the edges of more or less equal length are gathered together and to avoid as many crossing edges as possible.

Data sharing plans: All genomic and metagenomic data used in this study are publicly available

Acknowledgments

This work was supported by the French “Agence Nationale de la Recherche” Programs SAMOSA (ANR-13-ADAP-0010), CINNAMON (ANR-17-CE02-0014-01), EFFICACY (ANR-19-CE02-0019) and France Génomique (ANR-10-INBS-09) as well as the European Union program Assemble+ (Horizon

2020, under grant agreement number 287589). We acknowledge Christophe Six for his help with cloning some of the *Synechococcus* strains used in this study and Francisco M. Cornejo-Castillo for useful discussions. We also thank the support and commitment of the *Tara* Oceans coordinators and consortium, Agnès b. and E. Bourgois, the Veolia Environment Foundation, Région Bretagne, Lorient Agglomeration, World Courier, Illumina, the EDF Foundation, FRB, the Prince Albert II de Monaco Foundation, the *Tara* schooner, and its captains and crew. *Tara* Oceans would not exist without continuous support from 23 institutes (http://oceans.taraexpeditions.org).

References

1. H. Tettelin, *et al.*, Genome analysis of multiple pathogenic isolates of *Streptococcus agalactiae*: Implications for the microbial "pan-genome." *Proc Natl Acad Sci USA* **102**, 13950–13955 (2005).
2. M. López-Pérez, F. Rodriguez-Valera, Pangenome evolution in the marine bacterium *Alteromonas*. *Genome Biol Evol* **8**, 1556–1570 (2016).
3. T. D. Read, *et al.*, The genome sequence of *Bacillus anthracis* Ames and comparison to closely related bacteria. *Nature* **423**, 81–86 (2003).
4. C. Zhu, T. O. Delmont, T. M. Vogel, Y. Bromberg, Functional basis of microorganism classification. *PLOS Comput Biol* **11**, e1004472 (2015).
5. M. L. Reno, N. L. Held, C. J. Fields, P. V. Burke, R. J. Whitaker, Biogeography of the *Sulfolobus islandicus* pan-genome. *Proc Natl Acad Sci USA* **106**, 8605–8610 (2009).
6. S. S. Porter, P. L. Chang, C. A. Conow, J. P. Dunham, M. L. Friesen, Association mapping reveals novel serpentine adaptation gene clusters in a population of symbiotic *Mesorhizobium*. *ISME J* **11**, 248–262 (2017).
7. S. Kellner, *et al.*, Genome size evolution in the Archaea. *Emerg Top Life Sci* **2**, 595–605 (2018).
8. G. C. Kettler, *et al.*, Patterns and implications of gene gain and loss in the evolution of *Prochlorococcus*. *PLOS Genet* **3**, e231 (2007).
9. H. Doré, *et al.*, Evolutionary mechanisms of long-term genome diversification associated with niche partitioning in marine picocyanobacteria. *Front Microbiol* **11** (2020).
10. N. Kashtan, *et al.*, Single-cell genomics reveals hundreds of coexisting subpopulations in wild *Prochlorococcus*. *Science* **344**, 416–420 (2014).
11. P. B. Pearman, A. Guisan, O. Broennimann, C. F. Randin, Niche dynamics in space and time. *Trends Ecol Evol* **23**, 149–158 (2008).
12. T. O. Delmont, A. M. Eren, Linking pangenomes and metagenomes: the *Prochlorococcus* metapangenome. *PeerJ* **6**, e4320 (2018).
13. J.-H. Hehemann, *et al.*, Adaptive radiation by waves of gene transfer leads to fine-scale resource partitioning in marine microbes. *Nat Commun* **7**, 12860 (2016).
14. H. Koch, *et al.*, Genomic, metabolic and phenotypic variability shapes ecological

differentiation and intraspecies interactions of *Alteromonas macleodii*. *Sci Rep* **10** (2020).

15. J. P. Engelberts, *et al.*, Characterization of a sponge microbiome using an integrative genome-centric approach. *ISME J* **14**, 1100–1110 (2020).

16. B. J. Tully, E. D. Graham, J. F. Heidelberg, The reconstruction of 2,631 draft metagenome-assembled genomes from the global oceans. *Sci Data* **5**, 170203 (2018).

17. B. L. Hurwitz, A. H. Westveld, J. R. Brum, M. B. Sullivan, Modeling ecological drivers in marine viral communities using comparative metagenomics and network analyses. *Proc Natl Acad Sci USA* **111**, 10714–10719 (2014).

18. A. Meziti, *et al.*, Quantifying the changes in genetic diversity within sequence-discrete bacterial populations across a spatial and temporal riverine gradient. *ISME J* **13**, 767–779 (2019).

19. I. Raimundo, *et al.*, Functional metagenomics reveals differential chitin degradation and utilization features across free-living and host-associated marine microbiomes. *Microbiome* **9**, 43 (2021).

20. P. Flombaum, *et al.*, Present and future global distributions of the marine Cyanobacteria *Prochlorococcus* and *Synechococcus*. *Proc Natl Acad Sci USA* **110**, 9824–9 (2013).

21. N. Visintini, A. C. Martiny, P. Flombaum, *Prochlorococcus*, *Synechococcus*, and picoeukaryotic phytoplankton abundances in the global ocean. *Limnol Oceanogr* **6**, 207–215 (2021).

22. G. K. Farrant, *et al.*, Delineating ecologically significant taxonomic units from global patterns of marine picocyanobacteria. *Proc Natl Acad Sci USA* **113**, E3365–E3374 (2016).

23. A. G. Kent, *et al.*, Parallel phylogeography of *Prochlorococcus* and *Synechococcus*. *ISME J* **13**, 430–441 (2019).

24. N. A. Ahlgren, B. S. Belisle, M. D. Lee, Genomic mosaicism underlies the adaptation of marine *Synechococcus* ecotypes to distinct oceanic iron niches. *Environ Microbiol* **22**, 1801–1815 (2020).

25. C. A. Garcia, *et al.*, Linking regional shifts in microbial genome adaptation with surface ocean biogeochemistry. *Phil Trans Roy Soc B Biol Sci* **375**, 20190254 (2020).

26. L. J. Ustick, *et al.*, Metagenomic analysis reveals global-scale patterns of ocean nutrient limitation. *Science* **372**, 287–291 (2021).

27. A. C. Martiny, M. L. Coleman, S. W. Chisholm, Phosphate acquisition genes in *Prochlorococcus* ecotypes: Evidence for genome-wide adaptation. *Proc Natl Acad Sci USA* **103**, 12552–12557 (2006).

28. A. C. Martiny, Y. Huang, W. Li, Occurrence of phosphate acquisition genes in *Prochlorococcus* cells from different ocean regions. *Environmental Microbiology* **11**, 1340–1347 (2009).

29. L. Garczarek, *et al.*, Cyanorak v2.1: a scalable information system dedicated to the visualization and expert curation of marine and brackish picocyanobacteria genomes. *Nucl Acids Res* **49**, D667–D676 (2021).

30. A. G. Kent, C. L. Dupont, S. Yooseph, A. C. Martiny, Global biogeography of *Prochlorococcus* genome diversity in the surface ocean. *The ISME Journal* **10**, 1856–1865

(2016).

31. Q. Song, A. L. Gordon, M. Visbeck, Spreading of the Indonesian throughflow in the Indian Ocean. *J Phys Oceanogr* **34**, 772–792 (2004).

32. N. J. West, P. Lebaron, P. G. Strutton, M. T. Suzuki, A novel clade of *Prochlorococcus* found in high nutrient low chlorophyll waters in the South and Equatorial Pacific Ocean. *ISME J* **5**, 933–944 (2011).

33. D. B. Rusch, A. C. Martiny, C. L. Dupont, A. L. Halpern, J. C. Venter, Characterization of *Prochlorococcus* clades from iron-depleted oceanic regions. *Proc Natl Acad Sci USA* **107**, 16184–16189 (2010).

34. A. C. Martiny, S. Kathuria, P. M. Berube, Widespread metabolic potential for nitrite and nitrate assimilation among *Prochlorococcus* ecotypes. *Proc Natl Acad Sci USA* **106**, 10787–10792 (2009).

35. P. M. Berube, A. Rasmussen, R. Braakman, R. Stepanauskas, S. W. Chisholm, Emergence of trait variability through the lens of nitrogen assimilation in *Prochlorococcus*. *eLife* **8**, e41043–e41043 (2019).

36. P. M. Berube, *et al.*, Physiology and evolution of nitrate acquisition in *Prochlorococcus*. *ISME J* (2015) https:/doi.org/10.1038/ismej.2014.211.

37. M. Burnat, B. Li, S. H. Kim, A. J. Michael, E. Flores, Homospermidine biosynthesis in the cyanobacterium *Anabaena* requires a deoxyhypusine synthase homologue and is essential for normal diazotrophic growth. *Mol Microbiol* **109**, 763–780 (2018).

38. B. Wang, *et al.*, A guanidine-degrading enzyme controls genomic stability of ethylene-producing cyanobacteria. *Nat Commun* **12**, 5150 (2021).

39. J. W. Nelson, R. M. Atilho, M. E. Sherlock, R. B. Stockbridge, R. R. Breaker, Metabolism of free guanidine in Bacteria is regulated by a widespread riboswitch class. *Mol Cell* **65**, 220–230 (2017).

40. P. S. Novichkov, *et al.*, RegPrecise 3.0 – A resource for genome-scale exploration of transcriptional regulation in bacteria. *BMC Genomics* **14**, 745 (2013).

41. N. A. Kamennaya, A. F. Post, Characterization of cyanate metabolism in marine *Synechococcus* and *Prochlorococcus* spp. *Appl Environ Microbiol* **77**, 291–301 (2011).

42. N. A. Kamennaya, A. F. Post, Distribution and expression of the cyanate acquisition potential among cyanobacterial populations in oligotrophic marine waters. *Limnol Oceanogr* **58**, 1959–1971 (2013).

43. L. B. Jones, P. Ghosh, J.-H. Lee, C.-N. Chou, D. A. Y. 2018 Kunz, Linkage of the Nit1C gene cluster to bacterial cyanide assimilation as a nitrogen source. *Microbiol* **164**, 956–968 (2018).

44. J. K. Saunders, G. Rocap, Genomic potential for arsenic efflux and methylation varies among global *Prochlorococcus* populations. *ISME J* **10**, 197–209 (2016).

45. G. F. Riedel, Influence of salinity and sulfate on the toxicity of chromium(vi) to the estuarine diatom *Thalassiosira Pseudonana*. *Journal of Phycology* **20**, 496–500 (1984).

46. F. Pablo, J. L. Stauber, R. T. Buckney, Toxicity of cyanide and cyanide complexes to the marine diatom *Nitzschia closterium*. *Water Res* **31**, 2435–2442 (1997).

47. R. Pernil, S. Picossi, V. Mariscal, A. Herrero, E. Flores, ABC-type amino acid uptake

transporters Bgt and N-II of *Anabaena* sp. strain PCC 7120 share an ATPase subunit and are expressed in vegetative cells and heterocysts. *Mol Microbiol* **67**, 1067–1080 (2008).

48. M. L. Coleman, *et al.*, Genomic islands and the ecology and evolution of *Prochlorococcus*. *Science* **311**, 1768–1770 (2006).

49. C. M. Moore, *et al.*, Processes and patterns of oceanic nutrient limitation. *Nature Geosci* **6**, 701–710 (2013).

50. S. G. Tetu, *et al.*, Microarray analysis of phosphate regulation in the marine cyanobacterium *Synechococcus* sp. WH8102. *ISME J* **3**, 835–849 (2009).

51. L. L. Clark, E. D. Ingall, R. Benner, Marine phosphorus is selectively remineralized. *Nature* **393**, 426–426 (1998).

52. R. Feingersch, *et al.*, Potential for phosphite and phosphonate utilization by *Prochlorococcus*. *ISME J* **6**, 827–834 (2012).

53. A. Martinez, G. W. Tyson, E. F. Delong, Widespread known and novel phosphonate utilization pathways in marine bacteria revealed by functional screening and metagenomic analyses. *Environ Microbiol* **12**, 222–238 (2010).

54. O. A. Sosa, J. R. Casey, D. M. Karl, Methylphosphonate oxidation in *Prochlorococcus* strain MIT9301 supports phosphate acquisition, formate excretion, and carbon assimilation into purines. *Appl Environ Microbiol* **85**, e00289-19 (2019).

55. A. Martínez, M. S. Osburne, A. K. Sharma, E. F. DeLong, S. W. Chisholm, Phosphite utilization by the marine picocyanobacterium *Prochlorococcus* MIT9301. *Environ Microbiol* **14**, 1363–1377 (2012).

56. F. R. McSorley, *et al.*, PhnY and PhnZ comprise a new oxidative pathway for enzymatic cleavage of a carbon–phosphorus bond. *J Am Chem Soc* **134**, 8364–8367 (2012).

57. R. R. Malmstrom, *et al.*, Ecology of uncultured *Prochlorococcus* clades revealed through single-cell genomics and biogeographic analysis. *ISME J* **7**, 184–198 (2013).

58. J. W. Cooley, W. F. J. Vermaas, Succinate dehydrogenase and other respiratory pathways in thylakoid membranes of *Synechocystis* sp. strain PCC 6803: capacity comparisons and physiological function. *J Bacteriol* (2001) (January 27, 2022).

59. C. Whitfield, Biosynthesis and assembly of capsular polysaccharides in *Escherichia coli*. *Annu Rev Biochem* **75**, 39–68 (2006).

60. A. Buffet, E. P. C. Rocha, O. Rendueles, Nutrient conditions are primary drivers of bacterial capsule maintenance in *Klebsiella*. *Proc Roy Soc B Biol Sci* **288**, 20202876 (2021).

61. D. J. Scanlan, *et al.*, Ecological genomics of marine picocyanobacteria. *Microbiol Mol Biol Rev* **73**, 249–299 (2009).

62. F. Dempwolff, H. M. Wischhusen, M. Specht, P. L. Graumann, The deletion of bacterial dynamin and flotillin genes results in pleiotrophic effects on cell division, cell growth and in cell shape maintenance. *BMC Microbiol* **12**, 298 (2012).

63. D. J. Lea-Smith, *et al.*, Thylakoid terminal oxidases are essential for the cyanobacterium *Synechocystis* sp. PCC 6803 to survive rapidly changing light intensities. *Plant Physiol* **162**, 484–495 (2013).

64. D. J. Lea-Smith, P. Bombelli, R. Vasudevan, C. J. Howe, Photosynthetic, respiratory and

extracellular electron transport pathways in cyanobacteria. *Biochim Biophys Acta Bioenerget* **1857**, 247–255 (2016).

65. C. Kranzler, *et al.*, Coordinated transporter activity shapes high-affinity iron acquisition in cyanobacteria. *ISME J* **8**, 409–417 (2014).

66. C. Boulay, A. Wilson, S. D'Haene, D. Kirilovsky, Identification of a protein required for recovery of full antenna capacity in OCP-related photoprotective mechanism in cyanobacteria. *Proc Natl Acad Sci USA* **107**, 11620–11625 (2010).

67. C. Six, M. Ratin, D. Marie, E. Corre, Marine *Synechococcus* picocyanobacteria: Light utilization across latitudes. *Proc Natl Acad Sci USA* **118** (2021).

68. X. Xia, *et al.*, Phylogeography and pigment type diversity of *Synechococcus* cyanobacteria in surface waters of the northwestern Pacific Ocean. *Environ Microbiol* **19**, 142–158 (2017).

69. T. Grébert, *et al.*, Light color acclimation is a key process in the global ocean distribution of *Synechococcus* cyanobacteria. *Proc Natl Acad Sci USA* **115**, E2010–E2019 (2018).

70. J. E. Sanfilippo, *et al.*, Self-regulating genomic island encoding tandem regulators confers chromatic acclimation to marine *Synechococcus*. *Proc Natl Acad Sci USA* **113**, 6077–6082 (2016).

71. M. Costa, *et al.*, Structure of Hierridin C, synthesis of hierridins B and C, and evidence for prevalent alkylresorcinol biosynthesis in picocyanobacteria. *J. Nat. Prod.* **82**, 393–402 (2019).

72. A. A. Larkin, A. C. Martiny, Microdiversity shapes the traits, niche space, and biogeography of microbial taxa: The ecological function of microdiversity. *Environ Microbiol Rep* **9**, 55–70 (2017).

73. S. Sunagawa, *et al.*, Structure and function of the global ocean microbiome. *Science* **348**, 1261359–1261359 (2015).

74. B. Zhang, S. Horvath, A general framework for weighted gene co-expression network analysis. *Stat Appl Genet Mol Biol* **4**, Article17 (2005).

75. B. Szmrecsanyi, *Grammatical Variation in British English Dialects: A Study in Corpus-Based Dialectometry* (Cambridge University Press, 2012) https:/doi.org/10.1017/CBO9780511763380.

76. Oksanen, J., *et al.*, *Vegan: Community Ecology Package. R package Version 2.4-3* (2017).

77. P. Langfelder, S. Horvath, WGCNA: an R package for weighted correlation network analysis. *BMC Bioinfo* **9**, 559 (2008).

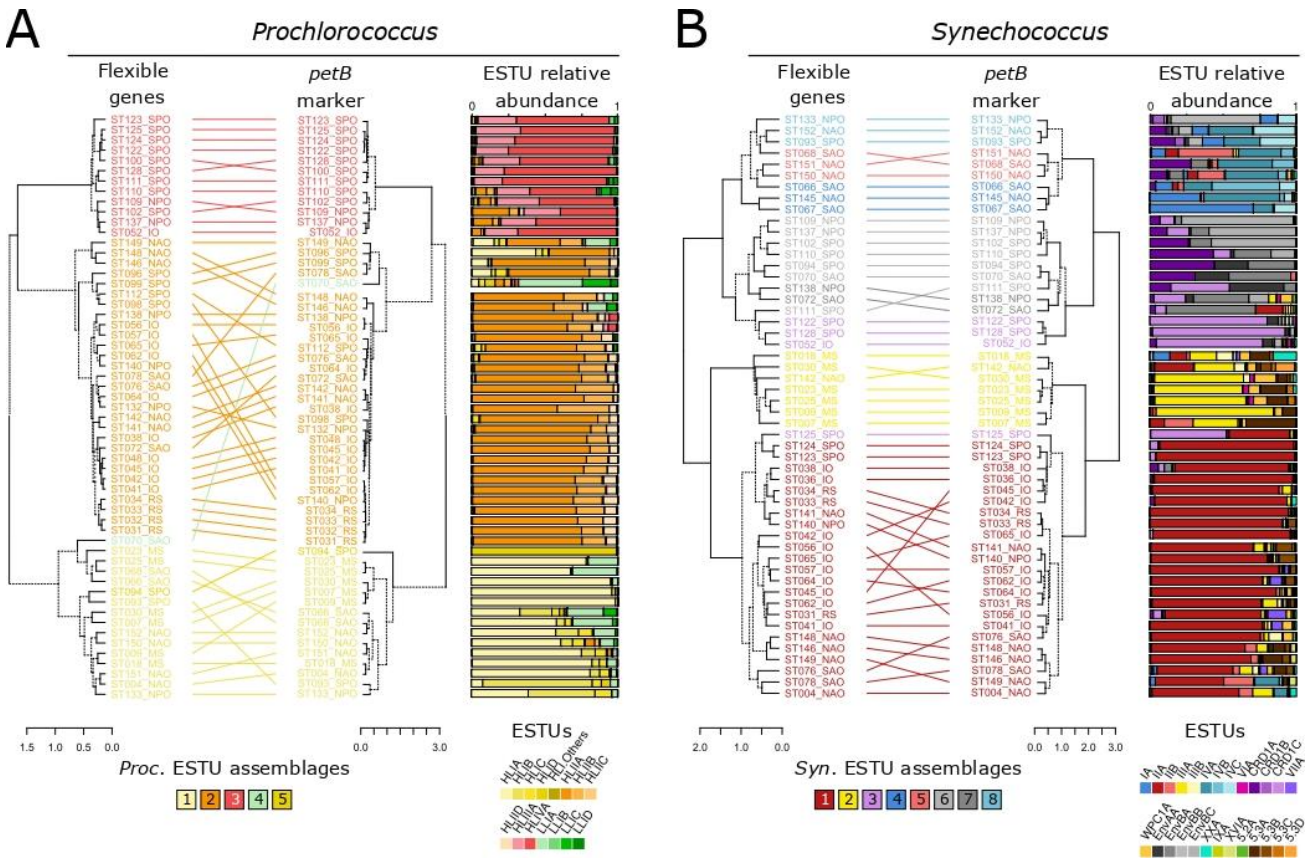

Figure 1. Comparison of clustering based on relative abundance profiles of ecologically significant taxonomic units (ESTUs) and of flexible genes for both picocyanobacteria. A. *Prochlorococcus*. B. *Synechococcus*. Leaves of the trees correspond to stations along the Tara Oceans transect that are colored according to the code shown at the bottom of the trees, corresponding to ESTU assemblages as determined by Farrant et al. (2016) by clustering stations exhibiting similar ESTU relative abundance profiles shown here on the right of each tree. ESTUs were colored according to the palette below each panel. Dotted lines in dendrograms indicate discrepancies between trees. Flexible genes correspond to genes that were not detected in a least one sample. Of note, due to a slightly different clustering method (cf. materials and methods), assemblage 7 (dark grey stations in 1B), which was discriminated from assemblage 6 in the Farrant et al. (2016) is now included into this assemblage. Abbreviations: IO, Indian Ocean; MS, Mediterranean Sea; NAO, North Atlantic Ocean; NPO, North Pacific Ocean; RS, Red Sea; SAO, South Atlantic Ocean; SO, Southern Ocean.

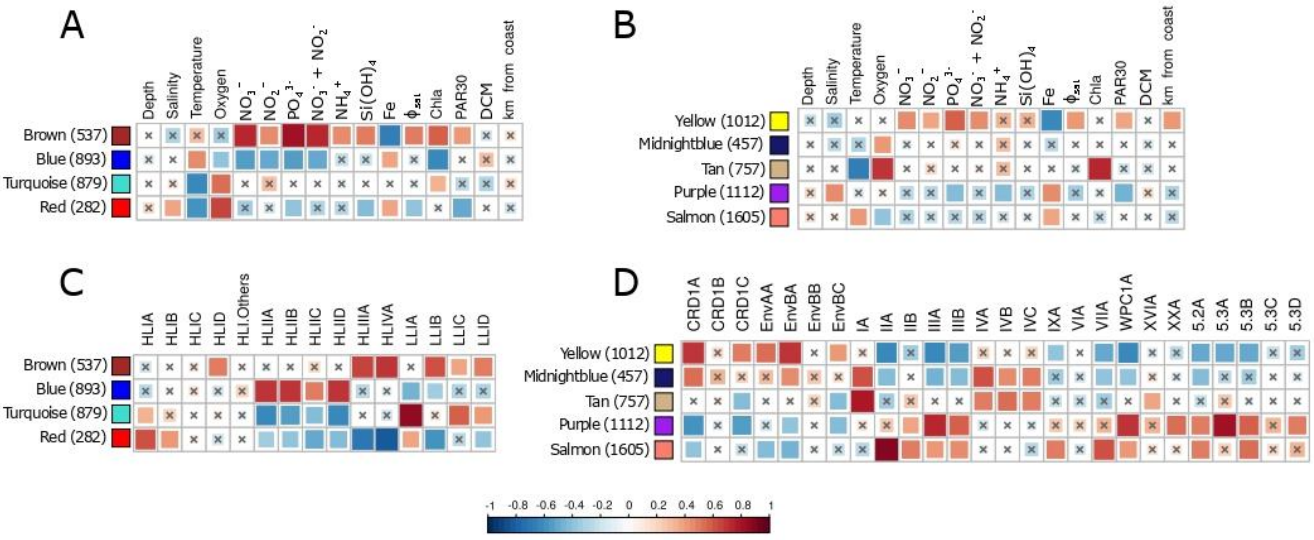

Figure 2. Correlation of picocyanobacterial module eigengenes to physico-chemical parameters and ESTU abundance. A, B. Correlation of module eigenges to physico-chemical parameters for *Prochlorococcus* (A) and *Synechococcus* (B). C, D. Correlation of module eigenges to relative abundance profiles of ESTUs sensu (Farrant et al., 2016). Pearson (A, B) and Spearman (B, D) correlation coefficient (R^2) is indicated by the color scale. Each module is identified by a specific color and the number between brackets specifies the number of genes in each module. Non-significant correlations (Student asymptotic p-value > 0.01) are marked by a cross. Φsat: index of iron limitation derived from satellite data. PAR30: satellite-derived photosynthetically available radiation at the surface, averaged on 30 days. DCM: depth of the deep chlorophyll maximum.

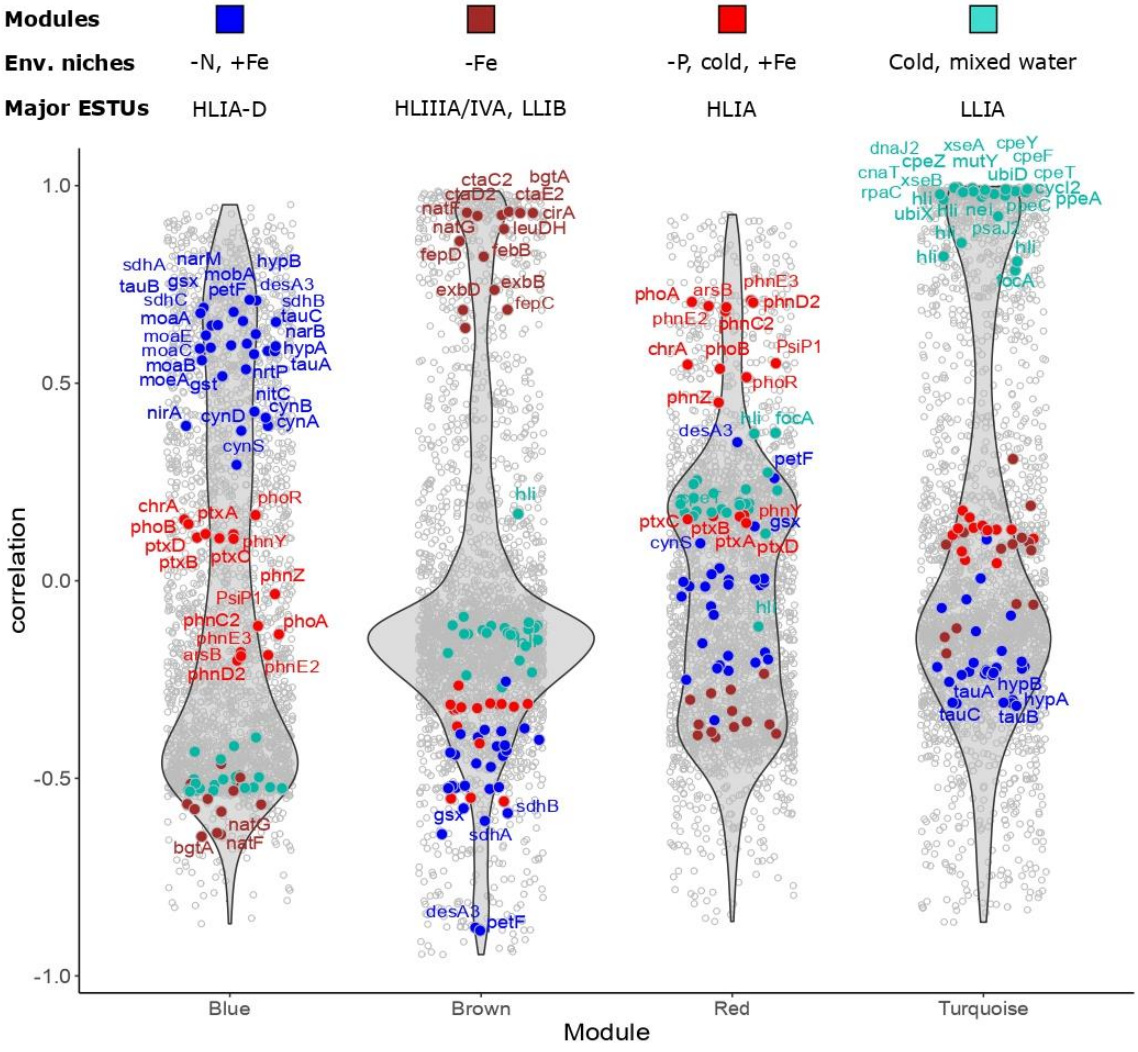

Figure 3. Violin plots highlighting the most representative genes of each *Prochlorococcus* module. For each module, each gene is represented as a dot positioned according to its correlation with the eigengene of each module, the most representative genes being localized on top of each violin plot. Genes mentioned in the text have been colored according to the color of the corresponding module, indicated by a colored bar above each module. Text between brackets indicates the most significant environmental parameter(s) and/or ESTU(s), as derived from **Fig. 2**.

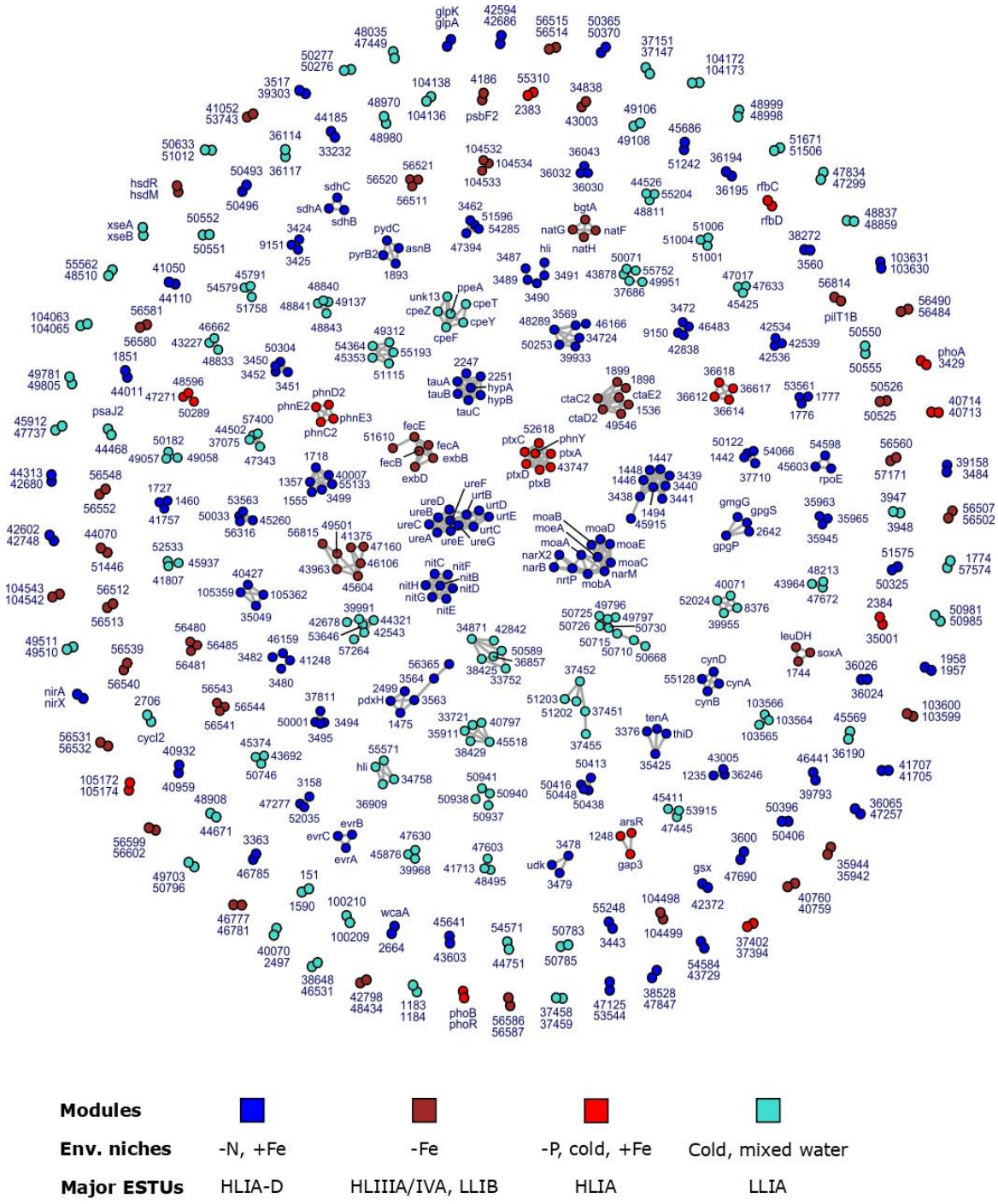

Figure 4. Delineation of *Prochlorococcus* CAGs, defined as a set of genes that are both adjacent in reference genomes and share a similar *in situ* distribution. Nodes correspond to individual genes with their gene name (or significant numbers of the CK number, e.g. 1234 for CK_00001234) and are colored according to their WGCNA module. A link between two nodes indicates that these two genes are less than 5 genes apart in at least one genome. Insert shows the most significant environmental parameter(s) and/or ESTU(s) for each module, derived from Fig. 2.

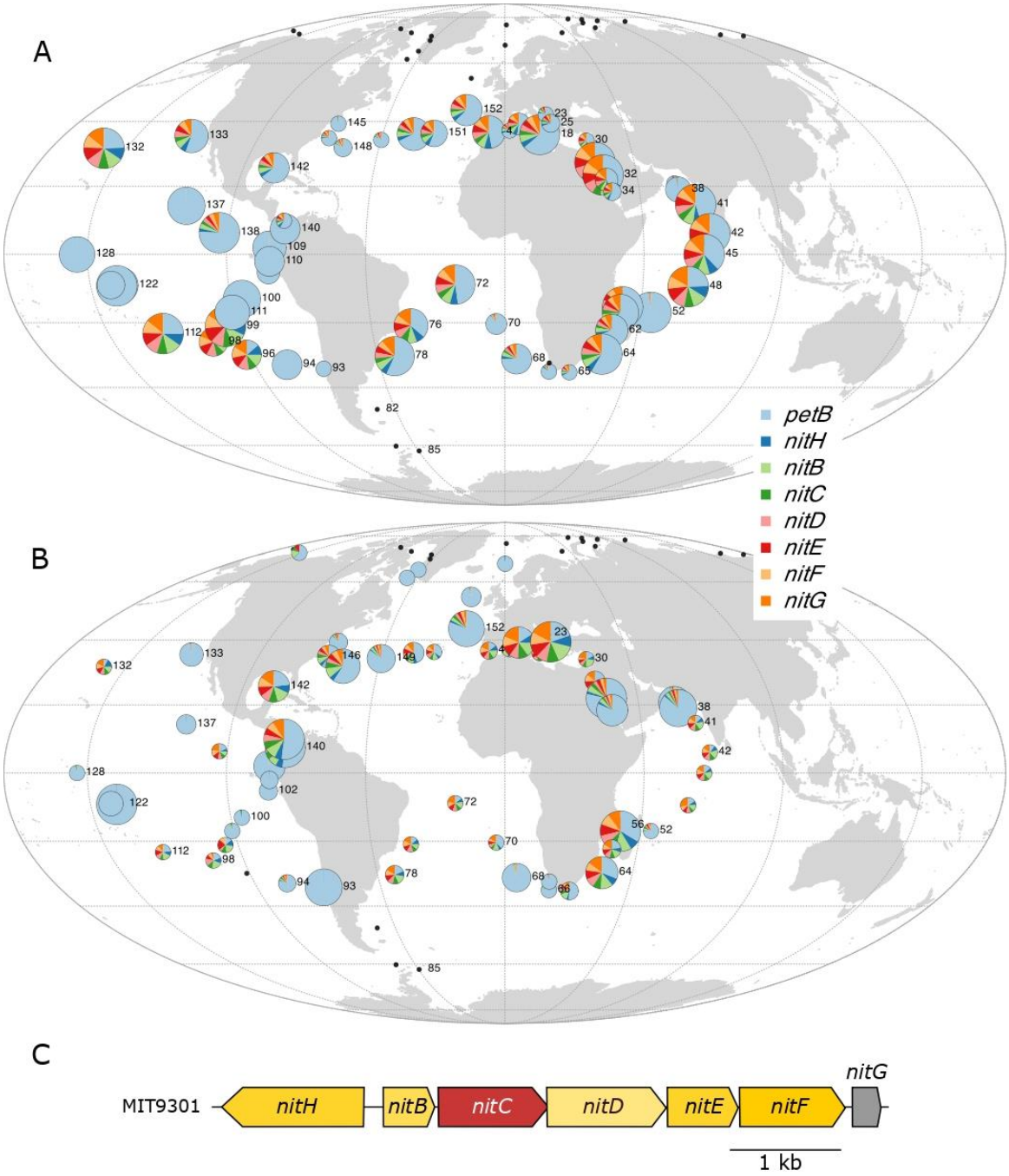

Figure 5. Global distribution map of CAG involved in nitriles or cyanides transport and assimilation. (*A*) *Prochlorococcus* (ProCAG_006) and (*B*) *Synechococcus* SynCAG_002. (*C*) Genomic region in *Prochlorococcus marinus* MIT9301. The size of the circle is proportional to relative abundance of *Prochlorococcus* as estimated based on the *petB* gene and this gene was also used to estimate the relative abundance of other genes in the population.

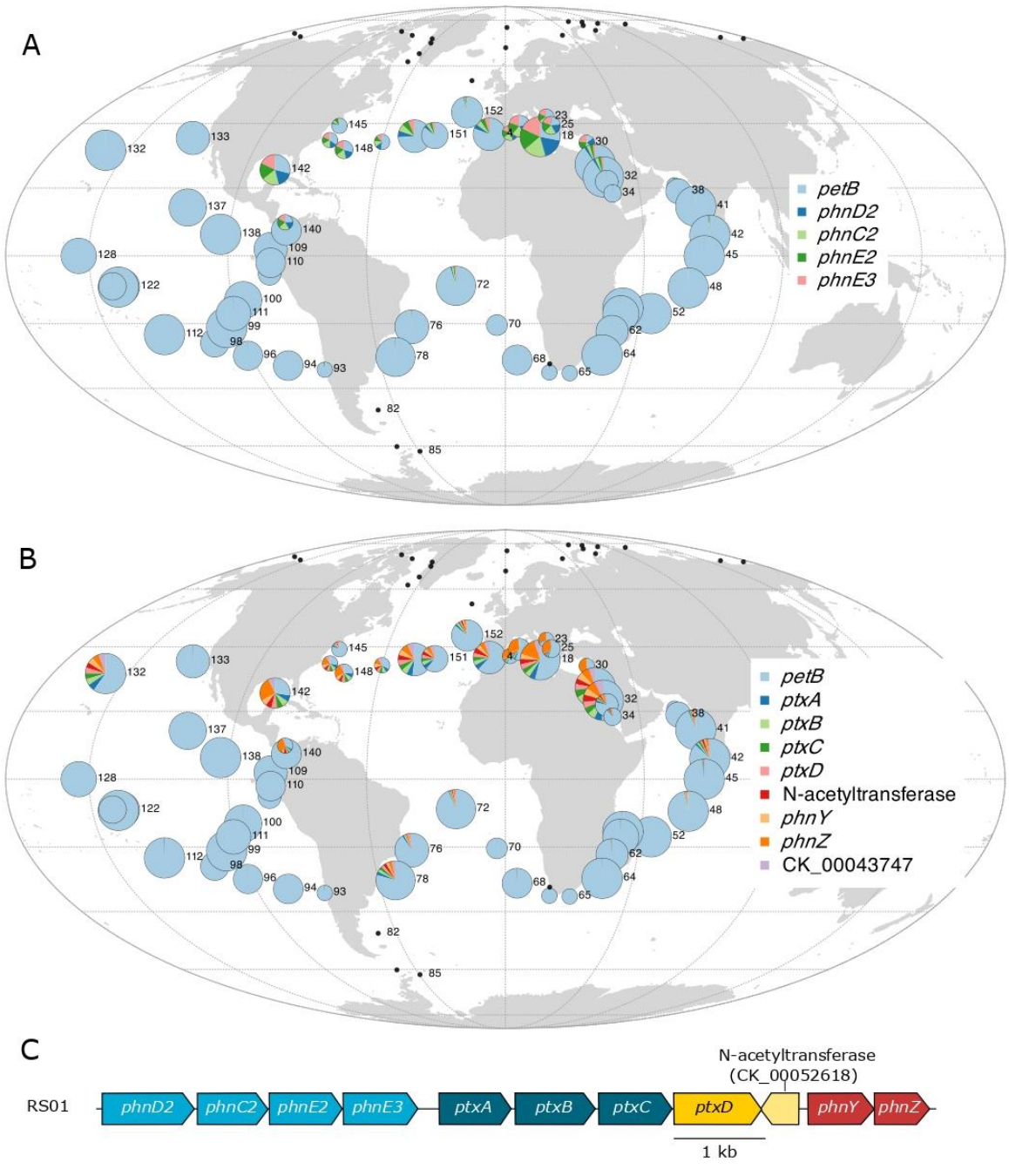

Figure 6. Global distribution map of CAGs putatively involved in phosphonate and phosphite transport and assimilation. *Prochlorococcus* (*A*) ProCAG_012 putatively involved in phosphonate transport, (*B*) ProCAG_013, involved in phosphonate/phosphite uptake and assimilation and phosphonate C-P bond cleavage, (*C*) Genomic region encompassing both *phnC2-D2-E2-E3* and *ptxABDC-phnYZ* specific of *Prochlorococcus* RS01.

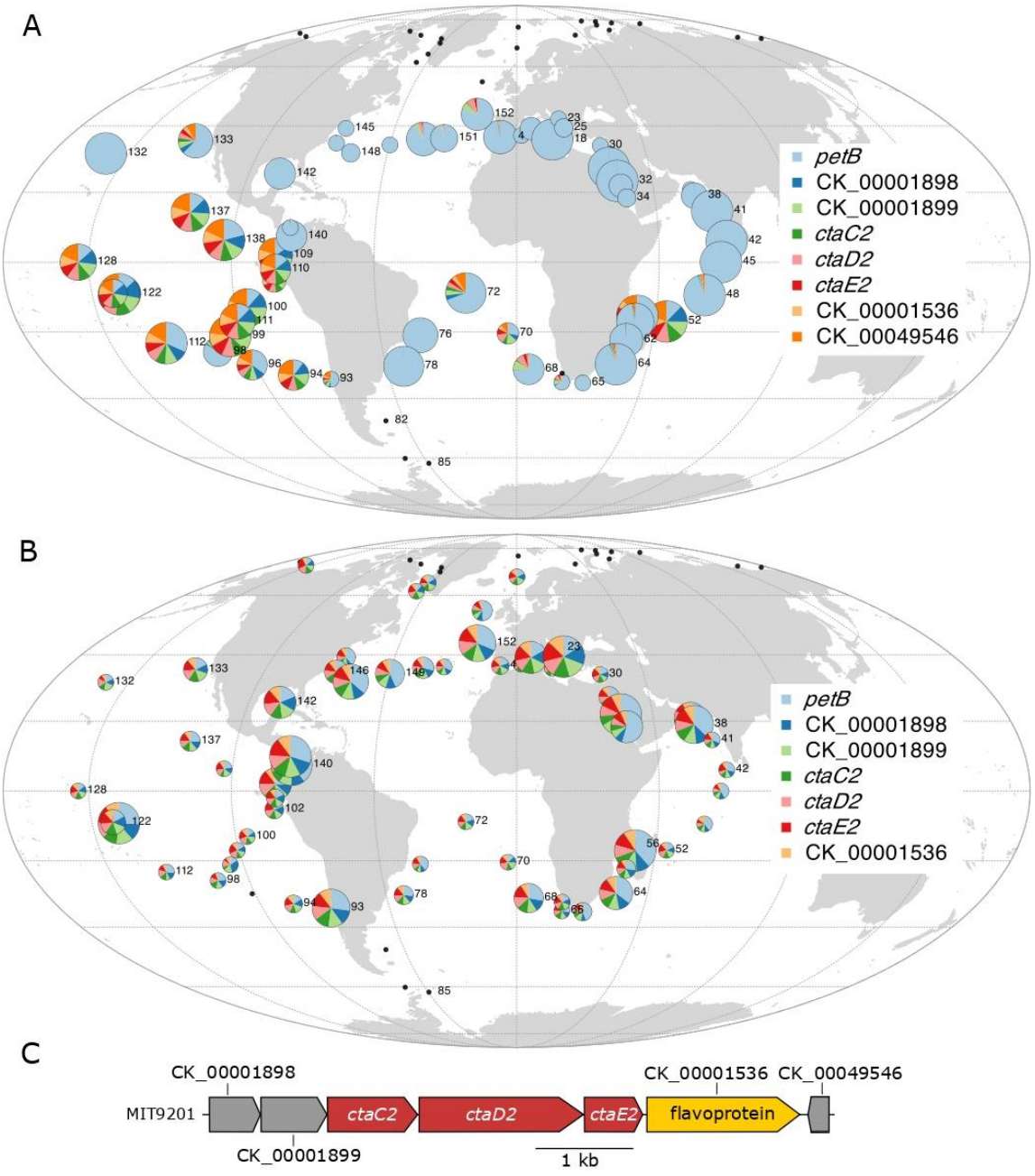

Figure 7. Global distribution map of the *Prochlorococcus* CAGs involved in biosynthesis of an alternative respiratory terminal oxidase (ARTO). (*A*) *Prochlorococcus* ProCAG_0XX, (*B*) *Synechococcus* SynCAG_0XX

Annexe C : Composition des milieux de cultures utilisés pour cultiver les souches de *Synechococcus* au cours de cette thèse

		Components (Final concentration in media µM unless stated otherwise)	AQUIL			PCRS-11			AQUIL PCRS-11	
			AQUIL (Price et al., 1989 : Table 2) **5 µM EDTA**	AQUIL (Price et al., 1989 : Table 3) **100 µM EDTA**	AQUIL (Price et al., 1989 : Table 3) **100 µM EDTA**	PCR-S11 (Rippka et al. 2000)	PCR-S11 (Moore et al. 2007)	PCR-S11 **2µM EDTA** (Roscoff)	AQUIL PCRS-11 **2µM EDTA**	AQUIL PCRS-11 **100 µM EDTA**
Macronutrients		$(NH_4)_2SO_4$				400	400	400		
	Na-PO_4	$NaH_2PO_4 \cdot H_2O$ $Na_2H\text{-}PO_4$	10	10	10	50	50	50	10	10
		$NaNO_3$	300	300	300	0	0	1000	300	300
		$Na_2SiO_3.9H_2O$	100	100	0				0	0
Buffers		HEPES, pH7.5				1000	1000	1000		
Trace Metals	Fe/EDTA	$Na_2EDTA \cdot 2H_2O$	5	100	100	8	8	2	2	100
		$FeCl_3 \cdot 6H_2O$	0,451	8,32	Variable				Variable	Variable
	Molybdenum	$Na_2MoO_4 \cdot 2H_2O$	0,1	0,1	0,1				0,1	0,1
		$(NH_4)6Mo_7O_{24} \cdot 4H_2O$				0,0002	0,0004	0,0004		
	Selenium	Na_2SeO_3	0,01	0,01	0,01				0,01	0,01
		SeO_2				0,0015	0	0,003		
	Zinc	$ZnSO_4 \cdot 7H_2O$	0,004	0,0797	0,0797	0,003	0,006	0,006		
		ZnCl2							0,006	0,0797
	Copper	$CuSO_4 \cdot 5H_2O$	0,000997	0,0196	0,0196	0,0015	0,003	0,003	0,003	0,0196
	Manganèse	$MnCl_2 \cdot 4H_2O$	0,023	0,121	0,121				0,06	0,121
		$MnSO_4 \cdot H_2O$				0,03	0,06	0,06		
	Cobalt	$CoCl_2 \cdot 6H_2O$	0,0025	0,0503	0,0503				0,003	0,0503

		$Co(NO_3)_2{\cdot}6H_2O$				0,0015	0,003	0,003		
	Tungsten	$Na_2WO_4{\cdot}2H_2O$				0,0003	0,0006	0,0006	0,0006	0,03
	Cadmium	$Cd(NO_3)_2{\cdot}4H_2O$				0,0015	0,003	0,003	0,003	0,15
	Nickel	$NiCl_2.6H_2O$				0,0015	0,003	0,003	0,003	0,15
	Chromium	$Cr(NO_3)_3{\cdot}9H_2O$				0,0003	0,0006	0,0006	0,0006	0,03
	Vanadium	VSO_5				0,0003	0,0006	0,0006	0,0006	0,03
	Aluminum	$KAl(SO_4)_2{\cdot}12H_2O$				0,003	0,006	0,006	0,006	0,3
	Iodine	KI				0,0015	0,003	0,003	0,003	0,003
	Boron	H_3BO_3				0,15	0,3	0,3		
	Bromine	KBr				0,003	0,006	0,006		
Salt (Red sea salt for PCR-S11 or SOW for AQUIL)	Boron	H_3B03	4,85E+02	4,85E+02	4,85E+02	Sea water	Sea water	Red Sea Salt 33.3g/L	4,85E+02	4,85E+02
	Bromine	K.Br	8,40E+02	8,40E+02	8,40E+02				8,40E+02	8,40E+02
		NaCl	4,20E+05	4,20E+05	4,20E+05				4,20E+05	4,20E+05
		$MgCl_2{\cdot}6H_2O$	5,46E+04	5,46E+04	5,46E+04				5,46E+04	5,46E+04
		$CaCl_2{\cdot}2H_2O$	1,05E+04	1,05E+04	1,05E+04				1,05E+04	1,05E+04
		KCl	9,39E+03	9,39E+03	9,39E+03				9,39E+03	9,39E+03
		Na_2S04	2,88E+04	2,88E+04	2,88E+04				2,88E+04	2,88E+04
		$NaHC0_3$	2,38E+03	2,38E+03	2,38E+03				2,38E+03	2,38E+03
		NaF	7,14E+01	7,14E+01	7,14E+01				7,14E+01	7,14E+01
		$SrCl_2{\cdot}6H20$	6,38E+01	6,38E+01	6,38E+01				6,38E+01	6,38E+01
Vitamins		Vitamin B12 Cyanocobalamin (µg/L)	0,55	0,55	0,55	10	10	1	0,55	0,55
		Biotin (µg/L)	0,5	0,5	0,5				0,5	0,5
		Thiamin HCl (µg/L)	100	100	100				100	100

Résumé

Les océans sont fortement impactés par le changement global, qui provoque une augmentation de la température de surface mais aussi une expansion des zones pauvres en Fer (Fe) alors que ce micronutriment limite déjà la croissance du phytoplancton dans près de 30 % de l'océan mondial. Dans ce contexte, on peut se demander si et comment le phytoplancton marin est capable de s'adapter à cette limitation et quelles seront les conséquences de l'appauvrissement en Fe sur la capacité des océans à séquestrer le CO_2 via la pompe à carbone biologique. De par son abondance, son ubiquité, la disponibilité de nombreuses souches et génomes, *Synechococcus* constitue l'un des modèles biologiques les plus pertinents disponibles à ce jour pour étudier les processus moléculaires impliqués dans l'adaptation du phytoplancton aux changements environnementaux en cours dans l'océan. Alors que les populations naturelles de *Synechococcus* ont longtemps été considérées comme dominées par quatre clades (I-IV), l'importance écologique d'un cinquième clade (appelé CRD1) a récemment été mise en évidence dans les zones limitées en Fe de l'océan mondial. En outre, il a été démontré que le clade CRD1 englobe 3 unités taxonomiques distinctes écologiquement significatives (ESTUs CRD1A à C), occupant des niches thermiques distinctes. Afin de mieux comprendre les rôles respectifs de la carence en Fe et de la température sur la distribution et la diversification génétique de *Synechococcus*, la comparaison de souches représentatives de chacun des trois ESTUs de CRD1 avec des membres des clades I-IV, utilisés comme références de thermotypes froids (I, IV) ou chauds (II, III) et colonisant des environnements riches en Fe, a permis de valider l'existence de trois thermotypes distinctes au sein au clade CRD1. De plus, l'acquisition de paramètres physiologiques supplémentaires à partir de cultures acclimatées à différentes températures et différents degrés de limitation en Fe a également révélé des spécificités des souches CRD1 par rapport aux autres clades. Des analyses comparatives des génomes de *Synechococcus* disponibles ont également suggéré que la dominance de ce clade dans les zones pauvres en Fe pourrait reposer sur une réduction du nombre de gènes codant pour des protéines riches en Fe et sur une augmentation du nombre de gènes codant pour des protéines utilisant des métaux alternatifs comme co-facteurs et surtout des protéines impliquées dans le transport, l'assimilation et le stockage du Fe. Enfin, l'analyse des métagénomes de *Tara* Oceans a révélé des gènes spécifiquement présents ou absents dans les niches pauvres en Fe qui ont permis de confirmer les résultats de génomique comparative et d'identifier de nouveaux gènes candidats potentiellement impliqués dans les mécanismes d'adaptation à la carence en Fe et à la température.

Abstract

The oceans are strongly impacted by global change, which is predicted to cause an increase of sea surface temperature but also an expansion of iron-poor areas (Fe). This micronutrient limits phytoplankton growth in nearly 30% of the global ocean. In this context, one may wonder if/how marine phytoplankton is able to adapt to such limitation and what will be the consequences of Fe depletion on the ocean ability to sequester CO2 via the biological carbon pump. Due to its abundance, ubiquity, the availability of numerous strains and genomes, Synechococcus constitutes one of the most relevant biological models available nowadays to study the molecular processes involved in the adaptation of phytoplankton to the environmental changes occuring the ocean. While natural populations of Synechococcus were long thought to be dominated by four clades (I-IV), the ecological importance of a fifth clade (called CRD1) has recently been demonstrated in Fe-limited areas of the world ocean. Furthermore, the CRD1 clade has been shown to encompass 3 distinct Ecologically Significant Taxonomic Units (ESTUs, CRD1A to C), occupying distinct thermal niches. In order to better understand the respective roles of Fe deficiency and temperature on the distribution and genetic diversification of Synechococcus, we compared the physiology of representative strains of each of the three CRD1 ESTUs with members of clades I-IV, used as controls for cold (I, IV) or warm (II, III) thermotypes and Fe-replete environments to validate the existence of three distinct thermotypes within the CRD1 clade. Moreover, the acquisition of additional physiological parameters from cultures acclimated to different temperatures and different degrees of Fe limitation also revealed specificities of CRD1 strains compared to other clades. Comparative analyses of Synechococcus genomes have also suggested that the dominance of this clade in Fe-depleted areas may rely on a reduction in the number of genes coding for Fe-rich proteins and an increase of genes coding for proteins using alternative metals as co-factors and especially involved in Fe transport, assimilation and storage. It made it possible to confirm the results of comparative genomics and to identify new candidate genes potentially involved in the mechanisms of adaptation to Fe and temperature. Finally, the analysis of Tara oceans metagenomes revealed genes specifically present of absent in the Fe-poor niches which made it possible to confirm the results of comparative genomics and to identify novel genes potentially involved in adaptation mechanisms to Fe-depletion and temperature.